Characterizing Roles for PD-1 and Capicua in Thymocyte Tolerance and Selection

by

Julia May

A thesis submitted in partial fulfilment of the requirements for the degree of

Doctor of Philosophy

In

Immunology

Department of Medical Microbiology and Immunology

University of Alberta

Abstract

The stochastic diversification of the T cell receptor (TCR) carries with it both the potential for recognizing virtually infinite foreign peptides, but also the potential for the erroneous recognition of self-peptides, which represents a threat of autoimmunity. During development in the thymus, T cells are positively selected based on weak self-reactivity and negatively selected when they demonstrate strong self-reactivity. Thymocytes are negatively selected when they recognize with high affinity self-peptides expressed ubiquitously (UbA, encountered in the thymic cortex) or in a tissue-restricted manner (TRA, encountered in the thymic medulla). To model negative selection to these differentially expressed antigens, here we used the MHCI-restricted HY^{cd4} (UbA) and OT-I (TRA) models. Negative selection serves to censor or silence self-reactive clones by instructed apoptosis (clonal deletion), diversion into nonconventional lineages (e.g. Treg), or functional inactivation (tolerance).

We previously showed that impairment in clonal deletion in a model for negative selection to TRA did not lead to a spontaneous loss of tolerance. In this study, we investigated the non-deletional tolerance established in cells that escaped clonal deletion in this model. Tolerance was established in a T cell-intrinsic manner in the thymus, and we provide the first epigenetic profile for thymocytes in this state. PD-1 is a co-inhibitory receptor that functions to depress the TCR signal. It has been negatively associated with T cell function under various contexts, but it has received the most attention for its role in maintaining T cell dysfunction during anti-tumour or anti-viral responses. We determined that PD-1 and PD-L1 were required for the establishment of thymic tolerance in our model. Tolerance was largely maintained following adoptive transfer of either mature thymocytes or splenic $CD8^+$ T cells into PD-$L1^{-/-}$ recipients, but CRISPR-mediated ablation of the *Pdcd1* locus resulted in broken tolerance.

Overall, these data suggest that the requirements for PD-1-mediated tolerance differ between the establishment versus the maintenance of tolerance.

Capicua (CIC) is an evolutionarily conserved transcriptional repressor that has recently been implicated for its role in early T cell development and expansion, and as a suppressor of autoimmunity. CIC has been postulated to participate in a negative feedback network for ERK signaling. Such a network was described in a study using human cell lines; ERK signaling attenuated CIC activity, while CIC repressed the transcription of a negative ERK regulator, DUSP6. A similar regulatory loop may also function in thymocytes, as known ERK regulators (DUSP6 among them) have been observed to be upregulated in the absence of CIC. In this study, we investigated the role of CIC in positive and negative selection using a $CIC^{FL/FL}$ CD4-cre knock-out model, which allows for the separation of early development events and selection proper. CIC deficiency resulted in impaired positive selection in mixed bone marrow chimeras for polyclonal thymocytes and in two MCHI-restricted TCR transgenic models. In contrast, negative selection in these transgenic models was largely unperturbed, suggesting CIC plays a unique role in the integration of the weak TCR signals associated with positive selection. Finally, CRISPR-mediated deletion of *Dusp6* was unable to rescue impaired positive selection in the CIC deficient thymocytes in HY^{cd4} mixed bone marrow chimeras, suggesting that this negative ERK regulator is not required for CIC's influence on selection. However, whether DUSP6 participates in this process redundantly alongside other regulators remains an unanswered question.

Preface

This thesis is an original work by Julia May. It contains content co-authored by collaborators and originally published in The Journal of Immunology:

- May, J. F., R. G. Kelly, A. Y. W. Suen, J. Kim, J. Kim, C. C. Anderson, G. R. Rayat, and T. A. Baldwin. 2024. Establishment of CD8+ T Cell Thymic Central Tolerance to Tissue-Restricted Antigen Requires PD-1. J. Immunol. Vol 212 (2): 271-283. Copyright © [2024] The American Association of Immunologists, Inc.

The research project that this thesis is a part of received research ethics approval from the University of Alberta Research Ethics Board. Project name, “Understanding the Cellular and Molecular requirements underlying negative selection in the Thymus”, Protocol No. (AUP220), (2014).

Acknowledgements

I would first like to express my deepest thanks to my supervisor, Dr. Troy Baldwin, for the opportunity to work in his lab. His unwavering support, guidance, and patience helped me overcome the challenges my projects (and graduate student life) posed.

I would like to thank my good friend Niall Pollock for always lending an understanding ear, being there to commiserate about frustrations, and helping to celebrate successes. You have been a never-ending source of positivity that has helped me stay sane.

Thanks to my dad, Gerry May, for providing the support and encouragement that carried me to – and through – graduate school.

I would like to thank Dr. Hanne Ostergaard and Dr. Colin Anderson for serving as my supervisory committee members. Their mentorship has been of great value to this research.

I would also like to express my gratitude to the University of Alberta staff that supported this project. The Flow Cytometry Core staff and their advice has been critical in my work. Additionally, this project would not have been possible without support from the HSLAS staff and their maintenance of our mouse colonies.

Thank you to all the members of the Baldwin lab. Thank you in particular to Bing Zhang for help with animal handling and maintaining the lab's day-to-day function over the years, and more recently, Thaisa Sandini for taking over his role. My fellow graduate students, Kevin Joannou, Shae Komant, and Rees Kelly, you made each day spent during this project brighter as we shared advice and jokes along the way. Thank you to Nikhil Bhatnagar, who contributed data to this thesis and acted as my experiment-partner at the end of my degree.

Finally, I would like to thank the Canadian Institutes of Health Research for funding and making this research possible.

Contents

List of Tables

List of Figures

List of recurring abbreviations

Ag – Antigen

APC – Antigen Presenting Cell

AT – Adoptive Transfer

BM – Bone Marrow

BMC – Bone Marrow Chimera

Bim – Bcl-2-interacting mediator of death

CIC – Capicua

CFSE – carboxyfluoroscein diacetate succinimidyl ester

CKO – Capicua knock-out

cTEC – Cortical Thymic Epithelial Cell

DC – Dendritic Cell

DN – Double Negative ($CD4^-$ $CD8^-$)

DP – Double Positive ($CD4^+$ $CD8^+$)

ERK – Extracellular Signal-Regulated Kinase

FACS – Fluorescence Activated Cell Sorting

Foxp3 – Forkhead Box p3

FR4 – Folate Receptor 4

HSC – Hematopoietic Stem Cell

HY – Transgene responsible for expression of a T cell receptor that recognizes a male-specific minor histocompatibility antigen (encoded by the Y chromosome)

IE – Independent Experiment

IELp – Intra-epithelial Lymphocyte Progenitors

iNKT – Invariant Natural Killer T cells

LAT – Linker for the Activation of T cells

LN – Lymph Node

M1 – Mature thymocyte subset 1 ($CD4^+CD8^-$ or $CD4^-$ $CD8^+$, $TCR\beta^+$ $H\text{-}2K^{b\ hi}$ $CD69^{hi}$)

M2 – Mature thymocyte subset 2 ($CD4^+CD8^-$ or $CD4^-$ $CD8^+$, $TCR\beta^+$ $H\text{-}2K^{b\ hi}$ $CD69^{lo}$)

MAPK – Mitogen-activated protein kinases

MFI – Median Fluorescence Intensity

MHC – Major Histocompatibility Complex

mTEC – Medullary Thymic Epithelial Cell

NFR – Nucleosome-Free Region

NOD – Non-Obese Diabetic

OVA – Chicken Ovalbumin

PD-1 – Programmed Cell Death Protein 1

pMHC – Peptide-MHC

RIP-mOVA – transgenic mice expressing membrane-bound OVA, driven by the rat insulin promoter

RTK – Receptor Tyrosine Kinases

SM – Semi-mature thymocyte ($CD4^+CD8^-$ or $CD4^-$ $CD8^+$, $TCR\beta^+$ $H\text{-}2K^{b\ lo}$)

SP – Single Positive ($CD4^+CD8^-$ or $CD4^-$ $CD8^+$)

T1D – Type I diabetes

TCM – T Central Memory

TCR – T Cell Receptor

TEM – T Effector Memory

T_{EX} – Terminally differentiated exhausted T cell

TFH – T Follicular Helper Cells

Tg – Transgenic

TIL – Tumour-Infiltrating T cell

T_{PEX} – Progenitor exhausted T cell

TRA – Tissue-Restricted Antigen

Treg – T Regulatory ($CD4^+$) cells

TSS – Transcription Start Site

tTreg – Thymic Treg

UbA – Ubiquitous Antigen

WT – Wildtype

Chapter 1 - Introduction

1.1 - The T cell compartment as a critical part of the immune system

The immune system is a complex and diverse grid comprised of a breadth of cell types, diffusible messengers, tissues, and physical phenomena that coordinate to precipitate protective responses against pathogens. Broadly, immunity can be categorized into two main branches: innate and adaptive immunity. Innate immunity includes the germline encoded mechanisms that provide 1) physical barriers to the outside world (such as the epithelial cell layers with associated mucosal secretions that line the respiratory or gastrointestinal tracts, and others), 2) small soluble molecules (such as complement, defensins, chemokines, cytokines, etc.), and 3) cellular mediators such as neutrophils or monocytes, which provide antimicrobial protection independently of antigen (Ag) specificity – and due to this feature, innate immunity is rapidly provoked (1). In contrast, adaptive immunity first arose in jawed vertebrates and is mediated by T and B lymphocytes, characterized by Ag-specific receptors diversified by unique enzymes that drive the rearrangement of their loci (2). T and B cells respond and expand based on the Ag-specificity of the T cell receptor (TCR) and B cell receptor (BCR), and establish immune memory, whereby subsequent responses are more rapid and robust.

The T cell compartment contains a myriad of subsets that encapsulate important effectors of an immune response, but also key regulatory nodes that inform both the type and magnitude of response carried out. $CD4^+$ T helper (Th) are T cells that function based on their αβ TCR engagement with peptide-MHCII (pMHCII); the differentiation of these cells into various subsets is thought to be based on signals from the extracellular milieu, the nature of the inciting Ag, and/or the qualities (i.e. size, TCR affinity, etc.) of the responding $CD4^+$ T cell population. Th

subsets include Th1, Th2, T regulatory cells (Treg), T follicular helper cell (TFH), Th17, Th9, Th22, and $CD4^+$ cytotoxic T lymphocytes (3). TFH cells, for example, support and promote humoral immune responses driven by B cells, and their early differentiation depends on numerous factors such as IL-6, inducible co-stimulator (ICOS), and TCR dwell time (4). The $CD8^+$ T cell is the other αβ TCR-expressing conventional T cell subset, which upon high affinity engagement with pMHCI, differentiate into effector T cells (cytotoxic T lymphocytes, CTL) that can eliminate intracellular pathogens by inducing apoptosis in infected cells via Fas/FasL interactions or release of cytolytic mediators.

1.2 - The T Cell Receptor

The αβ TCR is an Ag receptor comprised of two chains, α and β. The 5' ends of the genes encoding these subunits are arranged in arrays of variable (V), diversity (D), and joining (J) segments. The whole TCR complex consists of the αβ TCR heterodimer (responsible for specific Ag recognition) associated with CD3 γ/δ/ε/ζ subunits (which transmit the TCR signal; discussed below). The coreceptors CD4 and CD8 bind to MHC class I and II, respectively, which provide stabilization for the TCR-pMHC interaction and bring coreceptor-bound signaling molecule LCK into proximity with the TCR complex, allowing for the TCR signal to be kick-started (5).

The stochastic generation of the αβ TCR heterodimer involves RAG recombinase (a complex of *Rag1* and *Rag2* gene products) – in concert with additional accessory factors – binding DNA and generating double-stranded breaks at recombination signal sequences (RSS) flanking V, D, and J segments. The resulting error-prone repair, non-templated nucleotide addition, and combination of V and J segments for the TCRα chain and the V, D, and J segments for the TCRβ chain (along with their respective constant domains) produces the vastly diverse repertoire of TCR specificities required for preparedness for an outside world of virtually infinite

and changing foreign Ags (6). Development of the non-conventional γδ T cell similarly involves such recombination of the TCRγ and TCRδ loci. The stochasticity in the generation of this diverse repertoire means that TCRs can recognize self peptide presented in the context of MHC (facilitated by CD4/CD8 co-receptors) with a wide range of affinities. A low level of reactivity for self-MHC (in contrast to no self-reactivity whatsoever) is thought to characterize a functional TCR repertoire (development, homeostasis, and recruitment into responses) (7), and may be predictive of a given clone's capacity to bind foreign pMHC (8). Conversely, TCR affinities on the upper end of the spectrum of self-reactivity can potentially drive pathological responses to healthy tissues and must therefore be censored from the T cell repertoire. As a result, T cells undergo an education process in the thymus to retain a heterogenous functional population of low self-reactivities, while simultaneously silencing clones of high self-reactivity.

1.3 - T cell development and selection

Thymocyte development and selection is summarized in Figure 1.3-1. Hematopoietic stem cells give rise to $CD4^-$ $CD8^+$ (DN) T cell progenitors that traffic through the blood and seed the thymus at the cortico-medullary junction (9). These early DN thymocytes then differentiate through four sequential stages characterized by CD25 and CD44 expression: DN1 ($CD25^-$ $CD44^+$), DN2 ($CD25^+$ $CD44^+$), DN3 ($CD25^+$ $CD44^-$), and DN4 ($CD25^-$ $CD44^-$). At the DN2/3 stages, RAG1/2 are expressed and first begin rearrangement of the TCRβ, TCRγ, and TCRδ genes (10, 11). A process termed β-selection occurs, whereby the TCRβ subunit associates with the pre-TCRα chain and with CD3 proteins to form a pre-TCR complex whose signals validate the functionality of the TCRβ rearrangement and support the survival, proliferation, and differentiation of DN3 thymocytes (12, 13). Subsequent progression into the DN4 stage is

accompanied by extensive proliferation and the rearrangement of the TCRα locus, which continues until entry into the $CD4^+$ $CD8^+$ DP stage (14).

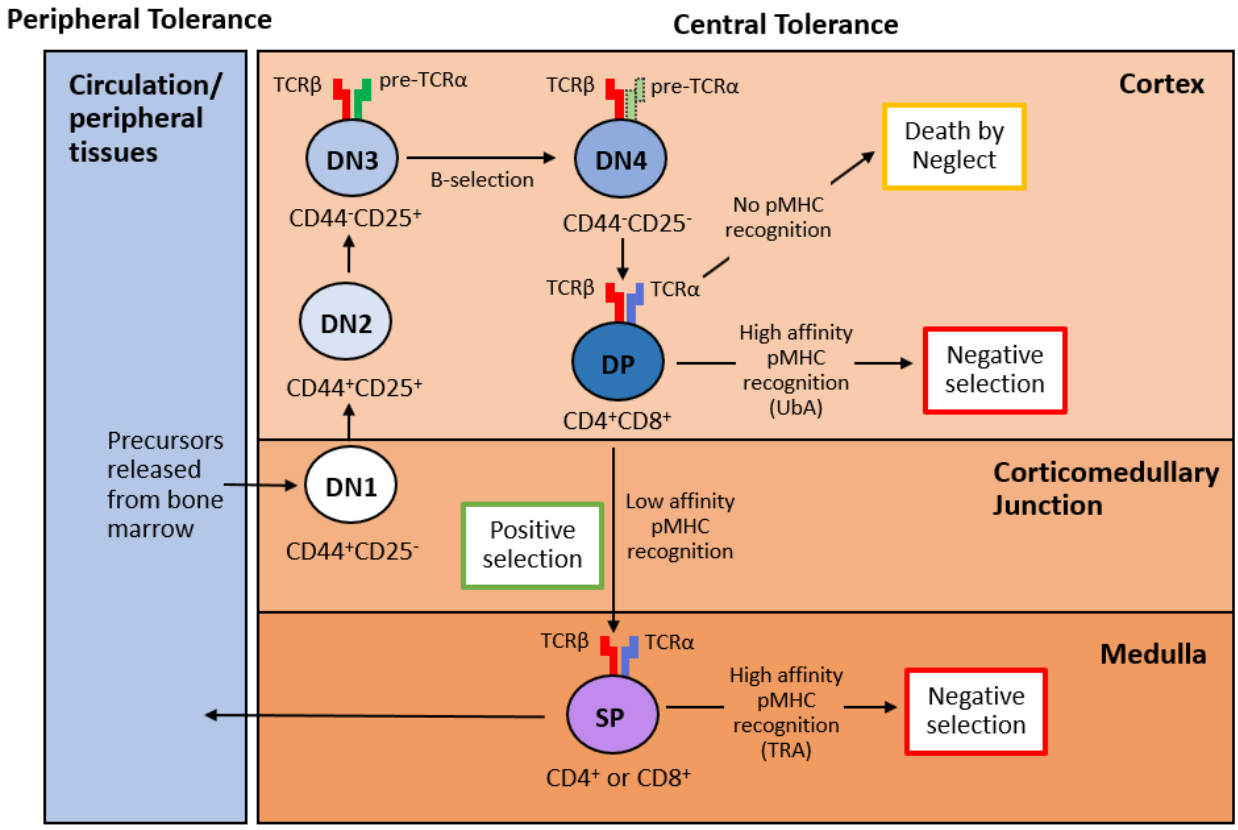

Figure 1.3-1: Development and selection of αβ T cells.

Early thymocyte progenitors enter the thymus at the corticomedullary junction. $CD4^-$ $CD8^-$ DN thymocytes progress through four developmental stages defined by CD44 and CD25 expression. β-selection occurs at the transition between DN3 and DN4 stages, during which thymocytes harbouring a functional TCRβ subunit are selected for. At the $CD4^+$ $CD8^+$ DP stage, the fully formed αβTCR scans ubiquituous (UbA) self-pMHC in the thymic cortex, and the affinity of the interactions between these entities signal thymocytes to undergo death by neglect, positive selection, or negative selection. Positively selected thymocytes differentiate into CD4/CD8 SP

stages and migrate to the medulla, where they retain the potential for negative selection as they encounter tissue-restricted Ag (TRA) self-pMHC presented therein. The population of mature SP thymocytes exiting the thymus is largely tolerant of self-peptides.

Upon formation of the αβTCR, DP thymocytes are "auditioned" based on the affinity of their TCR for self-pMHC presented by cortical thymic epithelial cells (cTEC), which present a unique pMHC ligandome due to their unique Ag-processing machineries. cTECs express the β5t catalytic subunit of the proteasome that produces a thymus-exclusive suite of MHCI ligands critical for positive selection of $CD8^+$ thymocytes (15, 16). cTECs also express the unique lysosomal proteases cathepsin L and thymus-specific serine protease (TSSP), which similarly produce unique ligands for endogenous loading on MHCII, and are required for the positive selection of $CD4^+$ thymocytes (17–19). If the TCR-self-pMHC interaction is too weak and fails to generate a productive signal, thymocytes die by neglect – they fail to experience positive selection and the accompanying survival signals. The pre-programmed cell death of DP thymocytes is thought to be supported by the unavailability of IL-7 signals due to a lack of CD127 (IL-7Rα) expression and paucity of IL-7 in the cortex (20). Thymocytes expressing TCRs with high affinity for self-pMHC undergo negative selection, whereby thymocytes are instructed to undergo apoptosis (clonal deletion), are rendered functionally impaired (anergy), or are diverted into non-conventional lineages such as Tregs, or $CD8\alpha\alpha^+$ intestinal epithelial lymphocytes (21). In the thymic cortex, thymocytes are auditioned based on ubiquitously-expressed Ags (UbA) (22). Following low-medium affinity encounters of the TCR with self-pMHC, positive selection occurs and DP thymocytes transition into the $CD4^+$ $CD8^-$ (CD4SP) or $CD4^-$ $CD8^+$ (CD8SP) stage and undergo CCR7-mediated migration into the thymic medulla (21).

In the medulla, SP thymocytes are exposed to a myriad of ectopically expressed tissue-restricted Ag (TRA) produced by medullary thymic epithelial cells (mTEC), upon which negative selection can occur during the 4-5 day thymocyte residency in this compartment before release into the periphery (23).

1.4 - TCR signaling during selection

The signaling machinery associated with the TCR is responsible for transmitting and integrating the mechanical force experienced by the TCR itself into complex and diverse functional and fate outcomes. Monomeric pMHC binding studies combined with fetal thymic organ culture previously defined the affinity threshold for negative selection at $K_D \leq 6$ μM, meaning that thymocytes binding self-pMHC with a lower affinity ($K_D > 6$ μM) experience positive selection (24, 25), in a manner largely independent of peptide concentration. This suggests striking precision in the TCR's ability to interpreting Ag affinity. Bids to explain this precision have culminated in the currently-held kinetic proofreading model (26), which proposes TCR-pMHC dwell-time as the deciding factor for interpreting affinity. Indeed, studies using optogenetic systems wherein the duration TCR-ligand interactions could be finely controlled have more recently provided support for this model (27, 28). Subtle differences in the duration of receptor occupancy are thought to be magnified by a sequence of downstream molecular events only triggered by longer TCR-pMHC interactions, termed proofreading steps. Examples of these events include CD4/8 coreceptor scanning (whereby the TCR complex "scans" the sea of coreceptors in the plasma membrane for those bound with LCK (29)), ZAP70 recruitment, LAT clustering, and diacylglycerol production (30).

Broadly, upon engagement of the TCR and LCK-bound coreceptors CD4 or CD8 with pMHC, tyrosine phosphorylation of the CD3 ITAMs by LCK results in the recruitment and

activation of ZAP70. Tyrosine residues on linker for activation of T cells (LAT) are phosphorylated by ZAP70, producing docking sites for other adapter molecules such as GADS, GRB2, SLP76, which facilitate the recruitment and activation of signaling molecules such as Vav1, PLCγ1, and SOS1 (31). The formation of the LAT signalosome is a crossroads for multiple downstream signals. For example, PLCγ1 generates second messengers from membrane lipids – diacylglycerol (which activates protein kinase C (PKC) and the MAP kinases (MAPK) pathways) and inositol (1, 4, 5)-trisphosphate (which triggers an increase in intracellular calcium and calcineurin activation). These signaling events culminate in the activation and/or nuclear translocation of activator protein 1 (AP-1), nuclear factor-κB (NF-κB), and nuclear factor of activated T cells (NFAT), whose activities combine with additional signals (CD28 co-stimulation and PI3K activation, cytokine signaling) to inform T cell development and behaviour (31).

The multitude of signaling events downstream of the TCR are a complex integration network. Each node (recruitment or phosphorylation event, or the diffusion of a second messenger), acts as a rheostat, independently contributing to a final fate outcome for the T cell. ZAP70 activity, for instance, while critical for TCR signaling under all contexts, is required over several days to generate the weak signal needed for positive selection, but is only required for 1 hour to induce negative selection (32). TCR-pMHC dwell-time is also thought to probabilistically regulate the recruitment of SOS1/GRB2 to LAT, which further promotes LAT clustering and cooperativity in the LAT signalosome (33–35). Additionally, LAT is required for both positive and negative selection (36, 37), and the slow kinetics of PLCγ1 recruitment to LAT help determine TCR sensitivity and therefore ligand discrimination (38). Further downstream of the TCR complex, the entry of Ca^{2+} into the cytoplasm acts as a second messenger. Low transient increases in cytosolic Ca^{2+} are associated with positive selection, supported by voltage-gated Na^{+}

channels (39); in contrast, negatively selecting signals result in sustained, consistently increased cytosolic Ca^{2+} (24, 40). The MAPK pathway is central to our current understanding of how weak and strong TCR signals are translated into positive or negative selection. During positive selection, the MAP kinases ERK1/2 experience weak but sustained activation and robust, transient activation during negative selection (41, 42). ERK1/2 have been shown to be required for positive selection, but not required for negative selection (42–44). In contrast, the MAP kinases P38 and JNK are dispensable for positive selection, but required for negative selection (45, 46), and their kinetics appear similar following these two signals (41). While each of these MAPKs is activated during both positive and negative selection, it is their activation kinetics and subcellular localizations that appear to influence their roles in these processes (24). Beyond the kinetics of individual signaling participants that occur within an individual T cell, other external factors exert influence on the functional avidity of the T cell fate response (or responses to TCR signaling in general) through their influence on the activation of the aforementioned intracellular pathways. The affinity of the TCR for self-pMHC is determined by diversity in the TCR, presented peptide, and MHC. However, the avidity of this interaction is additionally informed by the density of MHC, co-stimulatory, and adhesion molecules on adjacent APCs (antigen presenting cells), the availability/rate of presentation of peptide, coreceptors (CD4/CD8), and cytokines (47). Thus, the array of physical and chemical signals that cooperate to inform the strength of the TCR signal is extensive and context-dependent, and it can therefore be difficult to distinguish these influences from one another.

1.5 – T cell activation and tolerance

Following T cell development, mature naïve T cells exit the thymus and begin to patrol the periphery, receptive to activating stimuli and the subsequent precipitation of a productive T

cell response. In the event that a T cell recognizes Ag presented by MHC with high affinity, a TCR signal is initiated, but the ultimate fate and function of the T cell is determined by the activity of co-stimulatory and co-inhibitory receptors. CD28 is the prototypical co-stimulatory molecule, originally implicated in the proposed "two signal model", which introduced the paradigm that both TCR and co-stimulatory signaling are required for full T cell activation (48–50). Conversely, co-inhibitory receptors expressed on the T cell surface antagonize TCR and co-stimulatory signaling and T cell activation.

The expression of co-signaling receptors is responsive to changes in the local tissue environment. Activated APCs in the context of inflammatory responses are characterized by elevated production of antimicrobials, pro-inflammatory cytokines, chemo-attractants, and co-stimulatory ligands (importantly CD80/CD86, ligands of CD28). Alongside a strong TCR signal (signal 1), provision of co-stimulation to $CD4^+$ T cells (signal 2) leads to their activation, and these activated cells return the favour to APCs by engaging their membrane-bound CD40 with the T cell-expressed CD40L. This results in "licensing", whereby the APC is induced to increase Ag presentation, cross-present extracellular Ag on MHC I, and increase co-stimulatory capacity. Subsequently, a $CD8^+$ T cell response can then be efficiently provoked (51). Receipt of signal 1 without signal 2 is canonically associated with a failure to induce lymphocyte activation and the induction of tolerance. Accordingly, in this document, I will define tolerance as a state of active hypo-responsiveness (and lack of immune responsiveness) toward a given Ag due to a previous encounter with the Ag.

The question of tolerance arises when one asks whether and how APCs become activated in the first place. Originally, a scaffold to this question was provided by the self-non-self theory, which postulated that a bona fide immune response is triggered against foreign "non-self'

entities. Such entities are detected based on the engagement of evolutionarily conserved "pathogen-associated molecular patterns" (PAMPs) with evolutionarily conserved receptors on the surface of APCs (e.g. bacterially-derived lipopolysaccharide detected by TLR4) (52, 53). By contrast, Matzinger's competing "danger model" contests that "danger-associated molecular patterns" (DAMPs; e.g. ATP or F-actin released from damaged cells) is what induces an immune response. According to this model, self Ag can induce an immune response if associated with danger signals (e.g. some autografts), and non-self can be tolerated if not associated with danger signals (e.g. a fetus) (54). If '"foreignness" of a pathogen is not the important feature that triggers a response, and "self-ness" is no guarantee of tolerance', as Matzinger wrote (55), then whether danger signals are perceived is critical in determining the balance between full activation and tolerance, even at steady state in a healthy organism. Overall, the presence of PAMPs or DAMPs is conceptually important in producing a microenvironment favourable for the delivery of the co-stimulatory Signal 2. Whether this signal is great enough to overcome antagonistic co-inhibitory signals may be swayed contextually by factors such as the relative availability of Ag/co-signaling molecules and the time frame of T cell stimulation (acute vs. chronic).

1.6 - Central Tolerance

As mentioned above, the inherent self-reactivity required for both positive selection and naïve T cell homeostasis brings with it the threat presented by overtly self-reactive T cell clones, as recognition of self can lead to auto-aggressive pathological immune responses. Thus, tolerance is a term that broadly encapsulates the processes that prevent these pathologies. During selection in the thymus, these processes fall under the umbrella term, central tolerance.

In the thymic cortex, thymocytes undergo apoptosis due to either a failure of positive selection (56) or clonal deletion following negative selection (57, 58). The large number of thymocytes that fall into the latter group suggests that the stochastic generation of TCR specificity is MHC-biased (57). Critically, negative selection to ubiquitous self-Ag (UbA) in this compartment is dependent on rare $CD11c^+$ dendritic cells (DCs) (22, 40). The rarity of this subset in the thymus may be counterbalanced by its high level of co-stimulatory and adhesion molecule expression. Indeed, DCs deficient in intercellular adhesion molecule 1 (ICAM-1) were less effective in facilitating thymocyte arrest and sustained signaling associated with negative selection (40).

How is tolerance established toward Ags whose expression patterns are limited to specific tissues? Earlier studies showed that an absence of T cell reactivity toward such Ags was associated with their ectopic expression in thymic tissue (59–63). Later it was revealed that a hallmark of the thymic medulla is the ectopic expression of tissue-restricted Ags (TRA) by medullary thymic epithelial cells (mTECs) driven by the promiscuous transcription factor autoimmune regulator (AIRE) (64–67). Following positive selection, thymocytes upregulate CCR7, which promotes migration to the medulla. CCR7 upregulation is thus critical for tolerance, since failure to enter the medulla means a failure of thymocytes to establish tolerance to TRA. Indeed, mice lacking CCR7 or CCR7 ligands develop tissue specific autoimmunity (68). Direct Ag presentation by mTECs induce deletion in both $CD8^+$ and $CD4^+$ SP thymocytes (allowable through endogenous MHCII loading) (69, 70), although neighbouring APCs can do so as well through cross-presentation. Additionally, the increased expression of the co-stimulatory ligands CD80/86 in both mTECs and medullary APCs (important for negative selection in both the cortex and the medulla (71)) is another feature defining the medulla as a compartment

specialized for negative selection. Following encounter with high affinity Ag during selection, there are several possible fates that thymocytes can take on. Thus far, I have primarily discussed clonal deletion, for which the pro-apoptotic molecule, Bim, is critical. However, while the following sections will not include exhaustive discussion of all possible fates after negative selection, I will touch on those that are pertinent to this thesis.

1.6.1 - Clonal deletion

Bim is a member of the BCL-2 family and mediates cell death via the intrinsic apoptotic pathway. Bim is important for clonal deletion in superantigen-mediated models (72), TRA-mediated models (73–75), and UbA-mediated models (74, 76). However, in UbA-driven models of deletion, Bim deficiency did not rescue the development of a mature population of SP thymocytes, suggesting that it is not deletion that enforces tolerance to UbA. Rather, the receipt of a high affinity TCR signal implies a failure to receive a positive selection signal (77), or alternatively, premature eviction from the thymus in the case of CD8 T cells (78). Meanwhile, TRA are expressed in the thymic medulla, requiring developing thymocytes to first undergo successful positive selection and migration before they can engage with these antigens (79). Given the differences in developmental stage and tissue locale during negative selection to these different modes of self-peptide presentation, it's not surprising to observe different kinetics and requirements for this process. A recent study has estimated that 78 % of thymocytes undergoing clonal deletion do so in the cortex (71), which is in agreement with previous studies (57, 80) and likely in part thanks to the fact that DP thymocytes are particularly sensitive to TCR stimulation (14, 81, 82). However, clonal deletion can still occur up until the mature SP thymocyte stage (71). Bim expression is positively regulated by JNK signaling, which coincides with JNK's importance to clonal deletion (83, 84). During low affinity TCR signaling, thymocytes may

employ unique biochemical pathways to hamper clonal deletion until the receipt of bona fide (high affinity) negatively selecting signals. Such pathways may involve Schnurri-2 (85) or NCoR1 (86), to dampen pro-apoptotic Bax activation or inhibit Bim expression, respectively.

1.6.2 - T regulatory cells

T regulatory cells (Treg) are a non-conventional T cell fate following negative selection – an example of agonist selection. Tregs generated in the thymus are referred to as thymic Tregs (tTreg). Characterized by the expression of the transcription factor Foxp3, they represent a mode of dominant tolerance, in which they suppress immune responses. Antigen-specific mechanisms for this purpose arise during the Treg:APC interaction and include the removal of pMHC complexes from presenting DC's surface through trans-endocytosis and the binding and downmodulation of co-stimulatory molecules (e.g. CD80/86) on Ag-bearing APCs. Some non-antigen-specific mechanisms include the production of anti-inflammatory cytokines and Treg surface enzymes CD39/CD73 leading to increased concentrations of adenosine in the local environment and subsequent inhibition of Ag presentation by DCs (87). High affinity TCR signaling induces the upregulation of CD25 (high affinity α-chain of the IL-2 receptor) – this generates a population of $CD25^{hi}$ $Foxp3^{-}$ Treg precursors which are destined to become full-fledged Tregs upon the upregulation of Foxp3 and the receipt of IL-2 signaling (88), likely provided by thymic DCs which are potent producers of the cytokine (89) (though Treg induction can lead to apoptosis if cytokine-mediated survival signals are not received (90)). This being said, there is evidence suggesting both TECs and bone marrow-derived APCs can drive thymic Treg development, thus it does not appear dependent on a dedicated APC (91). Rather, the generally cytokine- (IL-2 and IL-15) and co-stimulatory molecule-rich environment of the

medulla robustly support Treg development, providing rationale for the observation that the majority of thymic Tregs develop in the medulla (88, 92).

1.6.3 - Anergy

The establishment of a functionally unresponsive or hypo-responsive state in autoreactive T cells is known as anergy, which is an alternate fate for thymocytes following high affinity Ag encounter. This state is defined by a cell-autonomous inability to respond to subsequent activation with proliferation, differentiation, or effector function (93). Generally, anergy is associated with inhibited activation of TCR signaling molecules such as Ras and ERK, downregulated expression of critical signaling participants such as ZAP70, and in some MHCI-restricted models the downregulation of CD8 and the TCR (94). Transcriptional activation of anergy-associated genes such as *Cbl-b* by Egr2/3 (95, 96) or nuclear factor of activated T cells (NFAT1) is thought to provide a basis for reduced TCR signaling capacity in anergic cells, as ubiquitylation by Cbl-b tags signaling molecules for lysosomal degradation (97, 98). This mode of T cell tolerance has largely been investigated for its induction in peripheral tissues, although early studies showed that HY TCR Tg thymocytes that escape clonal deletion and circulate in the periphery are unresponsive to HY Ag (99, 100). Later studies have additionally provided evidence for the induction of this state in the thymus in superantigen, polyclonal, and Tg TCR models (93, 101–103). However, the contribution of anergy to central tolerance remains under-appreciated.

1.7 - Peripheral tolerance and states of T cell dysfunction

Mechanisms of central tolerance are not perfectly effective, especially considering that not all self-Ags are efficiently presented in the thymus. Thus, peripheral mechanisms work to both maintain the tolerance established during in the thymus, as well as establishing *de novo*

tolerance in the periphery to – for example – self-Ag presented inefficiently during selection or sequestered in immunologically privileged tissues. Peripheral tolerance thus also stands as an obstacle to desirable T cell responses to such threats as tumours or chronic infections, which are known to promote T cell dysfunction. In this section, I will discuss T cell-intrinsic dysfunction, which can be classified under the terms tolerance, exhaustion, and anergy. For the sake of brevity, this section will only touch on mechanisms of peripheral tolerance relevant to this thesis. It is a complex task to categorize and distinguish putatively different T cell states that are ultimately unified by hypo-responsiveness and altered activation. The distinction between these states is subtle and usually depends on 1) the circumstances under which the state was acquired, 2) the implications and associations attached to the experimental model used to assay the functional state in question, and 3) the phenotypic features. The last point (phenotypic features) includes functional, epigenetic, and transcriptional characteristics; the difficulty with categorizing on these grounds comes from the fact that each term for T cell dysfunction likely embodies multiple discrete biochemical forms of unresponsiveness.

1.7.1 - Peripheral deletion

Deletion can occur in the thymus during T cell development as well as in the periphery. In the latter compartment, Bim mediates peripheral deletion alongside the extrinsic pathway of apoptosis activated by death receptors such as Fas/FasL (77). Bim induces apoptosis through permeabilization of the outer mitochondrial membrane through Bax/Bak, and is thought important for the contraction of T cell responses following acute infections. Fas (also CD95) is a death domain-containing receptor that when stimulated by its ligand FasL, trigger the deletion of T cells that repeatedly experience TCR stimulation *in vivo* (104, 105), in an apoptosis pathway termed activation-induced cell death (AICD).

1.7.2 - Anergy

Anergy as a concept was originally divided into two main categories: clonal anergy and adaptive tolerance. Clonal anergy is thought to be induced *in vitro* in $CD4^+$ T cells following incomplete activation, which may occur with the following stimuli: strong TCR stimulation without co-stimulation or by weak TCR stimulation in the presence of co-stimulation. Cells in this state fail to proliferate but can still produce low levels of effector cytokines upon subsequent TCR stimulation. Co-stimulation through CD28 is canonically a critical factor in preventing the induction of anergy, but the mechanism by which this occurs is not certain. Co-stimulation may prevent the induction of anergy-driving inhibitory factors that restrain T cell function (such as CTLA-4) or via influence on the cell-cycle by promoting the production of growth factors (such as IL-2) (93). For example, when mTor (which coordinates progression through the cell cycle) activity is inhibited, anergy ensues (77). Indeed, the provision of exogenous IL-2 is known to rescue clonally anergic T cells from this state *in vitro*. *In vitro*, cyclosporine A (a calcineurin inhibitor) was shown to prevent the induction of anergy (106). The calcium/calmodulin/ calcineurin pathway activates and causes the nuclear translocation of NFAT1, and the activity of this transcription factor is thought to be critical for the establishment of the anergic state (93, 107).

Adaptive tolerance is, in contrast to clonal anergy, characterized by studies using *in vivo* models for both $CD8^+$ (108, 109) and $CD4^+$ T cells (110, 111). Early experiments involved the adoptive transfer of $CD8^+$ male antigen-specific female HY TCR transgenic T cells into athymic male recipients (108). Following rapid expansion in these recipients, transferred cells declined in numbers until the remaining T population was unresponsive to *in vitro* re-stimulation. Thus, a key difference in this case with *in vitro* anergy is whether the T cells in question have been

previously activated. However secondary transfer to Ag-free female recipients resulted in functional rescue, suggesting that persistent exposure to Ag is required to maintain this dysfunctional state (109). In contrast to clonal anergy, the *in vivo*-induced state termed adaptive tolerance is not thought to be reversed by the addition of exogenous IL-2 (93).

Despite the detailed characterization of clonal anergy and adaptive tolerance by early studies, these terms are not strictly adhered to in more recent studies; the umbrella term "anergy" will thus be used in this thesis to describe T cell-intrinsic functional hypo-responsiveness induced in lymphocytes following encounter with high affinity Ag under sub-optimal stimulation conditions (broadly this takes the shape of stimulation in the absence of co-stimulation, which may be incited by inadequate $CD4^+$ T cell help) (93, 94). I wish to briefly address the position held by some that anergy and tolerance are not equivalent terms due to differences in functional characteristics, transcriptional signatures, and reliance on persistent Ag to maintain the impaired state (112, 113). As a counter to this view, the studies taken as examples often compare T cell function between models in which impairment has been induced by widely different means and compared between both MHC I- and MHC II-restricted T cells. For example, some methods include *in vitro* impairment by treatment with ionomycin, soluble Ag encountered in blood or in the intestine (oral tolerance), or Ag encountered in the thymus during selection (112–115). For the purposes of this thesis, we will take the position that anergy is a mechanism of tolerance that manifests following high affinity TCR signaling under tolerogenic conditions (e.g. without co-stimulation), and that this state is characterized by the inability to produce cytokines *in vitro* or respond with proliferation when stimulated under optimal conditions, expression of co-inhibitory receptors (e.g. PD-1), and the reliance on persistent Ag exposure to maintain the dysfunctional state. With this being said, whether continuous exposure to Ag is unconditionally required to

maintain dysfunction is not absolute, as although evidence collected by our group and others supports this idea (109, 112, 113, 116–118), work done in a tolerance model using TCR_{GAG} transgenic T cells in Alb:GAG mice (115) showed that T cell dysfunction can be reacquired or persist even in the absence of high affinity Ag. Among other proposed methods for overcoming T cell dysfunction is the induction of proliferation (e.g. by *in vitro* exposure to IL-15 (119) or by provoking lymphopenia-induced proliferation (115)).

In a model where glucose-6-phosphate isomerase (GPI; a UbA) -reactive KRN TCR Tg $CD4^+$ T cells were adoptively transferred into Ag-expressing lymphoreplete recipients, Ag-specific T cells upregulated two novel markers that came to characterize a form of $CD4^+$ T cell anergy – FR4 and CD73 – and this process was dependent on the presence of $Foxp3^+$ Tregs (120). Once re-isolated, $FR4^{hi}$ $CD73^{hi}$ $CD4^+$ T cells failed to proliferate upon introduction into secondary Ag-harbouring lymphoreplete hosts, while non-anergic controls underwent multiple rounds of division. Folate receptor 4 (FR4) is thought to be important for folic acid uptake and the maintenance of Tregs, as their numbers are reduced *in vivo* when FR4 is blocked (121); it may serve a similar purpose for $FR4^{hi}$ $CD73^{hi}$ $CD4^+$ anergic T cells. CD73 is an adenosine-generating ecto-5'-nucleotidase which is associated with the suppression of T cell effector function (122).

Despite the established functional and genomic characteristics for anergy, it is likely a dynamic and heterogenous state (115, 123, 124). Co-inhibitory receptors restrain T cell responses following Ag encounter, representing a "checkpoint" in T fate and function. Checkpoint blockade is a therapeutic strategy popularized in recent years designed to promote immune cell function by the administration of co-inhibitory receptor-specific blocking antibodies. An anergic population changes over time in its mobilizability in response to this treatment; for example, recent

proliferation is thought to correlate with sensitivity to blockade (125). Thus, despite established dysfunction, previously tolerant cells can be induced to mediate anti-tumour responses. The degree to which function is thenceforth maintained may be limited by epigenetics (115). The way in which anergic populations may be programmed for heterogeneity is by the kinetics of the inciting TCR signal (upon establishment of anergy), which is discussed in the next section.

1.7.3 - Exhaustion

Normally, during the course of an acute infection, naïve T cells encounter foreign Ag, become activated and expand. Their differentiation into cytotoxic effector T cells leads to the control and clearance of the pathogen in question, after which point Ag-specific T cell populations contract and leave behind differentiated memory T cells that will respond upon secondary infections. In the case of chronic exposure to foreign Ag associated with either chronic viral infections or persistent populations of tumour cells, this normal course of T cell activity is thought to deviate into a state of hypo-responsiveness termed exhaustion (126). Exhaustion is characterized by heightened expression of co-inhibitory receptors (e.g. Lag-3 and PD-1) and progressive, hierarchical loss of effector function (proliferation, IL-2 production, TNF-α production, then IFN-γ production) following initial activation and subsequent chronic Ag stimulation (127).

Exhaustion and anergy/tolerance share some features, such as the upregulation of genes associated with reduced immune function such as *Lag-3* and *Pdcd1*, the downregulation of genes associated with effector function such as *Ifng,* and altered expression of master transcription factors such as *Eomes* and *T-bet* (112, 115). Exhaustion is usually distinguished from tolerance or anergy by the assumption that it manifests following normal activation and subsequent chronic TCR signaling, whereas in the cases of tolerance and anergy, initial activation is thought not to

be achieved (126). The first and classic model for T cell exhaustion (T_{EX}) is in the context of chronic LCMV clone 13 infection, which is typically contrasted with acute LCMV Armstrong infection. Differences between the transcriptional profiles of functional T effector/memory (T_{EFF}/T_{MEM}) populations with the dysfunctional T_{EX} manifest several weeks post-infection (128, 129). Further, in the first week of infection with LCMV clone 13, virus-specific T cells retain the potential to differentiate into functional memory cells after transfer into infection-free recipients (though this ability is lost between 2 and 4 weeks post-infection) (130).

T cell exhaustion is thought to be a plastic, adaptive state rather than a simple failure to respond: a compromise between clearance of a pathogen or transformed tissue and immunological pathology (131). Indeed, the surge in viremia (132, 133) following $CD8^+$ T cell depletion and development of viral escape mutants (134) in the context of chronic infections suggests that "exhaustion" is a state of functional hypo-responsiveness instead of unresponsiveness. Additionally, the exhausted T cell population is thought to be comprised of at least two subpopulations, T_{PEX} and T_{EX}. Progenitor (T_{PEX}) exhausted T cells are a stem cell-like population that shares features with both early exhausted T cells (impaired cytokine production and increased expression of inhibitory receptors such as PD-1) as well as memory T cells (increased expression of TCF1 and long-term self-renewal (135–138)) (139). The dynamic balance between these two subpopulations over time is thought to determine the severity of T cell exhaustion (140), as the T_{PEX} subset has been associated with superior anti-tumour activity (141, 142).

1.8 - Selection of tolerant fates

It is currently held that while clonal deletion is the primary fate that follows very high TCR stimulation during development, the non-deletional fate of agonist selection may be more

likely to occur following TCR stimulation with an affinity near the threshold for negative selection (47).

1.8.1 - CD8$^+$ T cell anergy

The OT-I TCR transgenic, for example, recognizes chicken ovalbumin (OVA) with high affinity, and clonal deletion is thus efficient when OT-I thymocytes develop in the presence of OVA (69). In contrast, the OT-3 transgenic (Tg) TCR recognizes OVA with moderate affinity, and induces less efficient clonal deletion under similar circumstances (123). In cases of escape from clonal deletion by T cell clones of TCR affinity near the negative selection threshold, tolerance is maintained at steady state, but reversed upon immunization or infection, suggesting these clones both 1) represent a greater risk for autoimmunity, and 2) are nevertheless restrained by tolerance (47).

In studies using male Ag-reactive Tg mature CD8$^+$ T cells , it has been proposed that anergy is induced following exposure to high concentrations of high affinity Ag under steady-state conditions, while clonal deletion is induced by low concentrations of the same Ag (94). Indeed, a recent study showed that NDFIP1 (a HECT-type ubiquitin ligase activator) was required for mature OT-I Tg T cells to become anergic upon transfer to recipients containing high doses of high affinity Ag OVA, but was dispensable for their deletion in the periphery in response to low OVA concentrations (143); this provides a potential molecular basis for diverging T cell fates following strong TCR signaling under tolerogenic conditions. Indeed, what exactly constitutes “low” and “high” doses of Ag under these circumstances is relative, and the distinction is likely not bimodal, instead existing on a spectrum. It has been proposed that the fates anergy and peripheral deletion are differentially favoured and sustained based on both Ag dose as well as Ag persistence, suggesting both are plastic and not “all or nothing” processes.

Acute exposure to low doses of Ag results in incomplete deletion and the preservation of putatively self-reactive T cell clones, which may later acquire effector function or experience further rounds of deletion, depending on the circumstances of subsequent Ag encounter (144). Work done using a similar model, wherein naïve OT-I T cells become unresponsive following transfer into iFABP-OVA Tg recipients, showed that anergic cells were resistant to reinvigoration by checkpoint blockade (PD-1- and other molecules were targeted). Strong Ag stimulation and ensuing proliferation during infection (with VSV-OVA) accompanied renewed sensitivity to anti-PD-1 blockade, further suggesting anergy is a plastic state (125). However, the degree to which the affinity of the TCR signal upon first encounter with high affinity Ag informs the plasticity of the anergic state is still unclear.

1.8.2 - $CD4^+$ T cell anergy

Currently, the strength of the TCR signal required to induce anergy in $CD4^+$ T cells is a contentious matter. In HA-reactive $CD4^+$ mature T cell clones, anergy has been shown to be induced by low avidity TCR engagement with pMHC if co-stimulation is provided *in vitro* (145), or by short-lived TCR engagement (although in this case, anergy was short-lived (~7 days)) *in vitro* and *in vivo* (146). Conversely, relatively highly self-reactive naïve ($CD44^{lo}$ $CD62L^{hi}$) Nur77-GFP^{hi} $Ly6c^-$ $CD4^+$ T cells in polyclonal mice demonstrate hypo-responsiveness and phenotype consistent with the anergic state, suggesting strong basal or "tonic" TCR signaling can also contribute to not only genuine anergy, but also anergy-like features within the heterogeneous peripheral naïve $CD4^+$ compartment (147). Skokos *et al.* showed using the MHCII-restricted AND TCR Tg, peptide ligands of low, moderate, and high affinity induced a hypo-responsiveness state in the absence of inflammation *in vivo*. However, only interactions with high affinity Ag resulted in Ca^{2+} flux and T cell migratory arrest. This suggests that not only can

a spectrum of TCR signals induce $CD4^+$ T cell anergy, but the divergence of the biochemical pathways engaged may underlie heterogeneity in hypo-responsive programs induced in different models (148) – the functional consequences of this prospect remain to be explored.

1.8.3 - Treg development

The functional avidity required to induce anergy may be similar to that required to induce Treg development. That is, the strength of the TCR signals that lead to Treg selection fall near the threshold for negative selection (73). Thus, how the decision between anergic and Treg fates is made is likely based on cytokines and stimuli from the extracellular milieu, however this question has not been directly addressed. Yet, there is also a growing appreciation for an interdependence between these fates (149), as – for instance – the adoptive transfer of peripheral anergic $Foxp3^-$ $CD44^{hi}$ $FR4^+$ $CD73^{hi}$ $CD4^+$ T cells into lymphopenic *Tcra*$^{-/-}$ mice results in their trans-differentiation into $Foxp3^+$ Tregs (150). Nevertheless, in addition to the cytokine and co-stimulation requirements for efficient Treg selection mentioned above, generally, strong TCR signaling is thought to favour Treg development. For example, the efficiency of Treg generation was directly correlated with TCR affinity for a fixed amount of a single model self-Ag in the thymus (151). The efficiency of Treg selection is thus thought to be a function of TCR affinity as well as other environmental cues such as availability of pMHC complexes (i.e. TCR avidity) (47). Indeed, there is evidence to suggest that the stochasticity involved in this selection process may influence the developmental programs, genomics, and functionality of the resulting Tregs. In the thymus, stronger TCR signals supported development through $CD25^+$ intermediates and produced Tregs that were protective against experimental auto-immune encephalitis (EAE) (and experienced higher rates of apoptosis), while weaker TCR signals supported development through $Foxp3^{lo}$ intermediates (152). Greater self-reactivity (inferred by $Nur77^{hi}$, $CD5^{hi}$, and/or

Ly6c^{lo} phenotype) has also been associated with enhanced suppressive activity *in vitro* and *in vivo* in other studies. In general, greater self-reactivity correlates with more efficient Treg selection in both the thymus and periphery (47). While early studies in tolerance to orally- or intravenously-administered Ag suggested that low Ag concentration preferentially induced Treg (peripheral, pTreg), higher concentrations preferentially induced anergy (47). More recently, studies using the BDC2.5 TCR Tg model (153) and the 5C.C7 TCR Tg model (154) cumulatively provided evidence to suggest that low doses of high affinity Ag is ideal for inducing pTreg development *in vitro* and *in vivo*. However, this ideal zone is thought to be flexible in the presence of cytokines (e.g. TGFβ) and CD28 co-stimulation (47).

Given that Treg development is dependent on strong TCR signals, it should come as no surprise that this process is closely tied to that of clonal deletion. Indeed, the induction of Foxp3 reflects only a step toward the Treg lineage and cells require subsequent IL-2 signaling for their confirmation into the lineage (discussed in the previous sections). Foxp3 induction has been proposed as a stepping-stone to late thymocyte deletion (71), as Foxp3 has been shown to induce a pro-apoptotic signature that was counteracted by common γ-chain (γc)-dependent cytokine signaling, resulting in the deletion of "failed" Tregs – those that failed to received cytokine-mediated survival signals (90). Why individual autoreactive T cell clones assume one fate versus another may be a matter of the spatial and temporal manner in which signals are received, at least in the thymus. As was mentioned briefly in the previous sections, the bulk of clonal deletion occurs in the cortex, while the bulk of Treg development occurs in the medulla. Indeed, two studies using pMHCII tetramer-based enrichment to observe the fates of Ag-specific polyclonal CD4^{+} thymocytes when high affinity neo-self Ag was encountered as ubiquitous (cortical) or tissue-restricted (medullary) (102, 103). Ubiquitously expressed neo-self Ag expression resulted

in the loss of Ag-specific CD4SP thymocytes, indicating efficient clonal deletion. Neo-self Ag expressed as a TRA resulted in enhanced tTreg generation rather than deletion. Cumulatively, the different physiological features of the cortex and medullary compartments are thought to provide contexts that favour one fate over another: where encountered Ag is interpreted differently due to the developmental stage of thymocytes therein (DP vs. SP), kinetics of Ag presentation, and environmental cues such as co-stimulatory molecule expression (155).

1.8.4 - Exhaustion

The term exhaustion was originally used to described T cell dysfunction in the context of chronic infection by LCMV clone 13, but later studies came to include dysfunctional anti-tumour responses (126). Overall, exhaustion is considered a form of dysfunction exclusive to the periphery. Similarities exist in exhausted T cells from chronic infection and those infiltrating tumours such as the co-expression of multiple co-inhibitory receptors (such as PD-1, Lag-3, and Tim-3), impaired cytokine production, and cytotoxicity, however the hierarchy of progressively lost functions has been a challenge to describe in tumour-specific response as they evolve across time and tissues (156). Additionally, although both cancer and chronic infections are thought to generate T_{EX}, how these circumstances do so is distinct. An anti-tumour response must often contend with tumour (self) Ag that contributed to central and peripheral tolerance; thus, lower affinity clones are likely favoured within the pool of tumour-reactive T cells. As was mentioned earlier, exhaustion is typically defined as dysfunction that manifests following a stage of initial activation and response, in contrast to tolerance and anergy, where full initial activation is not canonically thought to occur (126). Importantly, anti-tumour T cell responses destined for exhaustion are likely primed under immunosuppressive conditions (in the absence of inflammation, the presence of Tregs, or secreted inhibitory factors by tumour cells such as TGF-

β and IL-10) (156), in which case initial activation may be precluded. Thus, while the difference between exhaustion and anergy are canonically defined by the circumstances of their induction, how rigidly models for these processes adhere to their defined categories is a matter that requires further examining.

1.9 - Programmed cell death protein-1 (PD-1)

Co-stimulatory and co-inhibitory receptors participate in activation, differentiation, and ongoing function of T cells as they respond to foreign Ag, providing them with information the immunological state of the local environment and shaping cellular behaviour (reviewed in (157)). The co-inhibitory receptor programmed cell death protein-1 (PD-1) is thought to play a role in restraining initial T cell activation and in altering T cell differentiation and effector function to restrict immunopathology in the context of infections, anti-tumour responses, and autoimmunity (158). However, its role in central tolerance is currently unclear.

PD-1 is a surface glycoprotein part of the immunoglobulin (Ig) super family, containing an Ig Variable-type N-terminal extracellular domain, a transmembrane domain, and a cytoplasmic domain containing an immunoreceptor tyrosine-based inhibitory motif (ITIM) and an immunoreceptor tyrosine-based switch motif (ITSM) (159). PD-1 expression is induced in T and B lymphocytes following Ag receptor engagement (160). Following T cell activation, PD-1 can be upregulated within 24 hours and is generally thought to persist at the cell surface according to persistent Ag stimulation; however, it can also be induced on other immune subsets (e.g. NK cells, macrophages, some dendritic cell subsets) (158). There are two known ligands for PD-1: PD-L1 and PD-L2. PD-L1 is widely expressed in cells of hematopoietic origin (e.g. T cells, B cells, macrophages, dendritic cells) as well as non-hematopoietic origin (e.g. vascular and stromal endothelial cells, pancreatic islets, and keratinocytes). Importantly, there is

heightened PD-L1 expression in tissues of immune-privilege like the placenta and eye (158). PD-L2 expression is limited to dendritic cells, macrophages, and B cells (161) and PD-L2 binds PD-1 with higher affinity and differential kinetics compared with PD-L1:PD-1 (162). Ligands PD-L1/2 have also been shown to interact with other cell surface molecules aside from PD-1. PD-L1 interacts with co-stimulatory ligand CD80 in *cis*, which may disrupt PD-1:PD-L1 binding in *trans* (reviewed in (163)), and PD-L2 binds with repulsive guidance molecule-b (RGMb) expressed by T cells and APCs, the interaction between which is important for tolerance in the respiratory tract (164). The functions of the two PD-1 ligands are thought to largely overlap, with the exception of some evidence pointing toward minor unique modes for the ligands (158). Although the expression of both PD-L1 and PD-L2 is induced by inflammatory stimuli, given the more widespread expression of PD-L1, its relevance is more likely to be observed across a diversity of models such as allograft acceptance and most cancers (161).

1.9.1 - Molecular mechanism for dampening the TCR signal by PD-1

When PD-1 is engaged by either of its ligands, it has been shown to inhibit both signaling proximal and downstream of the TCR (Fig. 1.9.1-1). The ITSM in the cytoplasmic tail of PD-1 becomes phosphorylated by primarily by LCK but also other kinases proximal to the TCR (165) and the phosphatase SHP-2 (and to a lesser extent, SHP-1) is recruited, which then attenuates TCR signal propagation by dephosphorylating participants in the TCR signalosome (166). Overall, this serves to antagonize pathways including PI3K, AKT/mTOR, RAS/ERK, Vav1, and PLCγ, and this leads to decreased T cell activation, proliferation, survival, and function (161). In contribution to this effect, engagement of PD-1 is thought to inhibit both signals stemming from the co-stimulatory receptor CD28 (165) as well as the TCR itself (167). Additionally, a study examining *in situ* kinetics of the P14 Tg TCR engaging with LCMV epitope gp33-41 presented

by H2-D^b provided evidence to suggest that PD-1 may limit T cell Ag recognition by restraining the mechanical cooperativity between TCR and CD8. This effect was dependent on SHP and LCK activity, and resulted in fewer and shorter interactions between TCR and pMHC (168).

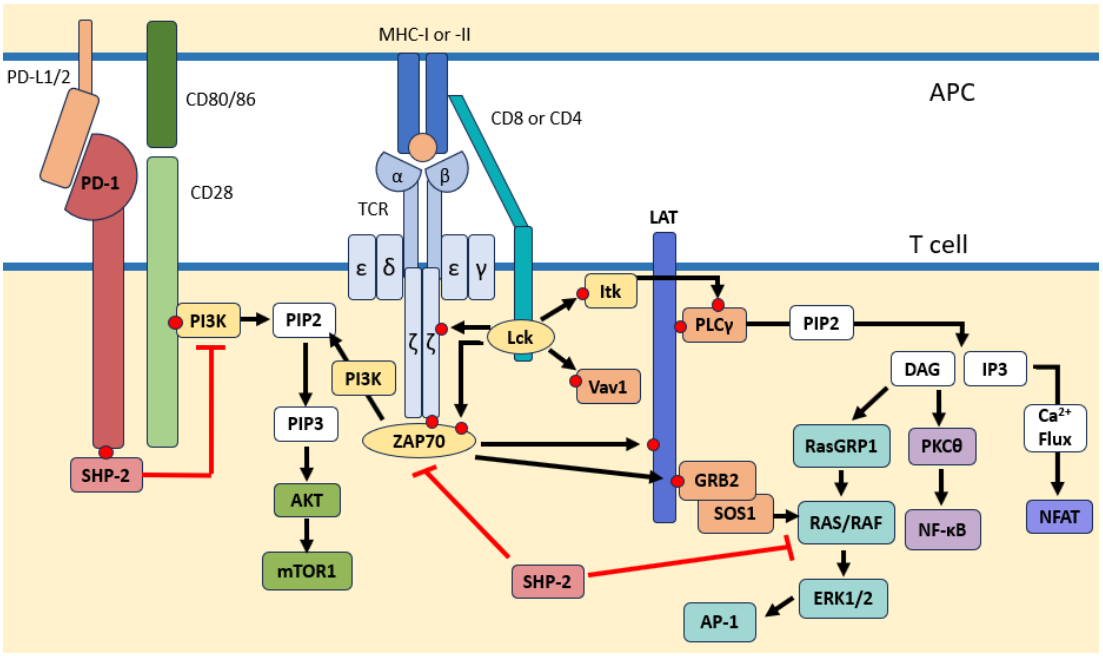

Figure 1.9.1-1: PD-1 regulates signaling downstream of the TCR and CD28.

The TCR signal is propagated when TCR recognizes peptide presented in the context of MHC (pMHC, class I or II) (31). LCK associated with coreceptors (CD8 or CD4) is localized to the TCR signalosome at the time of cooperative binding of pMHC by both TCR and coreceptor, and then phosphorylates the ITAM motifs in the CD3 subunits. ZAP70 is then recruited to the resulting phosphorylated sites and is itself activated by phosphorylation by LCK. ZAP70 phosphorylates transmembrane adaptor protein linker for activation of T cells (LAT), providing

docking sites for many other adapters and effectors in the signaling cascade. PLCγ1 is recruited to LAT and activated, after which it acts on phosphatidylinositol-4.5-bisphosphate (PIP2) and catalyzes the production of diacylglycerol (DAG) and inositol (1,4,5)-trisphosphate (IP3) that lead to Ca^{2+} flux, the recruitment and activation of Ras guanyl-releasing protein 1 (RasGRP1), and protein kinase C (PKCθ), which activate the nuclear factor of activated T cells (NFAT), mitogen-activated protein kinase (MAPK/ERK)/AP-1, and NF-κB pathways, respectively. These pathways cooperate to control T cell proliferation, migration, differentiation, and effector function. Co-stimulation through CD28 engagement with CD80/86 recruits phosphatidylinositol 3-kinase (PI3K) (associated with the CD28 cytoplasmic domain) to the TCR signalosome. PI3K phosphorylates PIP2 to generate phosphatidylinositol (3,4,5) triphosphate (PIP3), which regulate the recruitment and activation of AKT. AKT activates mechanistic target of rapamycin (mTOR), whose activity is important for the energetic demands of cell division (169).

1.9.2 - PD-1 function

As was mentioned above, PD-1 expression is induced upon activation in T cells and regulates the magnitude of their initial response, function during the effector phase, and the differentiation and recall of memory T cells (161). For example, while primary Ag encounter (presented by resting DCs) induces tolerance in $CD8^+$ T cells, PD-1 deficiency instead can transform this interaction into one of productive priming (170). In a study using 2-photon intravital microscopy, it was found that the period during which effector T cells arrest their migration and secrete cytokine (namely, IFN-γ) following Ag stimulation was prolonged by PD-1 blockade, which the authors interpreted to mean that PD-1 participates in a mechanism for shaping the magnitude of effector responses according to the amount of Ag present in an

inflamed tissue (171). Additionally, the differentiation, identity, and capacity for recall in $CD8^+$ memory T cells were shown to be influenced (and restrained) by PD-1 signaling during viral infection (172, 173).

Numerous roles have been proposed for PD-1 in the diverse processes across the T cell lifetime. During development, the threshold for positive selection is thought to be regulated by PD-1 signaling (174, 175). Earlier studies identified PD-1 expression on DP thymocytes undergoing negative selection in the HY^{cd4} UbA model system (176), but subsequent investigations revealed PD-1 was not required for negative selection in that model (177). Additionally, previous work in our lab determined that PD-1 is required for tolerance in the OT-$I^{-/-}$ > RIP-mOVA TRA model system, but was not required for clonal deletion (116). Beyond this, the body of information available on contributes to tolerance in the thymus is otherwise limited. In addition to being expressed in activated cells, PD-1 is upregulated under steady state conditions in memory T cells, tolerant T cells, Tregs, and some myeloid cells (161). Indeed, PD-1 is well known for its role in autoimmunity. PD-1 deficiency is associated in the C57BL/6 and BALB/c mouse strains with autoimmune glomerulonephritis and cardiomyopathy, and with accelerated disease in autoimmune-prone strains such as the non-obese diabetic strain (NOD), other disease models such as experimental autoimmune encephalomyelitis (EAE) and autoimmune enteritis (161, 166). It was also shown that PD-1 was important for establishing peripheral tolerance, since recent thymic emigrants (RTE) (originating from transplanted HSC in bone marrow chimeras) or adoptively transferred thymocytes (into lymphopenic recipients) lacking PD-1 mediated multi-organ inflammatory disease; in contrast, PD-1 was not required for tolerance in established mature T cells in the same adoptive transfer model (177). Low affinity tonic pMHC encounter is sufficient to induce the upregulation of PD-1 on T cells undergoing

lymphopenia-induced proliferation (LIP) and the combination of the lack of PD-1 and lymphopenia synergize to precipitate autoimmunity (178). PD-1:PD-L1 signaling has been reported to promote pTreg differentiation, maintenance, and function by enhancing and sustaining Foxp3 expression (179–181). However, in a Treg-specific PD-1 conditional knock-out model (Foxp3^{cre} Pdcd1$^{fl/fl}$), PD-1 was in contrast shown to inhibit Treg activation and function (182); similar results have been observed in other mouse models, and higher PD-1 expression in human Tregs has been associated with reduced suppressive capacity (reviewed in (183)).

PD-1 has primarily received interest in the literature for its role as a mechanism exploited during chronic infections and cancers for immune evasion. PD-1 was first associated with T cell exhaustion in the context of chronic LCMV infection, where it was found upregulated on dysfunctional T cells, and that *in vivo* blockade of the ligand PD-L1 enhanced virus-specific proliferation, cytokine production, and cytotoxicity (184). Since then, PD-1 has emerged as a forerunner candidate for immunotherapeutic targeting for the purpose of overcoming T cell exhaustion in clinical contexts (126, 161). However, despite great clinical efficacy in treating various human cancers, in more than a decade of application (185), most patients do not experience complete responses. Some experience failed responses to primary treatments and others relapse after a period of initial response (186). Among the roadblocks in the success of PD-1-targeting blocking therapies is the apparent importance of timing in the function of PD-1. In iFABP-OVA mice, adoptively transferred OVA-specific OT-I T cells encounter high affinity Ag in the small intestine and are rendered nonresponsive, but this tolerance was overcome with PD-L1 blockade (or PD-1 germline deficiency) when the treatment was administered the day of adoptive transfer (187), but not 30 d later (188). In the NOD model, blockade of PD-1 was more effective in precipitating autoimmunity in older compared with younger prediabetic NOD mice

(189). Additionally, it was recently shown that PD-1 blockade enhanced both responses by PD-1$^+$ CD8$^+$ T cells as well as immunosuppression by PD-1$^+$ Tregs, and that the relative frequencies of these populations was predictive of therapy success, which complicates predictions for blockade outcomes (190). Another roadblock in PD-1-targeting immunotherapies is the development of immune-related adverse events (IRAE) that have been observed to occur, with especially high rates in PD-1:CTLA-4 combination therapies (161). The mechanism by which these conditions manifest remains largely mysterious, but is likely complex given the multitude of circumstances wherein PD-1 is upregulated and influencing TCR signaling, as is discussed above. Lastly, PD-1 is not required for exhaustion, and some dysfunctional features have been shown to be in fact exacerbated in its absence; during chronic LCMV infection, the absence of PD-1 on CD8$^+$ T cells resulted in the accumulation of terminally differentiated T_{EX} (191). Immediate overstimulation and proliferation in the absence of PD-1 was associated with improved cytotoxicity and localization of T_{EX}, but at the expense of the long-term stability of the T_{EX} response. These data suggested that PD-1 functions to balance excessive activation with the longevity of the TEX population. Collectively, these data indicate that PD-1 contributes to the regulation of T cell function following both low and high affinity TCR signaling, underscoring the importance of PD-1 for regulating responses to the ambient and dynamic milieu perceived by the TCR when encountering both foreign- and self-Ag.

1.10 - Capicua

1.10.1 - CIC: Origin, structure, and regulation

Capicua (CIC) was first identified in *Drosophila* as a transcriptional repressor of genes downstream of the receptor tyrosine kinase (RTK) pathway, and is involved in the regulation of embryogenesis (192, 193). Earlier studies in *Drosophila* additionally provided evidence for the

CIC as a direct target of RTK signaling activation and phosphorylation, which promotes the cytoplasmic localization and degradation of CIC, releasing the repression of CIC transcriptional targets.

Two isoforms exist for CIC in *Drosophila* as well as humans and mice: the short form (CIC-S) and the long form (CIC-L), the difference between the two being a long form-specific N terminal region (194). CIC functions as a negative regulator of RTK signaling (e.g. signaling through epidermal growth factor receptor, EGFR) by binding octameric TGAATGAA-like motifs in the promoters and enhancers of RTK-responsive genes via cooperative activity between two evolutionarily conserved regions, an HMG-box and a separate conserved motif (C1) (193, 195). Regulation of CIC activity is summarized in Figure 1.10.1-1. The RTK-RAS-MAPK pathway has been shown to suppress CIC activity (expression level and nuclear localization by EGFR signaling (196–198). The c-Src and the MAPK ERK were specifically implicated in this regulation, evidence for the latter case stemming a study using chemical MEK1/2 inhibitors (199, 200). CIC is thought to be degraded in the nucleus following ERK signaling (197), but whether this can additionally occur in the cytoplasm of mammalian cells has not been demonstrated. Additional points of regulation for CIC include long noncoding RNA-mediated repression of CIC expression (201) and ATXN1/1L interaction and stabilization of CIC (194). CIC expression is widespread across murine tissues, which is reflective of its diverse roles; however, importantly for this study, CIC expression is also substantial in thymic tissue (202–204) and specifically in lymphocytes (205).

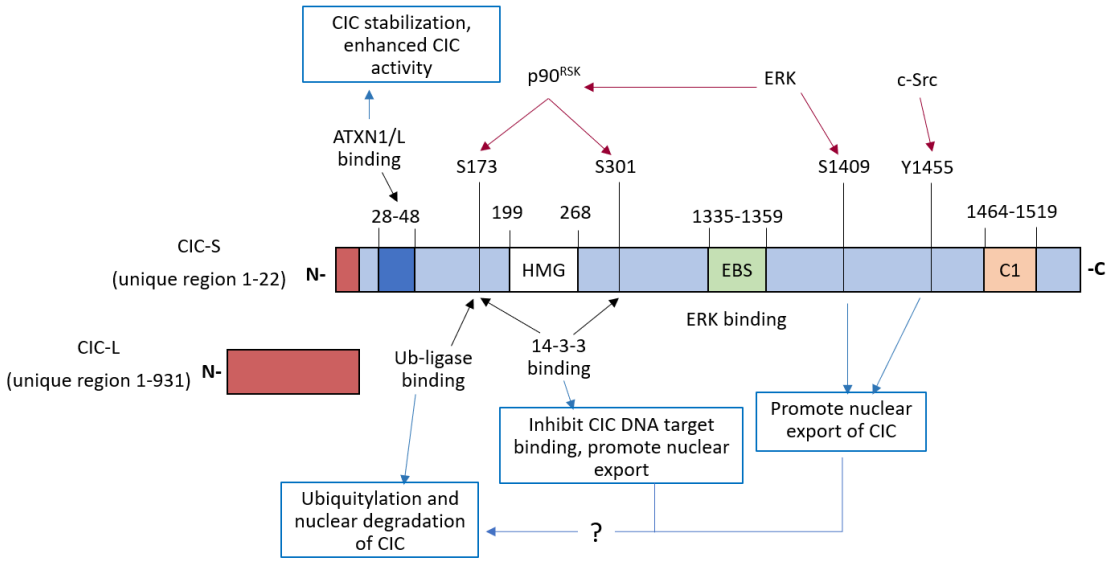

Figure 1.10.1-1: Capicua structure and regulation**.**

Schematic illustration of (mammalian) isoforms CIC-S and CIC-L, which differ at the N-terminus. Work in human cell lines demonstrated that EGFR signaling leads to the phosphorylation of CIC at multiple serine and threonine residues by ERK and ERK-activated $p90^{RSK}$ kinase activity. Phosphorylation of serine 173 allows for association with 14-3-3, which is thought to inhibit CIC binding to target DNA sequences (206) and mediate its nuclear export (207). ERK binds CIC at residues 1335-1359 (208), and phosphorylate serine 1409, which is thought to mask the nuclear localization sequence of CIC and inhibit its activity through nuclear exclusion (206). C-Src kinase phosphorylates tyrosine 1455, which also leads to cytoplasmic translocation (200). P-S173 provides a platform for E3 ligase binding, CIC ubiquitylation and proteasomal degradation (197). ATXN1 and homolog ATXN1L bind CIC residues 28-48 and stabilize CIC (194, 202), rendering it less sensitive to proteasomal degradation (209). Black arrows indicate noncovalent binding. Red arrows indicate enzymatic activity. Blue arrows indicate functional impact.

1.10.2 - General CIC function

In mammals, mutations and deficiency in CIC has been shown to be linked to numerous disease states, developmental defects, and disruption of the homeostasis of various systems: alveolar and central nervous system development, embryogenesis, neuronal cell differentiation. Indeed, germline deficiency of CIC results in embryonic or perinatal lethality (with incomplete penetrance) in mice associated with defects in lung alveolarization (204). Beyond *Drosophila*, CIC is conserved from *C. elegans* to mammals, and also acts as a tumour suppressor in the context of various cancer types (193). CIC target genes implicated in its role in cancer progression are oncogenic transcription factors *ETV1, ETV4,* and *ETV5* (193). CIC has been identified as a clinical biomarker for human lung and gastric adenocarcinoma progression and metastasis (198), and inactivation of CIC in adult mice induces T cell acute lymphoblastic lymphoma (T-ALL) either ubiquitously (hUBC-cre-driven ablation (210)) or in the hematopoietic compartment (210, 211). However, loss of CIC in T cells in studies using a Vav1-cre-driven knock-out model failed to show similarly robust T-ALL phenotypes, rather, disease manifested with late onset and incomplete penetrance (211, 212).

1.10.3 - CIC in thymocyte development

CIC has been primarily investigated for its role in immune cells using knock-out models such as Tek-cre and Vav1-cre which result in CIC deficiency in the HSC compartment (211, 213). The $CIC^{FL/FL}$ Vav1-cre model was associated with a lymphoproliferative, systemic, autoimmune-like phenotype characterized by splenomegaly, hyperglobulinemia, and immune cell infiltration of various organs (212). The autoimmune phenotype in this model was attributed to enhanced TFH differentiation and germinal centre responses following the de-repression of the CIC gene target *Etv5* in CIC deficient mice. Another study reported a positive regulatory role

for CIC in both positive and negative selection using the Vav1-cre knock-out model (213), and that CIC deficiency resulted in attenuated TCR signaling in DP thymocytes. However, deletion of CIC in the HSC compartment prior to T cell lineage commitment means that early thymic events (prior to the DP stage) and selection itself (concurrent with the DP stage) cannot be distinguished. Indeed, CIC deletion in the HSC compartment in the Tek-cre model in combination with bone marrow transplantation was suggestive of a role for CIC in the normal expansion of early T cell precursors, indicating that changes in these early events likely confound analysis of positive and negative selection that occur later (211). In support of this, T cell specific deletion of CIC designed to occur concurrently with selection in the CD4-cre knock-out model did not show impaired generation of polyclonal SP thymocytes as was the case in the Vav1-cre model (213). Cumulatively, this indicates our current understanding of CIC's role in selection itself (independent of pre-DP events) is limited.

Various studies in human cell lines and murine thymocytes have implicated CIC in the regulation of the MAPK pathway (204, 207, 213), which is critical to translating the TCR signal into thymocyte fates following selection (24, 42, 45, 214), as was described earlier. How CIC influences MAPK signaling is still an open question. Genomic and transcriptomic analyses in human and murine primary cells and cell lines (e.g. central nervous system, embryonic stem cells, neural stem cell lines) have described CIC gene targets, the set of which is enriched for Ras/MAPK effector genes (196, 215, 216). RNA-sequencing also confirmed some of these targets in DP thymocytes from Vav1-cre $CIC^{FL/FL}$ mice based on their upregulation relative to WT controls (*Etv1*, *Etv4, Etv5, Spry4, Dusp6, Dusp4,* and *Spred1*) (213). Of these putative targets in thymocytes, *Spry4, Dusp6, Dusp4,* and *Spred1* in particular are of interest, as they are known negative regulators of ERK activation (217–219). Indeed, a recent study using human cell

lines showed that CIC participates in a negative regulatory circuit involving ERK1/2, $P90^{RSK}$, and DUSP6. CIC was shown to repress *Dusp6* transcription, while ERK signaling led to the phosphorylation and nuclear export of CIC, leading to the de-repression of *Dusp6*, allowing its subsequent negative regulation on ERK (207). Overall, these studies provide grounds for investigating CIC as a participant in the machinery involved with integrating the TCR signal in thymocytes, and thus, selection.

1.11 - Rationale and thesis objectives

1. PD-1 is upregulated and influences T cell function in a multitude of contexts which include both steady-state homeostasis and bona fide Ag-specific responses. The immune checkpoint represented by PD-1 is an obstacle to both desirable (e.g. anti-tumour) and undesirable (i.e. autoimmunity) T cell responses; whether these two functions can be uncoupled will depend on a closer examination of PD-1 function across the T cell lifetime. Indeed, blocking PD-1 signaling as an immunotherapeutic target remains fraught with incomplete responses (185, 186), divergent potential effects on different immune cell subsets (such as with Tregs, as discussed above), and the development of immune-related adverse events (IRAE) that have been observed to occur following these therapies (161). This is therefore a motivating factor in the continued investigation of the mechanism PD-1-induced T cell dysfunction. While some evidence points to a role for PD-1 in modulating the threshold for positive selection (174, 175), the role of PD-1 during thymocyte development is under-appreciated. If PD-1 signaling is blocked in this tissue, is the establishment of tolerance disrupted, and is this a cause of IRAEs, or a genuine mechanism of a successful immunotherapy? Autoreactive T cell clones can already be found in the circulation of healthy individuals (161); similarly, if PD-1

signaling is blocked in this cells, to what extent can established tolerance be broken and what are the requirements for doing so? In this thesis I will investigate PD-1's role in establishing tolerance in the thymus to tissue-restricted Ag, and assess the features and requirements for maintaining this tolerance.

2. Previous work implicating CIC in thymocyte selection has largely involved models (such as Vav1-cre) that delete CIC prior to T cell lineage commitment, meaning that its role in either early thymocyte development events (pre-DP) or thymocyte selection itself (concurrent with the DP stage) cannot be differentiated. This is of particular concern, since work conducted by Tan *et al.* suggested that CIC indeed plays a role in the normal development and expansion of early T cell precursors (211). Despite these caveats associated with previous studies proposing a role for CIC in selection, transcriptional analyses in $CIC^{FL/FL}$ Vav1-cre DP thymocytes have linked CIC with repression of various negative regulators of ERK signaling (213), and CIC's participation in an ERK-DUSP6 negative feedback loop has been demonstrated in human cell lines (207). In this thesis, I will describe our investigation of CIC's role in both positive and negative selection (in a polyclonal and Tg TCR backgrounds), tolerance, and whether the negative ERK regulator DUSP6 is a key effector in CIC's influence on selection.

1.12 - Overall theses to be explored

1. PD-1 is required for establishing tolerance to tissue-restricted Ag. Continuous PD-1 signaling is required to maintain this tolerance, but its disruption by anti-PD-1 blocking antibodies or withdrawal of PD-L1 is insufficient to break tolerance.
2. Since ERK signaling downstream of the TCR signal is known to inhibit CIC activity, the integration of strong TCR signals (i.e. negative selection) is not greater perturbed by CIC

deficiency. Rather, the integration of weak TCR signals (as seen with positive selection) is uniquely disrupted by CIC deficiency.

Chapter 2 - Materials and Methods

Mice

C57BL/6j (WT, strain 000664), C57BL/6-Tg(Ins2-TFRC/OVA)296Wehi/WehiJ (RIP-mOVA, strain 005431) (220), NOD.B6-*Cd274*^{tm1Shr}/J (PD-L1$^{-/-}$, strain 018307) (221), C57BL/6-Tg(Cd8a-cre)1Itan/J (CD8-cre, strain 008766) (222), B6.Cg-*Foxn1*^{nu}/J (Nude, strain 000819) (223) mice were sourced from Jackson Laboratory. C57BL/6-*Pdcd1*$^{tm1.1Mrl}$ (PD-1$^{fl/fl}$, strain 13976) were purchased from Taconic Biosciences. The PD-L1$^{-/-}$ mice were backcrossed to C57BL/6j mice at least 5 generations prior to intercrossing with RIP-mOVA mice. OT-I Bim$^{-/-}$ mice were provided by Dr. Maureen McGargill (St. Jude Children's Research Hospital, Memphis, TN, USA). PD-1$^{-/-}$ mice were provided by Dr. Tasuku Honjo (Kyoto University, Kyoto, Japan) (224) and BTLA$^{-/-}$ were obtained from Dr. Kenneth Murphy (Washington University, St. Louis, MO) (225). CIC^{flox} mice were obtained from Dr. Quimin Tan (University of Alberta, Edmonton, Canada) (226). HY^{cd4} mice have been previously described (227). Mice with compound genotypes were intercrossed in-house. Across this study, both male and female mice were used and age-matched where possible. All mice were maintained via protocols approved by the University of Alberta Animal Care and Use Committee.

Bone marrow chimeras

T cells were depleted from donor bone marrow by I.P. administration of 100 µg anti-Thy1.2 (clone 30H12) -2 and -1 d prior to harvest. In experiments using OT-II transgenic (228), marrow was stored in liquid nitrogen before use; T cell depletion was performed in this case using a 1:500 dilution of biotinylated anti-CD4/CD8 (see clones used in section below) in place of Isolation Cocktail from a StemCell negative selection kit (Cat. # 19853A). 1 d prior to

transplant, recipients were irradiated with 2 doses of 450 rad, separated by a 4-hour rest period. Bone marrow was flushed from the femurs and tibias of donor mice with PBS (2 % FBS, 2 mM EDTA) and filtered through a 70 µm nylon strainer. $5x10^6$ – $10x10^6$ total BM cells were transplanted to recipients via tail vein injection. On day 1 post-transplant, 100 µg of anti-Thy1.2 antibody (clone 30H12) was administered I.P. to the recipients. For the first 4 wk post-transplant, recipient mice were given water containing Novo-Trimel (via University of Alberta Health Sciences Lab Animal Services). Chimeras were allowed to recover for at least 8 wk before further manipulation or analysis.

Tissue collection

Mice were anaesthetized with isoflurane and euthanized via CO_2 asphyxiation. Organs were harvested and made into single-cell suspensions by grinding through either sterile wire or nylon mesh screens in petri dishes containing RP10 media (RPMI 1640, 2.05 mM L-glutamine [Hyclone], 10 % FBS, 5 mM HEPES, 50 mM 2-mercaptoethanol, 50 µg/mL penicillin/streptomycin, 50 µg/mL gentamycin sulfate). Cells were treated with ammonium-chloride-potassium lysis buffer to lyse RBCs. Viable cell numbers were determined using Trypan Blue exclusion dye and a hemocytometer (Fisher Scientific) under light microscopy (Zeiss).

Adoptive transfers

Whole spleen and thymus cell suspensions from adoptive transfer donors were analyzed by flow cytometry to determine the frequency of $CD8^+$ $V\alpha2^+$ (splenic) and CD8SP $V\alpha2^+$ $CD24^{lo}$ cells (thymic), respectively. $CD8^+$ T cell enrichment was performed using the StemCell EasySep Mouse $CD8^+$ T cell Isolation Kit (Cat. # 19853A) on pooled lymph nodes and spleen. The purities of isolated fractions were > 70 % in all cases. Unless otherwise stated, $5x10^6$ splenic or

$4x10^6$ thymic mature $CD8^+$ $V\alpha2^+$ OT-I T cells were adoptively transferred I.V. into sub-lethally irradiated recipients (1 dose, 450 rad). Co-adoptive transfers involved $5x10^6$ cells per donor for a total of $10x10^6$ $CD8^+$ $V\alpha2^+$ T cells transferred.

Cell culture and in vitro stimulation assays

Cells were cultured at $2.5x10^6$ cells/well in 48-well plates in RP10 media at 37˚C in a tissue culture incubator. Whole spleen cell stimulators from C57BL/6 mice were resuspended in RP10 media at $20x10^6$ cells/mL pulsed with or without 100 nM OVA peptide sourced from AnaSpec (SIINFEKL, AS-60193-1) for 1 h at 37˚C with gentle shaking every 15-20 minutes. Stimulator cells were washed three times before culture. Responder cells were either resuspended in PBS at $10x10^6$ cells/mL and stained with 1.25 μM CFSE or at $5x10^6$ cells/mL stained with 2 μM CellTrace Violet. Staining was conducted for 20 min at 37ºC with regular mixing before quenching with at least 4 volumes of RP10 media. Responder cells were mixed with stimulator cells at a ratio of 4:1 and incubated at 37˚C for indicated time points. Proliferation and division indices were calculated using FlowJo. Proliferation index is calculated as the number of divisions within the dividing cellular population, while the division index is calculated as the average number of divisions undergone by each cell in the starting culture.

Abs and flow cytometry

All staining was carried out in round-bottom 96 well plates using FACS buffer (PBS, 1 % FBS, 0.02 % sodium azide, 1 mM EDTA [pH 7.2]). Prior to staining, samples were pre-incubated with anti-Fc receptor blocking solution (24G.2 hybridoma supernatant) at a 1:20 dilution in FACS buffer. Surface staining was carried out at 4˚C for 15 min. Antibodies were sourced from either BD Biosciences, ThermoFisher, or BioLegend. Clones used were as follows: CD4

(RM4.5), CD8 (53-6.7), CD69 (H1.2F3), PD-1 (J43), CD19 (1D3), CD25 (7D4), Vα2 (B20.1), H-2K^b (AF6-88.5.5.3), CD24 (M1/69), IFN-γ (XMG1.2), TNFα (MP6-XT22), CD45.1 (A20), and CD45.2 (104). Live/Dead staining was performed using LIVE/DEAD Fixable Aqua, Lime, or Blue (Thermo FisherScientific) or Fixable Viability Dye eFluor 780 (eBioscience). Biotinylated H-2K^b-OVA monomers were obtained from the NIH tetramer facility and tetramerized in house. Intracellular staining was performed using BD Cytofix/Cytoperm Fixation/Permeabilization Solution Kit (BD Biosciences). Data was collected on either BD LSRFortessa SORP/X-20, or a Cytek Aurora spectral cytometer. Analysis was conducted using Flowjo software (TreeStar).

Blood glucose monitoring

Blood glucose concentrations of bone marrow chimeras were monitored weekly starting at 3 wk post-transplantation using a OneTouch Ultra2 blood glucose meter and OneTouch Ultra Test Strips. Adoptive transfer recipients were monitored every 3-4 days starting 4 d post-transfer for the first month, and every week subsequently. Blood samples were acquired by tail vein bleeding. When blood glucose readings exceeded 15 mM, another reading was taken 24 h later. Mice were confirmed diabetic upon two consecutive readings above 15 mM.

PD-1 blockade

For *in vitro* blockade experiments, cultured cells were treated continuously with 5 μg/mL of αPD-1 (clones: J43 or RMP1-14, BioXCell). For *in vivo* experiments, mice were treated I.P. with 250 μg antibody every second day for 2 wk beginning at least 8 weeks post-BM transplant. The blood glucose concentration of treated mice was monitored for at least 4 wk following the final antibody injection.

CRISPR/Cas9 gene editing

Two crRNAs targeting murine *pdcd1* were used in combination to acutely ablate the PD-1 locus (synthesized by IDT): 5' – GACACACGGCGCAAUGACAG – 3' (first verified by Nüssing *et al.* 2020) and 5' – AGGUACCCUGGUCAUUCACU – 3' (generated by IDT predesigned CRISPR-Cas9 guide RNA service). Both crRNAs were complexed 1:1 with Alt-R CRISPR-Cas9 tracrRNA (IDT, #1072532), then each gRNA/tracrRNA complex was mixed 1:1 (0.3 nmol total guide RNA/tracrRNA complex delivered per electroporation) and mixed with 10 ug of Alt-R S.p. Cas9 nuclease V3 (IDT, #1081059). For control experiments, the Alt-R CRISPR-Cas9 Negative Control crRNA #1 was sourced from IDT (#1072544). Nucleofections were carried out using the Lonza Primary Cell 4D-Nucleofector X kit (#V4XP-3032).

ATAC-seq

ATAC-seq libraries were prepared from sorted $CD8^+$ $V\alpha2^+$ $CD24^{lo}$ thymocytes from OT-I $Bim^{-/-}$ > RIP-mOVA chimeras; all samples were collected from the same cohort of mice on the same day. Sorted cells were washed with ice-cold PBS before treatment with the Active Motif ATAC-Seq Kit (#53150). Some alterations to the kit's protocol are as follows. Cells were lysed for 5 min before the 1 hr extended tagmentation step and DNA amplification with barcoded primers. Qiaxcel gel fragment analysis was carried out to assess the quality of the libraries. 2x50bp paired-end sequencing was performed on a NovaSeq 6000 (Centre for Health Genomics and Informatics, University of Calgary, Calgary, AB). Pre-processing and quality control were conducted according to the GalaxyProject ATAC-seq data analysis article (229–231). Reads were mapped to the mouse genome (assembly GRCm39) using Bowtie2 (232). Duplicate reads were removed using Picard MarkDuplicates and reads mapping to chrM were excluded. Peak summits were identified using MACS2 (233) from each replicate; coverage was assessed based on 100 bp

regions flanking 5' read start sites (200 bp total). I excluded regions that intersected with ENCODE blacklisted regions. Tn5 insertions were counted for each replicate and differentially accessible regions were identified with DESeq2 (ver 1.12.3).

Quantitative real-time polymerase chain reaction (qRT-PCR)

Mature naïve T $CD8^+$ cells were isolated from spleen by StemCell EasySep naïve mouse $CD8^+$ T cell Isolation Kit (Cat. 19858), and thymocyte subsets were isolated by fluorescence activated cell sorting (FACS). RNA was isolated from 0.8-1.0x10^6 unstimulated cells using RNeasy Plus Mini Kits (QIAGEN, Cat. No. 74134). cDNA was created from RNA samples using SuperScript III first-strand synthesis supermix for qRT-PCR (Invitrogen, Cat. 11752-050) or High-Capacity cDNA Reverse Transcription Kit (Applied Biosystems, Cat. 4368814). qRT-PCR was performed using a Mastercycler ep *realplex* 2S (Eppendorf) and PerfeCTa SYBR Green FastMix (Quanta, Cat. 95072-250) and primers listed in Table 2-1. Results were normalized to β-actin expression within in each sample.

Table 2-1: qRT-PCR primers

β-actin F	CTA AGG CCA ACC GTG AAA AG
β-actin R	ACC AGA GGC ATA CAG GGA CA
DUSP6 F	AAC ACT GGT GGA GAG TCG GT
DUSP6 R	CCG TCT AGA TTG GTC TCG CAG

Western blotting

Equipment and reagents for protein quantification were generously shared by the lab of Dr. Christopher Power. Whole splenocytes (5x10^6 cells per chimera) were harvested and lysed in ice-cold RIPA Lysis and Extraction Buffer (ThermoFisher Scientific, Cat. 89900) with 1.5X Halt Protease Inhibitor Cocktail, EDTA-free (100X, ThermoFisher Scientific Cat. 87785) for 1 hr with periodic vortexing. Samples were then centrifuged at 17 xg for 1 min at 4°C before

supernatant transfer into fresh tubes. Protein was quantified in lysates using the Bio-Rad DC Protein Assay Kit (Cat. 500-0116), a BioTek Synergy HT plate reader (Agilent), and Gen5 v1.11.5 plate reader software (BioTek Instruments). Sample buffer (10 % SDS, 500 mM DTT, 50 % glycerol, 250 mM Tris-HCl and 0.5 % bromophenol blue dye, pH 6.8) was added and samples were boiled for 10 min before long term storage.

SDS-page was set up using a Mini-PROTEAN Tetra Cell (Bio-Rad). Samples (20 µg total protein/well) were run on pre-cast (4-20 %) SDS-PAGE gels (Bio-Rad, Cat. 456-1094) and run in electrophoresis running buffer (25 nM Tris, 190 nM Glycine, 0.1 % SDS, pH 8.3). After electrophoresis (1.5 hr, 110V), gels were equilibrated in transfer buffer (25 nM Tris, 190 nM Glycine, 20 % methanol, pH 8.3) and protein samples were wet-transferred to nitrocellulose membranes at 0.14 A for 1 hr.

After transfer, membranes were blocked overnight using Fish Serum Blocking Buffer (Thermo, Cat. 37527) at 4°C. Membranes were then incubated with primary antibodies (MKP3 recombinant Rabbit Monoclonal Antibody SR39-09; ThermoFisher, Cat. MA5-31988) diluted 1:1000 in Fish Serum Blocking Buffer overnight at 4°C and washed with PBS-T (0.1 % Tween-20 in PBS). Secondary HRP-conjugated antibody (Peroxidase AffiniPure Donkey Anti-Rabbit IgG; Jackson ImmunoResearch, Cat. 711-035-152) was diluted 1:5000 in 4 % skim milk/PBS-T for 1 hr at RT. Protein of interest blots were imaged first, and β-actin loading control detection was done immediately after blots were imaged and washed. β-actin HRP-conjugated primary (Santa Cruz, Cat. Sc-47778 HRP) was diluted 1:1000 and incubation was performed for 1 hr at RT, and membranes were washed, then imaged. Band intensities were developed from blots using the Pierce ECL Kit (ThermoFisher, Cat. 42132) with ECL substrate (1:4 dilution in Milli-Q

H_2O) applied to blots for 5 min. Blots were imaged using HE Health Sciences Biomolecular Imager (Cy2 channel) and quantified using ImageJ software and normalized to β-actin bands.

Competitive lymphopenia-induced proliferation (LIP)

Whole splenocytes from each donor mouse were stained with either CTV or CFSE, which were used to differentiate donor origin. Recipient mice were rendered lymphopenic by 1 dose of 450 rad on the day of adoptive transfer. $2.5x10^6$ stained cells from each donor were injected (a total of $5x10^6$ cells) into the sublethally irradiated (or non-irradiated controls) recipients. Spleens were harvested 7 days post-adoptive transfer and analyzed by flow cytometry.

Statistical analysis

Statistical analyses were conducted using Prism software (Graph-Pad). Specific tests used are listed in figure legends. * $p \leq 0.05$, ** $p \leq 0.01$, *** $p \leq 0.001$, **** $p \leq 0.0001$. Data expressed in plots are represented as mean ± SD unless otherwise stated.

Chapter 3 - Characterizing the non-deletional tolerance that protects OT-I Bim$^{-/-}$ > RIP-mOVA chimeras from autoimmunity

This chapter contains content originally published in The Journal of Immunology:

- May, J. F., R. G. Kelly, A. Y. W. Suen, J. Kim, J. Kim, C. C. Anderson, G. R. Rayat, and T. A. Baldwin. 2024. Establishment of CD8+ T Cell Thymic Central Tolerance to Tissue-Restricted Antigen Requires PD-1. J. Immunol. Vol 212 (2): 271-283. Copyright © [2024] The American Association of Immunologists, Inc.

Introduction

Bim is a pro-apoptotic BH3-only member of the Bcl-2 family of proteins, which regulate cell death through their influence on mitochondrial integrity. The TCR signal positively regulates the expression of Bim in addition to the anti-apoptotic family member Bcl-2. Critically, Bim expression is induced following the strong TCR signal and protein kinase C activation (234) associated with negative selection (176, 235), and it has been proposed to be required for the induction of thymocyte apoptosis (72, 76). Despite this, Bim's role in clonal deletion and negative selection appears to vary with context. In models of ubiquitous antigen-mediated (UbA) negative selection, while deficiency in Bim results in a lack of Caspase-3 activation, mature UbA-reactive T cells still fail to develop, indicating intact negative selection (76, 236–238). Rather, UbA-specific DP thymocytes experience delayed deletion independently of Caspase-3 activation (238). In contrast, in tissue-restricted antigen (TRA) models of negative selection, deficiency in Bim resulted in impaired clonal deletion and the subsequent generation of mature self-reactive T cells (73–75). Despite the release of self-reactive T cells into the periphery, animals in these experiments did not develop autoimmunity, implying the existence of a robust

mechanism of non-deletional tolerance following high affinity TCR signaling (74). We previously demonstrated impairment in clonal deletion in the absence of Bim (74) using the OT-I TCR transgenic system (239). OT-I Bim$^{-/-}$ T cells that escaped thymic clonal deletion in RIP-mOVA recipients did not go on to cause autoimmunity due to functional impairments characterized by defects in activation, proliferation, and cytokine production. The mechanism(s) behind this impairment was unclear but may be due to cell-extrinsic suppression or cell-intrinsic anergy (93, 240, 241).

We generated bone marrow (BM) chimeras using RIP-mOVA recipients, wherein membrane-bound chicken ovalbumin (mOVA) is expressed under the control of the rat insulin promoter (RIP) (220). In these transgenic mice, membrane-bound OVA is expressed in pancreatic islet beta cells, the proximal tubular cells of the kidney, as well as medullary thymic epithelial cells (mTECs) thanks to the recruitment of tissue-specific or promiscuous transcription factors (respectively) to the rat insulin promoter. By transferring BM from OT-I transgenic donors, wherein developing T cells recognize OVA with high affinity, into RIP-mOVA recipients, we were able to model negative selection to TRA. In this chapter, we aimed to further characterize the non-deletional tolerance that protected OT-I Bim$^{-/-}$ > RIP-mOVA chimeras from autoimmunity.

Results

TRA-specific T cells in OT-I Bim$^{-/-}$ > RIP-mOVA chimeras are functionally impaired via a cell-intrinsic mechanism

Previous work in our lab determined that activation marker induction and proliferation of OT-I splenocytes from OT-I Bim$^{-/-}$ > RIP-mOVA chimeras was diminished compared to that of wildtype (WT) OT-I CD45.1^{+} mice (74). We hypothesized that if a population of dominant

suppressors existed in OT-I Bim$^{-/-}$ > RIP-mOVA chimeras, they should suppress the activation and proliferation of wildtype OT-I T cells. We determined in previous work that *in vitro* co-culture with these impaired CD8^{+} T cells did not impair the WT ability to respond, suggesting the functional impairment seen in cells from OT-I Bim$^{-/-}$ > RIP-mOVA was cell-intrinsic. I next wanted to assay functional impairment *in vivo* and in the context of tolerance. General gating strategies are outlined in Fig. 3-1.

I co-adoptively transferred either whole spleen or enriched CD8^{+} T cells from OT-I Bim$^{-/-}$ > RIP-mOVA chimeras with splenocytes from CD45.1^{+} OT-I WT mice (1:1 ratio) into sub-lethally irradiated RIP-mOVA recipients. Neither whole spleen nor enriched CD8^{+} OT-I T cells from OT-I Bim$^{-/-}$ > RIP-mOVA chimeras alone were diabetogenic, suggesting that a dominant suppressor population of non-T cell origin was not responsible for functional impairment in these chimeras (Fig. 3-2A). Enriched CD8^{+} OT-I T cells from OT-I Bim$^{-/-}$ > RIP-mOVA chimeras co-adoptively transferred with WT OT-I T cells did not have a dominant suppressive effect on diabetogenicity. In these co-adoptive transfer recipients, WT OT-I T cells also expanded to a greater extent than those from OT-I Bim$^{-/-}$ > RIP-mOVA chimeras (Fig. 3-2B). Functional impairment of OT-I Bim$^{-/-}$ T cells from RIP-mOVA chimeras was also demonstrated by a reduced capacity for lymphopenia-induced proliferation compared to control cells from OT-I Bim$^{-/-}$ > WT chimeras (work done by previous lab member, Alexander Suen; Fig. 3-2C). Collectively, these data further suggest that a population of Ag-specific suppressors are not generated in OT-I Bim$^{-/-}$ > RIP-mOVA mice and that functional impairment of OT-I Bim$^{-/-}$ T cells from these chimeras is cell-intrinsic.

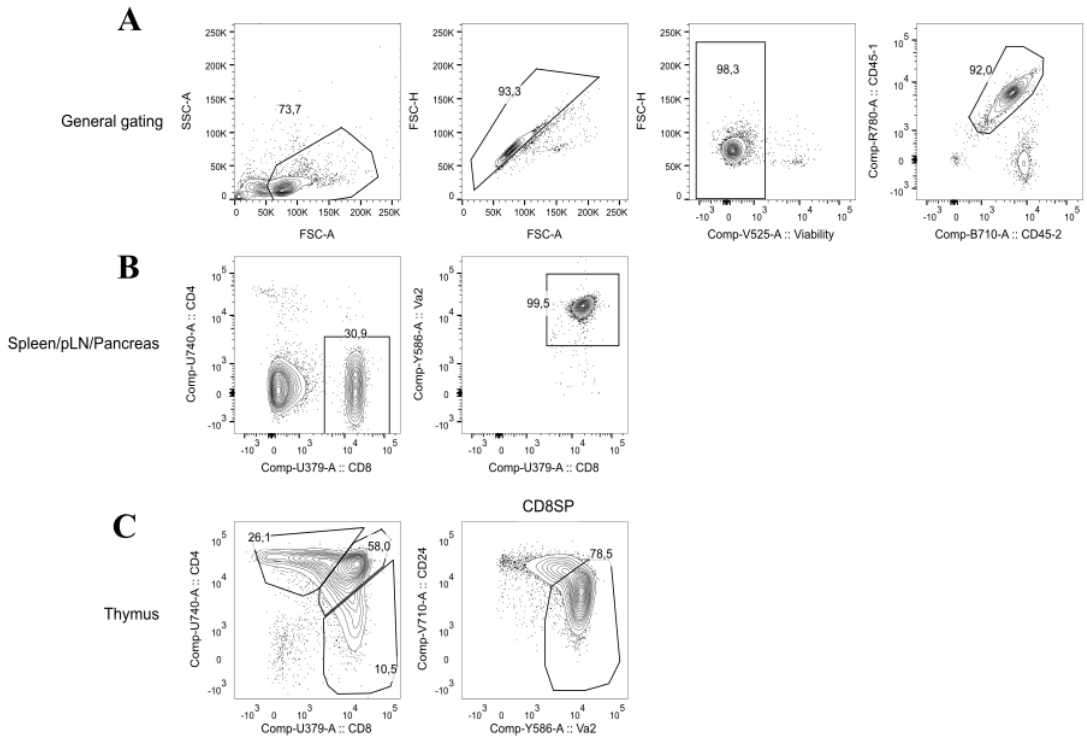

Figure 3-1: Gating strategy for analysis of OT-I transgenic thymic and peripheral T cells. Gates are ordered hierarchically from left to right. A, General gating strategy at the beginning of all analyses. B, Gating strategy for identifying peripheral OT-I T cells. C, Gating strategy for identifying OT-I thymocytes; the mature thymocyte gate is drawn within the CD8SP population.

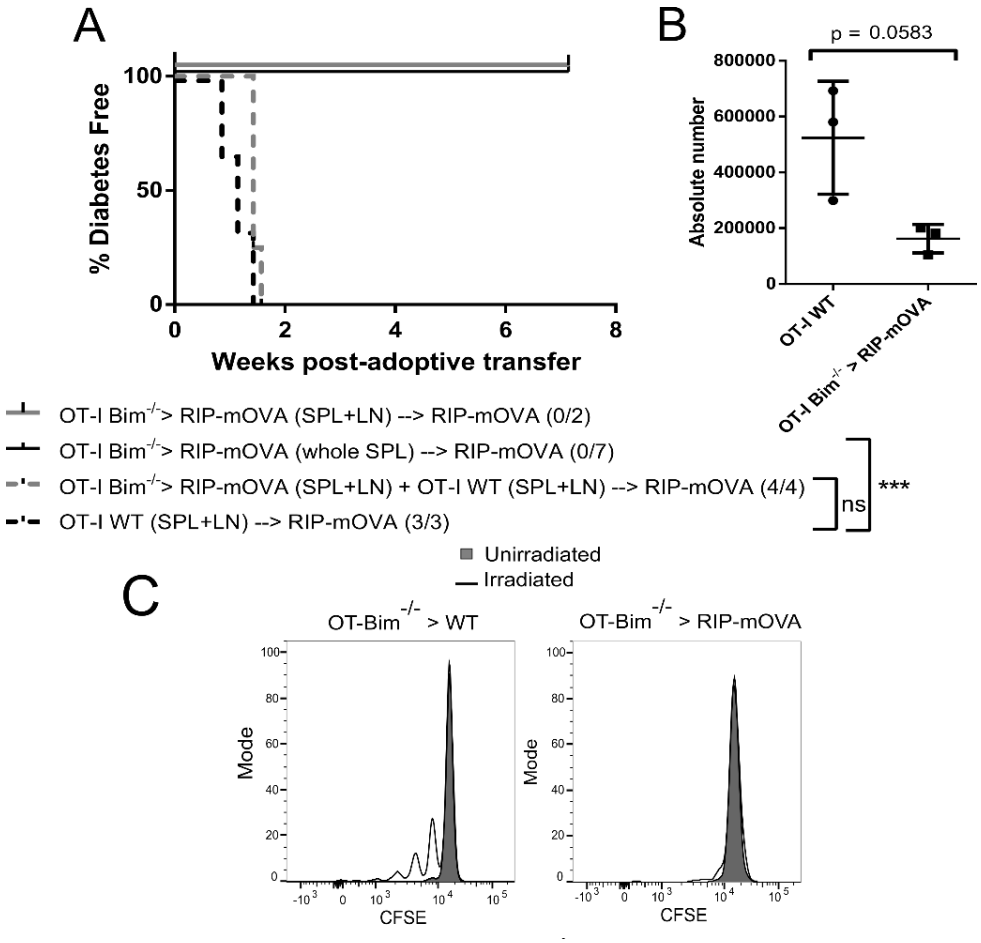

Figure 3-2: TRA-specific T cells from OT-I Bim$^{-/-}$ → RIP-mOVA chimeras demonstrate functional impairment *in vivo.*

A, Incidence of diabetes in sub-lethally irradiated RIP-mOVA recipients of adoptively transferred splenic CD8^{+} Vα2^{+} OT-I T cells from OT-I Bim$^{-/-}$ > RIP-mOVA and/or OT-I WT. Note that 7 recipients with OT-I Bim$^{-/-}$ > RIP-mOVA transfers received whole spleen while all other recipients in this experiment received CD8-enriched isolates from pooled spleen and lymph nodes (SPL+LN). Data are representative of 4 separate cohorts. B, Recipients of CD8-enriched isolates (SPL+LN) from OT-I Bim$^{-/-}$ > RIP-mOVA and OT-I WT described in A were analyzed for expansion of OVA-K^{b} tetramer^{+} cells from either donor cell population within the spleen. C, Lymphopenia induced proliferation of Vα2^{+} CD8^{+} splenocytes transferred from OT-Bim$^{-/-}$ > WT

or OT-I Bim$^{-/-}$ > RIP-mOVA chimeras into unirradiated (grey) or sub-lethally irradiated (open) recipients, measured by CFSE labelling (n = 2). Asterisks represent statistical significance as determined by Log-rank test (A) or paired T-test (B).

TRA-specific T Cells in OT-I Bim$^{-/-}$ > RIP-mOVA chimeras are rendered functionally impaired in the thymus.

After determining that the functional impairment of OT-I T cells from OT-I Bim$^{-/-}$ > RIP-mOVA chimeras was cell-intrinsic, I investigated whether this state was established during development in the thymus or in the periphery. The thymus is the initial site of high affinity antigen encounter and induction of non-responsiveness in thymocytes has been reported previously (242). The diagram shown in Figure 3-3 outlines the experiments described in this section. Some replicates for experiments in this section were carried out by former Baldwin lab student, Rees Kelly.

I stimulated CFSE-labelled thymocytes from OT-I Bim$^{-/-}$ > WT and OT-I Bim$^{-/-}$ > RIP-mOVA chimeras with OVA peptide-pulsed splenocytes and examined activation and proliferation. On day 2, expression of activation markers CD69 and CD25 was impaired in OT-I Bim$^{-/-}$ > RIP-mOVA thymocytes compared to OT-I Bim$^{-/-}$ > WT controls (Fig. 3-4A). Additionally, on day 3, thymocytes from OT-I Bim$^{-/-}$ > RIP-mOVA chimeras exhibited a defect in proliferation compared to OT-I Bim$^{-/-}$ > WT thymocytes (Fig. 3-4B). These impaired responses were not likely to be due to a reduction in more mature CD8SP thymocyte subsets in OT-I Bim$^{-/-}$ > RIP-mOVA recipients since the thymi of these mice demonstrated enhanced frequencies of mature (M2; CD69^{lo} H-2K$^{b\ hi}$) thymocytes over WT controls (Fig. 3-4D).

To determine if the observed *in vitro* defects in activation and proliferation acquired in the thymus translated into functional *in vivo* impairment, I adoptively transferred either thymocytes or splenocytes from OT-I $Bim^{-/-}$ > RIP-mOVA or OT-I $Bim^{-/-}$ > WT chimeras into sub-lethally irradiated RIP-mOVA recipients to assess diabetogenicity (Fig. 3-5). Most recipients of thymocytes and all recipients of splenocytes from OT-I $Bim^{-/-}$ > WT chimeras developed diabetes as expected. In contrast, none of the sub-lethally irradiated RIP-mOVA recipients that received thymocytes or splenocytes from OT-I $Bim^{-/-}$ > RIP-mOVA chimeras became diabetic. Collectively, these data suggest that functional impairment of OT-I $Bim^{-/-}$ > RIP-mOVA T cells is established in the thymus.

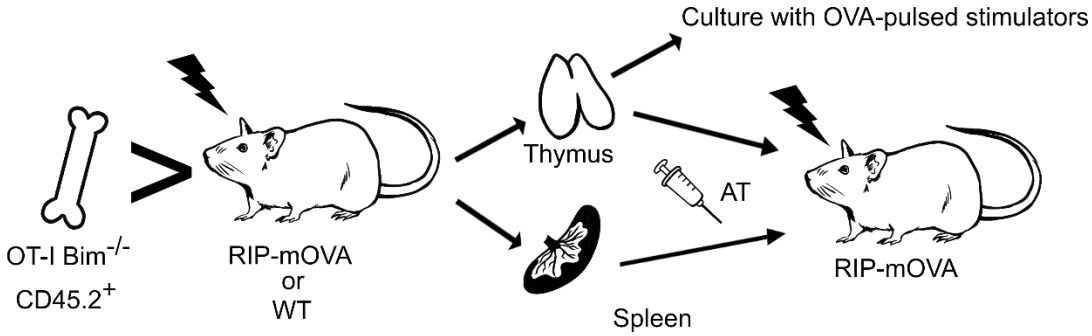

Figure 3-3: Diagram describing experiments outlined in Figures 3-4 and 3-5.

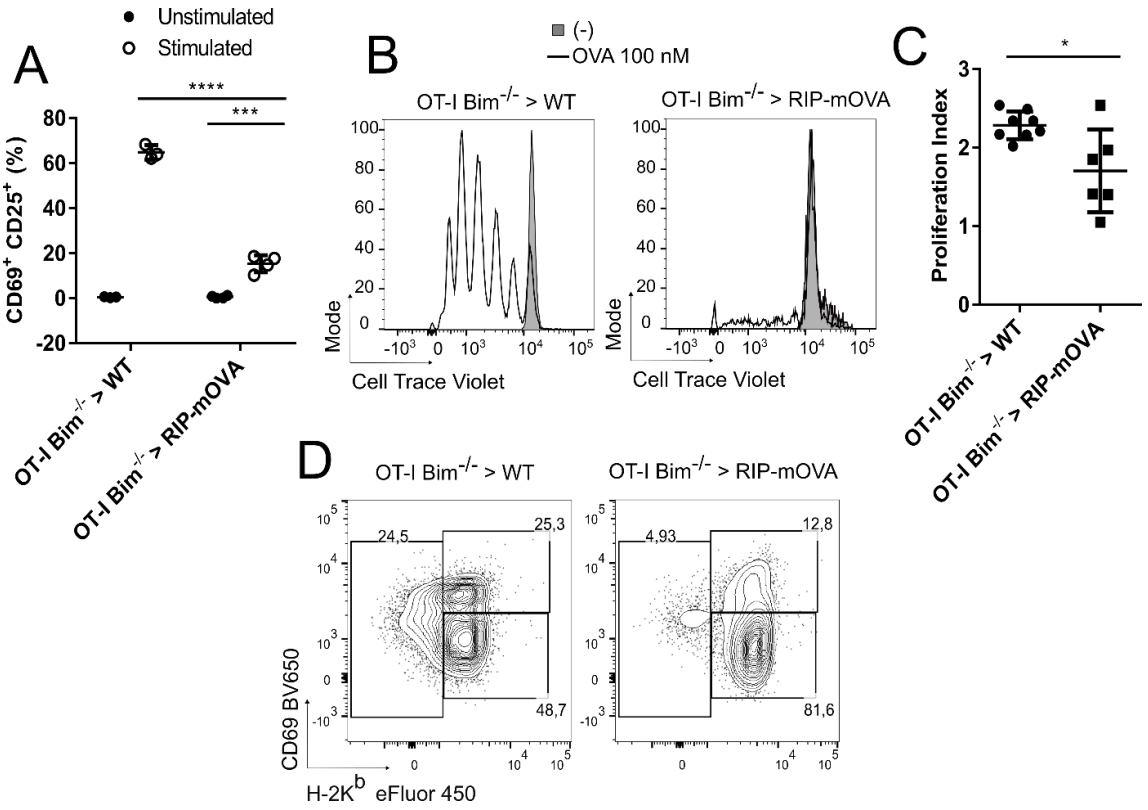

Figure 3-4: TRA-specific thymocytes from OT-I Bim$^{-/-}$ → RIP-mOVA chimeras are functionally impaired.

Activation marker induction (A), representative histograms for thymocyte proliferation (B), and compiled proliferation indices (C) of OT-I Bim$^{-/-}$ > RIP-mOVA or OT-I Bim$^{-/-}$ > WT thymocytes following *in vitro* stimulation. Open histograms represent culture with OVA peptide-pulsed stimulators, while greyed histograms represent no-peptide control stimulators. D, Distribution of Vα2^{+} CD8SP OT-I thymocytes among semi-mature (SM; H-2K$^{b\ lo}$), Mature 1 (M1; CD69^{hi} H-2K$^{b\ hi}$), and Mature 2 (M2; CD69^{lo} H-2K$^{b\ hi}$) population. For each assay described above, the number of independent experiments (IE) ≥ 3. Asterisks represent statistical significance as determined by a two-way ANOVA with Sidak's multiple comparisons test (A) or unpaired T-test with Welch's correction (C).

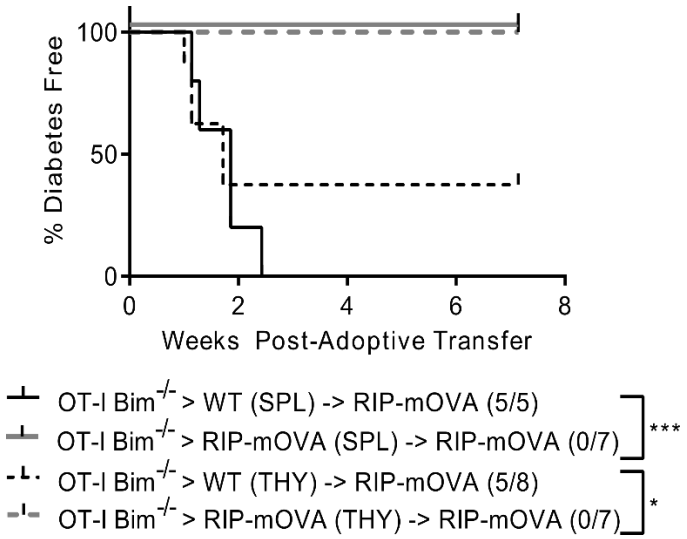

Figure 3-5: Both thymocytes and mature peripheral TRA-specific T cells from OT-I $Bim^{-/-}$ → RIP-mOVA chimeras demonstrate functional impairment *in vivo.*

From either OT-I $Bim^{-/-}$ > RIP-mOVA or > WT bone marrow chimeras, 2-5x10^6 $V\alpha2^+$ $CD24^{lo}$ thymocytes (THY) or $V\alpha2^+$ OT-I T splenocytes (SPL) from whole spleen were transferred to sub-lethally irradiated RIP-mOVA recipients, which were then monitored for the induction of diabetes. Log-rank (Mantel-Cox) test results are relative to organ transfer groups. Asterisks represent statistical significance as determined by a Log-rank test.

Tolerant TRA-specific T cells in OT-I $Bim^{-/-}$ > RIP-mOVA chimeras share phenotypic features with the state conventionally defined as "exhausted".

T cell dysfunction in general has come to be defined under numerous terms, one of which being "exhaustion". To further characterize the functionally impaired TRA-specific T cells I observed in our OT-I $Bim^{-/-}$ > RIP-mOVA chimeras, I assessed their expression of markers associated with exhaustion. Recently, TOX and TCF1 have been under investigation for their suspected roles in stem-like exhausted T cell populations (243–245). TOX specifically is thought to be associated with commitment into an exhausted, self-renewing population of T cells,

whereas TCF1 is thought to contribute to the maintenance of the "exhausted" identity (135–137). I found that T cells in OT-I Bim$^{-/-}$ > RIP-mOVA pancreatic lymph nodes displayed elevated expression of TOX, but I was unable to observe an increase in TCF1 expression in any of the tissues analyzed (Fig. 3-6).

The functional impairment seen in OT-I Bim$^{-/-}$ > RIP-mOVA thymocytes and splenocytes may be driven by co-inhibitory molecules and/or other factors that inhibit T cell activity. As such, I investigated whether various known co-inhibitors were differentially expressed in OT-I > RIP-mOVA thymocytes and splenocytes that escaped clonal deletion compared to OT-I > WT controls. I found enhanced PD-1 expression on OT-I T cells from both the thymus and periphery of OT-I > RIP-mOVA (Fig. 3-7) and OT-I Bim$^{-/-}$ > RIP-mOVA chimeras compared to OT-I cells from WT recipients, while the expression of other co-inhibitory molecules was not appreciably altered (Fig. 3-8).

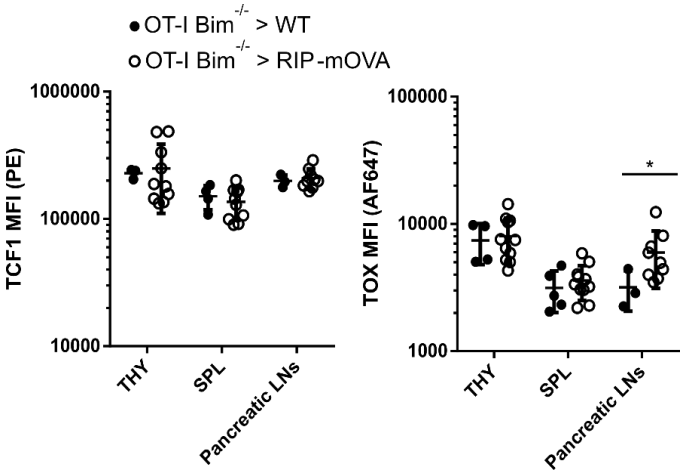

Figure 3-6: TCF1 and TOX expression in spleen, thymus, and pancreatic lymph nodes of in OT-I Bim-/- > RIP-mOVA and OT-I Bim-/- > WT chimeras.

The number of independent experiments (IE) ≥ 4. Asterisks represent statistical significance as determined by unpaired T-test with Welch's correction.

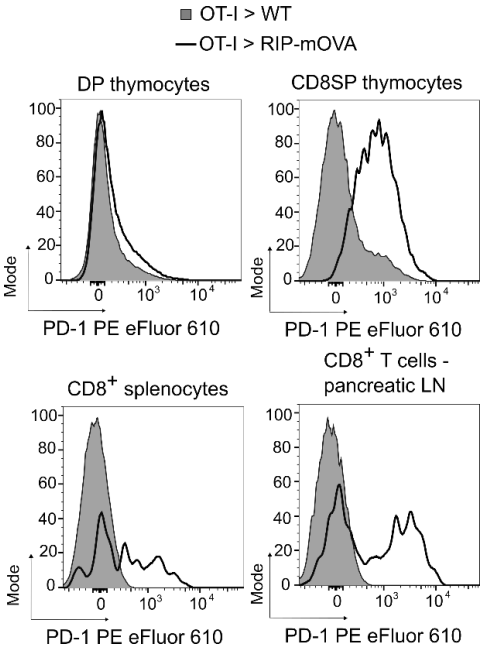

Figure 3-7: PD-1 is highly expressed in tolerant OT-I T cells.

PD-1 expression on OT-I T cells across organs in OT-I > RIP-mOVA (open histogram) and OT-I > WT (greyed histogram) bone marrow chimeras. Data is representative of n ≥ 3.

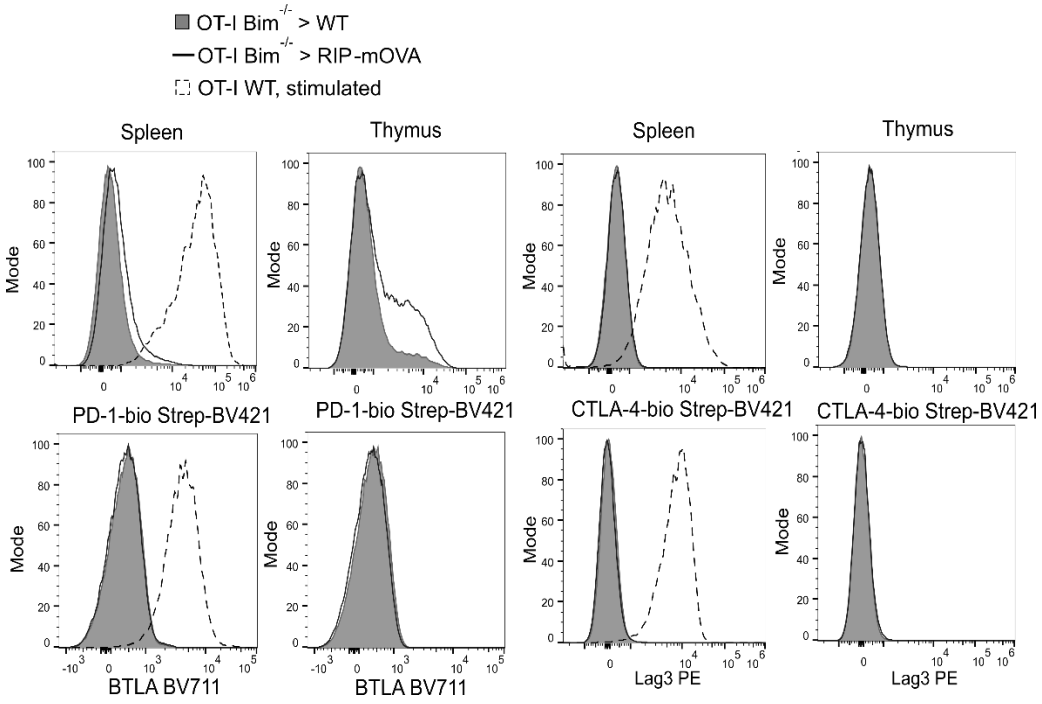

Figure 3-8: Co-inhibitory molecule expression in OT-I Bim$^{-/-}$ > RIP-mOVA and OT-I Bim$^{-/-}$ > WT chimeras.

As a positive control for co-inhibitory molecule expression, WT OT-I splenocytes were stimulated for 24 hr with high affinity peptide OVA (100 nM).

Epigenetic profiling of tolerance in OT-I Bim$^{-/-}$ > RIP-mOVA chimeras

Given the increase in PD-1 expression I observed association with dysfunction – which is also a marker of T cell exhaustion (reviewed in (245)) – and TOX expression, these data provided rationale for the comparison of our observed functionally impaired TRA-specific T cells with those observed in exhaustion studies (for example, in cases of persistent antigen exposure such as with chronic LCMV infection) (245). So far, I have provided evidence that cell-intrinsic functional impairment was established in the thymus in tolerant OT-I Bim$^{-/-}$ > RIP-

mOVA chimeras. Thus, I used ATAC-seq to assess the epigenetic landscape in thymocytes from these chimeras to get a more complete picture of the nature of the dysfunction I observed.

Mature $CD8^+$ $V\alpha2^+$ $CD24^{lo}$ thymocytes were collected from both OT-I $Bim^{-/-}$ > WT and OT-I $Bim^{-/-}$ > RIP-mOVA chimeras using fluorescence activated cell sorting (FACS), and nuclei were isolated for the preparation of ATAC-seq libraries. Once sequencing was complete, I called peaks in nucleosome-free regions (NFRs) on individual replicates and defined a set of non-redundant peaks present in both replicates for each experimental group. I quantified the number of reads mapping to regions within this merged peak set using DESeq2 (246). I then reviewed the overall correspondence between replicates by comparing peak overlaps in NFRs using occupancy analysis in the R Bioconductor package Diffbind (247, 248). Replicates in the OT-I $Bim^{-/-}$ > WT group clustered closely together, sharing significant peak overlaps, while replicates in the OT-I $Bim^{-/-}$ > RIP-mOVA group were more dissimilar overall, but still shared a significant number of peaks (Fig. 3-9A-B). I additionally quantified signal within peaks to evaluate changes between groups and correspondence between replicates, again using DESeq2. Despite the discrepancy seen in occupancy analysis, the RIP-mOVA group replicates clustered together with similar proximity compared to the WT group when signal within shared peaks was analysed (Fig. 3-9C).

I next focused on differentially accessible regions between OT-I $Bim^{-/-}$ > WT and OT-I $Bim^{-/-}$ > RIP-mOVA chimeras using the DESeq2 object described above. With the set of total hits across all annotated regions (promoters, exons, introns, untranslated regions, intergenic regions), we used the R Bioconductor package clusterProfiler (249, 250) to conduct enrichment analysis on these accessible regions in the $Bim^{-/-}$ > RIP-mOVA group over the control WT chimeras (Fig, 3-10A). I then generated a subset of regions that fell within 3000 bp of a transcription start site

(TSS) to focus our analysis on chromatin organization most likely to impact the transcriptional permissibility of a given locus (Fig. 3-10B). This analysis revealed nucleosome-free regions enriched proximal to the promoters of *Nr4a1, Tnfrsf18*, and *Myb* – all markers that have previously been linked with T cell exhaustion and dysfunction (251–259) (Table 3-1, under-represented hits in Table 3-2). Interestingly, promoters of genes associated with T cell function and survival were also found enriched for nucleosome-free chromatin: *Ksr1, Il2,* and *Ifng* (Table 3-1); in contrast, down-regulation of such mediators is thought to define dysfunctional states like anergy and tolerance, reviewed in (112).

Using R Bioconductor packages clusterProfiler and ChIPseeker (260, 261), I annotated our differential ATAC-seq regions to genes, then used the associated gene information to test enrichment for GO sets from the Gene Ontology Consortium (262, 263). These annotations were organized by those enriched and those under-represented in OT-I $Bim^{-/-}$ > RIP-mOVA chimeras compared to WT controls. In agreement with our observation of functional impairment in RIP-mOVA chimeras, I observed an enrichment in GO annotations for regulatory pathways: for responses to stimuli, cell communication, and signaling (Table 3-3). Meanwhile, I observed an under-representation of GO annotations for development, signal transduction, differentiation, activation, and migration (Table 3-4).

Finally, I used the R Bioconductor package ATACseqTFEA (264) to assess transcription factor foot-printing between our RIP-mOVA and WT control chimeras (Table 3-5). I observed an under-representation of foot-prints for the AP-1 family (JunB, Fos, Fos:Jun), a group of transcription factors with pleiotropic roles in T cell activation, differentiation, and overall function downstream of the TCR (reviewed in (265, 266)). Downregulation of AP-1 transcription factor activity has previously been linked with the “exhausted” state, which harmonizes with our

observed T cell dysfunction (267). I detected under-representation of the binding of additional transcription factors positively associated with T cell function: CREB1 (222) and KLF13 (268, 269). I also recorded under-representation of foot-prints of transcription factors negatively associated with T cell function in RIP-mOVA chimeras compared to WT controls, such as EGR4 (270). Finally, I saw enrichment in the foot-print of FOXP1, thought to restrict T cell signaling, homeostasis, and anti-tumour immunity (271–273).

Here, I have defined an epigenetic landscape associated with central tolerance of TRA-specific $CD8^+$ T cells. Overall, TRA-specific mature thymocytes from OT-I $Bim^{-/-}$ > RIP-mOVA chimeras displayed an epigenetic profile characterized by accessible promoters and transcription factor binding classically suggestive of both T cell function and dysfunction. The co-habitation of these apparently opposing features suggests that while chromatin organization supports the endurance of the tolerant state, it may simultaneously support the potential for a re-mobilization of a T cell response.

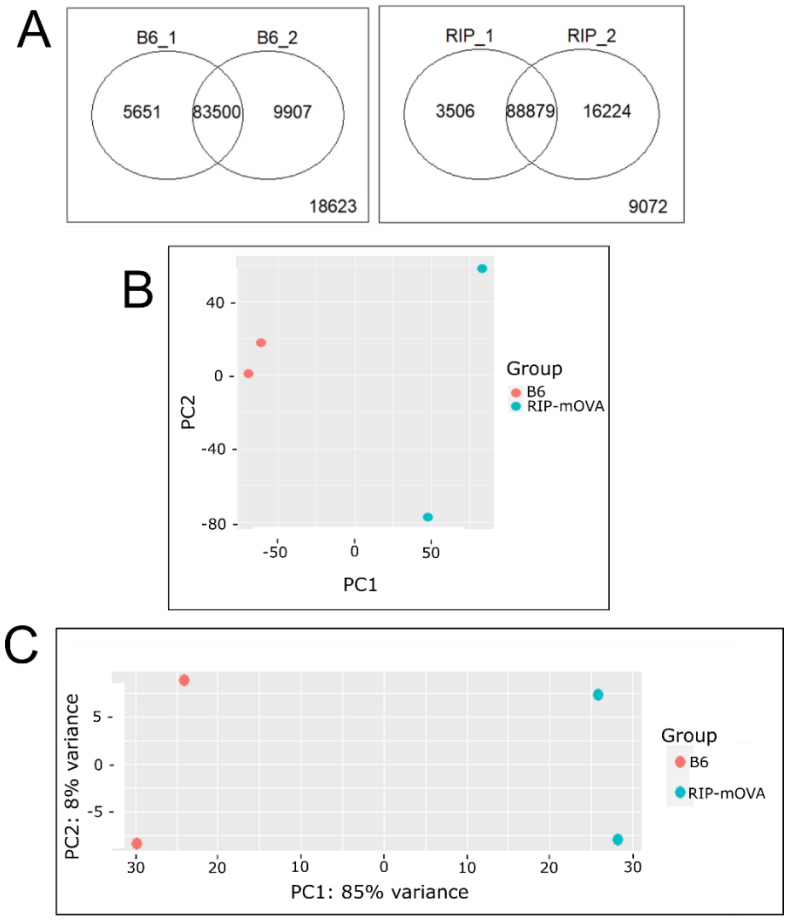

Figure 3-9: Correspondence between replicates in within ATAC-seq groups i) OT-I Bim$^{-/-}$ > WT (B6) and ii) OT-I Bim$^{-/-}$ > RIP-mOVA (RIP).

A, Overlap of NFRs between replicates for each experimental group. As the whole peak set (B6 and RIP-mOVA) is considered, the number in the bottom right of each box is the number of peaks not present in any sample within the box. B, Principal component analysis (PCA) analysis (occupancy analysis) of peak overlaps among all samples. C, Principal component analysis of signal quantity within peaks among all samples.

Table 3-1: Sample of hits for promoters of over-represented genes in the epigenetic landscape of OT-I Bim$^{-/-}$ > RIP-mOVA chimeras compared to WT controls.

Hits were selected based proximity to TSS and on known relevance to T cell biology below the threshold of adjusted p-value = 10e-6.

gene_name	log2FoldChange	Distance to TSS (bp)	padj
Ksr1	4.603014275	-7	2.5400E-31
Tnfrsf18	2.323314798	2188	5.4900E-55
Bmyc	2.074505647	1398	2.3403E-04
Myb	1.541577148	-416	2.1600E-07
Il15	1.470232062	-1	6.0100E-05
Il2	1.467390423	0	7.5293E-03
Ifng	1.462712598	868	1.9555E-03
Dusp1	1.459351329	-158	2.7133E-04
Cd47	1.285652478	0	2.1900E-05
Nr4a1	0.642097517	-10	7.6100E-07

Table 3-2: Sample of hits for promoters of under-represented genes in the epigenetic landscape of OT-I Bim$^{-/-}$ > RIP-mOVA chimeras compared to WT controls.

Hits were selected based on proximity to TSS and on known relevance to T cell biology below the threshold of adjusted p-value = 10e-6.

gene_name	log2FoldChange	Distance to TSS (bp)	padj
Pepd	-1.86583189	-1559	2.8700E-18
Akt2	-1.414015875	-140	8.0700E-05
Cd48	-1.410194449	0	1.0300E-05
Itgam	-1.231783707	0	1.7200E-08
Rgs10	-1.057700285	0	1.2100E-13
Rgs19	-0.92803691	-277	1.8231E-02
Cmah	-0.85263055	0	2.1666E-04
Il2rb	-0.735947851	-347	2.7776E-02
Ccr9	-0.619785507	0	6.0859E-04
Il7r	-0.619656312	0	2.7247E-02

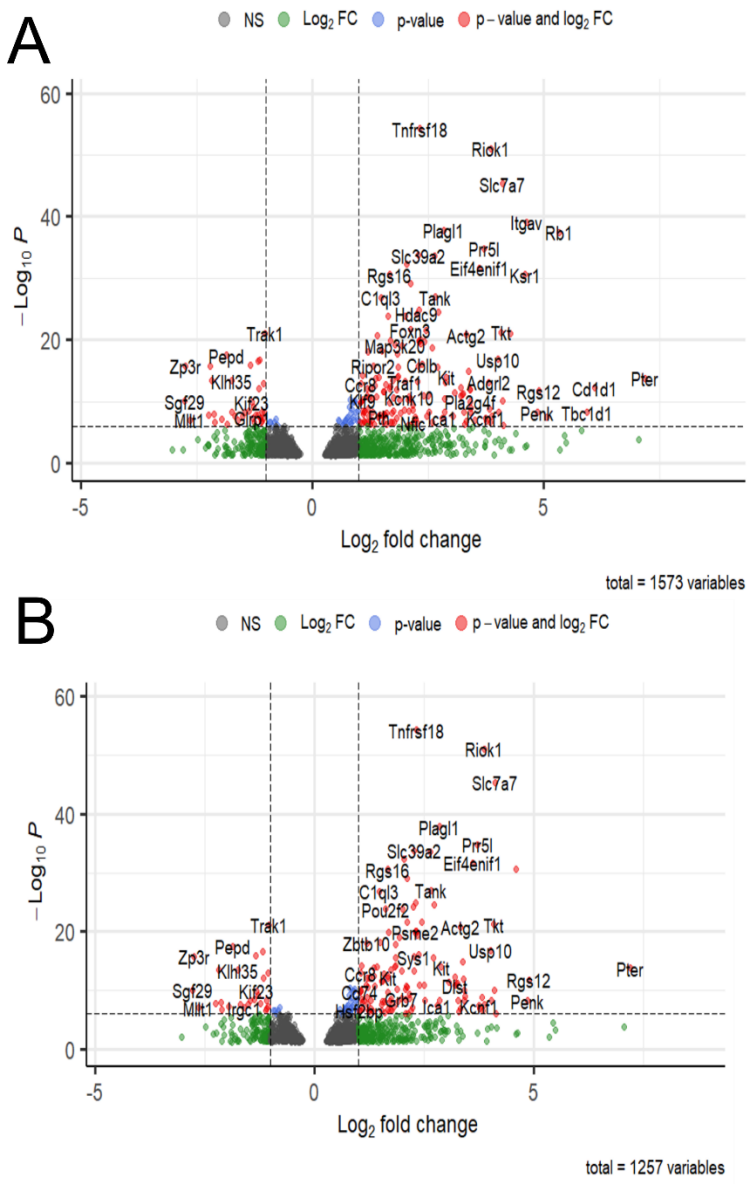

Figure 3-10: High affinity engagement with tissue-restricted antigen during development establishes a unique epigenetic "tolerance" profile in thymocytes.

A, Volcano plot showing differentially accessible regions across all possible annotated regions.

B, Volcano plot showing differentially accessible regions within 3000 bp (annotated as promoter region) of transcription start sites in OT-I Bim$^{-/-}$ > RIP-mOVA chimeras relative to OT-I Bim$^{-/-}$ > WT controls. Horizontal adjusted p-value threshold = 10e-6; vertical $\log_2$ fold change threshold = 1. Plot was generated using the R Bioconductor package EnhancedVolcano (274).

Table 3-3: Summary of functional annotations enriched in mature thymocytes from OT-I Bim$^{-/-}$ > RIP-mOVA chimeras.

GO ID	Description	Adjusted p-value
GO:0048523	negative regulation of cellular process	3.1172E-28
GO:0048583	regulation of response to stimulus	3.1172E-28
GO:0048731	system development	5.5680E-28
GO:0010646	regulation of cell communication	1.0832E-26
GO:0023051	regulation of signaling	1.1688E-26
GO:0009966	regulation of signal transduction	8.9244E-26
GO:0051239	regulation of multicellular organismal process	3.1122E-24
GO:0048870	cell motility	1.5987E-22
GO:0048513	animal organ development	4.5493E-22
GO:0016477	cell migration	1.0060E-21

Table 3-4: Summary of functional annotations under-represented in mature thymocytes from OT-I Bim$^{-/-}$ > RIP-mOVA chimeras.

GO ID	Description	Adjusted p-value
GO:0048731	system development	1.5825E-09
GO:0001775	cell activation	1.5189E-07
GO:0035556	intracellular signal transduction	1.5189E-07
GO:0030154	cell differentiation	1.5684E-07
GO:0051240	positive regulation of multicellular organismal process	1.5684E-07
GO:0048869	cellular developmental process	1.5684E-07
GO:0002521	leukocyte differentiation	1.8518E-07
GO:0016477	cell migration	1.8518E-07
GO:0046649	lymphocyte activation	1.8518E-07
GO:0045321	leukocyte activation	2.3997E-07

Table 3-5: Enrichment scores for transcription factor footprints in OT-I Bim$^{-/-}$ > RIP-mOVA relative to WT control.

Transcription factor hits are organized from most over-represented to most under-represented in RIP-mOVA chimeras relative to the WT control.

Transcription factor	Enrichment Score	Adjusted p-value
ZBTB33	0.145218686	5.31E-06
NFYB	0.077668738	1.51E-05
NFYA	0.065502445	6.28E-05
ZNF384	0.058396898	3.44E-28
Ahctf1	0.056327198	8.83E-08
CPEB1	0.053581969	8.43E-06
ASCL1	0.044179034	0.000912332
FOXC1	0.043772479	3.30E-09
Sox5	0.032405774	0.000328381
FOXP1	0.032386895	0.000819253
NFIC	0.027125052	3.68E-07
Ahr::Arnt	0.025614543	0.000819253
Arid3a	0.023549367	0.000348388
RREB1	-0.043471626	2.23E-06
FOS	-0.057070717	0.000551365
ZNF263	-0.058904132	7.76E-32
CTCF	-0.064364053	2.38E-27
CTCFL	-0.075345987	1.77E-31
Zfx	-0.075568042	7.90E-05
E2F6	-0.077864879	8.43E-06
ZNF143	-0.080631221	0.000982873
NRF1	-0.083155747	1.94E-12
SP2	-0.087092347	5.12E-62
RUNX2	-0.100815759	0.000123872
FOS::JUN(var.2)	-0.107981323	2.21E-06
SP3	-0.111354386	2.31E-34
KLF13	-0.111953635	9.55E-09
SP1	-0.113169283	4.20E-69
EGR4	-0.116592293	2.10E-06
Klf12	-0.121361717	2.72E-14
CREB1	-0.131212622	0.000225009
Crem	-0.157311544	4.48E-08
Atf2	-0.167956968	3.93E-15
FOSL1::JUND(var.2)	-0.177476137	8.62E-13
JUNB(var.2)	-0.1879324	3.37E-15

Discussion

Clonal deletion of strongly self-reactive thymocytes is a well-described mechanism of T cell central tolerance, however, potent non-deletional mechanisms also exist. Previously, we and others showed that while Bim is required for clonal deletion to TRA in OT-I $Bim^{-/-}$ > RIP-mOVA bone marrow chimeras (73), it is dispensable for tolerance (74, 75). In this chapter, I demonstrated that TRA-specific T cells that escape clonal deletion in these chimeras are rendered functionally impaired in a cell-intrinsic manner during antigen encounter in the thymus.

While the removal of autoreactive T cell clones via thymic clonal deletion has long been considered a primary mechanism for establishing T cell tolerance, conventional T cells that recognize self-peptides with high affinity can be readily found in healthy individuals (275). Like in the case of regulatory T cells, some of these T cells are actively selected for, while in other cases these T cells may be products of failed clonal deletion. By deleting Bim and blocking clonal deletion, a large population of highly self-reactive T cells are released into the periphery, yet tolerance is maintained (Fig. 3-2A) (74, 75). Similarly, recent studies in polyclonal mice have revealed limited deletion of TRA-specific T cells; rather, tolerance was enforced by Treg-mediated suppression (103), or T cell-intrinsic functional impairment (102, 276). Indeed, we and others previously observed an increased number and frequency of anergic-phenotype $CD4^{+}$ thymocytes and splenocytes when Bim was absent (57, 101). I observed functional impairment in thymocytes as well as in peripheral T cells, suggesting tolerance to TRA established by non-deletional means first occurs in the thymus (Fig. 3-4A-C). These data are consistent with the recent findings of Malhotra *et al.* where MHCII-restricted thymocytes specific for a TRA showed reduced responsiveness (102). Similar findings were reported for thymocytes in an allo-reactive

MHCI-restricted TCR transgenic model (242) and in a super-antigen mediated model of tolerance (277).

In previous studies where thymocytes were found to be functionally impaired, it was not determined if the impairment was due to cell-extrinsic dominant suppression or through cell-intrinsic mechanisms. In addition to $CD4^+$ $Foxp3^+$ Treg, there is mounting evidence supporting the existence of a $CD8^+$ T regulatory subset, but the precise signals controlling differentiation into this fate are not well understood (278). In our co-adoptive transfer experiments, neither the total splenocyte nor the $CD8^+$ T cell compartment appeared to contain dominant suppressors. In addition to previous *in vitro* work in our lab, these findings indicate that the functional impairment observed when clonal deletion is prevented is cell-intrinsic in nature. Furthermore, it would suggest that simple impairment of clonal deletion does not lead to the generation of $CD8^+$ T regulatory cells and that other factors are involved. However, it remains possible that the mechanisms of tolerance vary with the antigen, quantity of antigen, and presenting APC, as has been previously suggested (102, 103).

Using ATAC-seq, I characterized the epigenetic profile associated with the dysfunctional state displayed by mature thymocytes in our model. Our tolerant thymocytes displayed an epigenetic profile suggestive of commonalities with the exhausted state, as I detected accessible chromatin proximal to the promoters of genes previously linked with T cell exhaustion (*Nr4a1, Tnfrsf18,* and *Myb*) (251–259) (Table 3-1). *Nr4a1,* a member of the NR4A family of nuclear orphan receptors, is a transcription factor whose expression is associated with high affinity TCR signaling, reviewed in (251), and is thought to enforce T cell dysfunction in the context of tolerance and exhausted anti-tumour T cell responses (252, 253). *Tnfrsf18*, also known as Glucocorticoid-induced TNFR-related protein (GITR), is a co-stimulatory receptor that was

recently associated with exhausted T cells (PD-1^{hi} CTLA-4^{hi} CD38^{hi}) in a single-cell RNA-seq study of breast tumour infiltrates (254). GITR upregulation is thought to indicate ongoing TCR stimulation and promotes T cell activation, function, and survival (255). T cell dysfunction is known to emerge in response to chronic T cell activation, thus the upregulation of GITR alongside other co-stimulatory effector molecules speaks for the inherent relationship between dysfunctional and activated transcriptional signatures (279). *Myb* is a transcription factor important to cellular self-renewal in several contexts, most importantly for this discussion in CD8^{+} T cells (257, 258). *Myb* has recently been described as a key control point for the development and identity maintenance of self-renewing stem-like exhausted T cells (259). Conversely, I also detected accessible chromatin in the promoters of genes linked with normal T cell function and survival (*Ksr1, Il2,* and *Ifng*) (Table 3-1); expression of these genes has previously been shown to be down-regulated in the context of exhaustion (reviewed in (112)). *Ksr1,* or Kinase Suppressor of Ras1, has been posited as a positive modulator of the sensitivity of the MAPK cascade in T cells (280, 281). Among the first identified features of T cell exhaustion is the loss of capacity to produce IL-2, along with the capacities for proliferation and cytotoxic killing *ex vivo*; eventually, exhausted T cells are found incapable of producing significant levels of IFN-γ (reviewed in (282)). However, the enrichment of nucleosome-free regions (NFRs) at these loci does not necessarily indicate their enhanced expression. For example, post-transcriptional regulation of *Ifng* transcripts is known to limit IFN-γ production in dysfunctional tumour-infiltrating T cells (TILs) (283) and for numerous other cytokine transcripts in a DO11 CD4^{+} transgenic model for peripheral tolerance (284); accordingly, we previously showed mature T cells from OT-I Bim$^{-/-}$ RIP-mOVA chimeras to be poor producers of IFN-γ following *in vitro* stimulation (116). Thus, the epigenetic profile of tolerant TRA-specific thymocytes

demonstrates accessible chromatin in regions generally associated with both exhaustion and normal T cell function.

I detected an under-representation of AP-1 transcription factor foot-printing in dysfunctional thymocytes from OT-I $Bim^{-/-}$ > RIP-mOVA chimeras (Table 3-5). Decreased activity of this family of transcription factors has been linked to T cell dysfunction described for both exhaustion and anergy (114, 267), which in combination with our findings, suggests this feature is broadly shared among states of T cell dysfunction. Indeed, it has recently been proposed that Nur77 (*Nr4a1* gene), an immediate-early gene whose upregulation is dependent on the strength of the TCR signal (73), inhibits the activity of AP-1 transcription factors to restrict T cell function (252). While cooperation between transcription factors AP-1 and NFAT is important for productive T cell responses, NFAT activity without AP-1 promotes T cell dysfunction (107) (reviewed in (93)). AP-1 transcription factors are also thought to direct chromatin remodeling during T cell activation toward an epigenetic profile required for the effector phenotype – wherein additional regions containing AP-1 binding sites are unlocked and the shift toward an activated state is amplified (285). In the absence of co-stimulation in the form of CD28 engagement, nuclear translocation of AP-1 is drastically reduced, while this is only true to a small degree for the transcription factor NFAT (285). Following T cell activation, AP-1 transcription factors experience transient upregulation (286), whereas NFAT can be retained within the nucleus for longer periods even in response to minor increases in intracellular Ca^{2+} (287–289). The Rao group recently postulated that the elevated basal Ca^{2+} in chronically stimulated anergic/exhausted $CD8^{+}$ T cells may allow for chronic nuclear occupation by NFAT and therefore the maintenance of the dysfunctional state (107). In the present study, I did not observe significant enrichment of the NFAT foot-print in our tolerant ATAC-seq data set;

however, I did observe a mild enrichment of NFRs in the *Nfat2* promoter (Fold change = 1.37, padj = 0.007693). It is possible that in RIP-mOVA mice, tolerant OVA-specific OT-I $CD8^+$ cells progressively accumulate "signal memory" with chronic exposure to high affinity Ag, and that predominance of NFAT activity may emerge over time in the periphery.

As an example of shared features between dysfunctional T cell states, inhibitory receptors linked with exhaustion in the context of chronic viral infection such as PD-1 and Lag-3 have also been identified in other contexts such as cancer and tolerance (115, 282, 290–294). Similarly, I found elevated expression of PD-1 (but not other co-inhibitory molecules, Fig. 3-8) in the dysfunctional TRA-specific $CD8^+$ T cells in our model, suggesting it acts as a specific enforcer of non-deletional tolerance in this context (Fig. 3-7). I additionally sought to assess the expression of TCF1 and TOX in our model of tolerance, as these transcription factors have recently been under investigation for their suspected roles in stem-like "exhausted" T cell populations. The exhausted $CD8^+$ population is heterogenous, both functionally and phenotypically (140, 295). Progenitor exhausted T cells (T_{PEX}) are a self-renewing stem-like lymphoid-resident population characterized by TOX and TCF1 expression which seeds the terminally differentiated (T_{EX}) exhausted effector T cell population (135, 138, 141, 243–245). The development of the T_{PEX} population is also thought to be driven by MYB activity (259), whose promoter is enriched in chromatin of open conformation in our dysfunctional T cell model (Table 3-1). Indeed, I found elevated TOX expression associated with T cell dysfunction in pancreatic lymph nodes our model (Fig. 3-6), similar to what has recently been observed during the course of type I diabetes (T1D) in non-obese diabetic (NOD) mice (244). Meanwhile, I failed to observe elevated TCF1 expression associated with dysfunction (Fig. 3-6), whose continuous

expression is thought to characterize T_{PEX} (reviewed in (245)). Thus, dysfunctional T cells in our model only share some canonical features associated with stem-like exhaustion.

There has been increasing interest in the epigenetic landscape of dysfunctional T cell states. On one hand, if a dysfunctional epigenetic state is inflexible, this would help to explain the maintenance of normal T cell tolerance in a complex milieu of stimuli. On the other hand, inflexibility presents a challenge for immunotherapies seeking to rescue dysfunctional immune responses with the end goal of viral or tumour clearance. I detected under-representation of the foot-printing of additional transcription factors positively associated with T cell function: CREB1, a positive modulator of cytotoxic $CD8^+$ T cell function (222), and KLF13, a transcription factor thought to support normal thymocyte apoptosis (268) and activation (269). I saw enrichment in the foot-print of FOXP1, thought to maintain naïve T cell quiescence through negative regulation of MAPK signaling and IL-7 responsiveness (271, 272). FOXP1 has also been shown to be upregulated in tumour-infiltrating T cells and represses anti-tumour immunity (273). These additional transcription factor foot-prints differentially represented in our tolerant thymocytes further explain the T cell dysfunction I observed. In contrast, I also recorded under-representation of the foot-print of EGR4, a zinc finger transcription factor thought to restrict T cell activation and effector function (270).

Whether persistent Ag is required to maintain T cell dysfunction is likely dependent on the model utilized, as evidence exists both in favour (109, 116–118) and against its requirement (115, 296). Nevertheless, cessation of chronic exposure to Ag may aid in resetting nuclear occupancy by NFAT and allow for normal NFAT:AP-1 activity to occur again, releasing the "epigenetic lockdown". Finally, blocking of inhibitory receptor PD-1 has seen variable success in "reinvigorating" exhausted T cell responses. Mechanistic studies of these treatments have

suggested the dysfunctional T cell epigenetic program stands as an obstacle to their success (296). Overall, the epigenetic profile of dysfunctional thymocytes in our model demonstrates features both positively and negatively associated with T cell function, which has been observed in other models, as discussed above. Accessible chromatin in genes positively associated with T cell function such as the *Tnfrsf18* (GITR, a co-stimulatory receptor) promoter represent the potential for rescue from the dysfunctional state. Indeed, simultaneous PD-1-blocking and GITR agonizing bi-specific antibody treatment was recently proposed as an optimized strategy beyond singly target PD-1 in cancer immunotherapies (256).

Collectively, I have characterized a state of T cell-intrinsic tolerance established upon encounter with high affinity TRA during thymocyte selection in the absence of clonal deletion. This study details the first description of the epigenetic profile of tolerant $CD8^+$ TRA-specific thymocytes. Based on its elevated expression in OT-I $Bim^{-/-}$ > RIP-mOVA chimeras, I have implicated PD-1 as an enforcer of this dysfunctional state. The following chapter will investigate this further, which, in combination with our defined epigenetic profile, will provide insight into how this dysfunctional state is established and maintained.

Chapter 4 - Signaling through PD-1 is required to establish and maintain tolerance to TRA

This chapter contains content originally published in The Journal of Immunology:

- May, J. F., R. G. Kelly, A. Y. W. Suen, J. Kim, J. Kim, C. C. Anderson, G. R. Rayat, and T. A. Baldwin. 2024. Establishment of CD8+ T Cell Thymic Central Tolerance to Tissue-Restricted Antigen Requires PD-1. J. Immunol. Vol 212 (2): 271-283. Copyright © [2024] The American Association of Immunologists, Inc.

Introduction

In the previous chapter, I investigated the phenotypic and functional profile of tolerant transgenic $CD8^+$ T cells that escape clonal deletion in OT-I $Bim^{-/-}$ > RIP-mOVA chimeras. Tolerance in this context is characterized by an epigenetic profile sharing features with T cell exhaustion and cell-intrinsic functional impairment established in the thymus. The tolerance I observed was robust, even in the absence of clonal deletion, suggestive of a non-deletional mechanism that begins in the thymus and persists in the periphery. Due to increased PD-1 expression in the thymus of OT-I $Bim^{-/-}$ > RIP-mOVA chimeras (Fig. 3-8), in this chapter, I wished to explore the extent and mechanism by which PD-1 contributed to tolerance, especially since a majority of studies have limited their investigations in its role to mature T cells in the periphery (77).

Programmed cell death protein 1 (PD-1) is an inducible co-inhibitory receptor expressed on T cells, B cells, and some subsets from the myeloid lineage (297). PD-1 ligation impairs T cell responses and thus PD-1 blockade forms the basis for some promising cancer immunotherapies by improving the function of anti-tumour $CD8^+$ T cells in the tumour microenvironment, reviewed in (298). PD-1 is thought to function through its recruitment of the

phosphatase SHP2, which negatively regulates the activation of TCR-proximal signaling molecules (299) and CD28-driven co-stimulation (165, 300). On lymphocytes at steady state, PD-1 expression is limited to a small fraction of thymic and peripheral cells, but is induced on thymocytes and peripheral T cells following strong TCR interactions (160, 301). The ligands for PD-1, PD-L1 and PD-L2, are expressed on the thymic epithelium and professional antigen presenting cells in the thymus and throughout the periphery (302, 303). PD-1 deficiency results in autoimmunity in pre-clinical models (159) and single nucleotide polymorphisms in PD-1 are linked to autoimmunity in humans (304–306). In the thymus, transgenic overexpression of PD-1 has been shown to modulate positive selection (174), while PD-1 deficiency in UbA-mediated models of negative selection showed little or no impact (177, 307). Studies examining a role for PD-1 in thymic tolerance induced by TRA are currently lacking.

Thus far, I explored the fate and function of MHCI-restricted thymocytes specific for a TRA in the absence of clonal deletion. To investigate the requirements for tolerance in OT-I $Bim^{-/-}$ > RIP-mOVA chimeras, I used genomic and transplantation strategies to manipulate the PD-1 signal in the context of this model.

Results

PD-1 signals in the T cell compartment necessarily support tolerance to TRA

Given that I observed enhanced PD-1 expression on tolerant OT-I $CD8^+$ T cells from OT-I $Bim^{-/-}$ > RIP-mOVA chimeras and that previous literature supports a role for PD-1 in enforcing tolerance in general (297), I hypothesized that PD-1 was playing an active role in establishing and/or maintaining the functional impairment seen in TRA-specific T cells that escaped clonal deletion in OT-I $Bim^{-/-}$ > RIP-mOVA chimeras.

Work by previous students in our lab determined that PD-1 is required for tolerance in the OT-I$^{-/-}$ > RIP-mOVA model, but was not required for clonal deletion (116); we also previously observed 100 % incidence of diabetes in OT-I PD-1$^{-/-}$ > RIP-mOVA chimeras compared to 0 % in OT-I WT > RIP-mOVA controls. In the present study, I generated chimeras with a 1:9 ratio of OT-I (WT or PD-1$^{-/-}$) to non-transgenic BM to better approximate endogenous frequencies of self-reactive T cells. I found recipients of OT-I PD-1$^{-/-}$ BM still developed diabetes, but that disease onset was delayed and penetrance was not complete, suggesting that disease in this model is not simply an artifact of supra-physiological numbers of OVA-specific CD8^{+} T cells (Fig. 4-1). These findings suggested that only a fraction of the overall pool of OT-I T cells needed to be PD-1$^{-/-}$ to induce autoimmunity and further supports the case that functional impairment of OT-I T cells in OT-I Bim$^{-/-}$ > RIP-mOVA was cell intrinsic and not due to a population of dominant suppressors.

To provide further support for the idea that PD-1 signals received during thymic selection contributed to tolerance in OT-I Bim$^{-/-}$ > RIP-mOVA chimeras, I stimulated thymocytes and splenocytes from these chimeras alongside those from OT-I Bim$^{-/-}$ PD-1$^{-/-}$ > RIP-mOVA chimeras and evaluated whether ablating PD-1 on a Bim$^{-/-}$ background would restore functionality. Activation marker induction (CD69 and CD25) was enhanced in the absence of PD-1 in the thymus and spleen, suggesting that PD-1 is an enforcer of tolerance in the absence of clonal deletion. Proliferation was enhanced when PD-1 was absent in peripheral T cells, but this trend was not statistically significant for thymocytes (Fig. 4-2).

To determine whether PD-1 signaling specifically within the T cell compartment was necessary to induce tolerance, I conditionally deleted PD-1 in CD8^{+} T cells using *pdcd1* floxed mice. CD8-Cre mice were intercrossed with OT-I, constitutive PD-1$^{-/-}$, and *pdcd1* floxed mice to

generate OT-I CD8-Cre PD-1$^{fl/ko}$ mice. Single-positive (SP) thymocytes can be further subsetted based on their maturity and susceptibility to negative selection; semi-mature (SM, TCRβ^{+} H-2K$^{b\ lo}$) SP thymocytes undergo apoptosis following strong TCR stimulation, while the subsequent mature 1 (M1, TCRβ^{+} H-2K$^{b\ hi}$ CD69^{hi}) and mature 2 (M2, TCRβ^{+} H-2K$^{b\ hi}$ CD69^{lo}) subsets become activated similarly to naïve peripheral T cells (reviewed in (88)). In OT-I CD8-Cre PD-1$^{fl/ko}$ > RIP-mOVA chimeras, the loss of PD-1 became evident at the SM-M1 CD8SP thymocyte stages (Fig. 4-3A) and all OT-I CD8-Cre PD-1$^{fl/ko}$ > RIP-mOVA chimeras experienced rapid onset of diabetes while OT-I CD8-Cre PD-1$^{fl/wt}$ > RIP-mOVA chimeras were protected (Fig. 4-3B). Therefore, PD-1 signaling specifically within the CD8^{+} T cell compartment is required to establish tolerance in this model. Here and in subsequent diabetes analyses, I euthanized mice from some groups early for the purpose of *ex vivo* analysis (indicated by tick marks). Thus, mice from some groups were not followed to the end of the study, and therefore in some cases our reported incidence of diabetes may be underestimated. The Kaplan-Meier graphs depicting the percentage of mice remaining diabetes-free is accurate as the data points censored early are not included in this calculation.

I additionally wished to determine whether the manifestation of diabetes in OT-I PD-1$^{-/-}$ > RIP-mOVA chimeras was in any manner influenced by a lack of CD4^{+} T cells competent for T regulatory cells (Treg) differentiation. I generated chimeras with a 1:1 ratio of OT-I (PD-1$^{-/-}$ or PD-1$^{+/-}$) to OT-II (WT, MHCII-restricted transgenic TCR, similarly specific for a peptide derived from chicken ovalbumin) (228). Despite delayed onset of disease, all RIP-mOVA recipients of OT-I PD-1$^{-/-}$ + OT-II marrow developed diabetes, albeit at a significantly later time point than was the case for the OT-I PD-1$^{-/-}$ control (Fig. 4-4). A caveat here is that I did not successfully collect Foxp3-staining data from this experiment, meaning that I did not observe the extent to

which OT-II marrow generated Treg cells. However, overall these results suggest that the presence of MHCII-restricted T cells is not sufficient for protection from diabetes in this model, suggesting that non-tolerant $CD8^+$ OT-I T cells drive disease independently from the $CD4^+$ subset.

To further solidify that the deletion of PD-1 specifically and not any co-inhibitory receptor impaired tolerance in this context, I investigated whether deletion of B and T lymphocyte attenuator (BTLA) impaired tolerance. BTLA is a co-inhibitory receptor expressed on thymocytes following positive selection (308), and has been thought to play a similar role to PD-1 in regulating T cell tolerance (225). I generated OT-I $BTLA^{-/-}$ > WT or RIP-mOVA chimeras and found that frequencies of DP and CD8SP thymocytes remained largely unaltered when BTLA was ablated (Fig. 4-5A), and that these chimeras did not develop diabetes, suggesting that elimination of just any co-inhibitory receptor does not impair tolerance (Fig. 4-5B). Finally, the absolute number of $V\alpha2^+$ CD8SP $CD24^{lo}$ thymocytes was significantly reduced in both $BTLA^{-/-}$ and WT control RIP-mOVA chimeras, suggesting that clonal deletion was intact in the absence of BTLA (Fig. 4-5C).

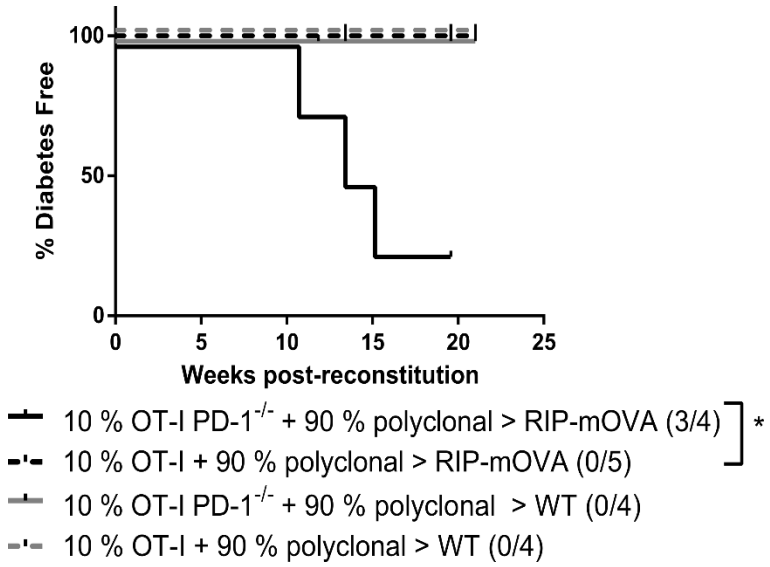

Figure 4-1: A minority of PD-$1^{-/-}$ TRA-specific $CD8^{+}$ T cells in the T cell compartment is sufficient to induce autoimmunity.

Incidence of diabetes in RIP-mOVA chimeras with a 1:9 mix of OT-I (PD-$1^{-/-}$ or WT) and polyclonal non-transgenic BM. Data were generated from two separate cohorts of chimeras. Asterisks represent statistical significance as determined by Log-rank test.

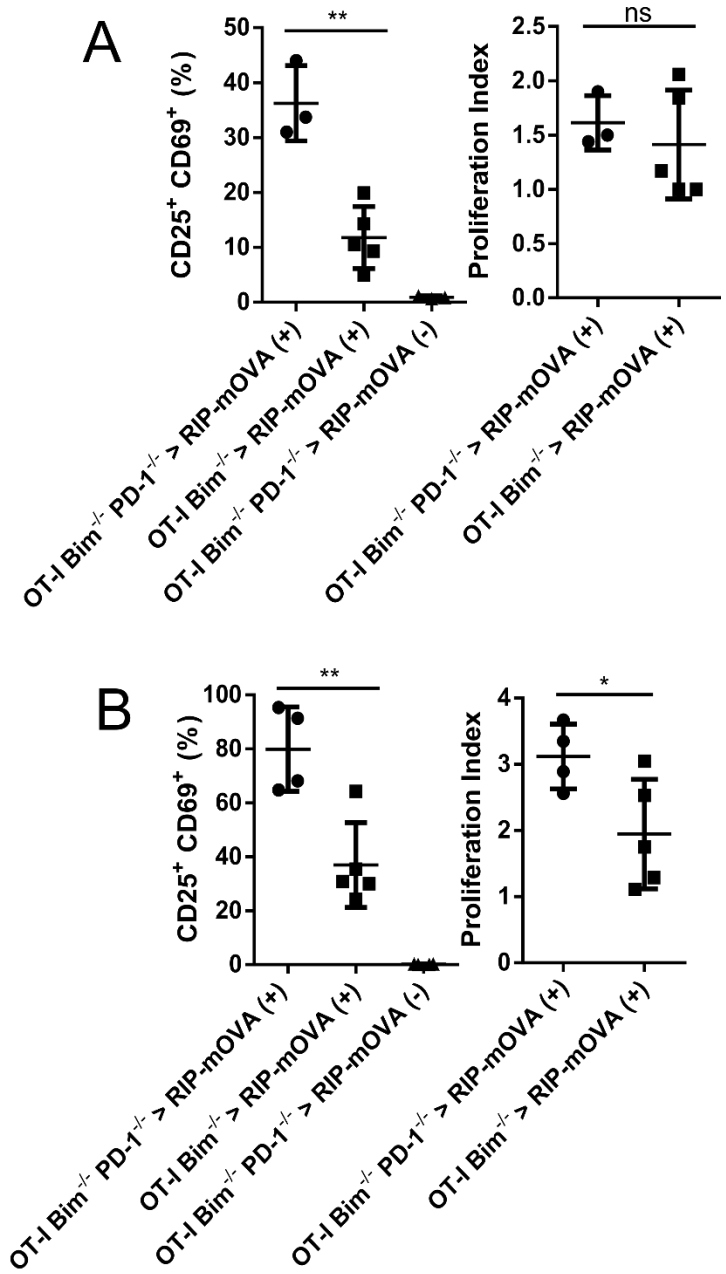

Figure 4-2: The absence of PD-1 enhances functionality in TRA-specific $CD8^+$ T cells from OT-I $Bim^{-/-}$ > RIP-mOVA chimeras.

Activation marker induction and compiled proliferation indices of OT-I $Bim^{-/-}$ > RIP-mOVA or OT-I $Bim^{-/-}$ $PD\text{-}1^{-/-}$ > RIP-mOVA thymocytes (A), and splenocytes (B) following *in vitro* stimulation. The number of independent experiments (IE) ≥ 3. Asterisks represent statistical significance as determined by unpaired T-test with Welch's correction.

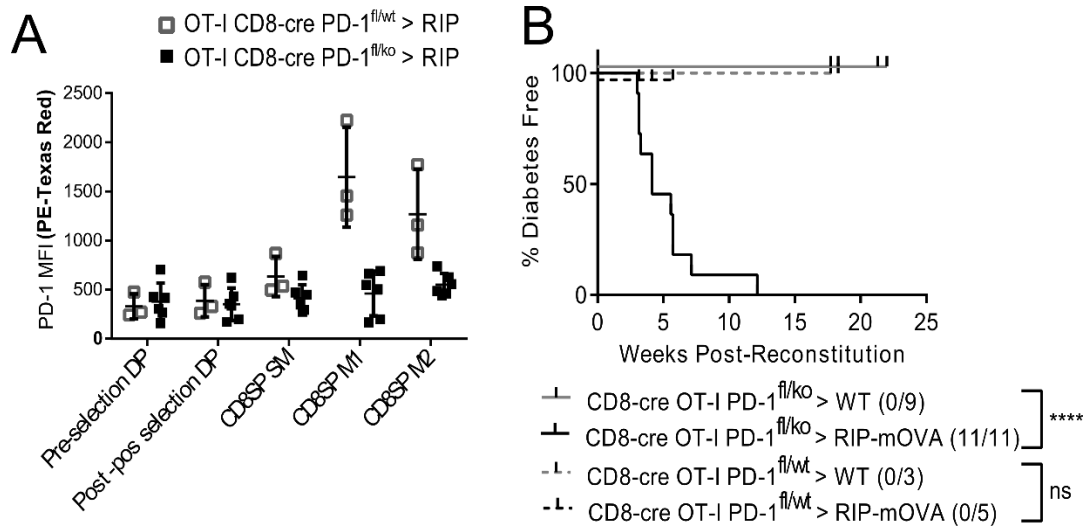

Figure 4-3: Conditional PD-1 ablation at the single-positive stage is sufficient for the induction of autoimmunity.

A, PD-1 expression in RIP-mOVA chimeras with OT-I CD8-cre PD-$1^{fl/wt}$ or PD-$1^{fl/ko}$ bone marrow. PD-1 expression was analyzed within the PD-1^{+} subset within each population shown. Pre-selection DP thymocytes ($CD69^{lo}$ $TCR\beta^{lo}$), post-positive selection DP ($CD69^{hi}$ $TCR\beta^{hi}$), SM thymocytes ($TCR\beta^{+}$ H-$2K^{b\ lo}$), M1 thymocytes ($TCR\beta^{+}$ H-$2K^{b\ hi}$ $CD69^{hi}$), M2 thymocytes ($TCR\beta^{+}$ H-$2K^{b\ hi}$ $CD69^{lo}$). B, Incidence of diabetes in RIP-mOVA or WT chimeras with CD8-cre OT-I PD-$1^{fl/ko}$ or PD-$1^{fl/WT}$ bone marrow; PD-$1^{fl/WT}$ > RIP-mOVA chimeras were sacrificed alongside their PD-$1^{fl/ko}$ counterparts to confirm the timing of PD-1 ablation. For each assay described above, the number of independent experiments (IE) ≥ 3. Asterisks represent statistical significance as determined by Log-rank test.

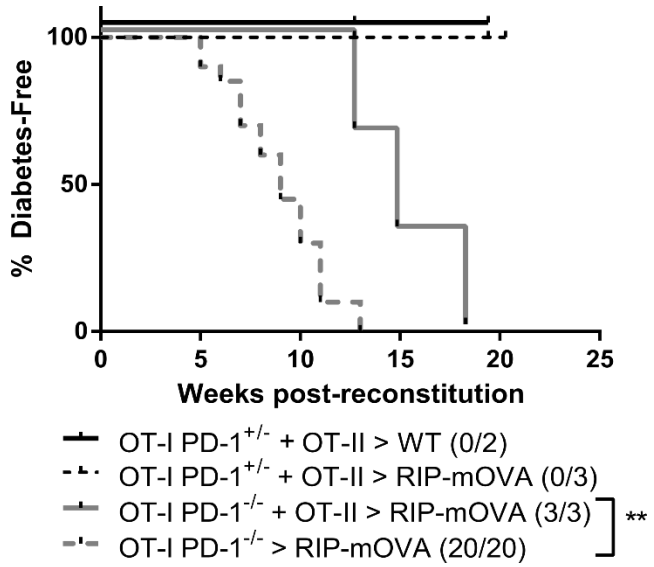

Figure 4-4: Co-transfer of OVA-specific MHCII-restricted OT-II marrow delays the onset of diabetes driven by OT-I PD-$1^{-/-}$ $CD8^{+}$ T cells.

Incidence of diabetes in RIP-mOVA or WT chimeras reconstituted with a 1:1 ratio of OT-I (PD-$1^{-/-}$ or PD-$1^{+/-}$) and OT-II (WT) marrow. Asterisks represent statistical significance as determined by Log-rank test.

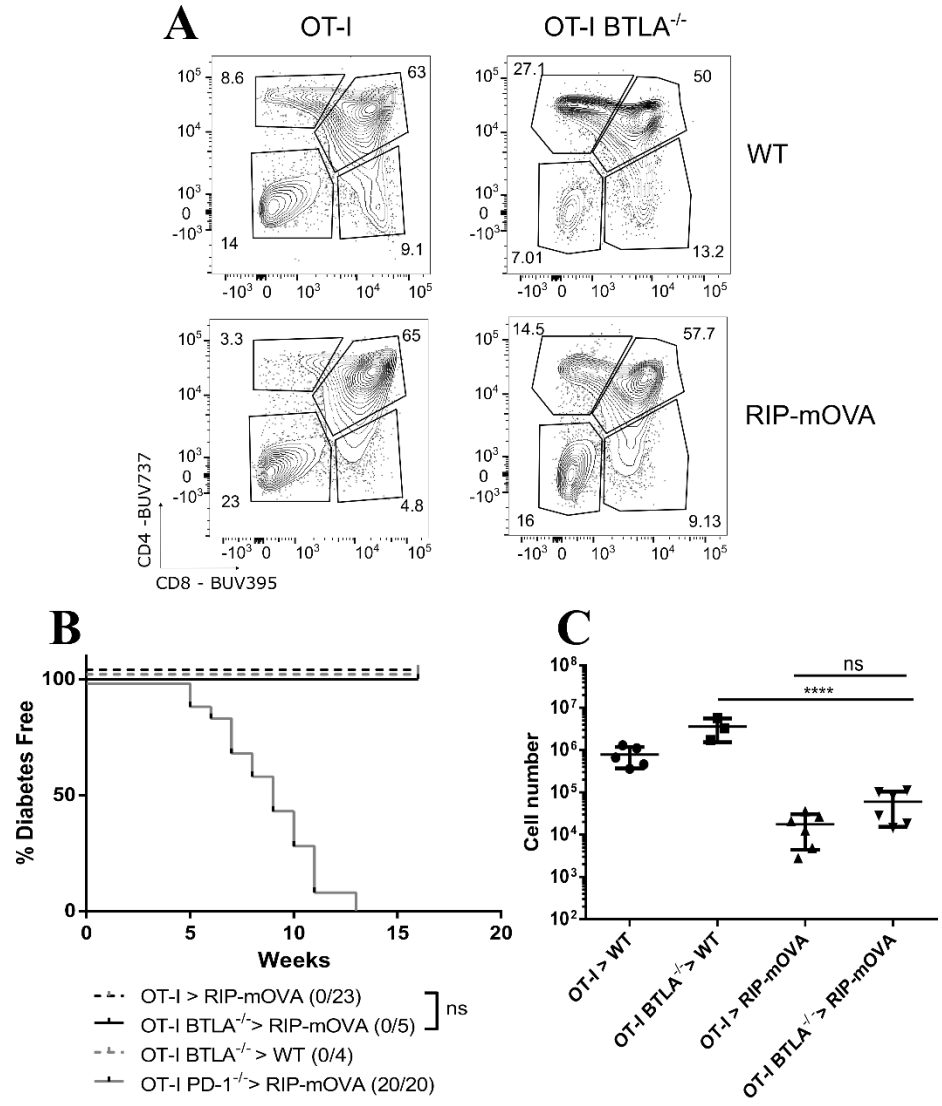

Figure 4-5: Co-inhibitory molecule BTLA is not required for tolerance to TRA in the OT-I > RIP-mOVA model.

A, Thymic profiles of WT or BTLA$^{-/-}$ OT-I > RIP or B6 chimeras. B, Incidence of diabetes in RIP-mOVA or WT chimeras with BTLA$^{-/-}$ (IE = 2) or WT bone marrow. C, Number of mature Vα2^{+} CD8SP CD24^{lo} thymocytes in the chimeras described in (A); OT-I > WT (n = 5), OT-I BTLA$^{-/-}$ > WT (n = 3), OT-I > RIP-mOVA (n = 6), OT-I BTLA$^{-/-}$ > RIP-mOVA (n = 6). Asterisks represent statistical significance as determined by Log-rank test (B) or two-way ANOVA with Sidak's multiple comparisons tests (C).

Acute PD-1 signaling within the thymic compartment is sufficient to induce tolerance to TRA that endures through anti-PD-1 blockade and the withdrawal of PD-L1-mediated signaling

I next investigated the specific requirements for the PD-1-driven tolerance induced in OT-I $Bim^{-/-}$ > RIP-mOVA chimeras. Given that OT-I T cells from OT-I $Bim^{-/-}$ > RIP-mOVA chimeras expressed PD-1 and are ostensibly impaired in a cell-intrinsic manner, I asked whether PD-1-dependent tolerance required continued PD-1 signaling or was stable even when PD-1 signaling was withdrawn. To address this question, I administered anti-PD-1 blocking antibodies to OT-I > RIP-mOVA or OT-I $Bim^{-/-}$ > RIP-mOVA bone marrow chimeras (some replicates for this experiment were carried out by previous student, Rees Kelly). This treatment failed to break tolerance, suggesting tolerance was stable even when PD-1 signaling was presumably interrupted (Table 4-1). Work from a previous student mirrored this result *in vitro*, as the addition of anti-PD-1 monoclonal antibodies failed to enhance the responses of TRA-specific $CD8^+$ T cells from OT-I $Bim^{-/-}$ > RIP-mOVA chimeras stimulated with OVA peptide-pulsed splenocytes.

Given potential limitations with the use of antibody-mediated blockade, I moved to an adoptive transfer approach with PD-$L1^{-/-}$ recipients. Since PD-L2 is another ligand for PD-1, I first determined if PD-L2 could compensate for the loss of PD-L1 and enforce tolerance in PD-$L1^{-/-}$ recipients. I generated OT-I $Bim^{-/-}$ > RIP-mOVA PD-$L1^{-/-}$ bone marrow chimeras and found these chimeras rapidly became diabetic, while those heterozygous for PD-L1 did not, suggesting PD-L2 could not compensate for the loss of PD-L1 in inducing or maintaining tolerance in this setting (Fig. 4-6). I then adoptively transferred splenocytes from OT-I $Bim^{-/-}$ > RIP-mOVA chimeras into sub-lethally irradiated RIP-mOVA PD-$L1^{-/-}$ recipients to acutely cease PD-L1-

dependent signaling (detailed in Fig. 4-7). In contrast to non-tolerant controls, most RIP-mOVA PD-L1$^{-/-}$ recipients that received OT-I Bim$^{-/-}$ > RIP-mOVA splenocytes did not become diabetic, and in the recipients in which diabetes was observed, disease was late-onset (Fig. 4-8A). 4 of the 12 recipients for this group were removed from the study at 8 weeks (indicated by tick-marks); while they may have become diabetic at later time points, they nevertheless remained healthy past the time where all positive control mice became diabetic. This suggested that a continuous PD-1 signal mediated by PD-L1 is not required for the maintenance of tolerance, but in the absence of PD-L1-mediated signals, tolerance wanes over extended periods of time.

Since functional impairment in tolerant chimeras is observable in thymocytes, I hypothesized that PD-1 signaling within the thymic compartment may be sufficient to establish tolerance in this model. To address this, I collected thymocytes from OT-I Bim$^{-/-}$ > RIP-mOVA chimeras and transferred them into sub-lethally irradiated RIP-mOVA PD-L1$^{-/-}$ recipients so that PD-1 signaling would be limited to the thymus. Like the splenocyte adoptive transfer, transferred thymocytes remained tolerant for an extended period in contrast to non-tolerant controls, with tolerance waning at late time points in some cases (Fig. 4-8B). These data suggest that acute PD-1 signaling in the thymus is sufficient for the establishment of tolerance, but continued PD-L1-dependent signals only support the maintenance of tolerance at late time points.

Table 4-1: Incidence of diabetes in chimeras treated with αPD-1 antagonist antibody or isotype control.

Chimera	**OT-I > RIP-mOVA**			**OT-I Bim$^{-/-}$ > RIP-mOVA**		
Treatment	None	αPD-1 (J43)	Isotype	None	αPD-1 (J43)	Isotype
Incidence of Diabetes	0/23	0/4	0/2	0/33	0/4	0/2

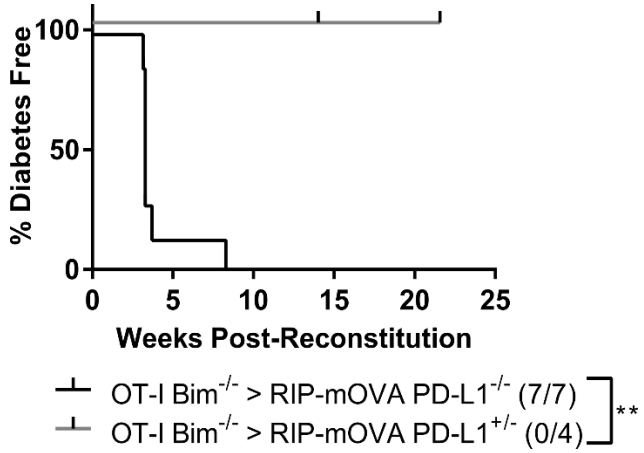

Figure 4-6: PD-L1 expression is required on cells of non-hematopoietic origin to establish tolerance.

Incidence of diabetes in OT-I Bim$^{-/-}$ > RIP-mOVA PD-L1$^{-/-}$ chimeras.

The number of independent experiments ≥ 3. Asterisks represent statistical significance as determined by Log-rank test.

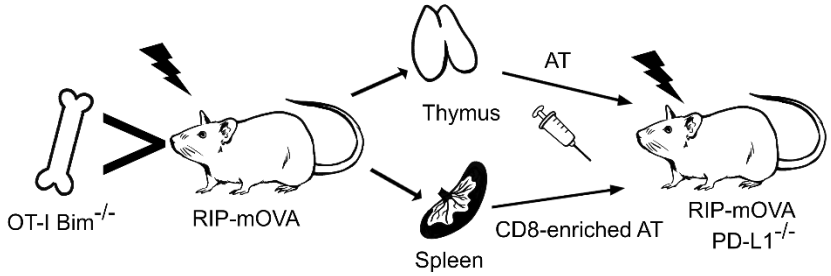

Figure 4-7: Schematic demonstrating experiments depicted in Figure 4-8.

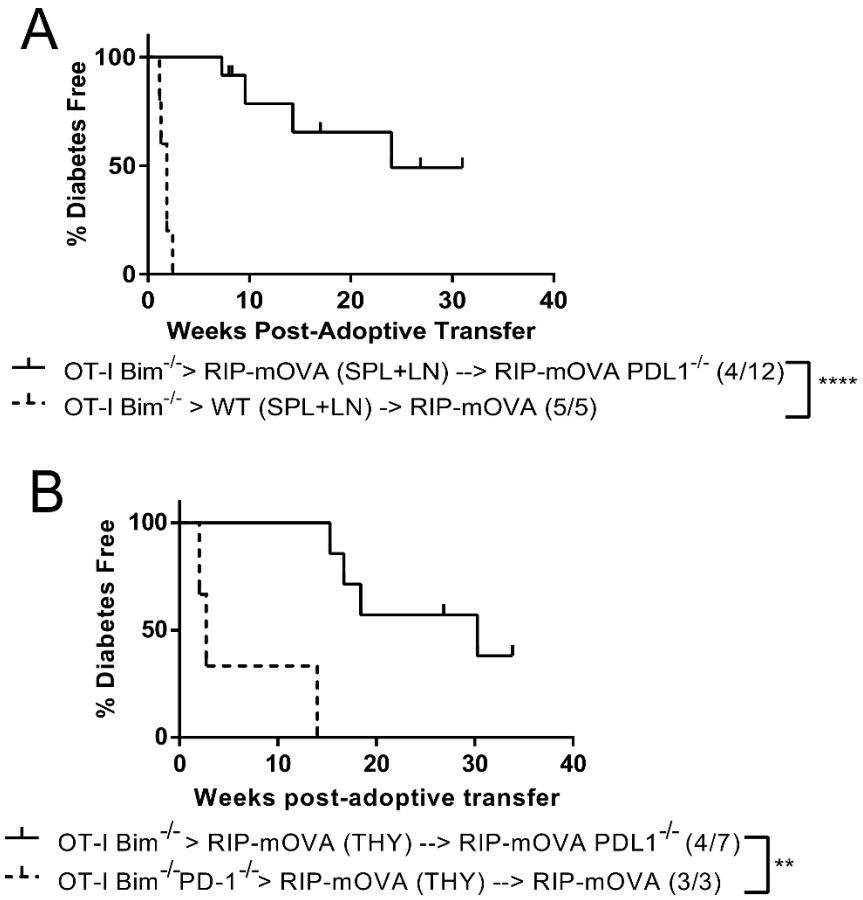

Figure 4-8: Acute PD-1 signaling within the thymic compartment is sufficient to induce tolerance to TRA.

A, Incidence of diabetes in sub-lethally irradiated RIP-mOVA PD-L1$^{-/-}$ recipients of adoptively transferred CD8-enriched CD8^{+} Vα2^{+} splenocytes from OT-I Bim$^{-/-}$ > RIP-mOVA chimeras. B, Incidence of diabetes in sub-lethally irradiated RIP-mOVA PD-L1$^{-/-}$ recipients of adoptively transferred thymocytes from OT-I Bim$^{-/-}$ > RIP-mOVA chimeras. Asterisks represent statistical significance as determined by Log-rank test.

CRISPR-mediated ablation of PD-1 results in a loss of tolerance in CD8$^+$ OT-I T cells from OT-I Bim$^{-/-}$ > RIP-mOVA chimeras

To further explore whether continuous PD-1 signaling was required for the maintenance of tolerance, I devised an alternate approach for interrupting the PD-1 signal. I enriched CD8$^+$ OT-I T cells from the spleens of OT-I Bim$^{-/-}$ > RIP-mOVA chimeras, used CRISPR to ablate the PD-1 locus, and immediately transferred these cells into sub-lethally irradiated RIP-mOVA recipients using a protocol described by Nüssing *et al.* 2020 (309). A portion of these nucleofected cells were rested *in vitro* for 2 days in the presence of IL-7 (10 ng/mL) before stimulation with anti-CD3/anti-CD28 plate-bound antibodies to assess the efficiency of PD-1 deletion, which I found to range between 60-80 % (Fig. 4-9). I found that cells from OT-I Bim$^{-/-}$ > RIP-mOVA chimeras that had experienced PD-1 deletion rapidly lost their tolerant state in contrast to cells that received control (non-PD-1-targeting) gRNA/Cas9 treatments (Fig. 4-10). In contrast to adoptive transfers of TRA-specific T cells from OT-I Bim$^{-/-}$ > RIP-mOVA into RIP-mOVA PD-L1$^{-/-}$ recipients (Fig. 4-8), interruption of the PD-1 signal via CRISPR-mediated ablation of PD-1 reverses the tolerance I observed in OT-I T cells from OT-I Bim$^{-/-}$ > RIP-mOVA chimeras, suggesting that continuous signaling through PD-1 is required to maintain tolerance.

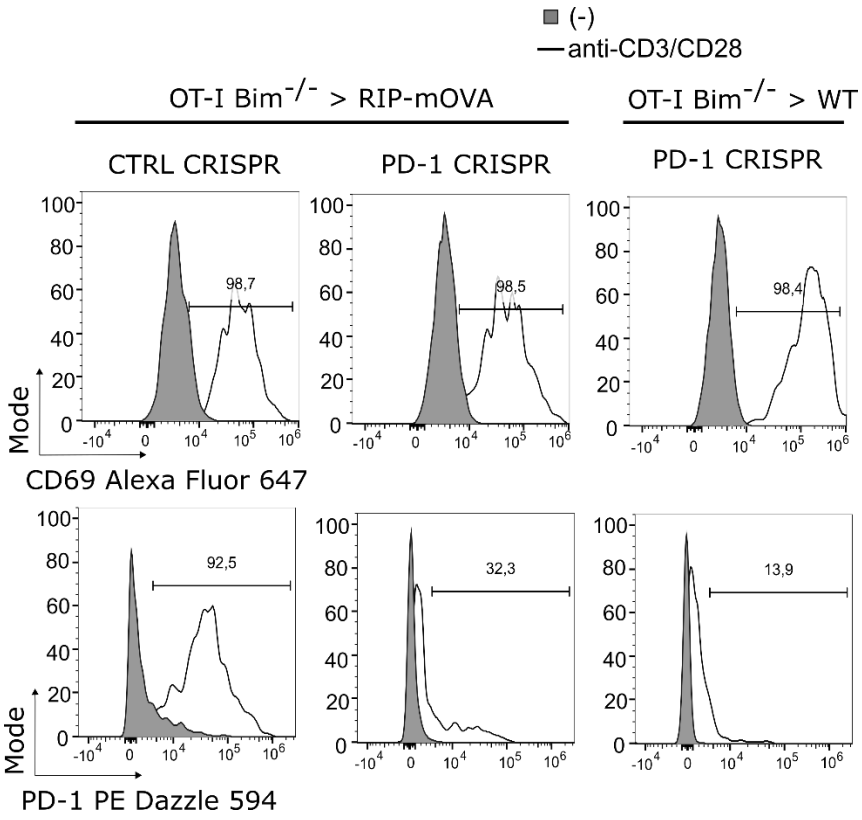

Figure 4-9: Successful deletion of PD-1 via CRISPR.

Representative histograms of PD-1 surface expression in CD8-enriched splenocytes from OT-I $Bim^{-/-}$ > RIP-mOVA chimeras electroporated with PD-1-targeting or control gRNA/Cas9 ribonucleoprotein complexes following stimulation with anti-CD3/anti-CD28 plate-bound antibodies for 2 days. Data is representative of cohorts described in Figure 4-10.

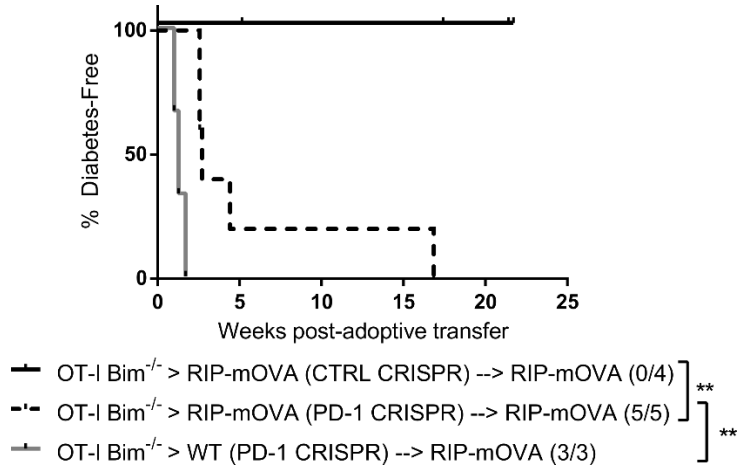

Figure 4-10: CRISPR-mediated ablation of PD-1 results in a loss of tolerance in OT-I T cells from OT-I Bim$^{-/-}$ > RIP-mOVA chimeras.

Incidence of diabetes in adoptive transfer recipients of CD8-enriched splenocytes from OT-I Bim$^{-/-}$ > RIP-mOVA chimeras electroporated with PD-1-targeting or control gRNA/Cas9 ribonucleoprotein complexes. The number of independent experiments (IE) ≥ 7. Asterisks represent statistical significance as determined by Log-rank tests.

Discussion

It is known that the co-inhibitory receptor PD-1 plays a role in regulating T cell function and is induced in DP thymocytes following strong TCR signaling. In the 2C TCR transgenic model of negative selection, PD-1 deficiency resulted in enhanced generation of DN thymocytes (307), suggesting the absence of PD-1 may substantially impact selection. However, no such effect was observed in MHCI- or MHCII-restricted male antigen reactive TCR transgenic models (177). In Chapter 3, I found that PD-1 was induced on OT-I CD8SP thymocytes that survived deletion in RIP-mOVA recipients. Previously, work in our lab established that deletion of PD-1 did not dramatically affect the number of OT-I CD8SP thymocytes in RIP-mOVA chimeras,

although there were increased numbers of OT-I T cells in the spleen and pancreatic lymph nodes of these mice (116), as was similarly observed for myelin oligodendrocyte glycoprotein (MOG)-specific $CD4^+$ T cells on a polyclonal background (310). I think it is unlikely that tolerance was broken in the absence of PD-1 (Fig. 4-1 and 4-3) due to the elevated numbers of Ag-specific cells, but rather that PD-1 signaling induced a tolerogenic program in the OT-I T cells, since OT-I $Bim^{-/-}$ > RIP-mOVA chimeras contain substantially more OT-I T cells than OT-I PD-$1^{-/-}$ > RIP-mOVA counterparts and tolerance was still enforced in OT-I $Bim^{-/-}$ T cells (74, 75).

PD-1 has primarily been investigated for its role in peripheral tolerance by limiting reactivation, function, and trafficking of self-reactive T cells (297), but a role for PD-1 in establishing tolerance in the thymus has not be reported. I found that PD-1 expression on thymocytes (Fig. 4-3) and PD-L1 expression on non-hematopoietic cells during development in the thymus were required to establish tolerance, since OT-I $Bim^{-/-}$ PD-$1^{-/-}$ > RIP-mOVA (116) and OT-I $Bim^{-/-}$ > PD-$L1^{-/-}$ RIP-mOVA chimeras (Fig. 4-6) rapidly developed diabetes. These data suggest it is during first encounter with high affinity antigen – in the thymus or periphery – that PD-1 signals are important for establishing tolerance, which is in contrast to previous studies (189, 311–313) proposing only a minor role for PD-1 in early tolerance induction (see review (314)). Indeed, it was recently shown that PD-1 could delay lethal autoimmunity in *Aire*$^{-/-}$ mice (315). In the absence of AIRE in this model, many TRA would not be expressed in the thymus and instead would be first encountered in the periphery, where concurrent PD-1 signals induced protection against autoimmunity. That PD-1 signaling during thymic selection is sufficient to induce tolerance is further supported by Thangavelu *et al.* where PD-1-deficiency in polyclonal thymocytes or recent thymic emigrants, but not established peripheral T cells, precipitated a lethal, multi-organ autoimmunity when adoptively transferred into $Rag^{-/-}$ recipients (177).

Finally, tolerance failed to establish and intestinal inflammation and mortality was driven by naïve OT-I T cells in iFABP-OVA mice when PD-L1 blockade treatment was administered the day of adoptive transfer, but not 30 days later (188).

When assessing the degree to which PD-1 was responsible for maintaining tolerance in the periphery, I found that PD-1 blockade in tolerant OT-I Bim$^{-/-}$ > RIP-mOVA chimeras was unable to break tolerance (Table 4-1). This may be due to the blockade treatment falling short of 100 % effectiveness; in this case, even low-level PD-1 signals may filter through and impact tolerance. I also found that PD-L1$^{-/-}$ RIP-mOVA recipients of adoptively transferred tolerant CD8^{+} cells from OT-I Bim$^{-/-}$ > RIP-mOVA chimeras experienced the development of diabetes with incomplete penetrance and late onset (Fig. 4-8). However, when I used CRISPR to interrupt the *Pdcd1* locus on tolerant CD8^{+} cells from OT-I Bim$^{-/-}$ > RIP-mOVA chimeras, I observed a rapid loss of tolerance and the manifestation of diabetes in recipients of these cells (Fig. 4-10). These data suggest that while PD-1 expression on TRA-specific CD8^{+} T cells is required for the maintenance of tolerance, signaling delivered through engagement with PD-L1 is not. I envision two main explanations for these observations. The first possible explanation is that the broad expression pattern of PD-L1 aids in delivering a strong signal through PD-1 to developing thymocytes, which is required to establish tolerance. The limited expression pattern of PD-L2 does not allow for sufficient engagement of PD-1 to establish tolerance. However, when PD-L1-mediated signals are discontinued in the periphery, tolerance is largely maintained until late time points, suggesting that the low-intensity signals delivered through PD-L2 are sufficient to maintain tolerance to some degree. One caveat to these experiments is that the transferred TRA-specific CD8^{+} T cells are PD-L1 sufficient; as I did not assess the level of PD-L1 expression on these cells, its potential contribution to tolerance cannot be accounted for. If strong PD-1

signaling is required to establish tolerance, and low-intensity PD-1 signals are sufficient to maintain tolerance as I propose, this would also explain why PD-1 blockade failed to break tolerance in our study, and that of the Fife group, who showed that established anergic peripheral T cells are not reinvigorated by PD-L1 blockade (188). If PD-1 blockade is not 100 % effective, residual PD-1 signals may maintain tolerance. The other explanation I propose for our observations is that PD-L1-driven tolerizing signals are context-dependent, and that simultaneous engagement of the TCR and PD-1 by an antigen-bearing thymic epithelial cell is required to induce tolerance during development. In contrast, PD-L2-driven signals delivered by antigen presenting cells may be sufficient to maintain tolerance in peripheral tissues. Indeed, the Sharpe group previously demonstrated in the NOD background distinct roles for PD-L1/PD-L2 in restraining self-reactive T cells in the pancreas (316).

I demonstrated that the provision of TRA-specific $CD4^+$ T cells by way of OT-II HSC co-transfer delayed the onset but was ultimately unable to prevent the development of diabetes driven by OT-I PD-$1^{-/-}$ T cells (Fig. 4-4), further solidifying the cell-intrinsic role for PD-1 in tolerance. In OT-II: RIP-mOVA double transgenic mice, OT-II thymocytes are subjected to clonal deletion and tTreg commitment, and do not mediate autoimmunity, despite the persistence of Ag-specific clonal deletion-escapees in the periphery (65, 69, 317). A caveat to this experiment is that despite the presumed competence of OT-II transgenic BM to produce TRA-specific $CD4^+$ Tregs, I did not assess this population in our chimeras. As a result, I cannot conclude that TRA-specific Tregs slowed the onset of diabetes driven by OT-I PD-$1^{-/-}$ T cells. However, delayed disease onset did not appear to simply be due to the proportional reduction in OT-I PD-$1^{-/-}$ autoimmune mediators, since 1:1 OT-I PD-$1^{-/-}$: OT-II BMCs all went diabetic between 15-20 weeks post-reconstitution, while previous work in our lab conversely showed that

1:1 OT-I PD-1$^{-/-}$: OT-I PD-1^{+} > RIP-mOVA chimeras all went diabetic between 5-10 weeks (116).

Chapter 5 - Capicua as a critical contributor to positive selection

Introduction

The transcriptional repressor, Capicua (CIC), has in recent years received attention for its potential role in thymocyte selection in part thanks to the spontaneous lymphoproliferative autoimmune-like disease that manifests in mice when CIC is deficient in the hematopoietic compartment (212). Deficiency in CIC has been associated with disproportionate generation of T follicular helper cells (TFH) and germinal centre (GC) responses, in a manner intrinsic to the T cell compartment (212). Studies using models that knock-out CIC in the HSC compartment such as Tek-cre (318) and Vav1-cre (319) have suggested that CIC is important to normal T cell development (211, 213). Acute ubiquitous deletion of CIC using a tamoxifen-inducible UBC-creER/T2 CIC$^{FL/FL}$ system resulted in dysregulated expansion of thymocytes in the early thymic progenitor (ETP) and CD4^{-} CD8^{-} DN1 populations (211). Vav1-cre-mediated disruption of the *Cic* locus resulted in impairment in both positive and negative selection, thought to be due to attenuation of the TCR signal (213). A caveat common to the studies described above is that the deletion of CIC in the HSC compartment (or generally prior to thymic colonization) precludes any distinction between early thymic events (ETP, DN) and positive/negative selection itself. Thus, in the present study, I wished to examine the impact of CIC on thymocyte selection using a CD4-cre-driven (320) CIC-knock-out (flox/flox, (226)) model, wherein gene editing occurs upon expression of the CD4 coreceptor and concurrently with the onset of positive selection.

I examined CIC's role in T cell biology using CD4-cre CIC$^{FL/FL}$ mice on a polyclonal background, and additionally intercrossed these mice with two different MHC-I-restricted TCR transgenic models. Here, I generated BM chimeras using the OT-I (239) and HY^{cd4} (227) transgenic TCR systems to model selection in the context of relatively high and low self-reactivity, respectively (321). In the HY^{cd4} system, expression of the HY male Ag-reactive TCRα-chain is delayed using conditional Cre/lox-based expression until the upregulation of CD4 at the CD4$^+$ CD8$^+$ DP thymocyte stage, in this case resulting in a correction of the premature αβTCR expression seen with other transgenic models.

Results

CIC deficiency is associated with alterations in conventional and non-conventional T cell populations

I first examined the role of CIC in thymic selection in a polyclonal setting by analyzing the *ex vivo* phenotype of CD4-cre CIC$^{FL/FL}$ T cells in the thymus and spleen of non-transgenic polyclonal mice.

I found that the overall impact of CIC deficiency on T cell populations was relatively subtle. Broadly, conventional T cell subsets in the thymus and periphery were unchanged except for a minor decrease in the frequency but not absolute numbers of CD4SP (CD25$^-$) thymocytes in the CD4-cre CIC$^{FL/FL}$ (Fig. 5-1A-C). As defects in positive selection have previously been reported in Vav1-cre-driven CIC knock-out models (213), I assessed the frequency of post-positive selection CD4$^+$ CD8$^+$ DP thymocytes by the co-upregulation of TCRβ and CD69. CD4-cre CIC$^{FL/FL}$ DP thymocytes appeared in the TCRβ^{hi} CD69^{hi} population at a lower frequency than did CIC-sufficient controls (Fig. 5-1D-E), suggesting lower rates of positive selection. Caspase-3 is cleaved in thymocytes undergoing apoptosis due to either clonal deletion or death by neglect,

and these populations can be distinguished as Caspase-3^{+} TCRβ^{hi} $CD5^{hi}$ or Caspase-3^{+} TCRβ^{lo} $CD5^{lo}$, respectively. The DP population did not show evidence of increased death by neglect, despite the lower proportion of post-positive selection DP thymocytes; the frequency of activated Caspase-3^{+} cells in the TCRβ^{lo} $CD5^{lo}$ subset was not elevated (Fig. 5-1F). This was similarly true for DP thymocytes undergoing clonal deletion (TCRβ^{hi} $CD5^{hi}$ subset) (Fig. 5-1F). CD4SP and CD8SP thymocytes trended higher in the proportion of cleaved Caspase-3^{+} cells, though these differences were not significant (Fig. 5-1G), suggesting negative selection experienced by these populations may be altered in the absence of CIC.

In the CD4-cre $CIC^{FL/FL}$, I observed a trending increase in the frequency of anergic phenotype $FR4^{hi}$ $CD73^{hi}$ $CD4^{+}$ T cells and a statistically significant increase in the frequency of the $Foxp3^{+}$ $CD25^{-}$ Treg progenitor population in the spleen, but not in the thymus (Fig. 5-2B). However, these differences did not extend to the total numbers of these populations (Fig. 5-2C). CIC deficiency was also associated with a decrease in the frequency of intra-epithelial lymphocyte progenitors (IELp) (Fig. 5-3B), which are thought to be a non-conventional fate for DP thymocytes after receiving a high affinity TCR signal (322–324). Another such non-conventional fate is the invariant natural killer T cell (iNKT), however the frequency of this population was unchanged in the absence of CIC (Fig. 5-3C). I observed increases in the frequencies of $CD44^{hi}$ $CD62L^{lo}$ (T effector memory, TEM-like) $CD4^{+}$ and $CD8^{+}$ splenocytes, similar to what has been recorded for the Vav1-cre $CIC^{FL/FL}$ model (212). However, this difference was not significant for the $CD4^{+}$ T cell subset (Fig. 5-2A). I also observed an increase – though not significant – in the frequency T follicular helper cells (TFH), as has previously been reported for both the Vav1-cre and CD4-cre-driven CIC knock-out models (212) (Fig. 5-3A).

The differences I observed thus far in subsets within the T cell compartment of CIC-deficient mice were suggestive of altered receipt of the TCR signal. Thus, I wished to assess whether conventional T cells that developed and circulate in the absence of CIC would display markers associated with altered TCR signaling strength. During positive selection, CD5 expression is set correlated to the strength of the TCR signal delivered by interactions with self-pMHC (325), and Helios has been shown to be upregulated following high affinity TCR signaling (58). While CD5 (Fig. 5-4A-B) and Helios (Fig. 5-4C-D) expression were unchanged, splenic $CD4^+$ T cells showed a significant increase in the expression of PD-1 (Fig. 5-4E-F). However, the increase in PD-1 expression may simply be due to increased TFH generation for the CD4-cre $CIC^{FL/FL}$ (Fig. 5-3A). These data suggest that in a polyclonal setting, the apparent self-reactivity of the T cell compartment is not altered in the CD4-cre $CIC^{FL/FL}$. Additionally, the frequency of $CD127^+$ $CD4^+$ and $CD8^+$ T cells in the thymus and spleen was decreased in the CD4-cre $CIC^{FL/FL}$ (Fig. 5-5A-B). CD127 (also known as the IL-7 receptor α-chain, IL-7Rα) is innately important to T cell selection and homeostasis (reviewed in (20)). Thus, differences in its expression suggest the phenotype associated with CIC deficiency may involve dysregulated receipt of IL-7 signals. Within the $CD127^+$ subset, the expression level of CD127 was also lower when CIC was absent (Fig. 5-5C).

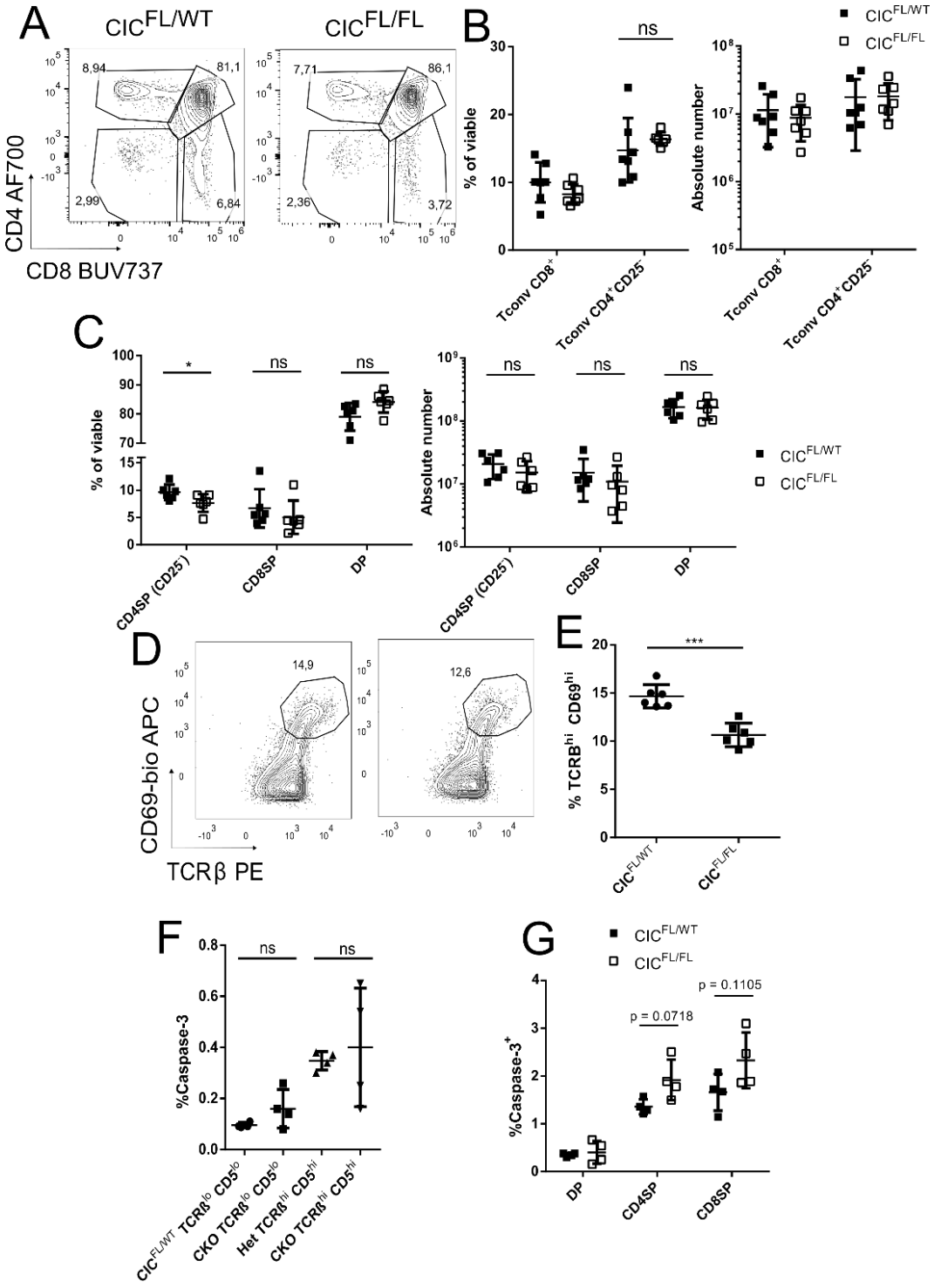

Figure 5-1: Alterations in the selection of conventional thymic subsets in CIC-deficient mice. A, Representative flow plot of profiles of $CIC^{+/-}$ and $CIC^{-/-}$ thymus. B, Frequencies (left) and absolute number (right) of conventional splenic T cell subsets. C, Frequencies (left) and absolute

numbers (right) of conventional thymic subsets. D, Representative flow plots of post-positive selection DP thymocytes, defined as $TCRB^{hi}$ $CD69^{hi}$. E, Summary of data from (D). F, Proportion of Caspase-3^{+} cells in DP thymocytes either undergoing death by neglect ($TCRB^{lo}$ $CD5^{lo}$) or clonal deletion ($TCRB^{hi}$ $CD5^{hi}$). G, Proportion of Caspase-3^{+} cells in conventional thymic subsets. Number of independent experiments per group ≥ 4. Asterisks represent statistical significance as determined by unpaired T-test with Welch's correction.

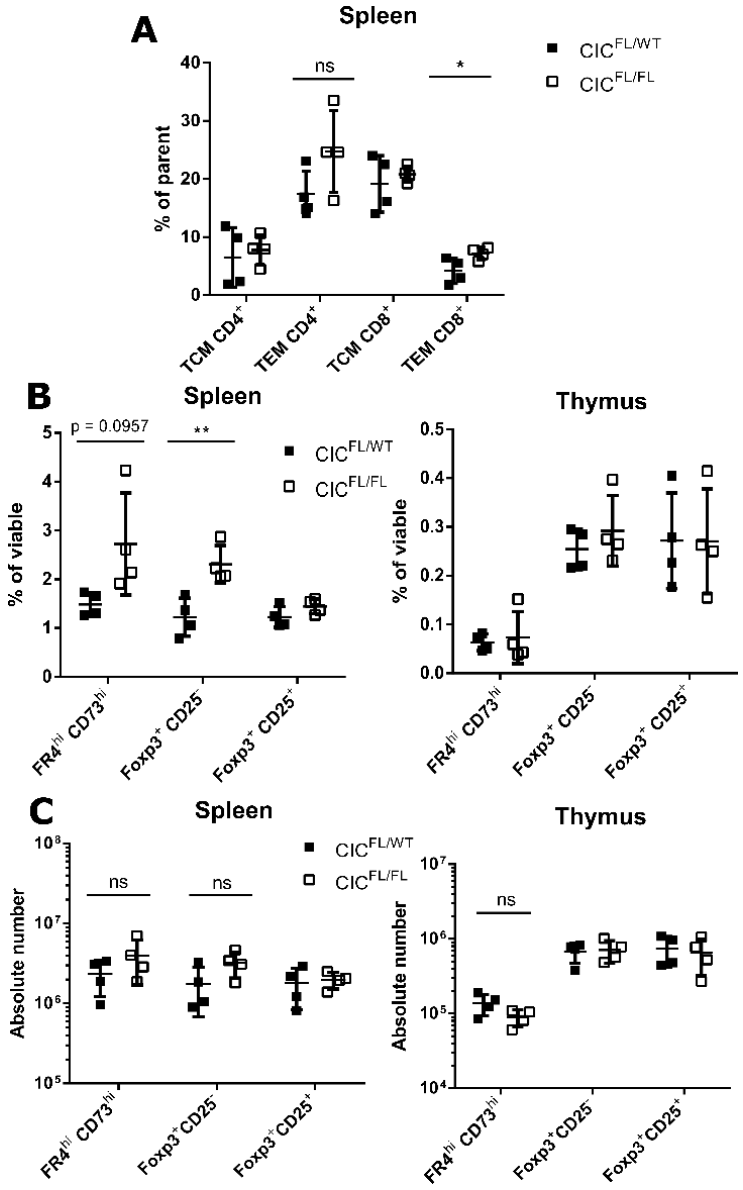

Figure 5-2: CIC deficiency increases the frequencies of some T cell populations associated with high affinity TCR signaling.

T cell subsets were analysed *ex vivo* from polyclonal $CIC^{FL/WT}$ and $CIC^{FL/FL}$ spleen or thymus. A, Frequencies of virtual memory T cell populations: T central memory (TCM, $CD62L^{hi}$ $CD44^{hi}$) and T effector memory (TEM, $CD62L^{lo}$ $CD44^{hi}$) in the spleen. B, Frequencies of anergic ($FR4^{hi}$ $CD73^{hi}$) and T regulatory cells (Treg, $Foxp3^{+}$ $CD25^{+}$), and Treg precursors ($Foxp3^{+}$ $CD25^{-}$) in the spleen (left) and thymus (right). C, Absolute numbers in the spleen (left) and thymus (right)

associated with the analysis in (B). Number of independent experiments per group ≥ 4. Asterisks represent statistical significance as determined by unpaired T-test with Welch's correction.

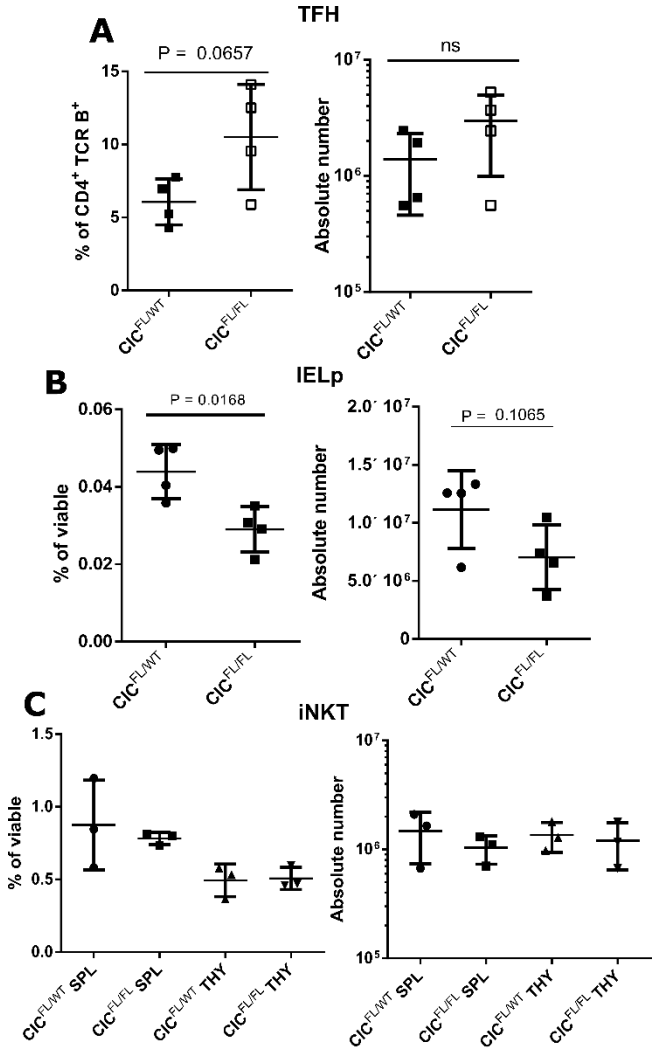

Figure 5-3: CIC deficiency is associated with alterations in the frequencies of non-conventional T cell populations.

Non-conventional T cell subsets were analysed *ex vivo* from polyclonal $CIC^{FL/WT}$ and $CIC^{FL/FL}$ spleen or thymus. A, Proportions (left) and absolute number (right) of T follicular helper (TFH, $CD4^+$ $CXCR5^+$ $PD\text{-}1^+$) cells (TFH) in spleen. B, Proportions (left) and absolute number (right) of

intra-epithelial lymphocyte progenitors (DP^{dull} $TCR\beta^{+}$ $CD5^{hi}$ $NK1.1^{-}$) in the thymus. C, Proportions (left) and absolute number (right) of invariant NKT cells (iNKT, $TCR\beta^{+}$ CD1d $tetramer^{+}$) in the spleen and thymus. Number of independent experiments per group ≥ 3. Asterisks represent statistical significance as determined by unpaired T-test with Welch's correction.

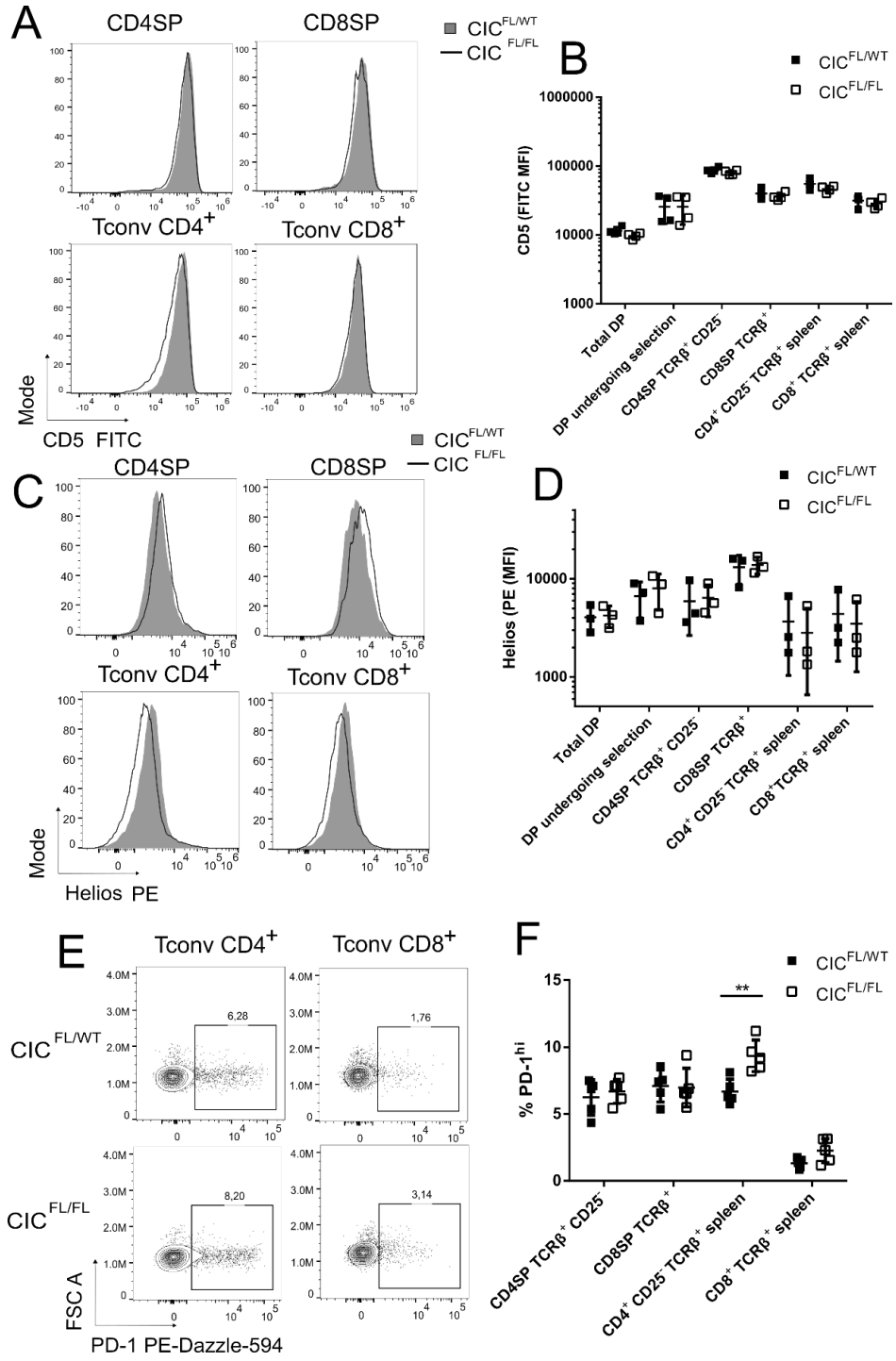

Figure 5-4: Deficiency in CIC does not result in altered self-reactivity of the conventional T cell compartment.

A, Representative histograms demonstrating CD5 expression in $CIC^{FL/WT}$ (grey) and $CIC^{FL/FL}$ (open) conventional T cell subsets from polyclonal mice. B, Summary of data shown in (A). C, Representative histograms demonstrating Helios expression in $CIC^{FL/WT}$ (grey) and $CIC^{FL/FL}$ (open) conventional T cell subsets from polyclonal mice. D, Summary of data shown in (C). E, Representative flow plots demonstrating differences in PD-1 expression in $CIC^{FL/WT}$ and $CIC^{FL/FL}$ conventional T cell subsets from the thymus of polyclonal mice. F, Summary of data shown in (E). Number of independent experiments per group ≥ 3. Asterisks represent statistical significance as determined by unpaired T-test with Welch's correction.

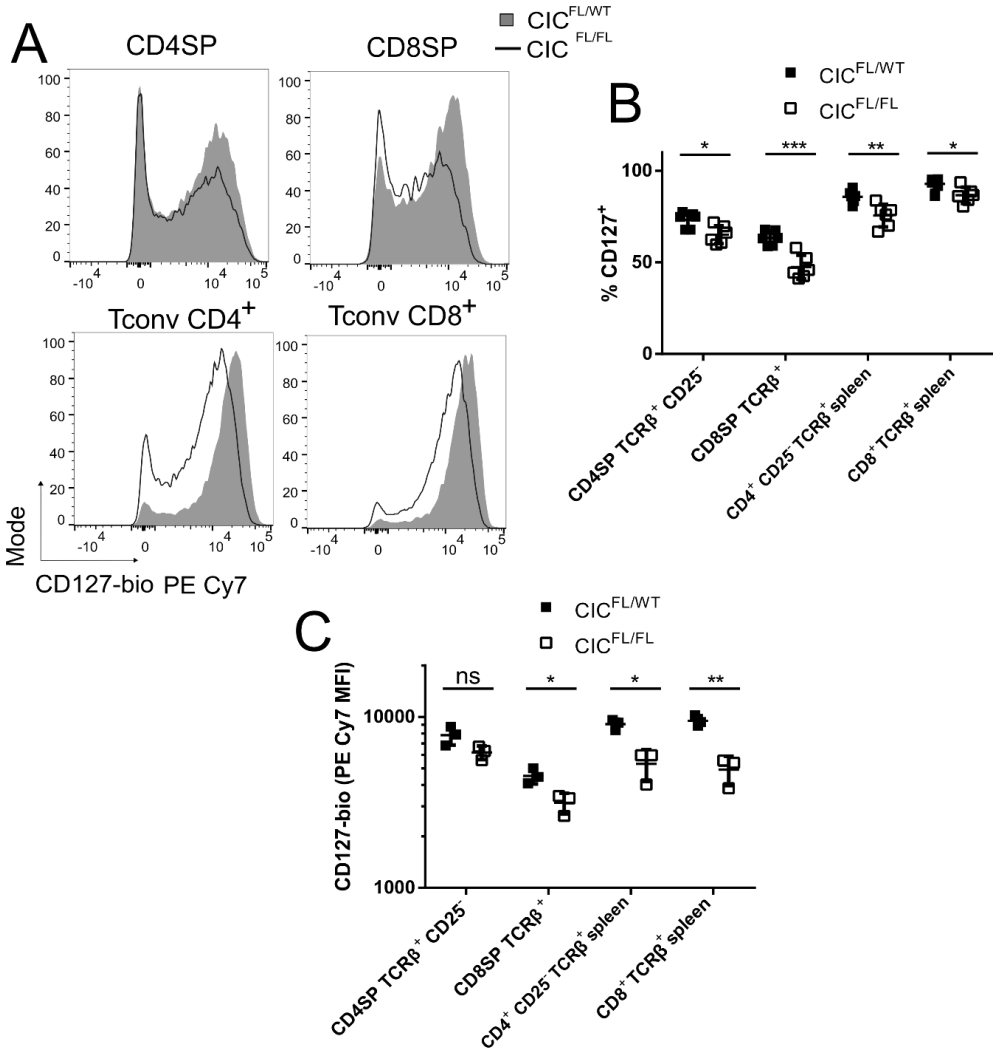

Figure 5-5: CIC deficiency is associated with diminished CD127 expression.

A, Representative histograms demonstrating CD127 expression in $CIC^{FL/WT}$ (grey) and $CIC^{FL/FL}$ (open) conventional T cell subsets from polyclonal mice. B, Summary of data shown in (A); represented is the percentage of each shown population positive for CD127 expression. C, CD127 expression (median fluorescence intensity) within the $CD127^{+}$ population quantified in (B). Number of independent experiments per group ≥ 3. Asterisks represent statistical significance as determined by unpaired T-test with Welch's correction.

CIC-deficient T cells show mild functional impairment *in vitro* and *in vivo*

In the previous section, I provided evidence for dysfunctional selection in the absence of CIC. To further characterize the T cell repertoire to follow from this potentially dysfunctional selection process, I assessed the functional capacity of mature $CD4^+$ and $CD8^+$ T cells from polyclonal CD4-cre $CIC^{FL/FL}$ mice.

In collaboration with undergraduate student Nikhil Bhatnagar, I labelled spleen-derived cells from both CD4-cre $CIC^{FL/FL}$ and CD4-cre $CIC^{FL/WT}$ mice with either CellTrace Violet (CTV) or carboxyfluorescein succinimidyl ester (CFSE) proliferation dyes. The diagram depicted in figure 5-6A describes both *in vitro* experiments (Fig. 5-6) and *in vivo* experiments (Fig. 5-7) carried out with these labelled splenocytes. I stimulated these cells *in vitro* using plate-bound α-CD3/α-CD28 antibodies. On day 2 post-stimulation, CIC deficiency in either $CD4^+$ or $CD8^+$ T cells did not result in differences in activation, based on the upregulation of CD25 and CD69 (Fig. 5-6B-C). The mean proliferation index of $CIC^{FL/FL}$ $CD8^+$ T cells was not significantly different from the control (Fig. 5-6D-E). However, the division index tended to be diminished for both $CD4^+$/$CD8^+$ populations, but these differences were not statistically significant. Thus, it is possible CIC-deficient T cells were overall less likely to divide *in vitro* following stimulation (Fig. 5-6F).

Splenocytes labelled as described in Fig. 5-6A were also co-adoptively transferred into sub-lethally irradiated (lymphopenic) recipients in parallel with *in vitro* experiments. Differential CTV/CFSE labelling was used to distinguish donor cells. Under lymphopenic conditions, $CIC^{FL/FL}$ $CD8^+$ T cells persisted to lower total numbers than did the $CIC^{FL/WT}$ control on day 7 post-adoptive transfer, while there was no difference in $CD4^+$ T cells (Fig. 5-7A). In contrast, in non-irradiated controls, no such differences emerged, suggesting that homeostatic proliferation

under lympho-replete conditions is not impacted by CIC deficiency (Fig. 5-7A). Proliferation index was significantly increased for $CIC^{FL/FL}$ $CD4^+$ T cells (Fig. 5-7B), which suggests that for total numbers to remain the same as shown in (Fig. 5-7A), cell death may have been increased in this population. However, I did not investigate cell death in these experiments. Finally, while division index was unchanged for $CIC^{FL/FL}$ $CD4^+$ T cells, it was diminished for the $CD8^+$ population (Fig. 5-7C). Overall, these data indicate that the capacity for LIP is altered in the absence of CIC and appears particularly limited in the $CD8^+$ compartment.

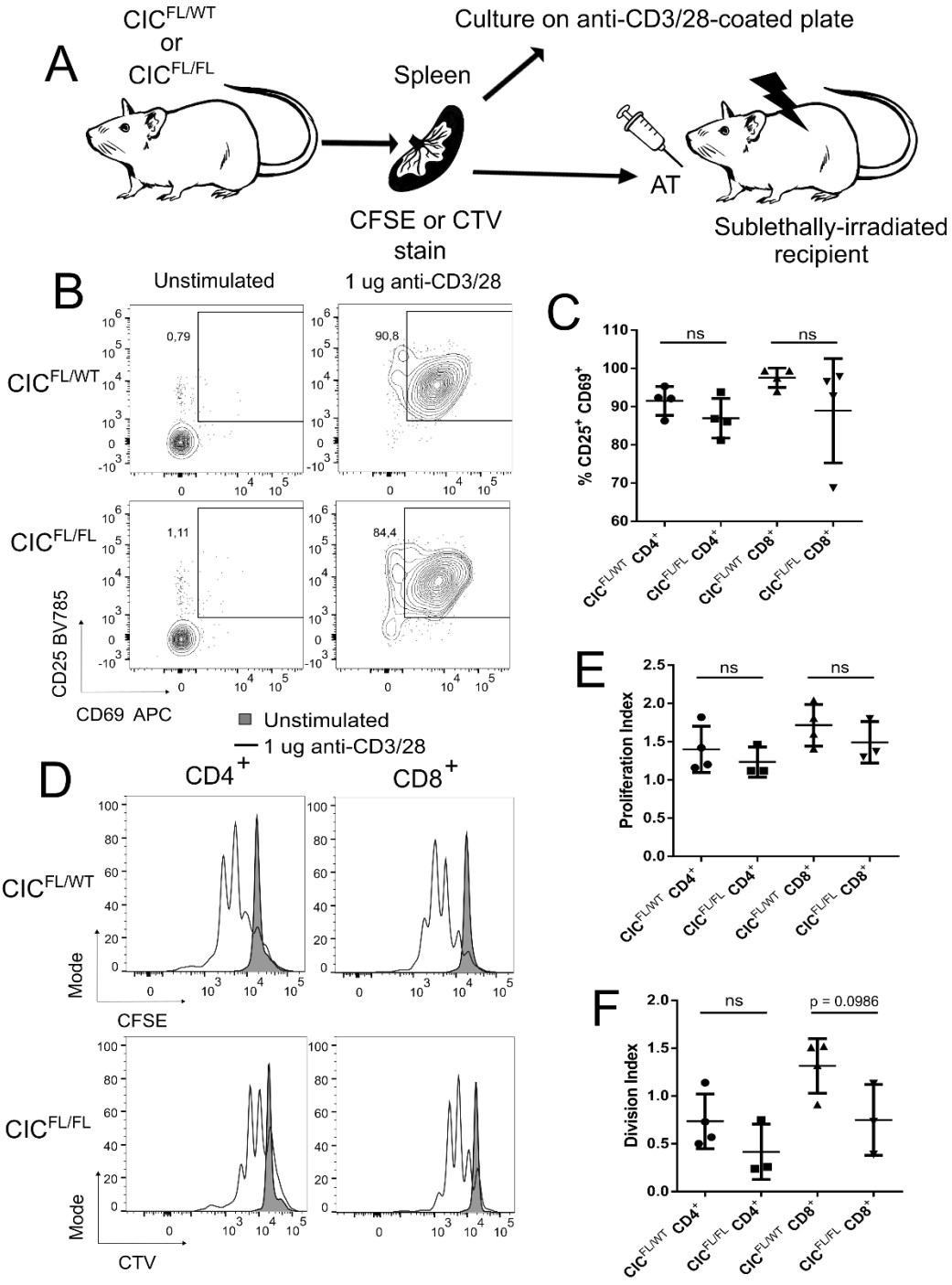

Figure 5-6: CIC deficiency results in a mild defect in proliferative responses to non-specific TCR stimulation *in vitro*.

A, Diagram describing experiments outlined in Figures 5-6 and 5-7. B, Activation marker CD25 and CD69 upregulation in polyclonal $CD4^+$ and $CD8^+$ T cells 2 days following stimulation with

plate-bound anti-CD3/28 antibodies *in vitro* (1 μg/mL for each antibody). C, Summary of data described in (B). D, Day 2 proliferation assessed by proliferation dye (CFSE or CTV) dilution in polyclonal $CD4^+$ and $CD8^+$ T cells; unstimulated PBS control (grey) and stimulated with plate-bound antibody. E, Summary of proliferation indices calculated from data described in (D). F, Summary of division indices calculated from data described in (D). Number of independent experiments per group ≥ 3. Asterisks represent statistical significance as determined by unpaired T-test with Welch's correction.

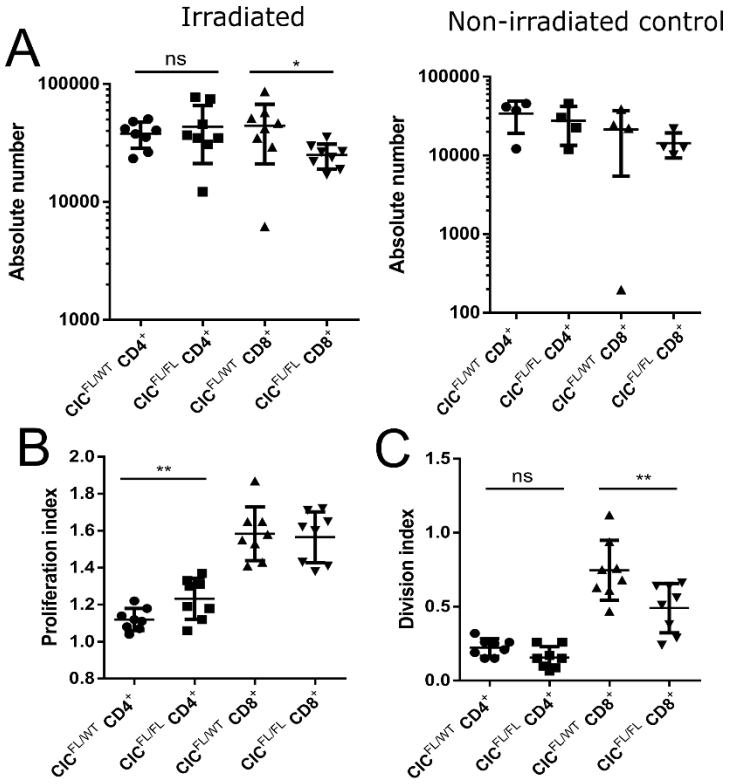

Figure 5-7: CIC deficiency results in altered capacity for lymphopenia induced proliferation in polyclonal T cells.

A, Number of TCRβ$^+$ CD4$^+$ and CD8$^+$ T cells recovered from the spleen of lymphopenic (irradiated, left) or lympho-replete control (non-irradiated, right) from either CIC$^{FL/WT}$ or CIC$^{FL/FL}$ donors 7 days post-adoptive transfer. Proliferation was assessed by proliferation dye (CFSE or CTV) dilution in polyclonal TCRβ$^+$ CD4$^+$ and CD8$^+$ T cells. B, Summary of proliferation indices calculated from data described in (A). Summary of division indices calculated from data described in (A). Number of independent experiments = 4. Asterisks represent statistical significance as determined by paired T-test.

Evidence of impaired selection and altered TCR signaling in competitive polyclonal BMCs

Due to the subtlety of the phenotype I observed directly *ex vivo* in polyclonal mice, I next wished to compare the selection of $CIC^{FL/FL}$ T cells in a setting with $CIC^{FL/WT}$ competitors to observe thymocytes developing in the presence or absence of CIC in parallel.

I generated $CIC^{FL/FL}$:$CIC^{FL/WT}$ (1:1) mixed bone marrow chimeras outlined in the diagram in figure 5-8A. The resulting CD4/CD8 thymic profiles of each donor were largely similar (Fig. 5-8B). However, while the total DP population was close to 50 % $CIC^{FL/FL}$-origin, this percentage decreased as thymocytes matured (Fig. 5-8C-D) and decreased between the mature SP thymocyte and peripheral $CD8^+$ T cell populations (Fig. 5-8E). This suggests CIC deficiency results in a T cell-intrinsic impairment in the positive selection of both CD4SP and CD8SP thymocytes as well as an impairment in peripheral $CD8^+$ T cell maintenance. However, while our data do not rule out the potential for altered thymic egress explaining differences in the peripheral $CD8^+$ population, in this case, one might expect an accumulation of $CIC^{FL/FL}$ CD8SP thymocytes rather than a deficit. Indeed, similar to observations I made directly *ex vivo* in polyclonal mice, the proportion of post-positive selection $CIC^{FL/FL}$ DP thymocytes was diminished compared to the $CIC^{FL/WT}$ control (Fig. 5-8F). Selection efficiencies (calculated by the number of SP per DP thymocyte) were also lower for CD8SP CD4-cre $CIC^{FL/FL}$ thymocytes, however the difference was not significant for the CD4SP subset (Fig. 5-8G).

Also consistent with our *ex vivo* data, the CD4-cre $CIC^{FL/FL}$ continued to display a lower proportion of $CD127^+$ $CD4^+$ and $CD8^+$ T cells in the thymus and spleen (Fig. 5-9A-B). Within the $CD127^+$ population, CD127 expression was also lower when CIC was absent (Fig. 5-9A-B). When developing in the presence of $CIC^{FL/WT}$ competitors, CIC-deficient DP thymocytes displayed decreased expression of CD5 (Fig. 5-9C), suggesting that positive selection may be

impaired due to the propagation of the TCR signal being diminished in the absence of CIC. The relative decrease in CD5 expression is also apparent in CD4SP thymocytes and peripheral $CD4^+$ and $CD8^+$ T cells. Interestingly, CD4-cre $CIC^{FL/FL}$ $CD4^+$ and $CD8^+$ T cells showed elevated expression of the marker Ki67, which is used to distinguish cycling cells that have exited the quiescent state (326) (Fig. 5-9D).

In $CIC^{FL/WT}$:$CIC^{FL/FL}$ mixed BMCs, CIC-deficient splenic $CD4^+$ and $CD8^+$ T cells showed marked increases in the proportions of PD-1^{hi} cells (Fig. 5-10A-B). However, for the $CD4^+$ population, this may primarily be due to enhanced generation of TFH ($CD4^+$ $CXCR5^+$ PD-1^+) for CD4-cre $CIC^{FL/FL}$ T cells in these mixed BMCs (Fig. 5-10C) compared with that of polyclonal mice directly *ex vivo* (Fig. 5-3A). The increase in both TFH generation and PD-1 expression in mixed BMCs suggests the added competition by $CIC^{FL/WT}$ was a contributor to these differences. Additionally, the proportion of CIC-deficient splenic $CD4^+$ $Foxp3^+$ $CD25^-$ cells was also observed to be elevated over those of the $CIC^{FL/WT}$ control, while no such difference arose in the thymus (Fig. 5-11).

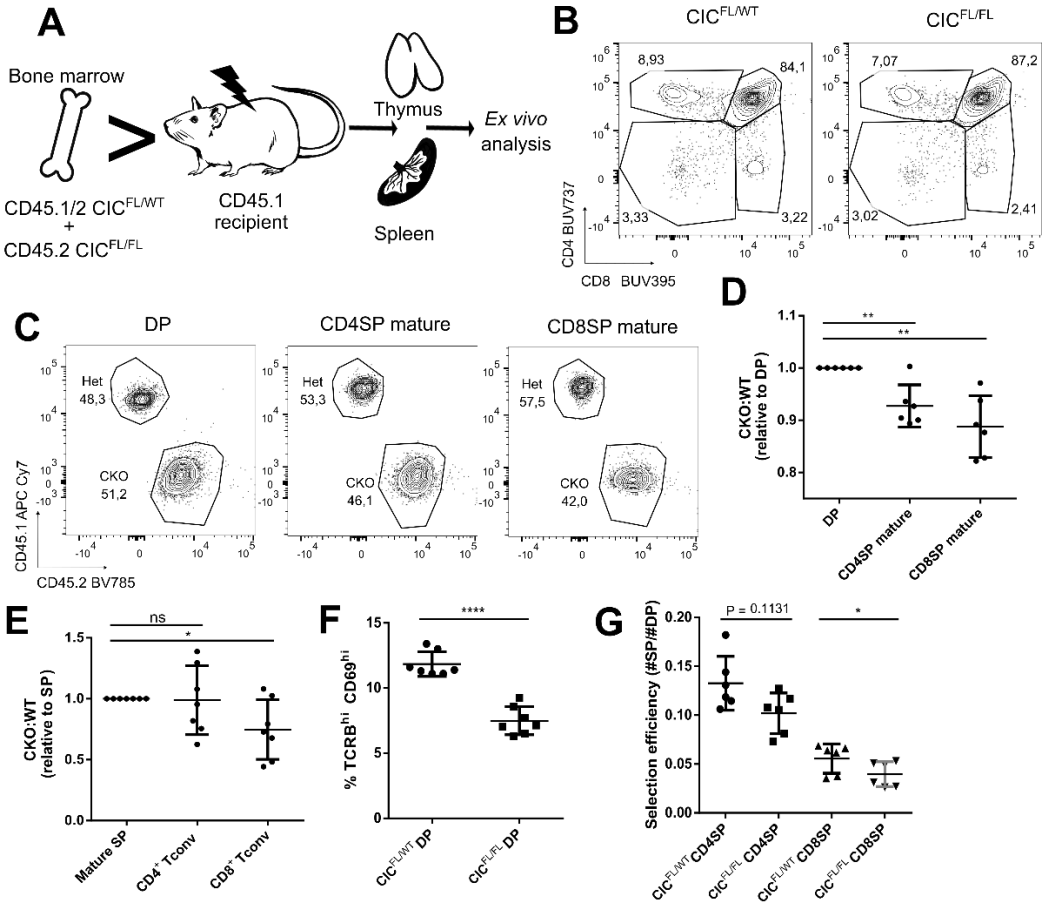

Figure 5-8: CIC-deficient T cells demonstrate a competitive disadvantage in polyclonal mixed bone marrow chimeras.

A, Diagram describing polyclonal mixed bone marrow chimera set-up. B, Representative flow plot of thymocytes of both donor origins within $CIC^{FL/WT}$:$CIC^{FL/FL}$ (1:1) mixed bone marrow chimeras. C, Donor composition of general thymic subsets after $CD45.1^{+}$ recipient cells are gated out. D, Percentage $CIC^{FL/FL}$-origin within the mature SP thymic subset relative to the DP subset (shown is a ratio, SP/DP). E, Percentage $CIC^{FL/FL}$-origin within the splenic T cell subset relative to the mature SP subset (shown is a ratio, splenic T cell/SP). F, Percentage of post-positive selection thymocytes within the DP subset within $CIC^{FL/WT}$ and $CIC^{FL/FL}$ donor populations. G, Selection efficiency of CD4SP and CD8SP thymocytes. Asterisks represent statistical significance as determined by paired T-test.

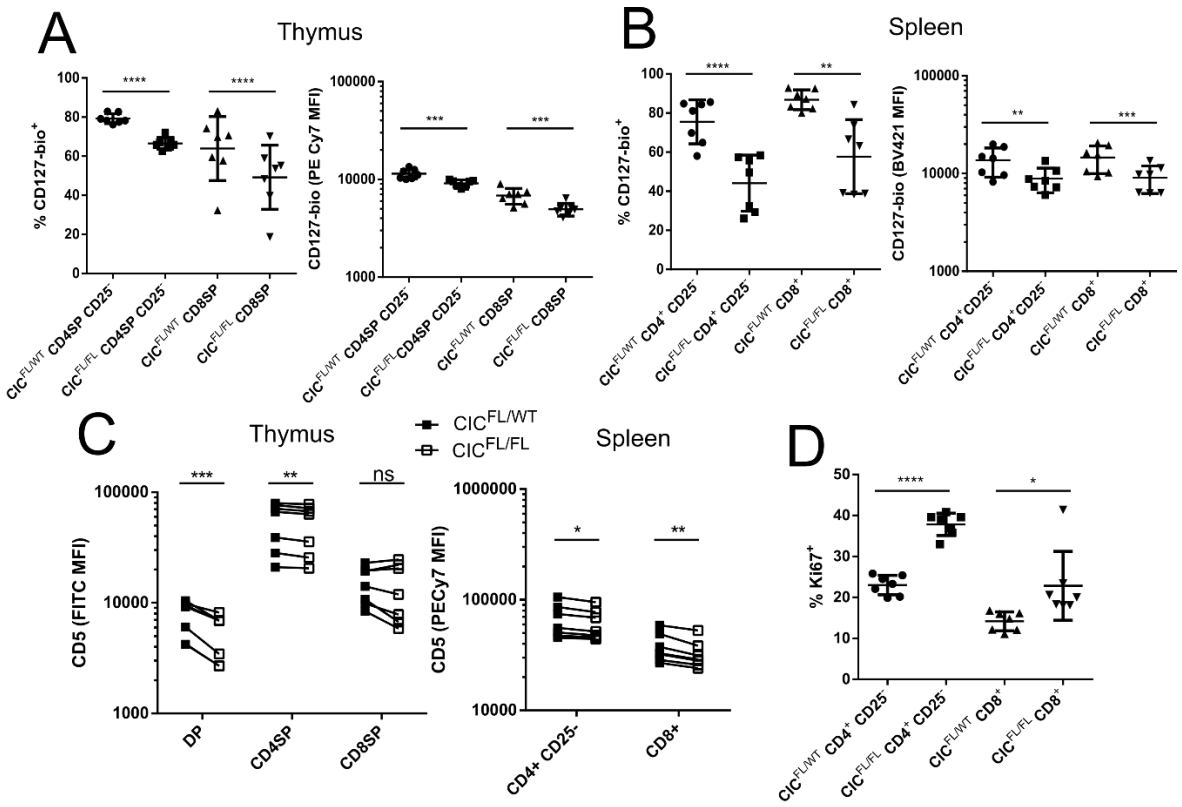

Figure 5-9: Phenotype of CIC-deficient T cells consistent with alterations in TCR signaling and homeostatic maintenance.

Cells were analyzed *ex vivo* from $CIC^{FL/WT}$:$CIC^{FL/FL}$ (1:1) polyclonal mixed bone marrow chimeras. A, CD127 expression in conventional thymic subsets; proportion of CD127-expressing cells (left) and CD127 expression (median fluorescence intensity) within the $CD127^+$ subset (right). B, CD127 expression in conventional splenic T cell subsets; proportion of CD127-expressing cells (left) and CD127 expression (median fluorescence intensity) within the $CD127^+$ subset (right). C, CD5 expression within thymic (left) and splenic (right) conventional T cell subsets. D, Proportion of Ki-67^+ cells within splenic conventional T cell subsets. Number of

independent experiments/cohorts = 2. Asterisks represent statistical significance as determined by paired T-test.

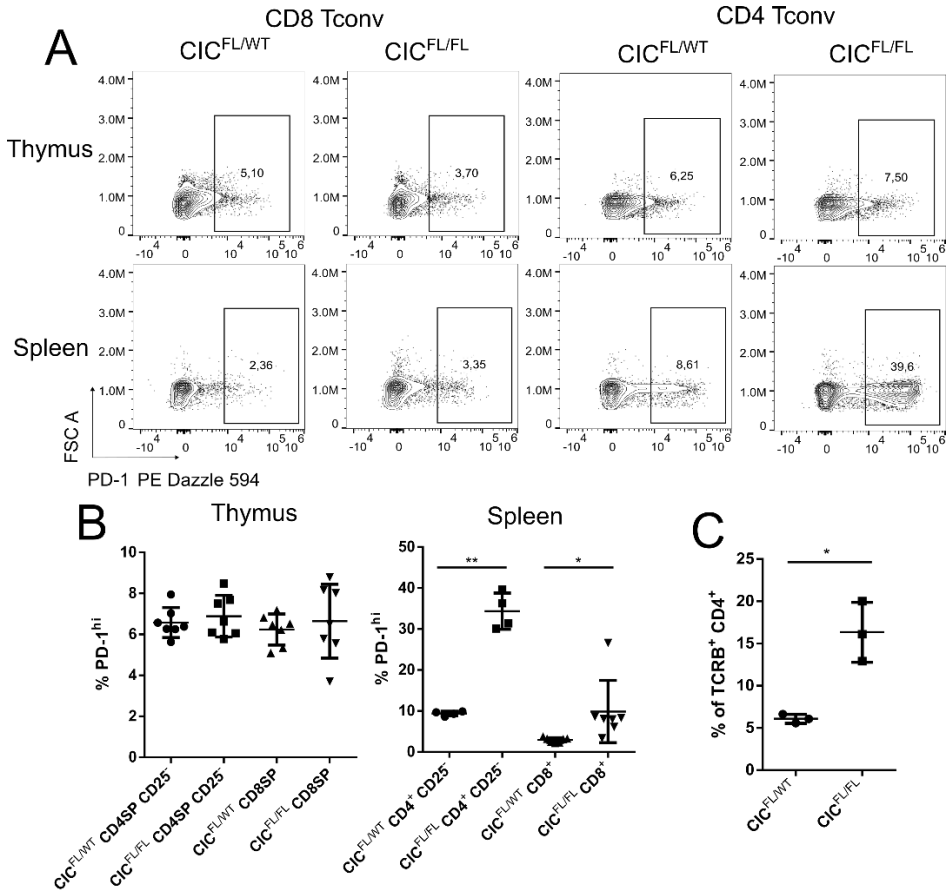

Figure 5-10: In CIC-deficient conventional T cells, the elevated proportion of the PD-1^{hi} subset is magnified in the periphery of competitive polyclonal bone marrow chimeras.

A, PD-1 expression in CD8$^+$ TCRβ$^+$ and CD4$^+$ TCRβ$^+$ CD25$^-$ conventional T cell subsets within the thymus and spleen of CIC$^{FL/WT}$:CIC$^{FL/FL}$ (1:1) polyclonal mixed bone marrow chimeras. B, Summary of data collected from experiment described in (A). C, Proportion of T follicular helper (TFH, CD4$^+$ CXCR5$^+$ PD-1$^+$) cells (TFH) in the spleen. Number of independent experiments/cohorts = 2, with the exception of PD-1 expression in splenic CD4$^+$ TCRβ$^+$ CD25$^-$

conventional T cells, in which case data is representative of a single cohort. Asterisks represent statistical significance as determined by paired T-test.

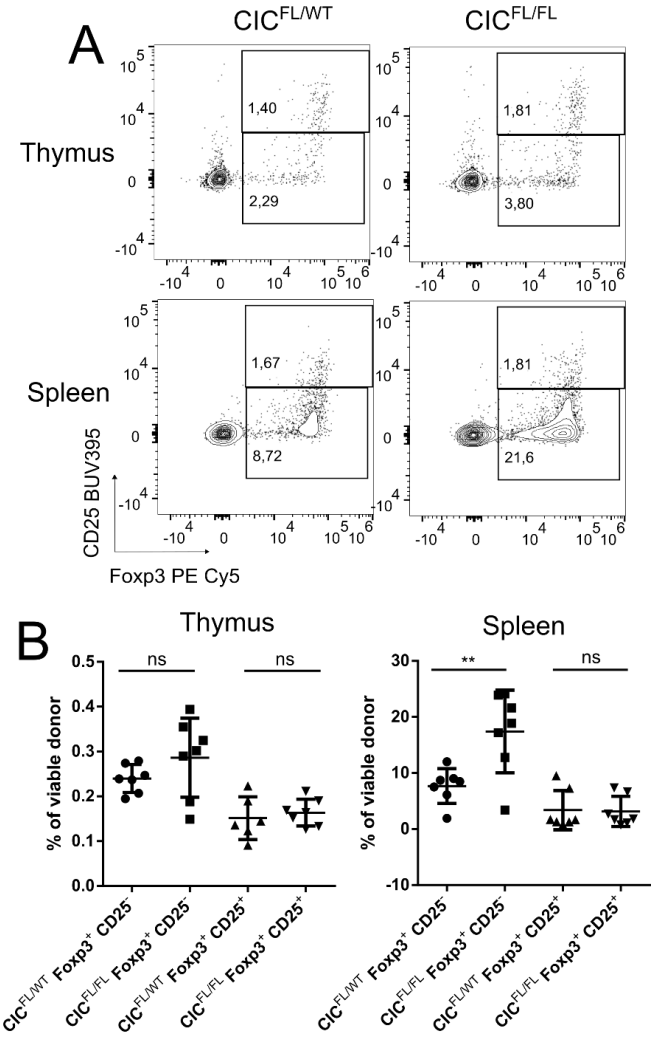

Figure 5-11: In CIC-deficient conventional T cells, the elevated proportion of the $CD4^+$ $Foxp3^+$ $CD25^-$ subset is magnified in the context of competitive polyclonal bone marrow chimeras. A, Treg ($CD4^+$ $Foxp3^+$ $CD25^+$) and Treg precursor ($CD4^+$ $Foxp3^+$ $CD25^-$) representation within the $CD4^+$ $TCR\beta^+$ population in the thymus and spleen of $CIC^{FL/WT}$:$CIC^{FL/FL}$ (1:1) polyclonal mixed bone marrow chimeras. B, Summary of data described in (A). Number of independent

experiments/cohorts = 2. Asterisks represent statistical significance as determined by paired T-test.

CIC deficiency leads to impairment in positive selection in two different transgenic models: OT-I and HY^{cd4}.

In the previous section, I noted phenotypic changes in CIC$^{FL/FL}$ T cells developing in competitive mixed BMCs consistent with dysregulation of the integration of the TCR signal. To better understand the nature of this dysregulation, I wished to examine CIC's influence on positive selection without the challenges associated with a diverse T cell repertoire.

I generated WT:CIC$^{FL/FL}$ (1:1) bone marrow chimeras with the physiological HY^{cd4} MHC I-restricted male Ag specific TCR transgenic system (227) using female recipients to study positive selection. Transgenic T3.70^{hi} thymocytes of CIC$^{FL/FL}$ origin showed decreased frequencies within the CD8SP gate (Fig. 5-12A-B), and selection efficiency was significantly decreased (Fig. 5-12C). Within the CD8SP T3.70^{+} population, the frequency of CD24^{lo} thymocytes was also decreased in the absence of CIC (Fig. 5-12D-E), indicating that positive selection was impaired.

Transgenic T3.70^{hi} T cells were identified according to the gates described in Fig. 5-13A. CIC deficiency was also associated with a decrease in expression of the transgenic HY-specific TCR (Fig. 5-13B) in the T3.70^{hi} DP and CD8SP thymic subsets. This may reflect a failure to fully upregulate the HY TCR due to impaired positive selection, which is supported by our observation of diminished CD5 expression on CIC$^{FL/FL}$ DP thymocytes (Fig. 5-13E-F). I additionally observed increased expression of PD-1 on CD8SP thymocytes and CD8^{+} peripheral

T cells (Fig. 5-13C-D), and CD5 expression saw sequential increases on CD8SP and $CD8^+$ peripheral T cells (Fig. 5-13E-F). Thus, as $CD8^+$ $T3.70^{hi}$ $CIC^{FL/FL}$ cells matured and egressed to the periphery, they increasingly displayed features associated with self-reactivity. Since our HY^{cd4} transgenic system is not on a $RAG^{-/-}$ background, it is possible that endogenous TCRα rearrangements mediate positive selection instead of the HY TCR in our chimeras, which may also explain decreased T3.70 staining in the thymus and elevated CD5 expression in the periphery. To limit this possibility, $T3.70^{hi}$ cells were gated as "true" HY^{cd4} Tg $CD8^+$ T cells; I presumed the $T3.70^{lo}$ population to potentially carry cells that expressed lower levels of HY TCR due to co-expression of endogenously rearranged alternate TCRα-chains. When $T3.70^{hi}$ and $T3.70^{lo}$ populations were compared (gating demonstrated in Fig. 5-14), differences in CD5 expression appeared to be exclusive to the $T3.70^{hi}$ population (Fig. 5-14B-D). I also observed a continuation in the trend of decreased CD127 expression in $CIC^{FL/FL}$ thymocytes and mature T cell (Fig. 5-15), and again this appeared largely exclusive to the $T3.70^{hi}$ population (Fig. 5-14D). If endogenous TCRα expression was a feature of the $T3.70^{lo}$ population and the above listed phenotypic differences were rescued in this population, then in this case the phenotype associated with CIC deficiency may be limited to the "true" HY TCR mono-expressing T cells. One potential explanation for this observation is that the influence of CIC is limited to T cell clones of lower self-reactivity (as with the HY TCR), and it plays a lesser role in clones with more highly self-reactive TCRs (endogenous rearrangements).

I also generated WT:$CIC^{FL/FL}$ (1:1) BMCs with the OT-I MHC I-restricted OVA-specific TCR transgenic system (239) (Fig. 5-16) using non-OVA-expressing C57BL/6J (B6) recipients in order to model positive selection in the context of a more highly self-reactive TCR (321, 327). Similarly to the HY^{cd4} model, $CIC^{FL/FL}$ cells in these chimeras displayed decreased frequencies

of CD8SP thymocytes within the OVA-K^b $tetramer^+$ population (Fig. 5-16A-B). The selection efficiency for CIC-deficient cells was also significantly lower than for the WT controls (Fig. 5-16C). The $CIC^{FL/FL}$ $tetramer^+$ subset also showed a decreased frequency of mature $CD24^{lo}$ CD8SP thymocytes (Fig. 5-16D-E). Broadly, evidence of impaired positive selection in these chimeras appeared overall less profound than what I observed with the less self-reactive HY^{cd4} mixed BMCs (Fig. 5-12).

Interestingly, DP $CIC^{FL/FL}$ OT-I thymocytes developing in these B6 recipients showed no difference CD5 expression, contrary to our findings with the HY^{cd4} model (Fig. 5-17A-B). This in combination with a milder overt impairment in positive selection suggests that a more highly self-reactive TCR may somewhat alleviate the impact of CIC deficiency. Alternatively, since the OT-I TCR is expressed prematurely at the DN stage (in contrast to the more physiological HY^{cd4} model), signaling through the transgenic αβTCR can occur prior to deletion of CIC. Thus, this is a caveat to our comparison between these models. Peripheral $CIC^{FL/FL}$ OT-I T cells showed decreased CD5 expression in the periphery, contrary to our findings with the HY^{cd4} model (Fig. 5-17A-B). Helios expression, a marker of high affinity TCR signaling, was significantly increased but sufficiently subtle as to call into question its biological relevance (Fig. 5-17E-F) (58). PD-1 expression was unchanged (Fig. 5-17C-D), suggesting that $CIC^{FL/FL}$ OT-I T cells developing in B6 recipients do not acquire overt features of high affinity signaling as I saw with HY^{cd4} mixed BMCs. Despite this, $CIC^{FL/FL}$ OT-I T cells in B6 recipients continued to display diminished CD127 expression; the proportion of $CD127^+$ % cells was decreased in the Tet^+ subset, although CD127 expression within the $CD127^+$ subset was not robustly altered (Fig. 5-18).

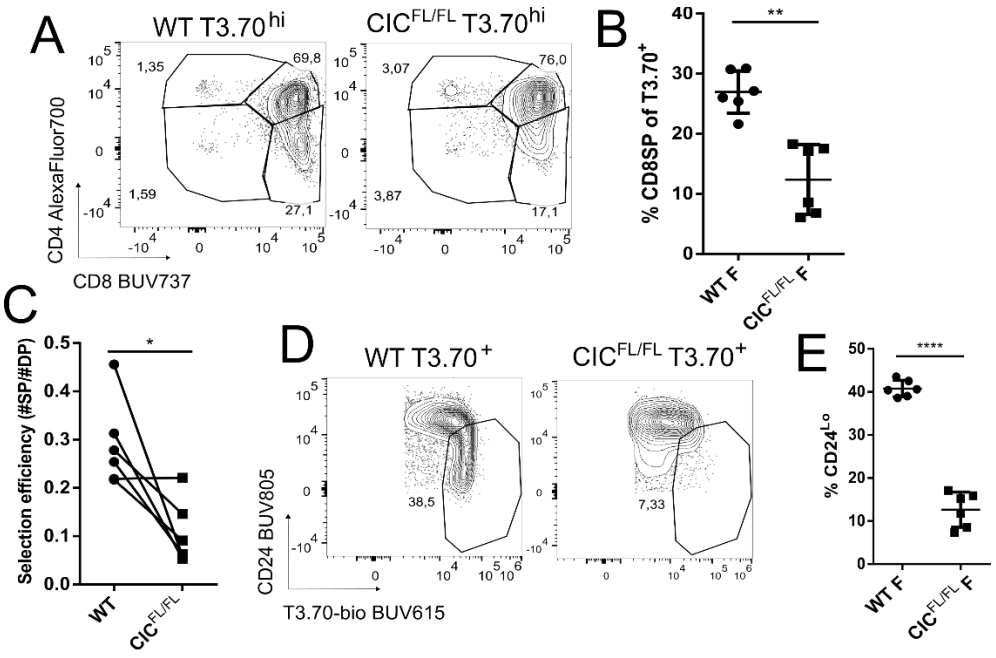

Figure 5-12: CIC-deficient T cells show impairment in positive selection in HY^{cd4} mixed bone marrow chimeras.

A, Representative flow plots of T3.70^{hi} thymocytes of both WT and CIC$^{FL/FL}$ donor origin within female mixed HY^{cd4} WT:CIC$^{FL/FL}$ (1:1) bone marrow chimeras. B, Proportion of T3.70^{hi} thymocytes that are CD8SP. C, Selection efficiency in chimeras described in (A), represented as a ratio of SP to DP thymocytes for both WT and CIC$^{FL/FL}$. D, Proportion of T3.70^{hi} CD24^{lo} mature CD8SP thymocytes within the T3.70^{+} donor population. E, Summary of data described in (D). Number of independent experiments/cohorts = 2. Asterisks represent statistical significance as determined by paired T-test.

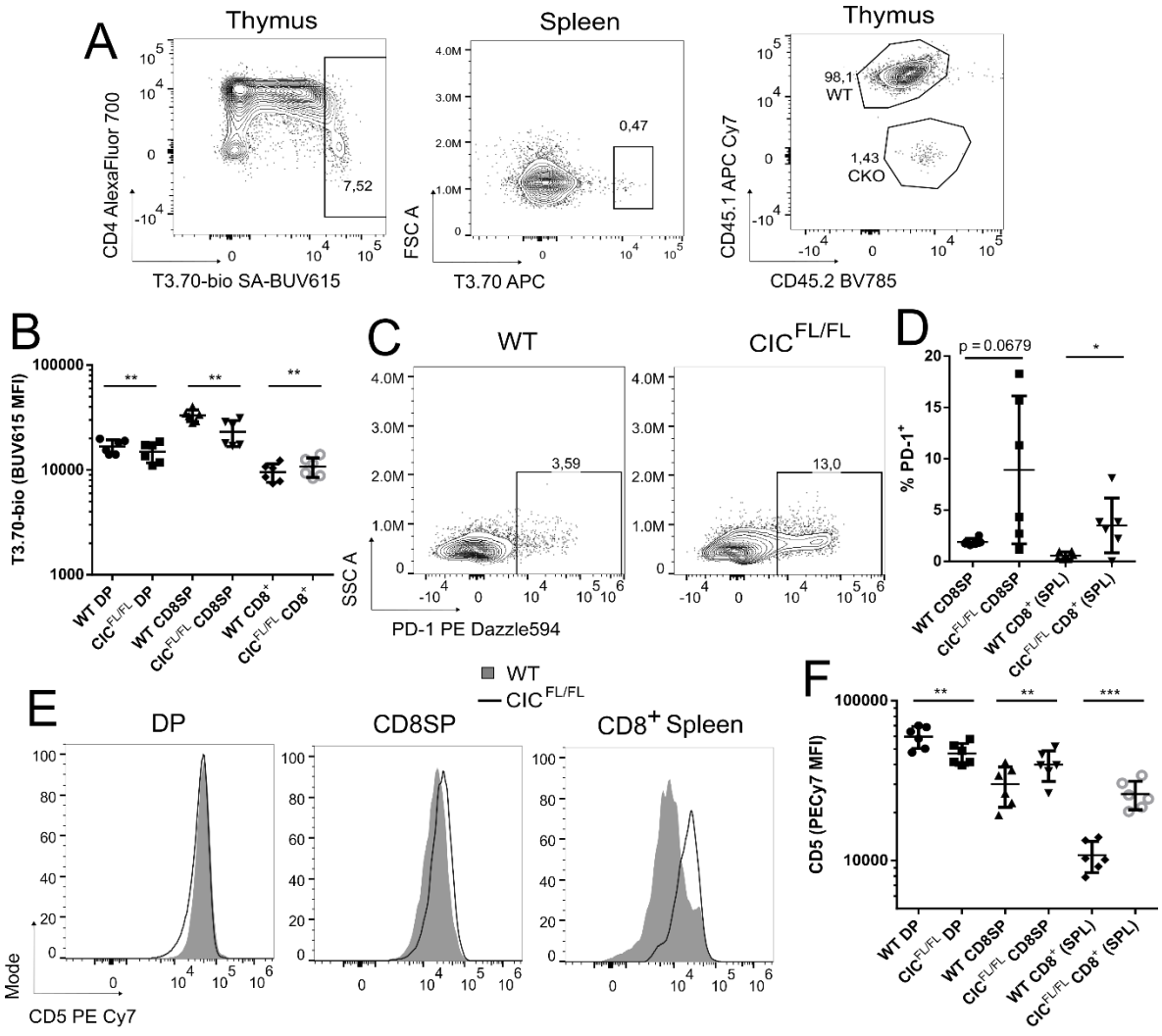

Figure 5-13: Phenotypes of CIC-deficient transgenic HY^{cd4} T cells in WT:CIC$^{FL/FL}$ (1:1) female bone marrow chimeras are suggestive of altered receipt of the TCR signal.

A, (Left, centre) Representative flow plots demonstrating how T3.70^{hi} T cells were gated in both thymus and spleen; (right) representative profile of WT and CIC$^{FL/FL}$ donor origins within the T3.70^{hi} gate in the thymus. B, T3.70 staining within CD8^{+} T3.70^{hi} donor-derived T cells. C, PD-1 expression within CD8SP T3.70^{hi} donor-derived thymocytes (spleen not shown). D, Summary of data described in (C). E, CD5 expression in CD8^{+} T3.70^{hi} donor-derived T cells. F, Summary of data described in (E). Number of independent experiments/cohorts = 2. Asterisks represent statistical significance as determined by paired T-test.

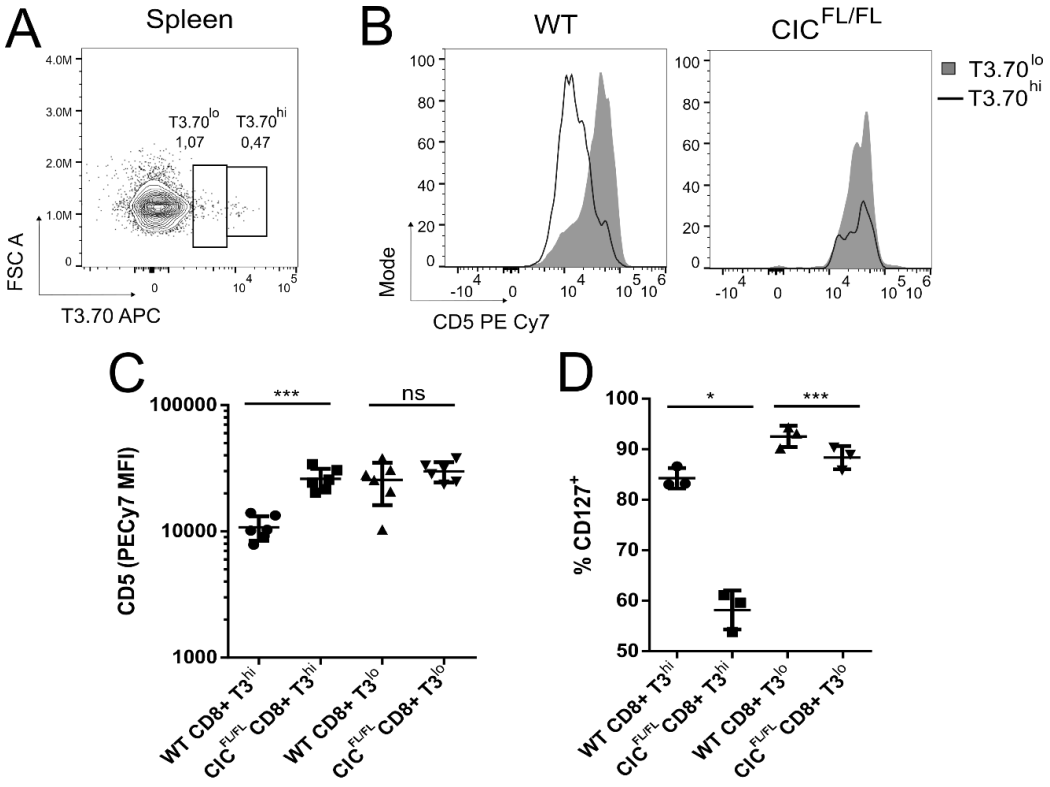

Figure 5-14: Phenotypic differences in CIC$^{FL/FL}$ T cells in HY^{cd4} bone marrow chimeras are largely limited to T3.70^{hi} populations.

A, Representative flow plots demonstrating how T3.70^{hi} and T3.70^{lo} populations were gated in the spleen. B, Flow plots demonstrating CD5 expression within T3.70^{hi} and T3.70^{lo} CD8^{+} donor-derived T cell populations in the spleen. C, Summary of data described in (B). D, Summary of the percentage of CD127^{+} within T3.70^{hi} and T3.70^{lo} populations in the spleen. Number of independent experiments/cohorts = 2. Asterisks represent statistical significance as determined by paired T-test.

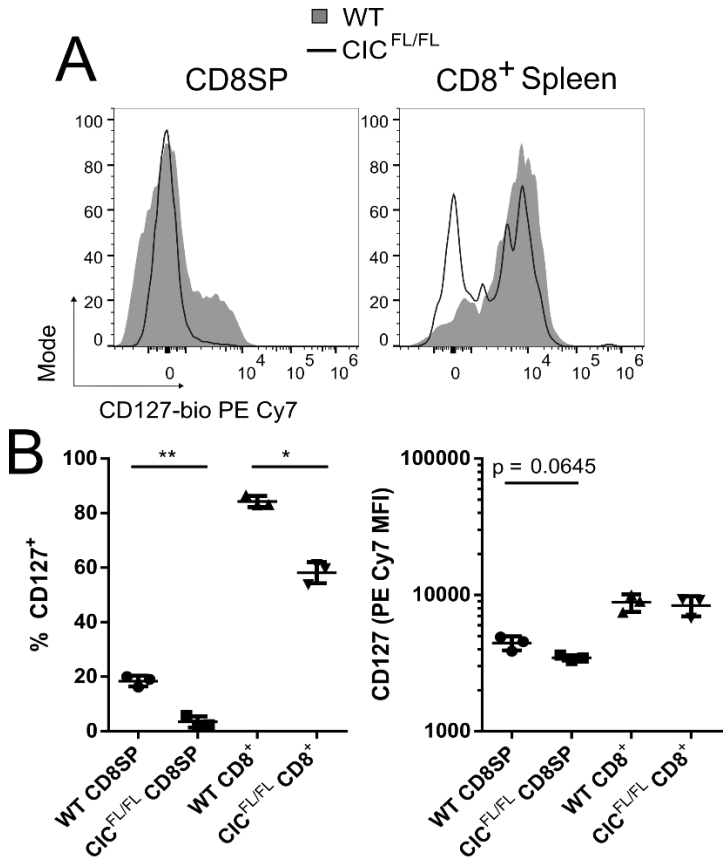

Figure 5-15: CIC-deficient transgenic HY^{cd4} T cells in WT:CIC$^{FL/FL}$ (1:1) female bone marrow chimeras show diminished CD127 expression.

A, CD127 expression within donor-derived T3.70^{hi} T cells within chimeras). B, Proportion of CD127^{+} (left) and CD127 expression within CD127^{+} subset (right) in donor-derived T cells. Number of independent experiments/cohorts = 1 unless otherwise stated. Asterisks represent statistical significance as determined by paired T-test.

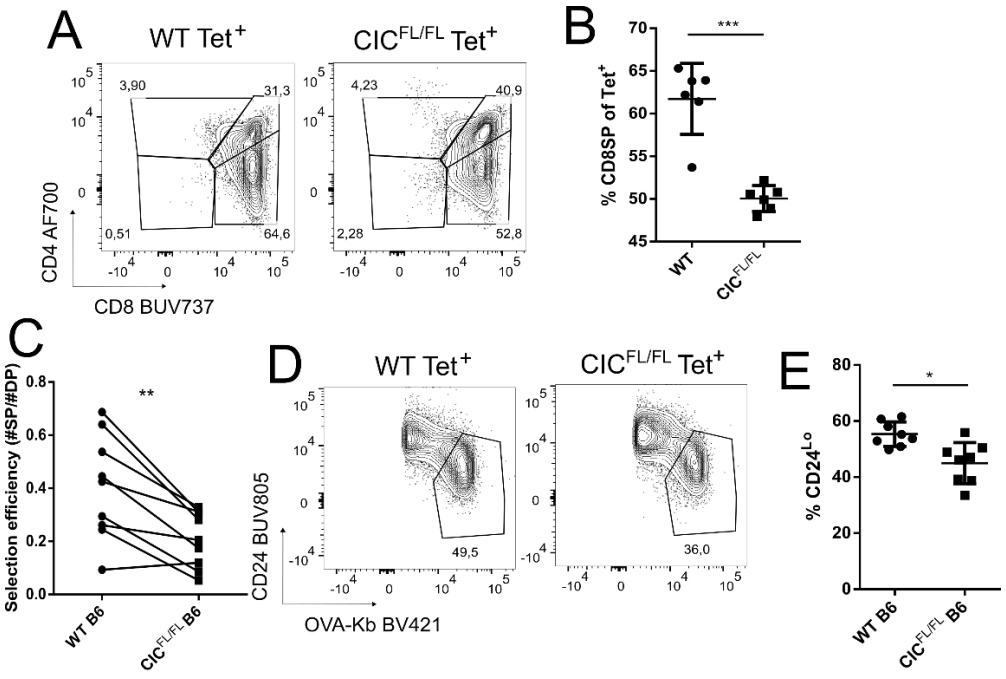

Figure 5-16: CIC deficiency leads to impairment in positive selection in OT-I > B6 chimeras. A, Representative flow plots of thymocytes of both donor origin within OT-I WT:CIC$^{FL/FL}$ (1:1) > WT (B6) mixed bone marrow chimeras. B, Proportion of tetramer-staining thymocytes that are CD8 single-positive; data are representative of one cohort. C, Positive selection efficiency in bone marrow chimeras calculated by the ratio of OT-I Tet^{+} CD8SP to total DP thymocytes. D, Proportion of Tet^{hi} CD24^{lo} mature CD8SP thymocytes within the Tet^{+} donor population. E, Summary of data described in (D). Number of independent experiments/cohorts = 2 unless otherwise stated. Asterisks represent statistical significance as determined by paired T-test.

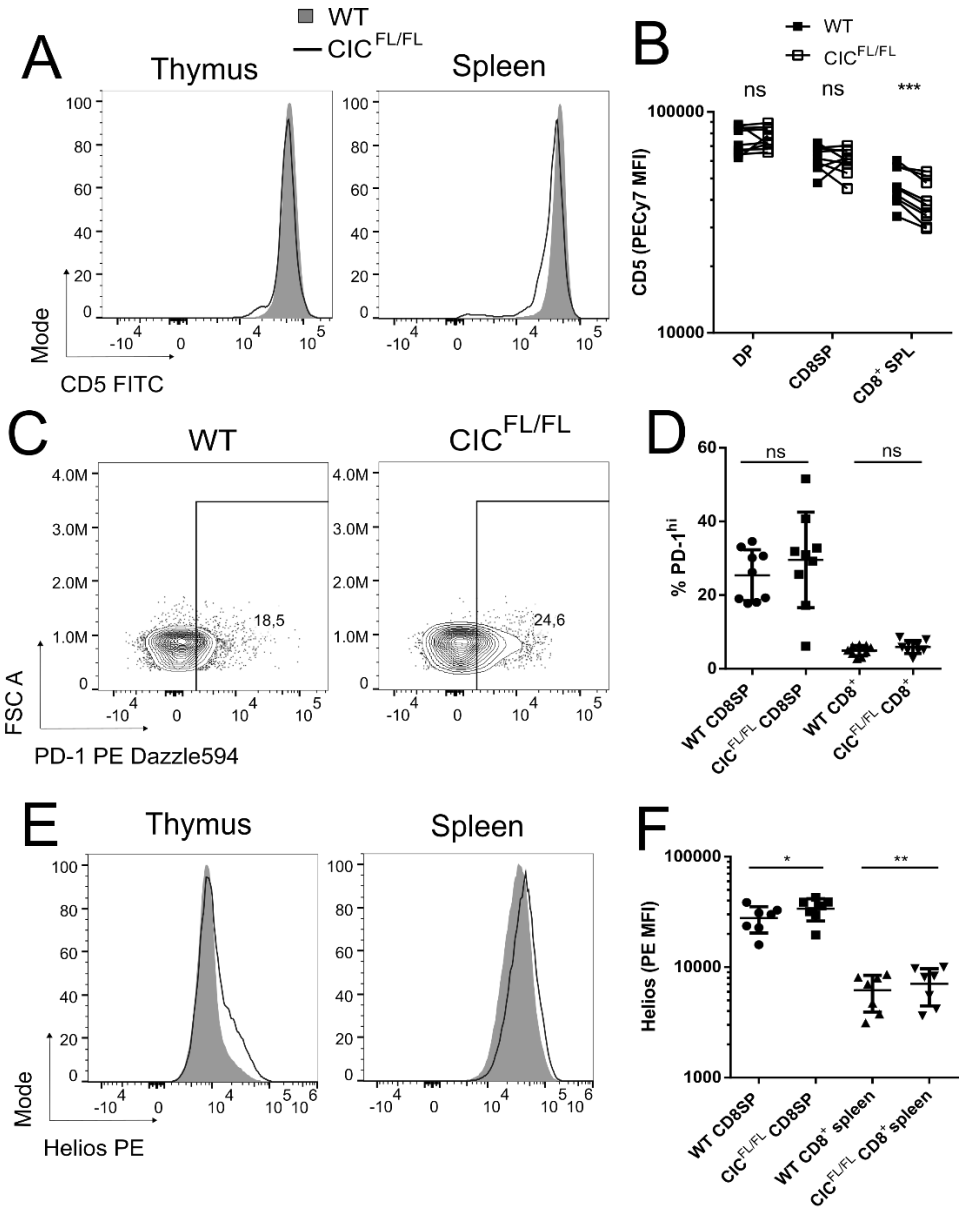

Figure 5-17: Phenotypes of CIC-deficient transgenic OT-I T cells in WT:CIC$^{FL/FL}$ > B6 bone marrow chimeras are suggestive of altered receipt of the TCR signal.

A, CD5 expression within Tet^{+} T cell subsets in mixed bone marrow chimeras. B, Summary of data described in (A). C, PD-1 expression within Tet^{+} donor-derived thymocytes within mixed bone marrow chimeras (spleen data not shown). D, Summary of data described in (C). E, Helios expression within Tet^{+} T cell subsets. F, Summary of data described in (E). Number of

independent experiments/cohorts = 2. Asterisks represent statistical significance as determined by paired T-test.

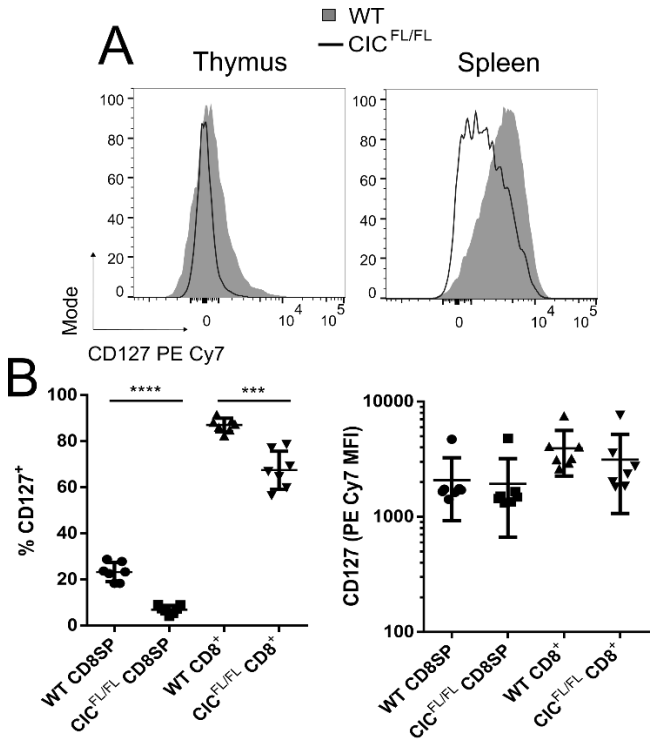

Figure 5-18: CIC-deficient transgenic OT-I T cells in WT:CIC$^{FL/FL}$ > B6 bone marrow chimeras showed diminished CD127 expression.

A, CD127 expression within donor-derived Tet^{+} T cells from the thymus (CD8SP) and spleen (CD8^{+}) of mixed bone marrow chimeras. B, Proportion of CD127^{+} (left) and CD127 expression within CD127^{+} subset (right) in donor-derived T cells. Number of independent experiments/cohorts = 2. Asterisks represent statistical significance as determined by paired T-test.

CIC-deficient T cells show intact negative selection and tolerance in two different transgenic models: OT-I and HYcd4

In the previous section, I demonstrated that CIC deficiency leads to an impairment in positive selection in two different TCR transgenic models. I next wanted to assess the impact of CIC deficiency on negative selection.

I generated HY^{cd4} WT:$CIC^{FL/FL}$ (1:1) BMCs using male recipients to study negative selection to ubiquitously expressed male-specific HY Ag. Normally, in the HY^{cd4} male thymus, clonal deletion occurs when DP thymocytes encounter high affinity HY Ag presented by cortical dendritic cells (22). In our mixed BMCs, I observed similar frequencies of CD8SP thymocytes within the transgenic $T3.70^{hi}$ population between cells of both WT and $CIC^{FL/FL}$ donor origins (Fig. 5-19A-B). When assessing clonal deletion by the ratio of CD8SP to DP among $T3.70^{hi}$ thymocytes in female and male BMCs, I observed a decrease from female to male in WT thymocytes (Fig. 5-19C). However, due to the poor rate of positive selection seen for $CIC^{FL/FL}$ in female chimeras, this ratio was similar to that of male chimeras. However, overall it appeared that HY^{cd4} $CIC^{FL/FL}$ thymocytes produced a similar phenotype to WT controls in male chimeras, and that negative selection appeared to be largely intact, as the SP/DP ratio was not significantly different between WT and $CIC^{FL/FL}$ thymocytes in male chimeras. In the donor-derived CD8SP compartment in male chimeras, the frequency of activated Caspase-3^{+} was not altered in the absence of CIC, suggesting that caspase-mediated cell death was not impacted by CIC deficiency (Fig. 5-19D).

I additionally generated OT-I WT:$CIC^{FL/FL}$ (1:1) BMCs using OVA-expressing RIP-mOVA recipients in order to model negative selection to tissue-restricted Ag. In our mixed BMCs, I observed similar frequencies of CD8SP thymocytes within the OVA-K^{b} $tetramer^{+}$ WT

or CIC$^{FL/FL}$ donor populations (Fig. 5-20A-B). When assessing clonal deletion using the ratio of CD8SP tetramer^{+} to DP thymocytes in B6 or RIP-mOVA recipients, I observed significant decreases from B6 to RIP-mOVA for both CIC-sufficient (WT) and CIC$^{FL/FL}$ cells (Fig. 5-20C), indicating that clonal deletion was intact in the absence of CIC. Additionally, OT-I WT:CIC$^{FL/FL}$ (1:1) > RIP-mOVA BMCs did not develop diabetes (Table 5-1), indicating that tolerance was intact when a portion of the T cell compartment is deficient in CIC.

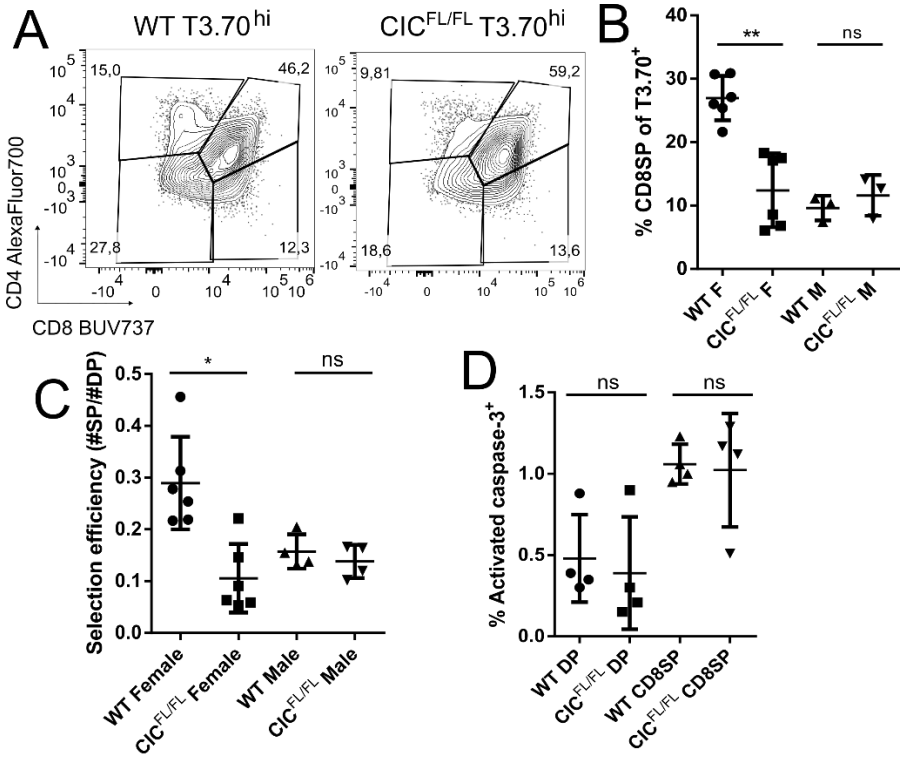

Figure 5-19: CIC-deficient T cells from mixed HY^{cd4} WT:CIC$^{FL/FL}$ (1:1) male bone marrow chimeras show intact negative selection.

A, Representative flow plots of T3.70^{hi} thymocytes of both WT and CIC$^{FL/FL}$ donor origin within male HY^{cd4} WT:CIC$^{FL/FL}$ (1:1) mixed bone marrow chimeras. B, Proportion of CD8SP thymocytes within the T3.70^{hi} thymic subset in female and male chimeras. C, Ratio (selection

efficiency) of CD8SP to DP within the T3.70^{hi} thymocyte subset in female (positive selection) and male (negative selection) chimeras. D, Proportion of activated Caspase-3^{+} thymocytes within thymic subsets. Number of independent experiments/cohorts = 2. Asterisks represent statistical significance as determined by paired T-test (B, D) or unpaired T-test with Welch's correction (C).

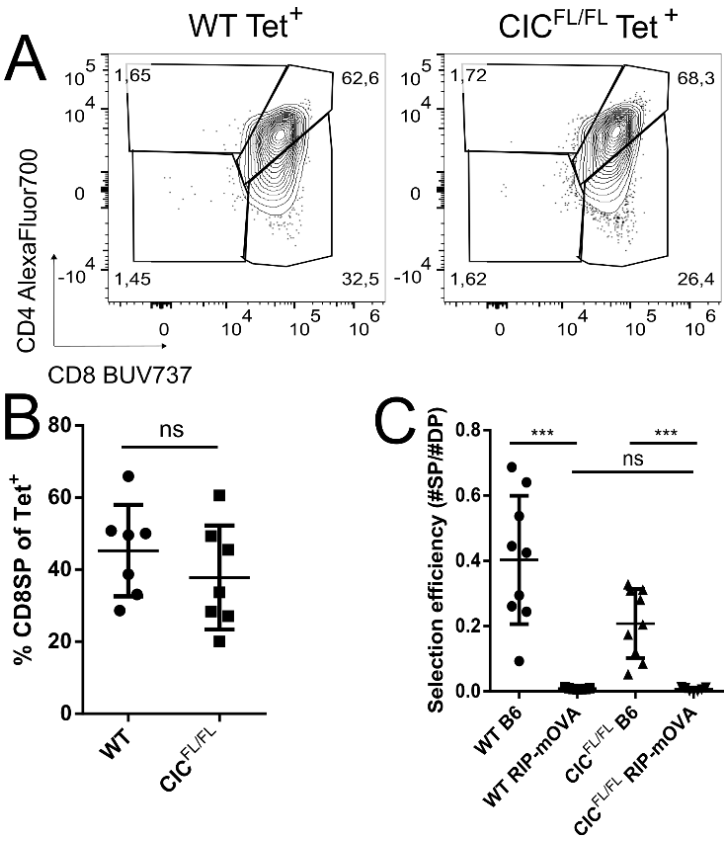

Figure 5-20: CIC-deficient T cells from mixed OT-I WT:CIC$^{FL/FL}$ (1:1) > RIP-mOVA bone marrow chimeras show intact negative selection.

A, Representative flow plots of Tet^{+} thymocytes of both WT and CIC$^{FL/FL}$ donor origin within OT-I WT:CIC$^{FL/FL}$ (1:1) mixed bone marrow chimeras. B, Proportion of CD8SP thymocytes within the Tet^{+} thymic subset in chimeras. C, Ratio of Tet^{+} CD8SP to total DP thymocytes in WT (B6, positive selection) and RIP-mOVA (negative selection) chimeras. Number of independent

experiments/cohorts = 2. Asterisks represent statistical significance as determined by paired T-test (B) or unpaired T-test with Welch's correction (C).

Table 5-1: Incidence of diabetes in OT-I WT:CIC$^{FL/FL}$ (1:1) > RIP-mOVA bone marrow chimeras. Blood glucose was tracked for at least 17 weeks post-reconstitution.

Chimera	**OT-I WT + CIC$^{FL/FL}$ > B6**	**OT-I WT + CIC$^{FL/FL}$ > RIP-mOVA**
Incidence of Diabetes	0/9	0/8

Dusp6 deletion does not rescue impaired positive selection in CD4-cre CIC$^{FL/FL}$ HY^{cd4} female chimeras

It is clear from our data that CIC plays a role in T cell positive selection, and potentially in peripheral T cell function and homeostasis. However, it is currently unknown how CIC functions in thymocytes or mature T cells in the periphery. Among the set of upregulated genes identified by RNA-seq in DP thymocytes from Vav1-cre CIC$^{FL/FL}$ compared with WT mice were *Etv1*, *Etv4, Etv5, Spry4, Dusp6, Dusp4,* and *Spred1* (213). And work in cell lines (293T and MCF7) has established CIC as a participant in an ERK-DUSP6 negative feedback loop (207), motivating us to interrogate DUSP6 as a CIC target in thymocytes, since ERK signaling is critical to positive selection (42, 43, 214).

I first conducted RT-qPCR on sorted populations of *ex vivo* polyclonal thymocytes and found that *Dusp6* expression appeared in general to be enhanced in the absence of CIC (Fig. 5-21). This enhancement was only significant for the DP subset, but was a non-significant trend in

other subsets. In parallel, I isolated naïve $CD8^+$ T cells from polyclonal spleen and similarly found a trending increase in the expression of *Dusp6*, although this was not significant (Fig. 5-21). A caveat to these data is that variability and low number of replicates has in part led to lack of significance in the differences I report.

In order interrogate whether regulation of DUSP6 expression is the mechanism by which CIC influences selection, I generated HY^{cd4} chimeras with either $CIC^{FL/WT}$ or $CIC^{FL/FL}$ BM and treated the HSCs with either control or *Dusp6*-targeting CRISPR gRNA (outlined in diagram in Fig. 5-22A) before transfer into lethally-irradiated female recipients. Special thanks to Dr. Niall Pollock for his help with western blotting experiments. Chimera set-ups are as follows: $CIC^{FL/WT}$ CTRL, $CIC^{FL/FL}$ CTRL, $CIC^{FL/WT}$ *Dusp6*, and $CIC^{FL/FL}$ *Dusp6*. After reconstitution, at time of analysis, protein lysates from whole splenocytes were harvested and analyzed by western blot. CRISPR-mediated deletion of *Dusp6* was confirmed, as splenocytes from chimeras that received edited BM had substantially reduced levels of DUSP6 protein (Fig. 5-22B-C). In agreement with the RT-qPCR data, DUSP6 expression appeared slightly elevated in splenocytes from HY^{cd4} $CIC^{FL/FL}$ CTRL chimeras compared with the $CIC^{FL/WT}$ control (Fig. 5-22C).

Finally, I analyzed the CRISPR-edited chimeras *ex vivo*. In CIC-sufficient chimeras, the ablation of DUSP6 alone did not appear to impact selection, as its deletion did not significantly affect thymic profiles (within the $T3.70^{hi}$ gate) (Fig. 5-23A), CD8SP or CD8SP $CD24^{lo}$ subset frequencies (Fig. 5-23B, 5-23D), selection efficiency (Fig. 5-23C), or number of transgenic donor-derived T cells in the spleen (Fig. 5-23E). The frequency of CD8SP thymocytes amongst $CIC^{FL/FL}$ thymocytes was not rescued by additional deletion in *Dusp6* (Fig. 5-23A-B) and this was also true for selection efficiency (Fig. 5-23C). The diminished frequency of the CD8SP $T3.70^+$ $CD24^{lo}$ mature subset I observed for $CIC^{FL/FL}$ thymocytes was not rescued with

disruption of the *Dusp6* locus (Fig. 5-23D), nor was the diminished size (in absolute cell numbers) of the splenic T cell compartment (Fig. 5-23E). Overall, deletion of *Dusp6* failed to rescue the impairment in positive selection experienced by $CIC^{FL/FL}$ thymocytes.

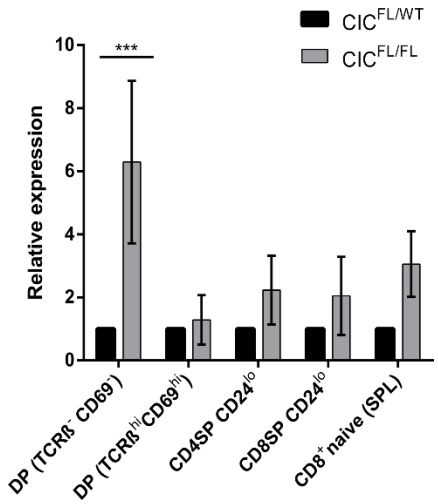

Figure 5-21: DUSP6 mRNA expression is enhanced in some T cell subsets of $CIC^{FL/FL}$ polyclonal mice.

DUSP6 mRNA abundance in sorted thymic subsets (FACS sort) and naïve $CD8^+$ T cells isolated from the spleen by magnetic separation from $CIC^{FL/FL}$ polyclonal mice expressed as a fold change over values in the $CIC^{FL/WT}$ subsets ($2^{-\Delta\Delta Ct}$). Pre-selection DP thymocytes ($TCR\beta^-$ $CD69^-$) (n = 2), post-positive selection DP thymocytes ($TCR\beta^{hi}$ $CD69^{hi}$), CD4SP mature ($TCR\beta^+$ $CD24^{lo}$), CD8SP mature ($TCR\beta^+$ $CD24^{lo}$), or $CD8^+$ naïve T cells ($CD44^{lo}$). Number of independent experiments = 3 unless otherwise stated. Asterisks represent statistical significance as determined by two-way ANOVA (Sidak's multiple comparison's test).

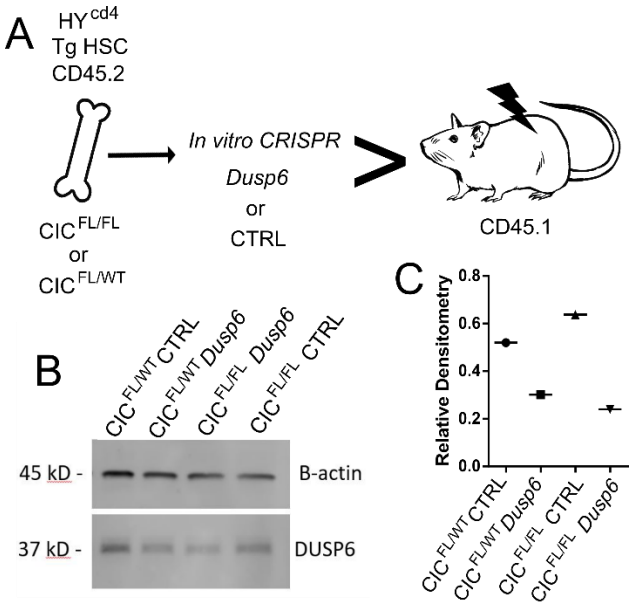

Figure 5-22: CRISPR-mediated interruption of the *Dusp6* locus is effective.

A, Diagram depicting *Dusp6* ablation using CRISPR in HYcd4 chimeras. Generated female HYcd4 chimeras with $CIC^{FL/FL}$ or $CIC^{FL/WT}$ HYcd4 marrow +/- CRISPR-mediated *Dusp6* ablation. B, DUSP6 expression in whole splenocytes from chimeras described in (A) verified by western blot. C, Relative densitometry from western blot in (B) assessed using ImageJ software. Number of independent experiments shown = 1.

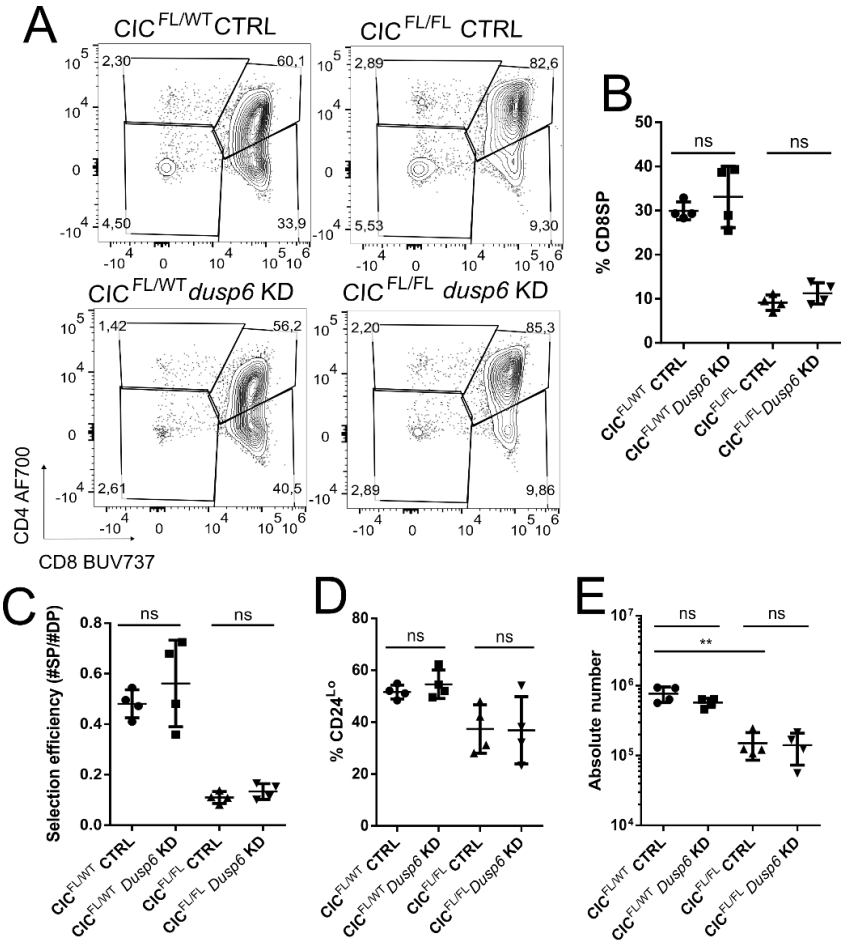

Figure 5-23: CRISPR-mediated DUSP6 knock-down does not rescue impaired positive selection in HY^{cd4} female mixed BMCs.

A, Representative flow plots for T3.70^{hi} thymocytes in the following HY^{cd4} female chimeras: CIC$^{FL/WT}$ CTRL, CIC$^{FL/FL}$ CTRL, CIC$^{FL/WT}$ *dusp6* KD, CIC$^{FL/FL}$ *dusp6* KD. B, Proportion of T3.70^{hi} thymocytes that are CD8SP. C, Selection efficiency in chimeras described in (A) represented as ratio of CD8SP to DP thymocyte within the T3.70^{hi} gate. D, Proportion of mature (CD24^{lo}) thymocytes within the donor T3.70^{+} CD8SP subset. E, Absolute number of T3.70^{hi} CD8^{+} donor-derived T cells in chimera spleens. Number of independent experiments = 2. Asterisks represent statistical significance as determined by unpaired T-test with Welch's correction.

Discussion

Recently, CIC has been implicated as an important contributor to thymocyte selection (211, 213). However, previous studies have focused mainly on models that ablate CIC expression in the whole hematopoietic compartment (e.g. Vav-1-cre, Tek-cre), meaning that roles for CIC in early thymic events (pre-DP stage) and in thymocyte selection itself have thus far not been distinguishable. In this current study, I showed that CIC plays an important role in positive selection (in particular for TCRs of low self-reactivity, potentially) but is not required for negative selection or tolerance.

In this chapter, I found features associated with CIC deficiency consistent with depressed TCR signaling in the thymus, such as a decreased frequency of post-positive selection DP thymocytes (Fig. 5-1D-E). In polyclonal mixed BMCs, I observed decreased CD5 expression on DP thymocytes (and to a lesser extent, mature peripheral T cells (Fig. 5-9C)), and made a similar observation in DP thymocytes from HY^{cd4} mixed BMCs (Fig. 5-13F). This is consistent with an interpretation of depressed TCR signaling, as TCR signal intensity experienced during positive selection is thought to program the expression level of CD5 (23). Indeed, Kim *et al.* (2021) reported decreased potential in Vav1-cre $CIC^{FL/FL}$ DP thymocytes for calcium influx and ERK activation following TCR crosslinking by anti-CD3/anti-CD4 antibodies (213). However, the same group failed to observe these results for CD4-cre $CIC^{FL/FL}$ DP thymocytes, suggesting that signaling deficiencies are likely due to dysfunction following an absence in CIC in pre-selection thymocytes rather than being reflective of CIC's role during selection itself. That CD4-cre $CIC^{FL/FL}$ DP thymocytes did not experience altered ERK activation is contrary to data collected from cell lines (293T and MCF7) that established CIC as a participant in an ERK-DUSP6 negative feedback loop (207). With this in mind, it is possible that CIC functions independently

of an ERK-DUSP6 negative feedback loop in DP thymocytes. Indeed, ablation of the *Dusp6* locus via CRISPR failed to rescue impaired positive selection in HY^{cd4} female chimeras in our study (Fig. 5-23). However, it is important to note that the study by Kim *et al.* (2021) induced ERK activation by anti-CD3 antibodies, which engage the TCR with high affinity and trigger activation-induced cell death in DP thymocytes *in vitro* (328, 329) and *in vivo* (330). Our male HY^{cd4} (Fig. 5-19) or OT-I > RIP-mOVA (Fig. 5-21) BMCs allowed us to model the receipt of a high affinity TCR signal in the thymus, and CIC deficiency did not disrupt negative selection in either of these experiments. Thus, it is rather possible that CIC specifically influences ERK negative feedback during the low affinity TCR signaling experienced during positive selection.

In contrast to what I observed in the thymus, features canonically associated with high affinity TCR signaling were apparent in the spleens of polyclonal mice in the absence of CIC. I observed an upregulation of CD44 and PD-1 (Fig. 5-2, 5-4), the former of the two having been previously reported for Vav1-cre $CIC^{FL/FL}$ model (212). However, the latter of these two observations may alternatively be explained by the increased generation of TFH ($CD4^+$ $CXCR5^+$ $PD\text{-}1^+$). Similarly to another group (212), the CD4-cre $CIC^{FL/FL}$ showed an increased proportion of $CD4^+$ $Foxp3^+$ $CD25^-$ T cells (Fig. 5-2B), a subset regarded as a less suppressive, less stable, precursor subset related to $CD4^+$ $Foxp3^+$ $CD25^+$ Tregs (331, 332). I also observed an increase in the proportion of $CD4^+$ $FR4^{hi}$ $CD73^{hi}$ cells (though this difference was not significant, Fig. 5-2B), which have been described in an Ag-specific arthritis model as an anergic subset. Both of these non-conventional subsets are thought to experience stronger TCR signaling than conventional T cells (57). This suggests that CIC-deficient T cells may experience tolerizing high affinity TCR signaling in peripheral tissues, but not in the thymus, where the proportion of these populations was unchanged. Thus, CIC deficiency does not appear to lead to the generation of T

cell clones of apparently high self-reactivity during selection in the thymus. Rather, this falls in line with evidence of lower affinity TCR signal intensity in thymocytes discussed above. Indeed, the frequency of another subset generated from agonist selection, IELp, was in fact lower in $CIC^{FL/FL}$ thymocytes (Fig. 5-3B). Overall, in the absence of CIC, thymocytes demonstrated features of low TCR signal intensity; the presentation of features of high TCR signal intensity in peripheral T cells suggests CIC may differentially support the normal integration of the TCR signal in both the thymus and periphery.

$CIC^{FL/FL}$ thymocytes in $CIC^{FL/FL}$:$CIC^{FL/WT}$ (1:1) mixed BMCs showed similarly aberrant selection to polyclonal thymocytes *ex vivo*, indicating that the $CIC^{FL/FL}$ phenotype is cell-intrinsic (Fig. 5-8), and upon the introduction of competition, I saw the emergence of decreased CD5 expression on $CIC^{FL/FL}$ cells (discussed above). Competition between CIC-sufficient and -deficient thymocytes during positive selection may magnify such markers of a depressed TCR signal, as positively selecting ligands (and survival-promoting stimuli such as IL-7 (20)) may be rendered even more limiting to a given clone (reviewed in (333)). Indeed, between the mature CD8SP thymocyte to peripheral $CD8^+$ subsets, cells of $CIC^{FL/FL}$-origin became proportionally outnumbered by the $CIC^{FL/WT}$, suggesting poorer homeostatic maintenance in the absence of CIC (the caveat here being that the contribution of differential thymic egress to this phenotype is unknown, given that I did not assay for rates of thymic egress) (Fig. 5-8E). Despite this, I observed an elevated proportion of $Ki67^+$ $CIC^{FL/FL}$ cells in polyclonal mixed BMCs (Fig. 5-9D), as Ki67 is expressed in G1, S, G2, and M phase of the cell cycle, and has canonically been used as an indicator of proliferation (326, 334), suggesting that peripheral $CIC^{FL/FL}$ may experience increased rates of cell death to account for the relative decline of their population. In a polyclonal setting, it is possible that T cell clones of low self-reactivity fail to thrive (successful competition

for positively selecting and/or homeostatic ligands), leading highly self-reactive clones to predominate. With the addition of competition, I saw a magnification of the frequency of PD-1^{hi} conventional CD4^{+} and CD8^{+} T cells in the spleen (Fig. 5-10), which coincides with further magnified generation of TFH (Fig. 5-10C). This suggests that – in addition to the agonist-selected lineages described in the above sections – CD4^{+} T cells that develop and circulate in the absence of CIC have a competitive advantage for acquiring the signals required for TFH differentiation such as long TCR-pMHCII dwell times (335).

Mature CD4-cre CIC$^{FL/FL}$ CD4^{+} and CD8^{+} T cells display mild (though not statistically significant) functional impairments *in vitro* following stimulation with anti-CD3/anti-CD28 antibodies (Fig. 5-6) and *in vivo* during lymphopenia-induced proliferation (LIP, Fig. 5-7). These data stand in contrast to previous reports of enhanced cytokine and proliferative responses by T cells from Vav1-cre CIC$^{FL/FL}$ mice to anti-CD3/anti-CD28 antibodies (212), further highlighting the differences between CD4-cre and Vav1-cre-driven knock-out models in this context. LIP helps us to assess the T cell capacity for proliferation in an environment of relatively abundant homeostatic resources (compared with lymphoreplete compartments) such as pMHC complexes and IL-7 or IL-5, collectively defined as T cell "space" (336, 337). Some factors known to proportionally influence the rate of LIP are the strength of TCR affinity for self-pMHC ligands and sensitivity to IL-7 received through the IL-7 receptor (IL-7R, whose unique α chain is CD127) (reviewed in (338)). It is thus reasonable to implicate both depressed TCR signaling and CD127 expression (Fig. 5-5, Fig. 5-9A-B) as contributors to altered LIP in the CD4-cre CIC$^{FL/FL}$. However, despite decreased CD127 expression spanning both CD4^{+} and CD8^{+} populations, LIP was only diminished in CD8^{+} CIC$^{FL/FL}$ cells, suggesting that differences in CD127 expression alone were not responsible for altered propensity for LIP.

Similarly to our polyclonal experiments, HY^{cd4} mixed BMCs showed features of depressed TCR signal intensity in the thymus (impaired positive selection, Fig. 5-12; decreased CD5 expression in DP thymocytes, Fig. 5-13F) and features of enhanced signal intensity/self-reactivity in the spleen (increased CD5 and PD-1 expression). In contrast to our results in the HY^{cd4} model, OT-I mixed BMCs presented a milder impairment in positive selection for $CIC^{FL/FL}$ thymocytes (Fig. 5-16). Peripheral markers of high affinity signaling (such as PD-1 and Helios) were in some cases significant but minor, and splenic Tet^{+} $CD8^{+}$ $CIC^{FL/FL}$ donor cells displayed decreased CD5 expression (Fig. 5-17), in contrast with the results from the HY^{cd4} chimeras. Additionally, in male HY^{cd4} and OT-I > RIP-mOVA chimeras, I saw no overt defects in negative selection (Fig. 5-19, 5-20). That I observed similar results with the fixed transgenic TCR chimeras as with the polyclonal suggests the phenotype I found associated with CIC deficiency is not simply due to alterations in the T cell repertoire, although such alterations may still have occurred in polyclonal mice. Indeed, changes in the frequencies of TCR β variable segments were observed for conventional $CD4^{+}$ ($CD25^{-}$ $Foxp3^{-}$) T cells and Treg $CD4^{+}$ ($CD25^{+}$ $Foxp3^{+}$) cells in Vav1-cre $CIC^{FL/FL}$ mice (213), but this may have been due to alterations in early thymocyte development (e.g. β-selection). That CIC deficiency produced a more robust effect in positively selected T cells of low self-reactivity (HY^{cd4}) compared with those of higher self-reactivity (OT-I) suggests CIC plays a preferential role in the integration of very low affinity positively selecting TCR signals, and this is further supported by the largely normal negative selection in the absence of CIC.

With this in mind, in the HY^{cd4} mixed chimeras, I compared $T3.70^{hi}$ and $T3.70^{lo}$ cells, the latter of which likely stems from co-expression of endogenously rearranged TCRα-chains. I observed the gulf in phenotype (CD5, CD127 expression) of splenic $T3.70^{+}$ $CD8^{+}$ to arise

preferentially in the T3.70^{hi} population (Fig. 5-14). Given that CIC deficiency appears to preferentially impact outcomes following low affinity TCR signaling, these results suggest that the endogenous α-chain rescues the aberrant phenotype of the CIC$^{FL/FL}$ due to enhancing self-reactivity relative to the low self-reactivity of the HY TCR. These are however speculations and can in the future be confirmed by crossing the HY^{cd4} transgenic onto a RAG-deficient background, wherein endogenous TCRα rearrangements can be precluded.

Here, I showed using the OT-I > RIP-mOVA system that CIC is not required for CD8^{+} T cell tolerance to TRA, as these chimeras did not develop diabetes in the absence of CIC (Table 5-1). However, it has previously been recorded that both CD4-cre and Vav1-cre CIC$^{FL/FL}$ mice develop T cell-intrinsic lymphoproliferative autoimmunity characterized by abnormal development of TFH cells and GC responses, indicating a role for CIC in maintaining peripheral tolerance. In this context, CIC is thought to modulate tolerance by restricting the activity of the transcription factor ETV5, which promotes TFH differentiation (212). Overall, despite the support that I demonstrated for a role for CIC in thymocyte development, its influence likely extends into the activities of mature peripheral T cells; disentangling thymic and peripheral roles for CIC will thus be important in future studies.

Chapter 6 - General Discussion

PD-1 Discussion

This chapter contains content originally published in The Journal of Immunology:

- May, J. F., R. G. Kelly, A. Y. W. Suen, J. Kim, J. Kim, C. C. Anderson, G. R. Rayat, and T. A. Baldwin. 2024. Establishment of CD8+ T Cell Thymic Central Tolerance to Tissue-Restricted Antigen Requires PD-1. J. Immunol. Vol 212 (2): 271-283. Copyright © [2024] The American Association of Immunologists, Inc.

Summary

Broadly, in the work presented here, I have investigated the mechanism as well as the functional and genomic consequences following high affinity TCR signaling triggered by a neo-self Ag whose expression models that of tissue-restricted Ag (TRA) during T cell development. We previously showed that when clonal deletion was precluded by the absence of Bim in developing thymocytes in OT-I $Bim^{-/-}$ > RIP-mOVA chimeras, autoimmunity in the form of diabetes did not develop despite the encounter of high affinity antigen, suggesting the presence of a robust mechanism non-deletional tolerance (74). The impetus for this present study was to characterize the functional impairment induced in thymocytes that escape clonal deletion in this model. I observed that PD-1 was critical in the establishment of tolerance in thymocytes that escaped clonal deletion. While PD-1 signaling was important for both this establishment as well as the maintenance of tolerance as these thymocytes matured and entered the periphery, I determined that the PD-1 ligand requirements for these processes differ. The summarized model for PD-1 function in our model is detailed in Figure 6-1. Overall, this study provides insight into the underappreciated role for PD-1 in central tolerance as well as in how the kinetics of the

necessary PD-1 signal may change based on whether tolerance is being established or maintained.

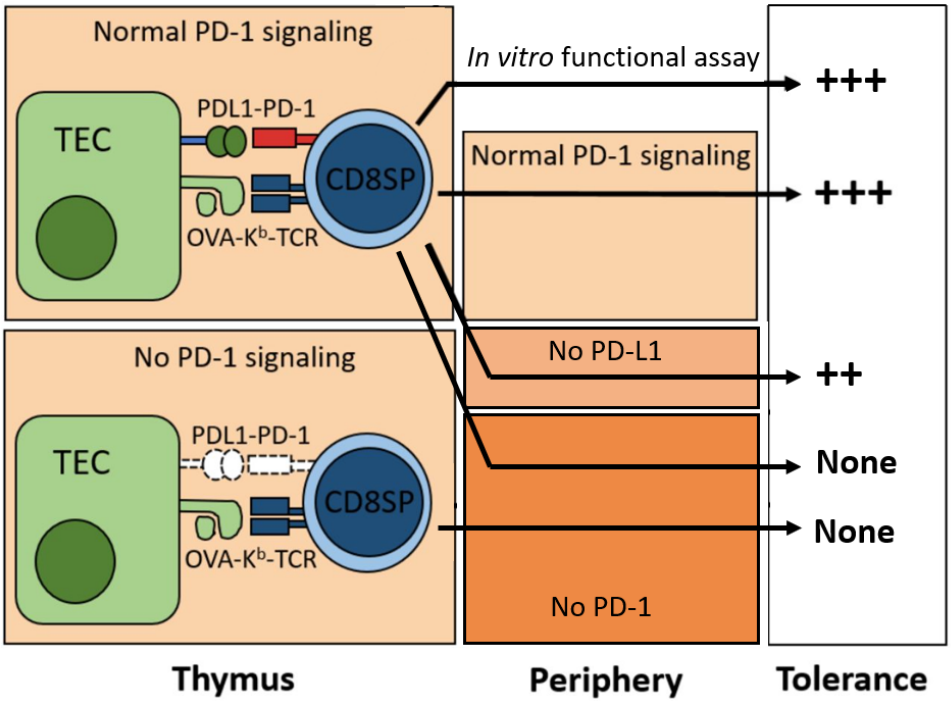

Figure 6-1: Model for PD-1 function in tolerance in OT-I Bim$^{-/-}$ > RIP-mOVA chimeras.

Here, I have investigated the non-deletional tolerance supported by PD-1 in OT-I Bim$^{-/-}$ > RIP-mOVA chimeras and described the first epigenetic profile characteristic of such a tolerant state. Mature OT-I T cells from such chimeras demonstrated cell-intrinsic functional impairment, as neither whole spleen isolates nor CD8^{+}-enriched fractions from these chimeras were diabetogenic in sublethally-irradiated recipients and did not have a dominant suppressive effect on non-tolerant WT OT-I T cells (Fig. 3-2). This functional impairment is established in the thymus of these chimeras, as OT-I Bim$^{-/-}$ > RIP-mOVA thymocytes displayed impaired responses to high affinity Ag (OVA) *in vitro* (Fig. 3-4) and were not diabetogenic, compared to cells from

Ag-naïve non-tolerant controls (Fig. 3-5). I also found that tolerance in this context was associated with the upregulation of markers typically associated with the "exhausted" state, TOX (Fig. 3-6), and PD-1 (Fig. 3-7). I characterized the epigenetic profile associated with tolerant thymocytes in OT-I $Bim^{-/-}$ > RIP-mOVA chimeras. Despite sharing some features previously reported for exhaustion, such as *Nr4a1* and *Tnfrsf18* promoters being enriched with NFRs (Table 3-1) or diminished AP-1 transcription factor footprinting (Table 3-5), I reported some features positively associated with T cell function (e.g. *Ksr1, Il2,* and *Ifng*).

I also demonstrated that continuous PD-1 signaling is required to maintain tolerance in TRA-specific $CD8^+$ T cells, but PD-L1 expressed on cells of non-hematopoietic origin is largely dispensable until later time points. Adoptively transferred cells (from thymus or spleen) from OT-I $Bim^{-/-}$ > RIP-mOVA chimeras into sublethally-irradiated RIP-mOVA $PD\text{-}L1^{-/-}$ recipients only caused autoimmune diabetes at late time points and with incomplete penetrance (Fig. 4-8). Meanwhile, deletion of PD-1 by CRISPR in mature splenic cells from these chimeras resulted in rapid loss of tolerance and development of autoimmune diabetes (Fig. 4-10). Conversely, while PD-L1 expression on cells of non-hematopoietic lineages did not appear critical for the maintenance of tolerance, it was critical for the establishment of tolerance, as OT-I $Bim^{-/-}$ > RIP-mOVA $PD\text{-}L1^{-/-}$ chimeras rapidly developed diabetes (Fig. 4-6).

Heterogeneity and epigenetic flexibility of T cell dysfunction

The exhausted T cell population is heterogenous, comprised of at least two subpopulations, T_{PEX} and T_{EX}. Progenitor (T_{PEX}) exhausted T cells are a stem cell-like population that shares features with both early exhausted T cells (impaired cytokine production and increased expression of inhibitory receptors such as PD-1) as well as memory T cells (increased expression of TCF1 and long-term self-renewal (135–138)) (139). The transcription factor MYB

was also recently found to support the development and functionally impaired identity of the T_{PEX} population (259). The pool of T_{PEX} is thought to differentiate into and replenish the terminally differentiated T_{EX} effector population in response to chronic Ag stimulation (140). The T_{PEX} population has been shown to be the exhausted subset with enhanced anti-tumour activity (141, 142) and sensitivity to reinvigoration by PD-1 blockade (135, 141, 259, 339) or PD-1:CTLA-4 combined blockade (136). Thus, the frequency of the T_{PEX} subset within the greater exhausted pool is thought to inform the severity of T cell exhaustion, which gradually progresses over time along with prolonged depletion of T_{PEX} as they produce T_{EX} progeny (140). In chapter 3, I discussed how NFAT activity in the context of decreased AP-1 binding in thymocytes (Table 3-5) is associated with T cell dysfunction and may underlie our observations in OT-I $Bim^{-/-}$ > RIP-mOVA chimeras. In the event of chronic Ag stimulation, nuclear occupation and activity by NFAT in the absence of AP-1 may accumulate "signal memory", due to NFAT's rapid nuclear import but slow export (288). NFAT activity induces TOX expression, which has been demonstrated as the initiator for the exhaustion-specific epigenetic program (340, 341). Although both T_{PEX} and T_{EX} rely on TOX for development, maintenance, and longevity (243, 340–342), TOX may thus translate chronic TCR stimulation to the terminally differentiated identity of T_{EX}, characterized by resistance to functional rescue either by discontinuing exposure to Ag or disrupting co-inhibitory signals (343). Importantly, NFAT activity is known to be important for not just exhaustion, but anergy as well, suggesting this mechanism may be applicable to T cell dysfunction in general (282).

Work done by the Schietinger group in an autochthonous liver cancer model showed that tumour-specific $CD8^+$ T cells differentiated through two discrete chromatin states associated with dysfunction and a sequential loss of TCF1 expression: 1) early in tumorigenesis, when effector

function could be rescued with *in vitro* culture with IL-15 (plastic program, likely reflecting T_{PEX} identity), and 2) late in tumorigenesis, when effector function could not be rescued (fixed program, likely reflecting T_{EX} identity) (343, 344). This distinction suggests that whether the epigenome presents an obstacle for rescue from the dysfunctional state is dependent on duration, frequency, and context of Ag encounter. As T cells transitioned to the late (fixed) dysfunctional state, the Schietinger group saw opening chromatin peaks that were enriched in E2F and Sp/KLF family TF motifs, which play diverse roles in proliferation, differentiation, development, and activation (345, 346). In contrast, dysfunction in our model was associated with under-representation of binding for these TFs (Table 3-5). They also observed chromatin regions enriched in AP-1 TF family motifs become closed with this transition, which coincides with our observation of diminished AP-1 foot-printing (Table 3-5). I found enhanced TOX but similar TCF1 expression in dysfunctional T cells from OT-I $Bim^{-/-}$ > RIP-mOVA chimera pLNs (Fig. 3-6) and the *Myb* promoter to be enriched in NFRs in our dysfunctional thymocytes (Table 3-1). While open chromatin at the *Myb* promoter suggests the presence of MYB-driven T_{PEX} in our model, the lack of a difference in TCF1 expression between RIP-mOVA and WT chimeras suggests dysfunctional T cells in our model more closely resemble terminally differentiated T_{EX}.

Puzzlingly, dysfunctional T cells in our model were sensitive to CRISPR-mediated disruption of PD-1 signaling (Fig. 4-10), a feature associated with the T_{PEX} subset. However, I showed that PD-1 blockade failed to reverse tolerance in our model (Table 4-1), which is more in line with expectations for T_{EX} populations. A possible explanation for these divergent observations may be that the relative sensitivity of the whole dysfunctional population to PD-1 disruption may reflect the composition of the population and frequency of the responsive T_{PEX} subset. How does PD-1 signaling influence the dynamic between progenitor T_{PEX} and terminally

differentiated T_{EX}? Tsui *et al.* (2022) proposed that PD-1 does not impact the development of T_{PEX}/T_{EX}, but rather limits the differentiation of $CD62L^+$ T_{PEX} into terminally exhausted effectors, which – although functionally impaired, and are themselves unable to expand – mediate viral clearance (259). In the NOD model for T1D, stem-like $TCF1^+$ autoimmune progenitors seed the population of pancreas-infiltrating $TCF1^-$ autoimmune mediators, which destroy β cells but are short-lived and therefore unable to independently sustain prolonged pathology (244). Together, these studies suggest that both T_{PEX}/T_{EX} contribute to the balance between the response to chronic Ag on one hand, and uncontrolled immune pathology on the other in the context of both tolerance and exhaustion, and that PD-1 regulates this balance. If PD-1 blockade is not 100 % effective and allows for low-level PD-1 signals to continue (in contrast with the complete ablation of PD-1 by CRISPR), this may be sufficient to maintain tolerance if blockade-sensitive T_{PEX} represent a minority of dysfunctional cells in our model. Schietinger *et al.* (2012) conducted a study using a model similar to ours, where TCR_{GAG} (TCR specificity for the Friend murine leukemia virus GAG epitope) transgenic mice were crossed with the Alb:GAG mouse strain, which expresses the *gag* transgene in hepatocytes via the albumin promoter (115). Despite only partial deletion of $CD8^+$ TCR_{GAG} thymocytes and their circulation in the periphery, these cells were functionally impaired and did not mediate liver injury. They observed enhanced Lag-3 expression, as has been reported for terminally exhausted cells during chronic LCMV infection (140), while I did not observe such a change (Fig. 3-8). Since co-expression of multiple inhibitory receptors correlates with more severe exhaustion (290), increased Lag-3 expression may similarly correlate with insensitivity of impaired T cells in the TCR_{GAG}-Alb:GAG model to rescue by discontinuation of Ag exposure (115). Meanwhile, impaired T cells in our model are

sensitive to rescue by this treatment (116), suggesting that our model imposes a less advanced state of dysfunction.

Similarly to what has been shown in studies in exhaustion models, anergy is thought to be a plastic and heterogeneous state. In a parallel to exhaustion being a progressive state, experiencing terminal differentiation and heightened resistance to reinvigoration over time, evidence suggests that tolerance is not a binary on/off state, but rather reflects a progressive range of responsiveness to Ag. The Fife group showed using the OT-I: iFABP-OVA Tg model that Ag-specific OT-I $CD8^+$ T cells were sensitive to PD-L1 blockade during the induction, but not the maintenance of anergy (188). They subsequently found that fully established tolerance could be reversed with strong TCR signaling in the presence of inflammatory stimuli, and susceptibility to PD-L1 blockade was renewed (125). Additionally, recent examination of naïve polyclonal $CD4^+$ T cells suggested that heterogeneity in basal TCR signaling may correlate with the degree of dysfunction in anergic cells (147). In a study investigating cell-intrinsic peripheral tolerance established in the context of lymphopenia, it was suggested that responsiveness was tunable in a manner dependent activation history of the cell and on perceived Ag dose, which may be curbed when T cell density is high (347). The interplay between the strength of the initial TCR signal and PD-1 during the induction of anergy influences the 'quality' (or depth of dysfunction) and persistence of remains largely mysterious.

Overall, the epigenetic, phenotypic, and functional profile of dysfunctional $CD8^+$ T cells in our model do not plainly align within either a T_{PEX} (plastic) or T_{EX} (fixed) exhausted program. This may be due to differential kinetics and circumstances of Ag encounter associated with our model and others discussed here. It may also be that our model does not see a predominance of either fixed or plastic dysfunction that can be parsed with the experiments I have carried out

here. Thus, future directions for this project might include a more comprehensive investigation of the T_{PEX}/T_{EX} phenotypic balance in OT-I Bim$^{-/-}$ > RIP-mOVA chimeras. For example, quantifying additional markers others have used for discerning exhausted subpopulations. T_{PEX} have been reported to be CD62L^{+} (259), T-bet^{hi} (140), Ly108^{+} (135), TCF1^{+} (135, 138, 141), CD38^{lo}, CD101^{lo}, CD30L^{lo}, and CD5^{hi} (344). T_{EX} have been reported to be Eomes^{hi} (140), Ly108^{-} (135), TCF1^{-} (135, 138, 141), CD38^{hi}, CD101^{hi}, CD30L^{hi}, and CD5^{lo} (344). Sorting subpopulations in our model based on these markers would allow us to verify whether they indeed possess the same functional features as those seen in exhaustion models as has been observed for self-reactive T cells in NOD mice (244). It will be interesting to examine the capacity for functional rescue in these populations (by removing Ag or disrupting PD-1 signaling), how they change as thymocytes migrate to the periphery and repeatedly encounter Ag, and how they change as functional rescue is achieved. These experiments may help us understand how and why dysfunctional T cell populations become resistant to functional rescue.

Comparing states of dysfunction

There exist commonalities and differences among dysfunctional T cell states reported in the literature compared with our study. Given that these states indeed share extensive similarities, I propose that lessons from reports on one state of dysfunction can facilitate our understanding of another. For example, earlier in this document, I explained our rationale for considering anergy a mechanism of tolerance (despite some opinions in the literature maintaining that they are distinct states). Thus, I consider dysfunctional OT-I T cells from our OT-I Bim$^{-/-}$ > RIP-mOVA chimeras to be both tolerant and anergic, as they nevertheless share features described for both states (Fig. 3-4, 3-7, (116)).

Impaired cytokine production is a shared feature between our model, and canonical definitions of exhaustion and anergy (112, 116, 348). However, in a study from Villarino *et al.* (2011), DO11 OVA-specific MHC II-restricted transgenic (Tg) T cells were adoptively transferred into recipient mice expressing soluble OVA in the blood and were rendered anergic despite having upregulated expression of cytokine mRNA. The disconnect between abundant cytokine mRNA and limited cytokine protein expression was mediated by post-transcriptional silencing. While I did not measure the transcript volume for cytokines in our dysfunctional T cells, I saw an enrichment in NFRs in the promoters near *Ifng* and *Il2* (Table 3-1). This suggests that, similarly to the anergic state observed by Villarino *et al.*, cytokine loci in our model may have the potential for equal or greater transcriptional activity despite limited cytokine production.

Overall, T cell dysfunction our model shares similarities with both canonical anergy and exhaustion. Some other examples I discussed are the under-representation of AP-1 transcription factor foot-printing (Table 3-5) (114, 267) and increased PD-1 expression (112, 170, 349). While much work has been done to characterize states of T cell dysfunction, cumulative evidence indicates that these broad terms (exhaustion, anergy, tolerance) likely represent a spectrum of functionally and biochemically disparate forms. Differences across studies may stem from heterogeneity in model systems rather than strict inherent boundaries between exhaustion and anergy, for example. This provides rationale for attention in future studies directed toward the mechanisms driving this heterogeneity.

Role of PD-1

As mentioned above, T cell dysfunction in our model was associated with increased PD-1 expression, which has been described as a feature of T cell dysfunction in studies investigating

tolerance, anergy, and exhaustion. In the context of anergy, co-stimulation through CD28 engagement feeds into the PI3K/AKT-mTOR pathway (350), which when blocked may promote the transition into the anergic state (351). The PD-1:PD-L1 interaction is an example, along with co-stimulation, of an additional signal that shapes the response downstream of the TCR (166). Importantly, signaling through PD-1 leads to the recruitment of SHP-1/2, whose phosphatase activity attenuates the activity of the PI3K and AKT pathways (77). However, developing thymocytes in our OT-I Bim$^{-/-}$ > RIP-mOVA chimeras first encounter high affinity Ag presented in the thymic medulla, where APCs express an abundance of co-stimulatory molecules (23). Thus, if self-reactive thymocytes receive high affinity TCR stimulation in the presence of co-stimulatory signals, and clonal deletion is precluded with the deletion of Bim, tolerance is likely established thanks to the negative regulation of PD-1 on the co-stimulatory signal. PD-1 and its recruitment of SHP-1/2 are also thought to dampen the phosphorylation-dependent signaling cascades stemming from the TCR itself in addition to CD28. When tolerance is established and PD-1 expression is elevated, PD-1's inhibition on the chronic TCR signal may contribute to chronic nuclear occupation by NFAT in the absence of AP-1 and "signal memory" described in the above. Indeed, PD-1 has been proposed to interfere with AP-1 signaling (352), and following PD-L1 blockade, the exhausted T cell epigenome became modestly more permissible for AP-1 binding and saw evidence of greater AP-1 activity (296).

In chapter 4, I described conflicting results as to the necessity of PD-1 in the maintenance of tolerance. While disruption of the PD-1 signal in OT-I Bim$^{-/-}$ > RIP-mOVA chimeras by PD-1 blockade (Table 4-1) and adoptive transfer into PD-L1$^{-/-}$ RIP-mOVA recipients (Fig. 4-8) failed to robustly reverse tolerance, CRISPR-mediated editing of the *Pdcd1* locus in mature dysfunctional T cells succeeded (Fig. 4-10). With the complete nature of CRISPR-mediated

ablation of the *Pdcd1* locus in contrast to blockade and adoptive transfer strategies theoretically permitting residual PD-1 signaling, these data suggest that continuous PD-1 signals are indeed required to maintain tolerance. PD-L1 is expressed on both cells of hematopoietic (T, B, DC, macrophage) and non-hematopoietic origin (vascular and stromal endothelial cells and other peripheral cell types). PD-L2 expression is, by contrast, more limited, being found predominantly on DCs, macrophages and B cells (161). In our OT-I Bim$^{-/-}$ > RIP-mOVA PD-L1$^{-/-}$ BMCs, PD-L1/2 expression is limited to hematopoietic lineages, which appear incapable of delivering a signal through PD-1 to establish tolerance (Fig. 4-6). Thus, PD-L1 expression on non-hematopoietic lineages appears critical for this process. This coincides with the current understanding of PD-1-PD-1 ligand signaling (requiring PD-1 ligand and pMHC expression on the same cell) (161), as thymocytes in our model first encounter high affinity Ag presented by medullary thymic epithelial cells. Similarly, the Sharpe group previously demonstrated in the NOD background that PD-L1 expression on non-hematopoietic lineages protects against autoimmune diabetes, and that PD-L1/2 expression on cells of hematopoietic origin was insufficient to protect animals from disease (316). Alternatively, since PD-L1 expression on cells of non-hematopoietic origin may provide a comparatively abundant source of PD-1 ligand relative to PD-L1/2 on hematopoietic lineages, it may be that high avidity or frequent signaling through PD-1 is required to establish tolerance, and that this is not attainable in OT-I Bim$^{-/-}$ > RIP-mOVA PD-L1$^{-/-}$ BMCs. However, the cell type delivering the PD-1 signal is still likely important, given that cells of hematopoietic origin are more abundant in the thymus than thymic epithelial cells (353), but their expression of PD-L1 is still insufficient to establish tolerance in OT-I Bim$^{-/-}$ > RIP-mOVA PD-L1$^{-/-}$ BMCs. In our adoptive transfers of cells (from thymus or spleen) from OT-I Bim$^{-/-}$ > RIP-mOVA chimeras into RIP-mOVA PD-L1$^{-/-}$ recipients (Fig. 4-8),

PD-L1 expression is limited to the (purified) transferred OT-I T cells and PD-L2 expression is limited to cells of recipient hematopoietic origin. Thus, it is PD-1 signals delivered from these sources that appear able to maintain tolerance until late time points. Together, these data suggest that PD-1 signals delivered through PD-L1 on thymic epithelial cells are sufficient to induce a tolerant state that can be largely maintained even when PD-1 ligands are subsequently limited to the hematopoietic compartment. This implies the tolerant state endures despite presumed Ag encounter on PD-L1$^{-/-}$ islets and weakened PD-1 signaling due to rarer PD-1:PD-1 ligand interactions in the periphery. The Fife group observed that PD-L1 blockade disrupted tolerance in naïve OT-I T cells upon transfer into iFABP-OVA mice, but not 30 days later (188), similar to our blockade experiment (Table 4-1). Similarly, the Anderson group demonstrated that PD-1 was critical for establishing tolerance in newly generated T cells under lymphopenic conditions, but not for the maintenance of tolerance in established peripheral T cells (177). This reinforces the idea that the requirements for PD-1 signaling may differ for the establishment versus the maintenance of tolerance. For example, if PD-1-targeting blockade is not 100 % effective, and some signals continue, then our data and the Fife group's data together suggest that the differential requirements may indeed involve the intensity of PD-1 signaling.

In the future, it will be interesting to assess the necessity for thymic PD-1 signaling by limiting PD-1 interactions to the periphery (e.g adoptive transfer of thymocytes from OT-I Bim$^{-/-}$ > RIP-mOVA PD-L1$^{-/-}$ chimeras into PD-L1$^{+/+}$ recipients), in which case failure to establish tolerance would further suggest it is PD-1 signals received specifically during first encounter with Ag in the thymus that are necessary for establishing tolerance. Indeed, recent thymic emigrants are thought uniquely sensitive to tolerizing factors compared to more mature circulating T cells, suggesting that PD-1 signals delivered in the thymus and periphery may lead

to functionally different outcomes (354). Rather, preliminary experiments suggest peripheral PD-1 signals are sufficient to establish *de novo* tolerance in T cells where PD-1 deficiency prevented the establishment of tolerance in the thymus. Adoptive transfer into sublethally-irradiated RIP-mOVA recipients of either thymocytes or spleen-derived OT-Is from diabetic OT-I $Bim^{-/-}$ > RIP-mOVA PD-$L1^{-/-}$ chimeras (n = 2 for both thymus and spleen) did not result in recipients becoming diabetic. Thus, PD-1 signaling is similarly capable of establishing tolerance in either the thymus or spleen, during either primary or successive encounters with high affinity Ag; in our model, the non-tolerant state acquired during OT-I thymocyte selection in the absence of PD-1 appears to be fully reversible by restoring the PD-1 signal in peripheral tissues. It would additionally be interesting to assess the T_{PEX}/T_{EX} of Ag-specific T cells in this context with the aforementioned comprehensive flow cytometry panel, especially if the balance of these populations differs when tolerance is induced in the thymus in OT-I $Bim^{-/-}$ > RIP-mOVA BMCs versus in the periphery when spleen-derived OT-Is from diabetic OT-I $Bim^{-/-}$ > RIP-mOVA PD-$L1^{-/-}$ chimeras are adoptively transferred into PD-L1-sufficient recipients. If a T_{PEX} phenotype is indeed associated with tolerance in our model, and the restoration of PD-1 signaling is sufficient to drive its formation, these experiments may indicate PD-1 impacts T_{PEX}/T_{EX} development, contrary to what has previously been suggested (259). Finally, one of the key hallmarks of exhaustion purported to distinguish it from tolerance or anergy is the bona fide initial activation and acquisition of effector function preceding the development of the dysfunctional state (126). Preliminary data suggest that TRA-specific OT-I $CD8^+$ T cells fail to establish tolerance in a RIP-mOVA PD-$L1^{-/-}$ thymus, but do not mediate autoimmunity upon subsequent adoptive transfer into PD-L1-sufficient RIP-mOVA recipients, supporting parallelism between our model of tolerance and the canonical definition of exhaustion.

ICB therapies

Immune checkpoint blockade (ICB) therapies targeting the PD-1:PD-L1 signaling axis have received considerable attention in the last 10 years for their effectiveness in treating a number of different cancers. A recent study proposed that ICB targeting the PD-1:PD-L1 signaling axis promoted the activation and expansion of newly recruited clones to an anti-tumour response, rather than reinvigorating pre-existing tumour-infiltrating T lymphocytes as is often suggested to underlie the success of PD-1 blockade (355). In this study, I provide evidence to support this alternate mechanism of anti-PD-1 ICB therapies. If PD-1 is indeed critical for the establishment of tolerance in the thymus (or in naïve clones) rather than its maintenance alone as I suggest, it follows that PD-1-targeting ICB may preferentially enhance recruitment of clones naïve to the PD-1 tolerogenic signal (also recent thymic emigrants), especially if blockade therapies fall short of 100% effectiveness.

Reinvigoration of "exhausted" $CD8^+$ T cells may remain a primary mechanism for responses to ICB treatments, but here I introduce new considerations for the understanding of these therapies. Despite the success of ICB therapies, clinical responses vary with different types of cancer, and immune-related adverse events (IRAE) are a persistent risk (298, 356). It is conceivable that should PD-1 blocking antibodies reach the thymus, normal selection processes may be hindered. While this provides a potential explanation for the development of some IRAEs, it may also be in some cases the mechanism behind successful cancer immunotherapies. Additionally, exhaustion is not an inert, but rather a hypo-responsive state adapted to limit immune pathology as I have discussed earlier in this thesis. This provides context for the occurrence of immune-related adverse events (IRAE) that can develop following such treatments (357); dysfunction is not necessarily a failure in an immune response, but a functional

adaptation. This highlights the need for a greater understanding of the mechanism by which PD-1 supports dysfunction and how this relates to ICB therapies. Overall, I provide evidence for a novel role for PD-1 in the establishment of tolerance to TRA in the thymus in escapees from clonal deletion. Additionally, I demonstrated the differential requirements for PD-1 and PD-L1 during the establishment and maintenance of tolerance to TRA.

Conclusion

In conclusion, I have investigated the tolerance established independently of clonal deletion by PD-1. I demonstrated that not only does this process occur in the thymus, but the requirements for the establishment and maintenance of this tolerance appear to be divergent, especially as they pertain to expression of the ligand PD-L1. This underscores the importance of understanding dysfunctional T cell states driven or supported by PD-1 signaling, if they are to be targets for reinvigorating immunotherapies. If thymic PD-1 signaling is interrupted by blockade therapies, is this a contributor to the development of IRAEs? In some cases, perhaps the interruption of these signaling events is the desired outcome? Finally, if PD-1 is important for the establishment of T cell dysfunction, it will be interesting in future studies to investigate how signals received at the onset inform the development of plastic versus fixed epigenetic states of dysfunction (e.g. investigation of models that induce dysfunction sensitive or insensitive to reinvigoration by blocking PD-1 signals, and epigenetic comparison of such states).

Capicua discussion

Summary

The work presented here examined thymocyte selection in the absence of CIC using the CD4-cre-driven deletion model that allowed us to isolate CIC's role during selection events at the DP thymocyte stage (post-β-selection). Meanwhile, previous studies saw the use of models

where the impact of CIC deletion prior to and during selection could not be disentangled (211, 213).

I found CIC deficiency to result in a lower frequency of $TCRB^{hi}$ $CD69^{hi}$ DP polyclonal thymocytes, suggesting poorer positive selection efficiency (Fig. 5-1), which I also demonstrated using polyclonal $CIC^{FL/WT}$:$CIC^{FL/FL}$ (1:1) mixed BMCs (Fig. 5-8). Directly *ex vivo* from polyclonal spleen, the frequencies of $FR4^{hi}$ $CD73^{hi}$ anergic, $Foxp3^{+}$ $CD25^{-}$ Treg precursor (Fig. 5-2) (though differences were not apparent for these populations in the thymus), and $CXCR5^{+}$ $PD\text{-}1^{+}$ TFH $CD4^{+}$ T cells (Fig. 5-3) were also elevated. The relative elevation of the latter two of these populations appeared further enhanced in polyclonal $CIC^{FL/WT}$:$CIC^{FL/FL}$ (1:1) mixed BMCs (Fig. 5-10, 5-11), suggesting that $CIC^{FL/FL}$ cells are more competitive for signals required for the generation of these lineages (i.e. strong TCR-pMHC interactions). Additionally, across polyclonal and the transgenic models I used (HY^{cd4} and OT-I), I found CIC deficiency to be associated with decreased CD127 expression in both SP thymocyte and mature peripheral T cell populations (Fig. 5-5, 5-9, 5-15, 5-18).

I also found that polyclonal $CIC^{FL/FL}$ T cells respond less robustly *in vitro* to non-Ag-specific TCR stimulation (Fig. 5-6) or *in vivo* to resource abundance in lymphopenic adoptive transfer recipients (Fig. 5-7), suggestive of functional impairment.

I identified that CIC deficiency led to defects in positive selection in mixed BMCs using both the HY^{cd4} (Fig. 5-12) and OT-I (Fig. 5-16) transgenic systems. In contrast, CIC deficiency did not impact negative selection in these models (Fig. 5-19, 5-20). Given this, and since selection efficiency was impaired to a greater extent and post-selection phenotypes of surviving transgenic $CIC^{FL/FL}$ T cells were more dissimilar from $CIC^{FL/WT}$ controls in the HY^{cd4}

background (Fig. 5-13, 5-17), I hypothesized that CIC plays a role in T cell development and/or function following weak TCR signals.

Finally, transcriptomic evidence in DP thymocytes in the Vav1-cre $CIC^{FL/FL}$ system has been suggestive of a role for CIC in modulating the expression of known ERK regulators (213), *Spry4, Dusp6, Dusp4,* and *Spred* (217–219). Despite this, I found that CRISPR-mediated deletion of *Dusp6* failed to rescue the impaired positive selection experienced by HY^{cd4} $CIC^{FL/FL}$ thymocytes in female mixed BMCs (Fig. 5-23). This implies either that *Dusp6* is not a critical downstream target for CIC in the context of thymocyte selection, or that it functions redundantly with other such targets. Nevertheless, it will thus be critical in future studies to identify direct targets of transcriptional regulation by CIC in the DP thymocyte population. Our proposed model for CIC function is detailed in Figure 6-2.

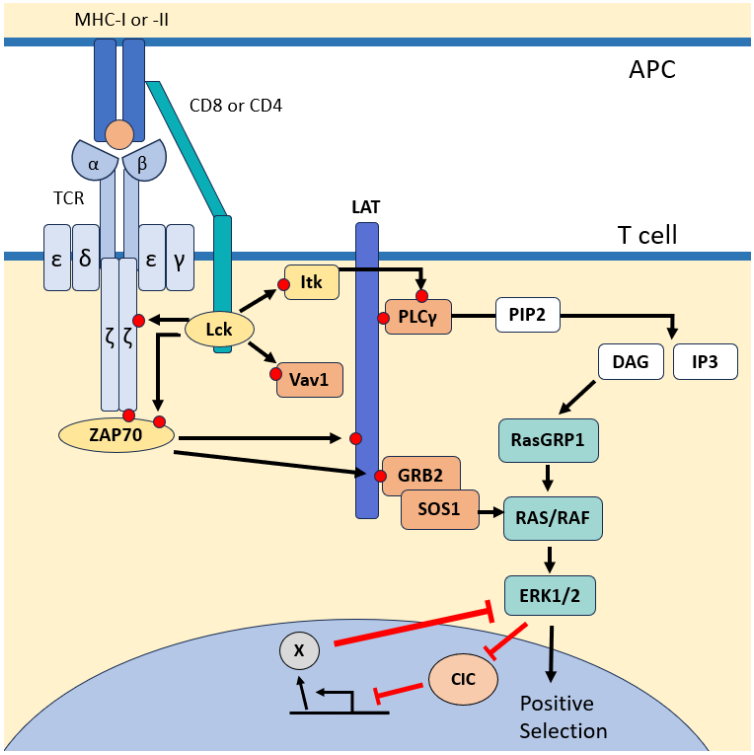

Figure 6-2: Model for CIC function downstream of the TCR.

X is representative of an ERK negative regulator of unknown identity. The work in this thesis provides evidence to suggest that X is not DUSP6. However, X may not be a single, but rather many regulatory gene products, of which DUSP6 may still be a redundant actor.

How does CIC influence signaling downstream of the TCR?

The molecular dynamics/interactions of CIC in thymocytes are poorly understood, as the set of gene targets repressed by CIC in thymocytes is still unknown. Currently, we are informed by a set of genes identified as direct CIC targets in other cell types (196, 215, 216), and shown to be upregulated by RNA-seq in DP thymocytes from Vav1-cre $CIC^{FL/FL}$ mice (*Etv1*, *Etv4, Etv5, Spry4, Dusp6, Dusp4,* and *Spred1*) (213). *Spry4, Dusp6, Dusp4,* and *Spred1* in particular are of interest, as they are known negative regulators of ERK activation (217–219). Since weak sustained ERK signaling is critical to positive selection (24, 42, 214), it is tempting to speculate that CIC deficiency causing dysregulated ERK kinetics in response to low affinity TCR signaling may alter how the functional outcome of the TCR signal is resolved. A potential avenue for further investigation would be to analyze how the kinetics of ERK activation in pre-selection DP thymocytes following stimulation with ligands of various affinities is impacted by the absence of CIC. Such a strategy was previously described using the OT-I transgenic model, whereby ERK phosphorylation was assayed following stimulation with a well-established suite of altered peptide ligand-K^b tetramers (24). Despite evidence of increased DUSP6 mRNA (Fig. 5-21) levels in $CIC^{FL/FL}$ thymocytes, disruption of the *Dusp6* locus by CRISPR did not rescue the impaired selection observed in the absence of CIC. While unhampered DUSP6 activity in the absence of CIC does not appear to be the underlying cause of the impairment in selection seen in $CIC^{FL/FL}$ mice (Fig. 5-23), it remains possible that DUSP6 functions as a part of a redundant pathway

downstream of CIC, especially since DUSP4, another negative regulator of the mitogen-activated protein kinase (MAPK) pathway, is another suspected CIC target. Among the next steps for this investigation should be to identify the loci bound by CIC in thymocytes (e.g. by ChIP-sequencing).

As mentioned above, positive selection hinges critically on the activity of ERK1/2, which along with the MAPK pathway at large, is subject to numerous layers of negative regulatory mechanisms which can exert their influence at both proximal and distal nodes of the TCR cascade (350, 358). Furthermore, signaling through receptor tyrosine kinases (RTK) and MAP kinases leads to the phosphorylation and inactivation of CIC (by dissociation from target promoters, nuclear export, and/or proteasomal degradation) (193, 359). If CIC activity is inhibited by ERK signaling, it then follows that the complete absence of CIC may simulate a situation of robust ERK activity (e.g. following negative selection), which may explain the lack of an effect of CIC deficiency on negative selection (Fig. 5-19, 5-20). Accordingly, following weak TCR signaling, regulatory mechanisms influenced by CIC may be uncoupled with the strength of the TCR signal. This may potentially lead to the uncoordinated and dysfunctional selection and activation outcomes I observed in this study. Once gene targets for CIC have been identified in DP thymocytes, transcriptional activity from those loci may be assessed under circumstances of low to high affinity TCR signaling to better understand the kinetics of CIC activity during selection.

How does CIC influence fate downstream of the TCR?

Overall, I observed that the impact of CIC deficiency appears limited to cases of low affinity TCR signaling, such as positive selection. If CIC indeed influences the MAPK pathway by controlling the expression of negative ERK regulators, as has been proposed by other groups

(described above), it may be through this regulatory loop that CIC serves to increase the sensitivity of the TCR to such low affinity signals. When it cannot do so, T cell clones of low self-reactivity fail to experience positive selection and they are censored from the repertoire, while clones of high self-reactivity may be allowed to predominate. Indeed, Kim *et al.* (2021) determined that in the Vav1-cre $CIC^{FL/FL}$ model, the frequencies of TCRβ variable (V) segments were altered in the $CD4^+$ conventional ($CD25^-$ $Foxp3^-$) and $CD4^+$ Treg ($CD25^+$ $Foxp3^+$) thymocyte populations, suggesting that impaired selection in the absence of CIC may alter the TCR repertoire (213). However, in our polyclonal mixed BMCs, SP thymocytes and mature peripheral T cells expressed lower levels of CD5 (Fig. 5-9C) and PD-1 expression was unchanged for SP thymocytes (Fig. 5-10), contrary to what I would expect for a more self-reactive repertoire. Conversely, I observed enhanced CD5 and PD-1 expression in the context of a fixed TCR on $CIC^{FL/FL}$ HY^{cd4} SP thymocytes and mature T cells in female chimeras (Fig. 5-13). Thus, alterations in the TCR repertoire due to simple decreased TCR sensitivity in the absence of CIC are likely only partially responsible for the CIC-deficient phenotype. However, given that CIC has been shown to be important for early (pre-selection) thymocyte development (211), it would be useful in the future to reassess the impact of CIC deficiency on TCR repertoire diversity in the context of the CD4-cre deletion system, so as to rule out any pre-selection effects of CIC deletion.

Canonically, pre-selection DP thymocytes do not express CD127, which is thought to contribute to their pre-programmed death in the absence of a productive positive selection signal (20). However, $CD4^+$ $CD8^{lo}$ intermediate thymocytes, the immediate progeny of post-selection DPs, are the first αβ TCR-expressing thymocytes capable of responding to IL-7. Indeed, in a study using a CD4-cre-driven CD127 deletion model, the Singer group showed that IL-7

signaling was important for the generation of CD8SP thymocytes and $CD8^+$ lineage specification (360). It is thus possible that decreased CD127 expression in the absence of CIC may contribute to the impairment in CD8SP thymocyte generation I observed with polyclonal (Fig. 5-8D, G) and MHC I-restricted TCR transgenic models HY^{cd4} and OT-I (Fig. 5-12, 5-16). However, IL-7 signaling has been shown not to be critical for the generation of CD4SP thymocytes (360), thus the mildly impaired selection I observed for this population in polyclonal mixed BMCs (Fig. 5-8D-G) suggests differences in CD127 expression must not be solely responsible. Rather, differential CD127 expression may influence the CIC-deficient phenotype depending on T cell subset. Indeed, if decreased CD127 expression contributes to impaired selection, it would thus make sense that the CD8SP subset experiences a greater effect compared with CD4SP. It will thus be interesting in future studies to investigate the impact of CIC deficiency using an MHC II-restricted transgenic TCR model.

How does CIC influence function downstream of the TCR?

While positive selection was impaired $CIC^{FL/FL}$ HY^{cd4} thymocytes in our female chimeras, the few $T3.70^{hi}$ cells that managed to reach maturity demonstrated both enhanced CD5 and PD-1 expression which – in the case of CD5 – appeared to increase further as T cells matured and entered the periphery (Fig. 5-13). Meanwhile, differences in CD5 expression were not present in the $T3.70^{lo}$ population. A possible explanation for this phenomenon is that stochastic receipt of survival-supporting TCR signals during selection led to some HY thymocytes receiving more signal than others, allowing for positive selection and homeostatic maintenance in the periphery for those cells. In support of this assertion, Tg T cells were gated according to very high T3.70 staining, suggesting that $CIC^{FL/FL}$ cells were not phenotypically distinct due to expression of an alternate TCRα-chain. However, I cannot eliminate the potential for endogenous TCRα

expression, even in the T3.70^{hi} population, highlighting the benefit of repeating these experiments in a RAG-deficient background, which would ensure HY TCR mono-expression. The introduction of competition in mixed BMCs may decrease the apparent abundance and therefore potential stochasticity in the delivery of positively selecting TCR-pMHC interactions; indeed, clonal frequency has been previously shown in Tg TCR models in several studies to be negatively correlated with the efficiency of positive selection (361–363). The fact that the surviving CIC$^{FL/FL}$ thymocytes with fixed TCR affinity developed features associated with self-reactivity suggests the absence of CIC doesn't simply reduce TCR sensitivity, but rather disrupts the normal integration of the TCR signal. I.e. despite displaying features associated with self-reactivity, CIC$^{FL/FL}$ HY^{cd4} thymocytes in female chimeras may not be functionally self-reactive, thus it will be interesting in future studies to assess function in these cells. As I have reported evidence to suggest the role of CIC varies depending on the self-reactivity of the TCR, functional outcomes of CIC deficiency may similarly vary. Finally, our current model (CD4-cre CIC$^{FL/FL}$) is unable to distinguish aberrant TCR signaling in the absence of CIC occurring in the thymus versus periphery. Therefore, another avenue of future study would be to assess phenotype and function when CIC is deleted post-positive selection (e.g. using a Rosa-creERT2 inducible deletion model or via CRISPR).

I observed diminished capacity for LIP in polyclonal CD8$^+$, but not for CD4$^+$ CIC$^{FL/FL}$ T cells (Fig. 5-7). Compared with CD4$^+$, CD8$^+$ T cells are known to be more sensitive to IL-7 and undergo LIP at an accelerated rate (364, 365). One proposed mechanism for this difference is the higher expression of monosialotetrahexosylganglioside (GM1)-containing lipid rafts in the plasma membrane of CD8$^+$ T cells, which recruit cytokine receptors, and whose formation is thought to be induced by the TCR-self-pMHC interaction (366). It may thus be interesting to

assay GM1 expression in the context of CIC deficiency, as decreased CD127 expression does not appear to be a complete explanation for differential LIP. In contrast, adoptive transfer into lymphoreplete (non-irradiated) recipients, which experimentally is more representative of steady-state homeostatic capability, did not result in differential recovery of $CIC^{FL/FL}$ T cells 7 days post-transfer (Fig. 5-7), overall suggesting that "defective homeostatic fitness" is not a comprehensive characterization of the CIC-deficient phenotype. Given these data, it was puzzling to observe an elevated proportion of $Ki67^{+}$ $CIC^{FL/FL}$ cells in polyclonal mixed BMCs (Fig. 5-9D), as Ki67 is expressed in G1, S, G2, and M phase of the cell cycle, and has canonically been used as an indicator of proliferation (326, 334). However, elevated Ki67 expression may broadly mean 1) increased rate of cell division, or 2) altered balance of the quiescent state, especially since time spent in the G1 phase does not necessarily imply continuation through phases S, G2, and M. If CD4-cre $CIC^{FL/FL}$ T cells are less inclined to expand under circumstances favourable to LIP (or following recolonization of BMC recipients) and simultaneously express Ki67 at an elevated rate, it is possible that these cells become blocked at the G1 phase of the cell cycle. An alternative explanation is that peripheral $CIC^{FL/FL}$ experience cell death at a greater rate, making the population at large less inclined to respond with proliferation or persist under homeostatic conditions.

Conclusion

In conclusion, I have shown that CIC is critical for positive selection, but dispensable for negative selection; however, how CIC influences positive selection – and, more broadly, TCR signal integration in general – remains a mystery. As I have mentioned in this discussion, to elucidate CIC's role and mechanism in T cell development and function, it will be critical to 1) identify its direct transcriptional targets in DP thymocytes undergoing selection by CHIP-seq, 2)

isolate CIC's role in the thymus from that in the periphery, for example, by acute deletion of CIC in mature peripheral T cells, and 3) investigation of CIC's role following TCR signals of varying affinities, for example, by analyzing ERK phosphorylation or other markers of activation *in vitro* following stimulation of $CIC^{FL/FL}$ OT-I thymocytes with peptide ligand-K^b tetramers (24).

Closing Remarks

The studies described here elucidate details in how PD-1 contributes to both the establishment and maintenance of tolerance to TRA. Although concern for PD-1 lies generally in its role in peripheral tissues, I provided evidence for its largely under-appreciated role in establishing tolerance in the thymus and provided the first description of the associated epigenetic profile. Through our findings, I have furthered our understanding of the mechanism by which PD-1 enforces tolerance – its action in the thymus upon primary encounter with high affinity Ag, and its signaling requirements for continuous protection in the periphery. I additionally showed that CIC plays a role in facilitating normal positive selection, while it does not appear important for negative selection. Overall, I have taken some early steps in elevating our understanding of the mechanism by which CIC influences selection (that has heretofore not seen in-depth investigation), which I hope will provide a spring-board for future inquiry.

References

1. Chaplin, D. D. 2010. Overview of the Immune Response. *J. Allergy Clin. Immunol.* 125: S3.

2. Flajnik, M. F., and M. Kasahara. 2009. Origin and evolution of the adaptive immune system: genetic events and selective pressures. *Nat. Rev. Genet.* 11: 47–59.

3. Sun, L., Y. Su, A. Jiao, X. Wang, and B. Zhang. 2023. T cells in health and disease. *Signal Transduct. Target. Ther.* 8: 1–50.

4. Crotty, S. 2014. T follicular helper cell differentiation, function, and roles in disease. *Immunity* 41: 529–542.

5. Gascoigne, N. R. J., T. Zal, P. P. Yachi, and J. A. H. Hoerter. 2010. Co-receptors and recognition of self at the immunological synapse. *Curr. Top. Microbiol. Immunol.* 340: 171–89.

6. Schatz, D. G., and Y. Ji. 2011. Recombination centres and the orchestration of V(D)J recombination. *Nat. Rev. Immunol.* 11: 251–263.

7. Hogquist, K. A., and S. C. Jameson. 2014. The self-obsession of T cells: how TCR signaling thresholds affect fate “decisions” and effector function. *Nat. Immunol.* 15: 815–23.

8. Mandl, J. N., J. P. Monteiro, N. Vrisekoop, and R. N. Germain. 2013. T Cell Positive Selection Uses Self-Ligand Binding Strength to Optimize Repertoire Recognition of Foreign Antigens. *Immunity* 38: 263–274.

9. Lind, E. F., S. E. Prockop, H. E. Porritt, and H. T. Petrie. 2001. Mapping Precursor Movement through the Postnatal Thymus Reveals Specific Microenvironments Supporting Defined Stages of Early Lymphoid Development. *J. Exp. Med.* 194: 127–134.

10. Capone, M., R. D. Hockett, and A. Zlotnik. 1998. Kinetics of T cell receptor β, γ, and δ rearrangements during adult thymic development: T cell receptor rearrangements are present in CD44+CD25+ Pro-T thymocytes. *Proc. Natl. Acad. Sci. U. S. A.* 95: 12522–12527.

11. Livák, F., M. Tourigny, D. G. Schatz, and H. T. Petrie. 1999. Characterization of TCR Gene Rearrangements During Adult Murine T Cell Development. *J. Immunol.* 162: 2575–2580.

12. Saint-Ruf, C., K. Ungewiss, M. Groettrup, L. Bruno, H. J. Fehling, and H. von Boehmer. 1994. Analysis and expression of a cloned pre-T cell receptor gene. *Science* 266: 1208–1212.

13. Dutta, A., B. Zhao, and P. E. Love. 2021. New insights into TCR β-selection. *Trends Immunol.* 42: 735–750.

14. Starr, T. K., S. C. Jameson, and K. A. Hogquist. 2003. Positive and Negative Selection of T Cells. *Annu. Rev. Immunol.* 21: 139–176.

15. Murata, S., K. Sasaki, T. Kishimoto, S. I. Niwa, H. Hayashi, Y. Takahama, and K. Tanaka. 2007. Regulation of CD8+ T cell development by thymus-specific proteasomes. *Science* 316: 1349–1353.

16. Sasaki, K., K. Takada, Y. Ohte, H. Kondo, H. Sorimachi, K. Tanaka, Y. Takahama, and S. Murata. 2015. Thymoproteasomes produce unique peptide motifs for positive selection of CD8+ T cells. *Nat. Commun.* 6: 7484.

17. Nakagawa, T., W. Roth, P. Wong, A. Nelson, A. Farr, J. Deussing, J. A. Villadangos, H. Ploegh, C. Peters, and A. Y. Rudensky. 1998. Cathepsin L: critical role in Ii degradation and CD4 T cell selection in the thymus. *Science* 280: 450–453.

18. Gommeaux, J., C. Grégoire, P. Nguessan, M. Richelme, M. Malissen, S. Guerder, B.

Malissen, and A. Carrier. 2009. Thymus-specific serine protease regulates positive selection of a subset of CD4+ thymocytes. *Eur. J. Immunol.* 39: 956–964.

19. Nedjic, J., M. Aichinger, N. Mizushima, and L. Klein. 2009. Macroautophagy, endogenous MHC II loading and T cell selection: the benefits of breaking the rules. *Curr. Opin. Immunol.* 21: 92–97.

20. Hong, C., M. A. Luckey, and J. H. Park. 2012. Intrathymic IL-7: The where, when, and why of IL-7 signaling during T cell development. *Semin. Immunol.* 24: 151.

21. Hogquist, K. A., T. A. Baldwin, and S. C. Jameson. 2005. Central tolerance: learning self-control in the thymus. *Nat. Rev. Immunol.* 5: 772–782.

22. McCaughtry, T. M., T. A. Baldwin, M. S. Wilken, and K. A. Hogquist. 2008. Clonal deletion of thymocytes can occur in the cortex with no involvement of the medulla. *J. Exp. Med.* 205: 2575–2584.

23. Klein, L., B. Kyewski, P. M. Allen, and K. A. Hogquist. 2014. Positive and negative selection of the T cell repertoire: what thymocytes see (and don't see). *Nat. Rev. Immunol.* 14: 377–391.

24. Daniels, M. A., E. Teixeiro, J. Gill, B. Hausmann, D. Roubaty, K. Holmberg, G. Werlen, G. A. Holländer, N. R. J. Gascoigne, and E. Palmer. 2006. Thymic selection threshold defined by compartmentalization of Ras/MAPK signalling. *Nature* 444: 724–729.

25. Naeher, D., M. A. Daniels, B. Hausmann, P. Guillaume, I. Luescher, and E. Palmer. 2007. A constant affinity threshold for T cell tolerance. *J. Exp. Med.* 204: 2553–9.

26. Mckeithan, T. W. 1995. Kinetic proofreading in T-cell receptor signal transduction. *Proc.*

Natl. Acad. Sci. U. S. A. 92: 5042–5046.

27. Yousefi, O. S., M. Günther, M. Hörner, J. Chalupsky, M. Wess, S. M. Brandl, R. W. Smith, C. Fleck, T. Kunkel, M. D. Zurbriggen, T. Höfer, W. Weber, and W. W. A. Schamel. 2019. Optogenetic control shows that kinetic proofreading regulates the activity of the T cell receptor. *Elife* 8: e42475.

28. Tischer, D. K., and O. D. Weiner. 2019. Light-based tuning of ligand half-life supports kinetic proofreading model of T cell signaling. *Elife* 8: e42498.

29. Stepanek, O., A. S. Prabhakar, C. Osswald, C. G. King, A. Bulek, D. Naeher, M. Beaufils-Hugot, M. L. Abanto, V. Galati, B. Hausmann, R. Lang, D. K. Cole, E. S. Huseby, A. K. Sewell, A. K. Chakraborty, and E. Palmer. 2014. Coreceptor scanning by the T cell receptor provides a mechanism for T cell tolerance. *Cell* 159: 333–345.

30. Mørch, A. M., F. Schneider, E. Jenkins, A. M. Santos, S. E. Fraser, S. J. Davis, and M. L. Dustin. 2022. The kinase occupancy of T cell coreceptors reconsidered. *Proc. Natl. Acad. Sci. U. S. A.* 119: e2213538119.

31. Gaud, G., R. Lesourne, and P. E. Love. 2018. Regulatory mechanisms in T cell receptor signalling. *Nat. Rev. Immunol.* 18: 485–497.

32. Au-Yeung, B. B., H. J. Melichar, J. O. Ross, D. A. Cheng, J. Zikherman, K. M. Shokat, E. A. Robey, and A. Weiss. 2014. Quantitative and Temporal Requirements Revealed for Zap-70 Catalytic Activity During T Cell Development. *Nat. Immunol.* 15: 687.

33. Houtman, J. C. D., H. Yamaguchi, M. Barda-Saad, A. Braiman, B. Bowden, E. Appella, P. Schuck, and L. E. Samelson. 2006. Oligomerization of signaling complexes by the multipoint

binding of GRB2 to both LAT and SOS1. *Nat. Struct. Mol. Biol.* 13: 798–805.

34. Huang, W. Y. C., Q. Yan, W. C. Lin, J. K. Chung, S. D. Hansen, S. M. Christensen, H. L. Tu, J. Kuriyan, and J. T. Groves. 2016. Phosphotyrosine-mediated LAT assembly on membranes drives kinetic bifurcation in recruitment dynamics of the Ras activator SOS. *Proc. Natl. Acad. Sci. U. S. A.* 113: 8218–8223.

35. McAffee, D. B., M. K. O'Dair, J. J. Lin, S. T. Low-Nam, K. B. Wilhelm, S. Kim, S. Morita, and J. T. Groves. 2022. Discrete LAT condensates encode antigen information from single pMHC:TCR binding events. *Nat. Commun.* 13.

36. Sommers, C. L., J. Lee, K. L. Steiner, J. M. Gurson, C. L. DePersis, D. El-Khoury, C. L. Fuller, E. W. Shores, P. E. Love, and L. E. Samelson. 2005. Mutation of the phospholipase C-gamma1-binding site of LAT affects both positive and negative thymocyte selection. *J. Exp. Med.* 201: 1125–1134.

37. Shen, S., M. Zhu, J. Lau, M. Chuck, and W. Zhang. 2009. The Essential Role of LAT in Thymocyte Development During the Transition from DP to SP. *J. Immunol.* 182: 5596–5604.

38. Lo, W. L., M. Kuhlmann, G. Rizzuto, H. A. Ekiz, E. M. Kolawole, M. P. Revelo, R. Andargachew, Z. Li, Y. L. Tsai, A. Marson, B. D. Evavold, D. Zehn, and A. Weiss. 2023. A single-amino acid substitution in the adaptor LAT accelerates TCR proofreading kinetics and alters T-cell selection, maintenance and function. *Nat. Immunol.* 24: 676–689.

39. Lo, W. L., D. L. Donermeyer, and P. M. Allen. 2012. A voltage-gated sodium channel is essential for the positive selection of CD4+ T cells. *Nat. Immunol.* 13: 880–887.

40. Melichar, H. J., J. O. Ross, P. Herzmark, K. A. Hogquist, and E. A. Robey. 2013. Distinct

temporal pattern of T cell receptor signals during positive versus negative selection in situ. *Sci. Signal.* 6: ra92.

41. Werlen, G., B. Hausmann, and E. Palmer. 2000. A motif in the αβ T-cell receptor controls positive selection by modulating ERK activity. *Nature* 406: 422–426.

42. McNeil, L. K., T. K. Starr, and K. A. Hogquist. 2005. A requirement for sustained ERK signaling during thymocyte positive selection in vivo. *Proc. Natl. Acad. Sci. U. S. A.* 102: 13574–13579.

43. Fischer, A. M., C. D. Katayama, G. Pagès, J. Pouysségur, and S. M. Hedrick. 2005. The role of erk1 and erk2 in multiple stages of T cell development. *Immunity* 23: 431–443.

44. McGargill, M. A., I. L. Ch'en, C. D. Katayama, G. Pagès, J. Pouysségur, and S. M. Hedrick. 2009. Cutting edge: Extracellular signal-related kinase is not required for negative selection of developing T cells. *J. Immunol.* 183: 4838–4842.

45. Rincón, M., A. Whitmarsh, D. D. Yang, L. Weiss, B. Dérijard, P. Jayaraj, R. J. Davis, and R. A. Flavell. 1998. The JNK Pathway Regulates the In Vivo Deletion of Immature CD4+CD8+ Thymocytes. *J. Exp. Med.* 188: 1817–1830.

46. Sugawara, T., T. Moriguchi, E. Nishida, and Y. Takahama. 1998. Differential roles of ERK and p38 MAP kinase pathways in positive and negative selection of T lymphocytes. *Immunity* 9: 565–574.

47. This, S., S. F. Valbon, M. È. Lebel, and H. J. Melichar. 2021. Strength and Numbers: The Role of Affinity and Avidity in the 'Quality' of T Cell Tolerance. *Cells* 10: 1530.

48. Bretscher, P., and M. Cohn. 1970. A theory of self-nonself discrimination. *Science* 169:

1042–9.

49. June, C. H., J. A. Ledbetter, M. M. Gillespie, T. Lindsten, and C. B. Thompson. 1987. T-cell proliferation involving the CD28 pathway is associated with cyclosporine-resistant interleukin 2 gene expression. *Mol. Cell. Biol.* 7: 4472–81.

50. Mueller, D. L., M. K. Jenkins, and R. H. Schwartz. 1989. Clonal expansion versus functional clonal inactivation: a costimulatory signalling pathway determines the outcome of T cell antigen receptor occupancy. *Annu. Rev. Immunol.* 7: 445–80.

51. Laidlaw, B. J., J. E. Craft, and S. M. Kaech. 2016. The multifaceted role of CD4(+) T cells in CD8(+) T cell memory. *Nat. Rev. Immunol.* 16: 102–11.

52. Janeway, C. A. 1989. Approaching the asymptote? Evolution and revolution in immunology. *Cold Spring Harb. Symp. Quant. Biol.* 54: 1–13.

53. Janeway, C. A. 1992. The immune system evolved to discriminate infectious nonself from noninfectious self. *Immunol. Today* 13: 11–6.

54. Pradeu, T., and E. L. Cooper. 2012. The danger theory: 20 years later. *Front. Immunol.* 3: 287.

55. Matzinger, P. 2002. The danger model: a renewed sense of self. *Science* 296: 301–5.

56. Surh, C. D., and J. Sprent. 1994. T-cell apoptosis detected in situ during positive and negative selection in the thymus. *Nature* 372: 100–103.

57. Stritesky, G. L., Y. Xing, J. R. Erickson, L. A. Kalekar, X. Wang, D. L. Mueller, S. C. Jameson, and K. A. Hogquist. 2013. Murine thymic selection quantified using a unique method to capture deleted T cells. *Proc. Natl. Acad. Sci. U. S. A.* 110: 4679–84.

58. Daley, S. R., D. Y. Hu, and C. C. Goodnow. 2013. Helios marks strongly autoreactive CD4+ T cells in two major waves of thymic deletion distinguished by induction of PD-1 or NF-κB. *J. Exp. Med.* 210: 269–285.

59. Jolicoeur, C., D. Hanahan, and K. M. Smith. 1994. T-cell tolerance toward a transgenic beta-cell antigen and transcription of endogenous pancreatic genes in thymus. *Proc. Natl. Acad. Sci. U. S. A.* 91: 6707–11.

60. Antonia, S. J., T. Geiger, J. Miller, and R. A. Flavell. 1995. Mechanisms of immune tolerance induction through the thymic expression of a peripheral tissue-specific protein. *Int. Immunol.* 7: 715–25.

61. von Herrath, M. G., J. Dockter, and M. B. Oldstone. 1994. How virus induces a rapid or slow onset insulin-dependent diabetes mellitus in a transgenic model. *Immunity* 1: 231–42.

62. Klein, L., M. Klugmann, K. A. Nave, V. K. Tuohy, and B. Kyewski. 2000. Shaping of the autoreactive T-cell repertoire by a splice variant of self protein expressed in thymic epithelial cells. *Nat. Med.* 6: 56–61.

63. Smith, K. M., D. C. Olson, R. Hirose, and D. Hanahan. 1997. Pancreatic gene expression in rare cells of thymic medulla: evidence for functional contribution to T cell tolerance. *Int. Immunol.* 9: 1355–65.

64. Anderson, M. S., E. S. Venanzi, L. Klein, Z. Chen, S. P. Berzins, S. J. Turley, H. Von Boehmer, R. Bronson, A. Dierich, C. Benoist, and D. Mathis. 2002. Projection of an immunological self shadow within the thymus by the aire protein. *Science* 298: 1395–1401.

65. Anderson, M. S., E. S. Venanzi, Z. Chen, S. P. Berzins, C. Benoist, and D. Mathis. 2005. The

cellular mechanism of Aire control of T cell tolerance. *Immunity* 23: 227–239.

66. Liston, A., S. Lesage, J. Wilson, L. Peltonen, and C. C. Goodnow. 2003. Aire regulates negative selection of organ-specific T cells. *Nat. Immunol.* 4: 350–354.

67. Liston, A., D. H. D. Gray, S. Lesage, A. L. Fletcher, J. Wilson, K. E. Webster, H. S. Scott, R. L. Boyd, L. Peltonen, and C. C. Goodnow. 2004. Gene dosage--limiting role of Aire in thymic expression, clonal deletion, and organ-specific autoimmunity. *J. Exp. Med.* 200: 1015–1026.

68. Kurobe, H., C. Liu, T. Ueno, F. Saito, I. Ohigashi, N. Seach, R. Arakaki, Y. Hayashi, T. Kitagawa, M. Lipp, R. L. Boyd, and Y. Takahama. 2006. CCR7-dependent cortex-to-medulla migration of positively selected thymocytes is essential for establishing central tolerance. *Immunity* 24: 165–177.

69. Gallegos, A. M., and M. J. Bevan. 2004. Central tolerance to tissue-specific antigens mediated by direct and indirect antigen presentation. *J. Exp. Med.* 200: 1039–1049.

70. Hinterberger, M., M. Aichinger, O. P. Da Costa, D. Voehringer, R. Hoffmann, and L. Klein. 2010. Autonomous role of medullary thymic epithelial cells in central CD4(+) T cell tolerance. *Nat. Immunol.* 11: 512–519.

71. Breed, E. R., M. Watanabe, and K. A. Hogquist. 2019. Measuring Thymic Clonal Deletion at the Population Level. *J. Immunol.* 202: 3226–3233.

72. Bouillet, P., J. F. Purton, D. I. Godfrey, L. C. Zhang, L. Coultas, H. Puthalakath, M. Pellegrini, S. Cory, J. M. Adams, and A. Strasser. 2002. BH3-only Bcl-2 family member Bim is required for apoptosis of autoreactive thymocytes. *Nature* 415: 922–926.

73. Moran, A. E., K. L. Holzapfel, Y. Xing, N. R. Cunningham, J. S. Maltzman, J. Punt, and K.

A. Hogquist. 2011. T cell receptor signal strength in Treg and iNKT cell development demonstrated by a novel fluorescent reporter mouse. *J. Exp. Med.* 208: 1279–1289.

74. Suen, A. Y. W., and T. A. Baldwin. 2012. Proapoptotic protein Bim is differentially required during thymic clonal deletion to ubiquitous versus tissue-restricted antigens. *Proc. Natl. Acad. Sci. U. S. A.* 109: 893–898.

75. Gray, D. H. D., F. Kupresanin, S. P. Berzins, M. J. Herold, L. A. O'Reilly, P. Bouillet, and A. Strasser. 2012. The BH3-Only Proteins Bim and Puma Cooperate to Impose Deletional Tolerance of Organ-Specific Antigens. *Immunity* 37: 451–462.

76. Hu, Q., A. Sader, J. C. Parkman, and T. A. Baldwin. 2009. Bim-mediated apoptosis is not necessary for thymic negative selection to ubiquitous self-antigens. *J. Immunol.* 183: 7761–7.

77. Xing, Y., and K. A. Hogquist. 2012. T-Cell tolerance: Central and peripheral. *Cold Spring Harb. Perspect. Biol.* 4: 1–15.

78. Badr, M. E., Z. Zhang, X. Tai, and A. Singer. 2023. CD8 T cell tolerance results from eviction of immature autoreactive cells from the thymus. *Science* 382: 534–541.

79. Nitta, T., S. Nitta, L. Yu, M. Lipp, and Y. Takahama. 2009. CCR7-mediated migration of developing thymocytes to the medulla is essential for negative selection to tissue-restricted antigens. *Proc. Natl. Acad. Sci. U. S. A.* 106: 17129–17133.

80. McDonald, B. D., J. J. Bunker, S. A. Erickson, M. Oh-Hora, and A. Bendelac. 2015. Crossreactive αβ T Cell Receptors Are the Predominant Targets of Thymocyte Negative Selection. *Immunity* 43: 859–69.

81. Peterson, D. A., R. J. DiPaolo, O. Kanagawa, and E. R. Unanue. 1999. Cutting Edge:

Negative Selection of Immature Thymocytes by a Few Peptide-MHC Complexes: Differential Sensitivity of Immature and Mature T Cells. *J. Immunol.* 162: 3117–3120.

82. Ebert, P. J. R., L. I. R. Ehrlich, and M. M. Davis. 2008. Low ligand requirement for deletion and lack of synapses in positive selection enforce the gauntlet of thymic T cell maturation. *Immunity* 29: 734–45.

83. Whitfield, J., S. J. Neame, L. Paquet, O. Bernard, and J. Ham. 2001. Dominant-negative c-Jun promotes neuronal survival by reducing BIM expression and inhibiting mitochondrial cytochrome c release. *Neuron* 29: 629–643.

84. Putcha, G. V., S. Le, S. Frank, C. G. Besirli, K. Clark, B. Chu, S. Alix, R. J. Youle, A. LaMarche, A. C. Maroney, and E. M. Johnson. 2003. JNK-mediated BIM phosphorylation potentiates BAX-dependent apoptosis. *Neuron* 38: 899–914.

85. Staton, T. L., V. Lazarevic, D. C. Jones, A. J. Lanser, T. Takagi, S. Ishii, and L. H. Glimcher. 2011. Dampening of death pathways by Schnurri 2 is essential for T cell development. *Nature* 472: 105–109.

86. Wang, J., N. He, N. Zhang, D. Quan, S. Zhang, C. Zhang, R. T. Yu, A. R. Atkins, R. Zhu, C. Yang, Y. Cui, C. Liddle, M. Downes, H. Xiao, Y. Zheng, J. Auwerx, R. M. Evans, and Q. Leng. 2017. NCoR1 restrains thymic negative selection by repressing Bim expression to spare thymocytes undergoing positive selection. *Nat. Commun.* 8: 959.

87. Shevyrev, D., and V. Tereshchenko. 2020. Treg Heterogeneity, Function, and Homeostasis. *Front. Immunol.* 10: 495736.

88. Kurd, N., and E. A. Robey. 2016. T cell selection in the thymus: a spatial and temporal

perspective. *Immunol. Rev.* 271: 114–126.

89. Weist, B. M., N. Kurd, J. Boussier, S. W. Chan, and E. A. Robey. 2015. Thymic regulatory T cell niche size is dictated by limiting interleukin 2 from antigen-bearing dendritic cells and feedback competition. *Nat. Immunol.* 16: 635–641.

90. Tai, X., B. Erman, A. Alag, J. Mu, M. Kimura, G. Katz, T. Guinter, T. McCaughtry, R. Etzensperger, L. Feigenbaum, D. S. Singer, and A. Singer. 2013. Foxp3 transcription factor is proapoptotic and lethal to developing regulatory T cells unless counterbalanced by cytokine survival signals. *Immunity* 38: 1116–28.

91. Klein, L., and K. Jovanovic. 2011. Regulatory T cell lineage commitment in the thymus. *Semin. Immunol.* 23: 401–409.

92. Cowan, J. E., S. M. Parnell, K. Nakamura, J. H. Caamano, P. J. L. Lane, E. J. Jenkinson, W. E. Jenkinson, and G. Anderson. 2013. The thymic medulla is required for Foxp3+ regulatory but not conventional CD4+ thymocyte development. *J. Exp. Med.* 210: 675–681.

93. Schwartz, R. H. 2003. T CELL ANERGY. *Annu. Rev. Immunol.* 21: 305–334.

94. Redmond, W. L., and L. A. Sherman. 2005. Peripheral Tolerance of CD8 T Lymphocytes. *Immunity* 22: 275–284.

95. Safford, M., S. Collins, M. A. Lutz, A. Allen, C. T. Huang, J. Kowalski, A. Blackford, M. R. Horton, C. Drake, R. H. Schwartz, and J. D. Powell. 2005. Egr-2 and Egr-3 are negative regulators of T cell activation. *Nat. Immunol.* 6: 472–480.

96. Zheng, Y., Y. Zha, G. Driessens, F. Locke, and T. F. Gajewski. 2012. Transcriptional regulator early growth response gene 2 (Egr2) is required for T cell anergy in vitro and in vivo. *J.*

Exp. Med. 209: 2157–2163.

97. Jeon, M. S., A. Atfield, K. Venuprasad, C. Krawczyk, R. Sarao, C. Elly, C. Yang, S. Arya, K. Bachmaier, L. Su, D. Bouchard, R. Jones, M. Gronski, P. Ohashi, T. Wada, D. Bloom, C. G. Fathman, Y. C. Liu, and J. M. Penninger. 2004. Essential role of the E3 ubiquitin ligase Cbl-b in T cell anergy induction. *Immunity* 21: 167–177.

98. Fathman, C. G., and N. B. Lineberry. 2007. Molecular mechanisms of CD4+ T-cell anergy. *Nat. Rev. Immunol.* 7: 599–609.

99. Kisielow, P., H. Blüthmann, U. D. Staerz, M. Steinmetz, and H. Von Boehmer. 1988. Tolerance in T-cell-receptor transgenic mice involves deletion of nonmature CD4+8+ thymocytes. *Nature* 333: 742–746.

100. Carlow, D. A., S. J. Teh, and H. S. Teh. 1992. Altered thymocyte development resulting from expressing a deleting ligand on selecting thymic epithelium. *J. Immunol.* 148: 2988–2995.

101. Hu, Q. N., A. Y. W. Suen, L. M. Henao Caviedes, and T. A. Baldwin. 2017. Nur77 Regulates Nondeletional Mechanisms of Tolerance in T Cells. *J. Immunol.* 199: 3147–3157.

102. Malhotra, D., J. L. Linehan, T. Dileepan, Y. J. Lee, W. E. Purtha, J. V. Lu, R. W. Nelson, B. T. Fife, H. T. Orr, M. S. Anderson, K. A. Hogquist, and M. K. Jenkins. 2016. Polyclonal CD4+ T cell tolerance is established by distinct mechanisms, according to self-peptide expression patterns. *Nat. Immunol.* 17: 187–195.

103. Legoux, F. P., J. B. Lim, A. W. Cauley, S. Dikiy, J. Ertelt, T. J. Mariani, T. Sparwasser, S. S. Way, and J. J. Moon. 2015. CD4+ T cell tolerance to tissue-restricted self antigens is mediated by antigen-specific regulatory T cells rather than deletion. *Immunity* 43: 896–908.

104. Kawabe, Y., and A. Ochi. 1991. Programmed cell death and extrathymic reduction of Vbeta8+ CD4+ T cells in mice tolerant to Staphylococcus aureus enterotoxin B. *Nature* 349: 245–248.

105. Strasser, A., and M. Pellegrini. 2004. T-lymphocyte death during shutdown of an immune response. *Trends Immunol.* 25: 610–615.

106. Jenkins, M. K., C. A. Chen, G. Jung, D. L. Mueller, and R. H. Schwartz. 1990. Inhibition of antigen-specific proliferation of type 1 murine T cell clones after stimulation with immobilized anti-CD3 monoclonal antibody. *J. Immunol.* 144: 16–22.

107. Martinez, G. J., R. M. Pereira, T. Äijö, E. Y. Kim, F. Marangoni, M. E. Pipkin, S. Togher, V. Heissmeyer, Y. C. Zhang, S. Crotty, E. D. Lamperti, K. M. Ansel, T. R. Mempel, H. Lähdesmäki, P. G. Hogan, and A. Rao. 2015. The transcription factor NFAT promotes exhaustion of activated CD8+ T cells. *Immunity* 42: 265–278.

108. Rocha, B., and H. Von Boehmer. 1991. Peripheral Selection of the T Cell Repertoire. *Science* 251: 1225–1228.

109. Rocha, B., C. Tanchot, and H. Von Boehmer. 1993. Clonal anergy blocks in vivo growth of mature T cells and can be reversed in the absence of antigen. *J. Exp. Med.* 177: 1517–1521.

110. Tanchot, C., D. L. Barber, L. Chiodetti, and R. H. Schwartz. 2001. Adaptive Tolerance of CD4 + T Cells In Vivo: Multiple Thresholds in Response to a Constant Level of Antigen Presentation . *J. Immunol.* 167: 2030–2039.

111. Pape, K. A., R. Merica, A. Mondino, A. Khoruts, and M. K. Jenkins. 1998. Direct Evidence That Functionally Impaired CD4+ T Cells Persist In Vivo Following Induction of Peripheral

Tolerance. *J. Immunol.* 160: 4719–4729.

112. Schietinger, A., and P. D. Greenberg. 2014. Tolerance and Exhaustion: Defining Mechanisms of T cell Dysfunction. *Trends Immunol.* 35: 51–60.

113. Choi, S., and R. H. Schwartz. 2007. Molecular mechanisms for adaptive tolerance and other T cell anergy models. *Semin. Immunol.* 19: 140–152.

114. Macián, F., F. García-Cózar, S. H. Im, H. F. Horton, M. C. Byrne, and A. Rao. 2002. Transcriptional mechanisms underlying lymphocyte tolerance. *Cell* 109: 719–731.

115. Schietinger, A., J. J. Delrow, R. S. Basom, J. N. Blattman, and P. D. Greenberg. 2012. Rescued Tolerant CD8 T Cells Are Preprogrammed to Reestablish the Tolerant State. *Science* 335: 723–727.

116. May, J. F., R. G. Kelly, A. Y. W. Suen, J. Kim, J. Kim, C. C. Anderson, G. R. Rayat, and T. A. Baldwin. 2023. Establishment of CD8+ T Cell Thymic Central Tolerance to Tissue-Restricted Antigen Requires PD-1. *J. Immunol.* 212: 271–283.

117. Ramsdell, F., and B. J. Fowlkes. 1992. Maintenance of in vivo tolerance by persistence of antigen. *Science* 257: 1130–1134.

118. Calbo, S., H. Delagrèverie, C. Arnoult, F.-J. Authier, F. Tron, and O. Boyer. 2008. Functional tolerance of CD8+ T cells induced by muscle-specific antigen expression. *J. Immunol.* 181: 408–417.

119. Teague, R. M., B. D. Sather, J. A. Sacks, M. Z. Huang, M. L. Dossett, J. Morimoto, X. Tan, S. E. Sutton, M. P. Cooke, C. Öhlén, and P. D. Greenberg. 2006. Interleukin-15 rescues tolerant CD8+ T cells for use in adoptive immunotherapy of established tumors. *Nat. Med.* 12: 335–341.

120. Martinez, R. J., N. Zhang, S. R. Thomas, S. L. Nandiwada, M. K. Jenkins, B. A. Binstadt, and D. L. Mueller. 2012. Arthritogenic self-reactive CD4+ T cells acquire an FR4hiCD73hi anergic state in the presence of Foxp3+ regulatory T cells. *J. Immunol.* 188: 170–181.

121. Yamaguchi, T., K. Hirota, K. Nagahama, K. Ohkawa, T. Takahashi, T. Nomura, and S. Sakaguchi. 2007. Control of Immune Responses by Antigen-Specific Regulatory T Cells Expressing the Folate Receptor. *Immunity* 27: 145–159.

122. Deaglio, S., K. M. Dwyer, W. Gao, D. Friedman, A. Usheva, A. Erat, J. F. Chen, K. Enjyoji, J. Linden, M. Oukka, V. K. Kuchroo, T. B. Strom, and S. C. Robson. 2007. Adenosine generation catalyzed by CD39 and CD73 expressed on regulatory T cells mediates immune suppression. *J. Exp. Med.* 204: 1257–1265.

123. Enouz, S., L. Carrié, D. Merkler, M. J. Bevan, and D. Zehn. 2012. Autoreactive T cells bypass negative selection and respond to self-antigen stimulation during infection. *J. Exp. Med.* 209: 1769–1779.

124. Zehn, D., and M. J. Bevan. 2006. T Cells with Low Avidity for a Tissue-Restricted Antigen Routinely Evade Central and Peripheral Tolerance and Cause Autoimmunity. *Immunity* 25: 261–270.

125. Nelson, C. E., L. J. Mills, J. L. McCurtain, E. A. Thompson, D. M. Seelig, S. Bhela, C. F. Quarnstrom, B. T. Fife, and V. Vezys. 2019. Reprogramming responsiveness to checkpoint blockade in dysfunctional CD8 T cells. *Proc. Natl. Acad. Sci. U. S. A.* 116: 2640–2645.

126. Jiang, W., Y. He, W. He, G. Wu, X. Zhou, Q. Sheng, W. Zhong, Y. Lu, Y. Ding, Q. Lu, F. Ye, and H. Hua. 2020. Exhausted CD8+T Cells in the Tumor Immune Microenvironment: New Pathways to Therapy. *Front. Immunol.* 11: 622509.

127. Wherry, E. J., J. N. Blattman, K. Murali-Krishna, R. van der Most, and R. Ahmed. 2003. Viral persistence alters CD8 T-cell immunodominance and tissue distribution and results in distinct stages of functional impairment. *J. Virol.* 77: 4911–4927.

128. Doering, T. A., A. Crawford, J. M. Angelosanto, M. A. Paley, C. G. Ziegler, and E. J. Wherry. 2012. Network Analysis Reveals Centrally Connected Genes and Pathways Involved in CD8+ T Cell Exhaustion versus Memory. *Immunity* 37: 1130–1144.

129. Crawford, A., J. M. Angelosanto, C. Kao, T. A. Doering, P. M. Odorizzi, B. E. Barnett, and E. J. Wherry. 2014. Molecular and transcriptional basis of CD4+ T cell dysfunction during chronic infection. *Immunity* 40: 289–302.

130. Angelosanto, J. M., S. D. Blackburn, A. Crawford, and E. J. Wherry. 2012. Progressive loss of memory T cell potential and commitment to exhaustion during chronic viral infection. *J. Virol.* 86: 8161–70.

131. Frebel, H., V. Nindl, R. A. Schuepbach, T. Braunschweiler, K. Richter, J. Vogel, C. A. Wagner, D. Loffing-Cueni, M. Kurrer, B. Ludewig, and A. Oxenius. 2012. Programmed death 1 protects from fatal circulatory failure during systemic virus infection of mice. *J. Exp. Med.* 209: 2485–99.

132. Jin, X., D. E. Bauer, S. E. Tuttleton, S. Lewin, A. Gettie, J. Blanchard, C. E. Irwin, J. T. Safrit, J. Mittler, L. Weinberger, L. G. Kostrikis, L. Zhang, A. S. Perelson, and D. D. Ho. 1999. Dramatic rise in plasma viremia after CD8(+) T cell depletion in simian immunodeficiency virus-infected macaques. *J. Exp. Med.* 189: 991–8.

133. Schmitz, J. E., M. J. Kuroda, S. Santra, V. G. Sasseville, M. A. Simon, M. A. Lifton, P. Racz, K. Tenner-Racz, M. Dalesandro, B. J. Scallon, J. Ghrayeb, M. A. Forman, D. C.

Montefiori, E. P. Rieber, N. L. Letvin, and K. A. Reimann. 1999. Control of viremia in simian immunodeficiency virus infection by CD8+ lymphocytes. *Science* 283: 857–60.

134. Pircher, H., D. Moskophidis, U. Rohrer, K. Bürki, H. Hengartner, and R. M. Zinkernagel. 1990. Viral escape by selection of cytotoxic T cell-resistant virus variants in vivo. *Nature* 346: 629–33.

135. Utzschneider, D. T., M. Charmoy, V. Chennupati, L. Pousse, D. P. Ferreira, S. Calderon-Copete, M. Danilo, F. Alfei, M. Hofmann, D. Wieland, S. Pradervand, R. Thimme, D. Zehn, and W. Held. 2016. T Cell Factor 1-Expressing Memory-like CD8(+) T Cells Sustain the Immune Response to Chronic Viral Infections. *Immunity* 45: 415–427.

136. Siddiqui, I., K. Schaeuble, V. Chennupati, S. A. Fuertes Marraco, S. Calderon-Copete, D. Pais Ferreira, S. J. Carmona, L. Scarpellino, D. Gfeller, S. Pradervand, S. A. Luther, D. E. Speiser, and W. Held. 2019. Intratumoral Tcf1+PD-1+CD8+ T Cells with Stem-like Properties Promote Tumor Control in Response to Vaccination and Checkpoint Blockade Immunotherapy. *Immunity* 50: 195-211.e10.

137. Chen, Z., Z. Ji, S. F. Ngiow, S. Manne, Z. Cai, A. C. Huang, J. Johnson, R. P. Staupe, B. Bengsch, C. Xu, S. Yu, M. Kurachi, R. S. Herati, L. A. Vella, A. E. Baxter, J. E. Wu, O. Khan, J. C. Beltra, J. R. Giles, E. Stelekati, L. M. McLane, C. W. Lau, X. Yang, S. L. Berger, G. Vahedi, H. Ji, and E. J. Wherry. 2019. TCF-1-Centered Transcriptional Network Drives an Effector versus Exhausted CD8 T Cell-Fate Decision. *Immunity* 51: 840-855.e5.

138. Wu, T., Y. Ji, E. Ashley Moseman, H. C. Xu, M. Manglani, M. Kirby, S. M. Anderson, R. Handon, E. Kenyon, A. Elkahloun, W. Wu, P. A. Lang, L. Gattinoni, D. B. McGavern, and P. L. Schwartzberg. 2016. The TCF1-Bcl6 axis counteracts type I interferon to repress exhaustion and

maintain T cell stemness. *Sci. Immunol.* 1: eaai8593.

139. Chi, X., S. Luo, P. Ye, W. L. Hwang, J. H. Cha, X. Yan, and W. H. Yang. 2023. T-cell exhaustion and stemness in antitumor immunity: Characteristics, mechanisms, and implications. *Front. Immunol.* 14: 1104771.

140. Paley, M. A., D. C. Kroy, P. M. Odorizzi, J. B. Johnnidis, D. V. Dolfi, B. E. Barnett, E. K. Bikoff, E. J. Robertson, G. M. Lauer, S. L. Reiner, and E. J. Wherry. 2012. Progenitor and terminal subsets of CD8+ T cells cooperate to contain chronic viral infection. *Science* 338: 1220–1225.

141. Im, S. J., M. Hashimoto, M. Y. Gerner, J. Lee, H. T. Kissick, M. C. Burger, Q. Shan, J. S. Hale, J. Lee, T. H. Nasti, A. H. Sharpe, G. J. Freeman, R. N. Germain, H. I. Nakaya, H. H. Xue, and R. Ahmed. 2016. Defining CD8+ T cells that provide the proliferative burst after PD-1 therapy. *Nature* 537: 417–421.

142. Baharom, F., R. A. Ramirez-Valdez, K. K. S. Tobin, H. Yamane, C. A. Dutertre, A. Khalilnezhad, G. V. Reynoso, V. L. Coble, G. M. Lynn, M. P. Mulè, A. J. Martins, J. P. Finnigan, X. M. Zhang, J. A. Hamerman, N. Bhardwaj, J. S. Tsang, H. D. Hickman, F. Ginhoux, A. S. Ishizuka, and R. A. Seder. 2021. Intravenous nanoparticle vaccination generates stem-like TCF1+ neoantigen-specific CD8+ T cells. *Nat. Immunol.* 22: 41–52.

143. Wagle, M. V., J. M. Marchingo, J. Howitt, S. S. Tan, C. C. Goodnow, and I. A. Parish. 2018. The Ubiquitin Ligase Adaptor NDFIP1 Selectively Enforces a CD8+ T Cell Tolerance Checkpoint to High-Dose Antigen. *Cell Rep.* 24: 577–584.

144. Redmond, W. L., B. C. Marincek, and L. A. Sherman. 2005. Distinct requirements for deletion versus anergy during CD8 T cell peripheral tolerance in vivo. *J. Immunol.* 174: 2046–

2053.

145. Korb, L. C., S. Mirshahidi, K. Ramyar, A. A. Sadighi Akha, and S. Sadegh-Nasseri. 1999. Induction of T Cell Anergy by Low Numbers of Agonist Ligands. *J. Immunol.* 162: 6401–6409.

146. Mirshahidi, S., L. C. K. Ferris, and S. Sadegh-Nasseri. 2004. The magnitude of TCR engagement is a critical predictor of T cell anergy or activation. *J. Immunol.* 172: 5346–5355.

147. Zinzow-Kramer, W. M., A. Weiss, and B. B. Au-Yeung. 2019. Adaptation by naïve CD4 $^{+}$ T cells to self-antigen–dependent TCR signaling induces functional heterogeneity and tolerance. *Proc. Natl. Acad. Sci.* 116: 15160–15169.

148. Skokos, D., G. Shakhar, R. Varma, J. C. Waite, T. P. Cameron, R. L. Lindquist, T. Schwickert, M. C. Nussenzweig, and M. L. Dustin. 2007. Peptide-MHC potency governs dynamic interactions between T cells and dendritic cells in lymph nodes. *Nat. Immunol.* 8: 835–844.

149. Kalekar, L. A., and D. L. Mueller. 2017. Relationship between CD4 Regulatory T Cells and Anergy In Vivo. *J. Immunol.* 198: 2527–2533.

150. Kalekar, L. A., S. E. Schmiel, S. L. Nandiwada, W. Y. Lam, L. O. Barsness, N. Zhang, G. L. Stritesky, D. Malhotra, K. E. Pauken, J. L. Linehan, M. G. O'Sullivan, B. T. Fife, K. A. Hogquist, M. K. Jenkins, and D. L. Mueller. 2016. CD4+ T cell anergy prevents autoimmunity and generates regulatory T cell precursors. *Nat. Immunol.* 17: 304–314.

151. Lee, H. M., J. L. Bautista, J. Scott-Browne, J. F. Mohan, and C. S. Hsieh. 2012. A broad range of self-reactivity drives thymic regulatory T cell selection to limit responses to self. *Immunity* 37: 475–486.

152. Owen, D. L., S. A. Mahmud, L. E. Sjaastad, J. B. Williams, J. A. Spanier, D. R. Simeonov, R. Ruscher, W. Huang, I. Proekt, C. N. Miller, C. Hekim, J. C. Jeschke, P. Aggarwal, U. Broeckel, R. S. LaRue, C. M. Henzler, M. L. Alegre, M. S. Anderson, A. August, A. Marson, Y. Zheng, C. B. Williams, and M. A. Farrar. 2019. Thymic regulatory T cells arise via two distinct developmental programs. *Nat. Immunol.* 20: 195–205.

153. Turner, M. S., L. P. Kane, and P. A. Morel. 2009. Dominant role of antigen dose in CD4+Foxp3+ regulatory T cell induction and expansion. *J. Immunol.* 183: 4895–4903.

154. Gottschalk, R. A., E. Corse, and J. P. Allison. 2010. TCR ligand density and affinity determine peripheral induction of Foxp3 in vivo. *J. Exp. Med.* 207: 1701–1711.

155. Klein, L., E. A. Robey, and C. S. Hsieh. 2019. Central CD4 + T cell tolerance: deletion versus regulatory T cell differentiation. *Nat. Rev. Immunol.* 19: 7–18.

156. Pauken, K. E., and E. J. Wherry. 2015. Overcoming T cell exhaustion in infection and cancer. *Trends Immunol.* 36: 265–276.

157. Chen, L., and D. B. Flies. 2013. Molecular mechanisms of T cell co-stimulation and co-inhibition. *Nat. Rev. Immunol.* 13: 227–242.

158. Jubel, J. M., Z. R. Barbati, C. Burger, D. C. Wirtz, and F. A. Schildberg. 2020. The Role of PD-1 in Acute and Chronic Infection. *Front. Immunol.* 11: 487.

159. Ishida, Y., Y. Agata, K. Shibahara, and T. Honjo. 1992. Induced expression of PD-1, a novel member of the immunoglobulin gene superfamily, upon programmed cell death. *EMBO J.* 11: 3887–3895.

160. Agata, Y., A. Kawasaki, H. Nishimura, Y. Ishida, T. Tsubata, H. Yagita, and T. Honjo.

1996. Expression of the PD-1 antigen on the surface of stimulated mouse T and B lymphocytes. *Int. Immunol.* 8: 765–772.

161. Sharpe, A. H., and K. E. Pauken. 2018. The diverse functions of the PD1 inhibitory pathway. *Nat. Rev. Immunol.* 18: 153–167.

162. Youngnak, P., Y. Kozono, H. Kozono, H. Iwai, N. Otsuki, H. Jin, K. Omura, H. Yagita, D. M. Pardoll, L. Chen, and M. Azuma. 2003. Differential binding properties of B7-H1 and B7-DC to programmed death-1. *Biochem. Biophys. Res. Commun.* 307: 672–677.

163. Javed, S. A., A. Najmi, W. Ahsan, and K. Zoghebi. 2024. Targeting PD-1/PD-L-1 immune checkpoint inhibition for cancer immunotherapy: success and challenges. *Front. Immunol.* 15: 1383456.

164. Xiao, Y., S. Yu, B. Zhu, D. Bedoret, X. Bu, L. M. Francisco, P. Hua, J. S. Duke-Cohan, D. T. Umetsu, A. H. Sharpe, R. H. DeKruyff, and G. J. Freeman. 2014. RGMb is a novel binding partner for PD-L2 and its engagement with PD-L2 promotes respiratory tolerance. *J. Exp. Med.* 211: 943–59.

165. Hui, E., J. Cheung, J. Zhu, X. Su, M. J. Taylor, H. A. Wallweber, D. K. Sasmal, J. Huang, J. M. Kim, I. Mellman, and R. D. Vale. 2017. T cell costimulatory receptor CD28 is a primary target for PD-1-mediated inhibition. *Science* 355: 1428–1433.

166. Keir, M. E., M. J. Butte, G. J. Freeman, and A. H. Sharpe. 2008. PD-1 and Its Ligands in Tolerance and Immunity. *Annu. Rev. Immunol.* 26: 677–704.

167. Mizuno, R., D. Sugiura, K. Shimizu, T. Maruhashi, M. Watada, I. Okazaki, and T. Okazaki. 2019. PD-1 Primarily Targets TCR Signal in the Inhibition of Functional T Cell Activation.

Front. Immunol. 10: 630.

168. Li, K., Z. Yuan, J. Lyu, E. Ahn, S. J. Davis, R. Ahmed, and C. Zhu. 2021. PD-1 suppresses TCR-CD8 cooperativity during T-cell antigen recognition. *Nat. Commun.* 12: 2746.

169. Gamper, C. J., and J. D. Powell. 2012. All PI3Kinase signaling is not mTOR: dissecting mTOR-dependent and independent signaling pathways in T cells. *Front. Immunol.* 3: 312.

170. Probst, H. C., K. McCoy, T. Okazaki, T. Honjo, and M. Van Den Broek. 2005. Resting dendritic cells induce peripheral CD8+ T cell tolerance through PD-1 and CTLA-4. *Nat. Immunol.* 6: 280–286.

171. Honda, T., J. G. Egen, T. Lämmermann, W. Kastenmüller, P. Torabi-Parizi, and R. N. Germain. 2014. Tuning of Antigen Sensitivity by TCR T Cell Receptor-Dependent Negative Feedback Controls T Cell Effector Function in Inflamed Tissues. *Immunity* 40: 235–247.

172. Allie, S. R., W. Zhang, S. Fuse, and E. J. Usherwood. 2011. Programmed Death 1 Regulates Development of Central Memory CD8 T Cells after Acute Viral Infection. *J. Immunol.* 186: 6280–6286.

173. Fuse, S., C.-Y. Tsai, M. J. Molloy, S. R. Allie, W. Zhang, H. Yagita, and E. J. Usherwood. 2009. Recall responses by helpless memory CD8+ T cells are restricted by the up-regulation of PD-1. *J. Immunol.* 182: 4244–4254.

174. Keir, M. E., Y. E. Latchman, G. J. Freeman, and A. H. Sharpe. 2005. Programmed Death-1 (PD-1):PD-Ligand 1 Interactions Inhibit TCR-Mediated Positive Selection of Thymocytes. *J. Immunol.* 175: 7372–7379.

175. Nishimura, H., T. Honjo, and N. Minato. 2000. Facilitation of β Selection and Modification

of Positive Selection in the Thymus of Pd-1–Deficient Mice. *J. Exp. Med.* 191: 891–898.

176. Baldwin, T. A., and K. A. Hogquist. 2007. Transcriptional Analysis of Clonal Deletion In Vivo. *J. Immunol.* 179: 837–844.

177. Thangavelu, G., J. C. Parkman, C. L. Ewen, R. R. E. Uwiera, T. A. Baldwin, and C. C. Anderson. 2011. Programmed death-1 is required for systemic self-tolerance in newly generated T cells during the establishment of immune homeostasis. *J. Autoimmun.* 36: 301–312.

178. Ellestad, K. K., J. Lin, L. Boon, and C. C. Anderson. 2017. PD-1 controls tonic signaling and lymphopenia-induced proliferation of T lymphocytes. *Front. Immunol.* 8: 1289.

179. Francisco, L. M., V. H. Salinas, K. E. Brown, V. K. Vanguri, G. J. Freeman, V. K. Kuchroo, and A. H. Sharpe. 2009. PD-L1 regulates the development, maintenance, and function of induced regulatory T cells. *J. Exp. Med.* 206: 3015–29.

180. Amarnath, S., C. W. Mangus, J. C. M. Wang, F. Wei, A. He, V. Kapoor, J. E. Foley, P. R. Massey, T. C. Felizardo, J. L. Riley, B. L. Levine, C. H. June, J. A. Medin, and D. H. Fowler. 2011. The PDL1-PD1 axis converts human TH1 cells into regulatory T cells. *Sci. Transl. Med.* 3: 111ra120.

181. Wang, L., K. Pino-Lagos, V. C. de Vries, I. Guleria, M. H. Sayegh, and R. J. Noelle. 2008. Programmed death 1 ligand signaling regulates the generation of adaptive Foxp3+CD4+ regulatory T cells. *Proc. Natl. Acad. Sci. U. S. A.* 105: 9331–6.

182. Tan, C. L., J. R. Kuchroo, P. T. Sage, D. Liang, L. M. Francisco, J. Buck, Y. R. Thaker, Q. Zhang, S. L. McArdel, V. R. Juneja, S. J. Lee, S. B. Lovitch, C. Lian, G. F. Murphy, B. R. Blazar, D. A. A. Vignali, G. J. Freeman, and A. H. Sharpe. 2021. PD-1 restraint of regulatory T

cell suppressive activity is critical for immune tolerance. *J. Exp. Med.* 218.

183. Pauken, K. E., J. A. Torchia, A. Chaudhri, A. H. Sharpe, and G. J. Freeman. 2021. Emerging concepts in PD-1 checkpoint biology. *Semin. Immunol.* 52: 101480.

184. Barber, D. L., E. J. Wherry, D. Masopust, B. Zhu, J. P. Allison, A. H. Sharpe, G. J. Freeman, and R. Ahmed. 2006. Restoring function in exhausted CD8 T cells during chronic viral infection. *Nature* 439: 682–687.

185. Ohaegbulam, K. C., A. Assal, E. Lazar-Molnar, Y. Yao, and X. Zang. 2015. Human cancer immunotherapy with antibodies to the PD-1 and PD-L1 pathway. *Trends Mol. Med.* 21: 24–33.

186. Sharma, P., S. Hu-Lieskovan, J. A. Wargo, and A. Ribas. 2017. Primary, Adaptive and Acquired Resistance to Cancer Immunotherapy. *Cell* 168: 707–723.

187. Reynoso, E. D., K. G. Elpek, L. Francisco, R. Bronson, A. Bellemare-Pelletier, A. H. Sharpe, G. J. Freeman, and S. J. Turley. 2009. Intestinal tolerance is converted to autoimmune enteritis upon PD-1 ligand blockade. *J. Immunol.* 182: 2102–2112.

188. Pauken, K. E., C. E. Nelson, T. Martinov, J. A. Spanier, J. R. Heffernan, N. L. Sahli, C. F. Quarnstrom, K. C. Osum, J. M. Schenkel, M. K. Jenkins, B. R. Blazar, V. Vezys, and B. T. Fife. 2015. Identification of autoreactive CD4+ and CD8+ T cell subsets resistant to PD-1 pathway blockade. *J. Immunol.* 194: 3551–3555.

189. Ansari, M. J. I., A. D. Salama, T. Chitnis, R. N. Smith, H. Yagita, H. Akiba, T. Yamazaki, M. Azuma, H. Iwai, S. J. Khoury, H. Auchincloss, and M. H. Sayegh. 2003. The programmed death-1 (PD-1) pathway regulates autoimmune diabetes in nonobese diabetic (NOD) mice. *J. Exp. Med.* 198: 63–69.

190. Kumagai, S., Y. Togashi, T. Kamada, E. Sugiyama, H. Nishinakamura, Y. Takeuchi, K. Vitaly, K. Itahashi, Y. Maeda, S. Matsui, T. Shibahara, Y. Yamashita, T. Irie, A. Tsuge, S. Fukuoka, A. Kawazoe, H. Udagawa, K. Kirita, K. Aokage, G. Ishii, T. Kuwata, K. Nakama, M. Kawazu, T. Ueno, N. Yamazaki, K. Goto, M. Tsuboi, H. Mano, T. Doi, K. Shitara, and H. Nishikawa. 2020. The PD-1 expression balance between effector and regulatory T cells predicts the clinical efficacy of PD-1 blockade therapies. *Nat. Immunol.* 21: 1346–1358.

191. Odorizzi, P. M., K. E. Pauken, M. A. Paley, A. Sharpe, and E. John Wherry. 2015. Genetic absence of PD-1 promotes accumulation of terminally differentiated exhausted CD8+ T cells. *J. Exp. Med.* 212: 1125–1137.

192. Jiménez, G., A. Guichet, A. Ephrussi, and J. Casanova. 2000. Relief of gene repression by Torso RTK signaling: role of capicua in Drosophila terminal and dorsoventral patterning. *Genes Dev.* 14: 224–231.

193. Lee, Y. 2020. Regulation and function of capicua in mammals. *Exp. Mol. Med.* 52: 531–537.

194. Lam, Y. C., A. B. Bowman, P. Jafar-Nejad, J. Lim, R. Richman, J. D. Fryer, E. D. Hyun, L. A. Duvick, H. T. Orr, J. Botas, and H. Y. Zoghbi. 2006. ATAXIN-1 interacts with the repressor Capicua in its native complex to cause SCA1 neuropathology. *Cell* 127: 1335–1347.

195. Forés, M., L. Simón-Carrasco, L. Ajuria, N. Samper, S. González-Crespo, M. Drosten, M. Barbacid, and G. Jiménez. 2017. A new mode of DNA binding distinguishes Capicua from other HMG-box factors and explains its mutation patterns in cancer. *PLoS Genet.* 13: e1006622.

196. Fryer, J. D., P. Yu, H. Kang, C. Mandel-Brehm, A. N. Carter, J. Crespo-Barreto, Y. Gao, A. Flora, C. Shaw, H. T. Orr, and H. Y. Zoghbi. 2011. Exercise and Genetic Rescue of SCA1 via

the Transcriptional Repressor Capicua. *Science* 334: 690–693.

197. Bunda, S., P. Heir, J. Metcalf, A. S. C. Li, S. Agnihotri, S. Pusch, M. Yasin, M. Li, K. Burrell, S. Mansouri, O. Singh, M. Wilson, A. Alamsahebpour, R. Nejad, B. Choi, D. Kim, A. von Deimling, G. Zadeh, and K. Aldape. 2019. CIC protein instability contributes to tumorigenesis in glioblastoma. *Nat. Commun.* 10: 661.

198. Okimoto, R. A., F. Breitenbuecher, V. R. Olivas, W. Wu, B. Gini, M. Hofree, S. Asthana, G. Hrustanovic, J. Flanagan, A. Tulpule, C. M. Blakely, H. J. Haringsma, A. D. Simmons, K. Gowen, J. Suh, V. A. Miller, S. Ali, M. Schuler, and T. G. Bivona. 2017. Inactivation of Capicua drives cancer metastasis. *Nat. Genet.* 49: 87–96.

199. Wang, B., E. B. Krall, A. J. Aguirre, M. Kim, H. R. Widlund, M. B. Doshi, E. Sicinska, R. Sulahian, A. Goodale, G. S. Cowley, F. Piccioni, J. G. Doench, D. E. Root, and W. C. Hahn. 2017. ATXN1L, CIC, and ETS Transcription Factors Modulate Sensitivity to MAPK Pathway Inhibition. *Cell Rep.* 18: 1543–1557.

200. Bunda, S., P. Heir, A. S. C. Li, Y. Mamatjan, G. Zadeh, and K. Aldape. 2020. c-Src Phosphorylates and Inhibits the Function of the CIC Tumor Suppressor Protein. *Mol. Cancer Res.* 18: 774–786.

201. Ni, C., W. Jiang, Z. Wang, Z. Wang, J. Zhang, X. Zheng, Z. Liu, H. Ou, T. Jiang, W. Liang, F. Wu, Q. Li, Y. Hou, Q. Yang, B. Guo, S. Liu, S. Li, S. Li, E. Yang, X. H. Zhu, X. Huang, Z. Wen, and C. Zhao. 2021. LncRNA-AC006129.1 reactivates a SOCS3-mediated anti-inflammatory response through DNA methylation-mediated CIC downregulation in schizophrenia. *Mol. Psychiatry* 26: 4511–4528.

202. Lee, Y., J. D. Fryer, H. Kang, J. Crespo-Barreto, A. B. Bowman, Y. Gao, J. J. Kahle, J. S.

Hong, F. Kheradmand, H. T. Orr, M. J. Finegold, and H. Y. Zoghbi. 2011. ATXN1 protein family and CIC regulate extracellular matrix remodeling and lung alveolarization. *Dev. Cell* 21: 746–757.

203. Kim, E., S. Park, N. Choi, J. Lee, J. Yoe, S. Kim, H. Y. Jung, K. T. Kim, H. Kang, J. D. Fryer, H. Y. Zoghbi, D. Hwang, and Y. Lee. 2015. Deficiency of Capicua disrupts bile acid homeostasis. *Sci. Rep.* 5: 8272.

204. Simón-Carrasco, L., G. Jiménez, M. Barbacid, and M. Drosten. 2018. The Capicua tumor suppressor: a gatekeeper of Ras signaling in development and cancer. *Cell Cycle* 17: 702–711.

205. Kim, M. S., S. M. Pinto, D. Getnet, R. S. Nirujogi, S. S. Manda, R. Chaerkady, A. K. Madugundu, D. S. Kelkar, R. Isserlin, S. Jain, J. K. Thomas, B. Muthusamy, P. Leal-Rojas, P. Kumar, N. A. Sahasrabuddhe, L. Balakrishnan, J. Advani, B. George, S. Renuse, L. D. N. Selvan, A. H. Patil, V. Nanjappa, A. Radhakrishnan, S. Prasad, T. Subbannayya, R. Raju, M. Kumar, S. K. Sreenivasamurthy, A. Marimuthu, G. J. Sathe, S. Chavan, K. K. Datta, Y. Subbannayya, A. Sahu, S. D. Yelamanchi, S. Jayaram, P. Rajagopalan, J. Sharma, K. R. Murthy, N. Syed, R. Goel, A. A. Khan, S. Ahmad, G. Dey, K. Mudgal, A. Chatterjee, T. C. Huang, J. Zhong, X. Wu, P. G. Shaw, D. Freed, M. S. Zahari, K. K. Mukherjee, S. Shankar, A. Mahadevan, H. Lam, C. J. Mitchell, S. K. Shankar, P. Satishchandra, J. T. Schroeder, R. Sirdeshmukh, A. Maitra, S. D. Leach, C. G. Drake, M. K. Halushka, T. S. K. Prasad, R. H. Hruban, C. L. Kerr, G. D. Bader, C. A. Iacobuzio-Donahue, H. Gowda, and A. Pandey. 2014. A draft map of the human proteome. *Nature* 509: 575–581.

206. Dissanayake, K., R. Toth, J. Blakey, O. Olsson, D. G. Campbell, A. R. Prescott, and C. Mackintosh. 2011. ERK/p90RSK/14-3-3 signalling has an impact on expression of PEA3 Ets

transcription factors via the transcriptional repressor capicúa. *Biochem. J.* 433: 515–525.

207. Ren, Y., Z. Ouyang, Z. Hou, Y. Yan, Z. Zhi, M. Shi, M. Du, H. Liu, Y. Wen, and Y. Shao. 2020. CIC Is a Mediator of the ERK1/2-DUSP6 Negative Feedback Loop. *iScience* 23: 101635.

208. Futran, A. S., S. Kyin, S. Y. Shvartsman, and A. J. Link. 2015. Mapping the binding interface of ERK and transcriptional repressor Capicua using photocrosslinking. *Proc. Natl. Acad. Sci. U. S. A.* 112: 8590–8595.

209. Wong, D., K. Lounsbury, A. Lum, J. Song, S. Chan, V. LeBlanc, S. Chittaranjan, M. Marra, and S. Yip. 2019. Transcriptomic analysis of CIC and ATXN1L reveal a functional relationship exploited by cancer. *Oncogene* 38: 273–290.

210. Simón-Carrasco, L., O. Graña, M. Salmón, H. K. C. Jacob, A. Gutierrez, G. Jiménez, M. Drosten, and M. Barbacid. 2017. Inactivation of Capicua in adult mice causes T-cell lymphoblastic lymphoma. *Genes Dev.* 31: 1456–1468.

211. Tan, Q., L. Brunetti, M. W. C. Rousseaux, H. C. Lu, Y. W. Wan, J. P. Revelli, Z. Liu, M. A. Goodell, and H. Y. Zoghbi. 2018. Loss of Capicua alters early T cell development and predisposes mice to T cell lymphoblastic leukemia/lymphoma. *Proc. Natl. Acad. Sci. U. S. A.* 115: E1511–E1519.

212. Park, S., S. Lee, C. G. Lee, G. Y. Park, H. Hong, J. S. Lee, Y. M. Kim, S. B. Lee, D. Hwang, Y. S. Choi, J. D. Fryer, S. H. Im, S. W. Lee, and Y. Lee. 2017. Capicua deficiency induces autoimmunity and promotes follicular helper T cell differentiation via derepression of ETV5. *Nat. Commun.* 8: 16037.

213. Kim, S., G. Y. Park, J. S. Park, J. Park, H. Hong, and Y. Lee. 2021. Regulation of positive

and negative selection and TCR signaling during thymic T cell development by capicua. *Elife* 10: e71769.

214. Mariathasan, S., A. Zakarian, D. Bouchard, A. M. Michie, J. C. Zúñiga-Pflücker, and P. S. Ohashi. 2001. Duration and strength of extracellular signal-regulated kinase signals are altered during positive versus negative thymocyte selection. *J. Immunol.* 167: 4966–4973.

215. Weissmann, S., P. A. Cloos, S. Sidoli, O. N. Jensen, S. Pollard, and K. Helin. 2018. The tumor suppressor CIC directly regulates MAPK pathway genes via histone deacetylation. *Cancer Res.* 78: 4114–4125.

216. Yang, R., L. H. Chen, L. J. Hansen, A. B. Carpenter, C. J. Moure, H. Liu, C. J. Pirozzi, B. H. Diplas, M. S. Waitkus, P. K. Greer, H. Zhu, R. E. McLendon, D. D. Bigner, Y. He, and H. Yan. 2017. Cic Loss Promotes Gliomagenesis via Aberrant Neural Stem Cell Proliferation and Differentiation. *Cancer Res.* 77: 6097–6108.

217. Kidger, A. M., and S. M. Keyse. 2016. The regulation of oncogenic Ras/ERK signalling by dual-specificity mitogen activated protein kinase phosphatases (MKPs). *Semin. Cell Dev. Biol.* 50: 125–132.

218. Sasaki, A., T. Taketomi, R. Kato, K. Saeki, A. Nonami, M. Sasaki, M. Kuriyama, N. Saito, M. Shibuya, and A. Yoshimura. 2003. Mammalian Sprouty4 suppresses Ras-independent ERK activation by binding to Raf1. *Nat. Cell Biol.* 5: 427–432.

219. Wakioka, T., A. Sasaki, R. Kato, T. Shouda, A. Matsumoto, K. Miyoshi, M. Tsuneoka, S. Komiya, R. Baron, and A. Yoshimura. 2001. Spred is a Sprouty-related suppressor of Ras signalling. *Nature* 412: 647–651.

220. Kurts, C., W. R. Heath, F. R. Carbone, J. Allison, J. F. A. F. Miller, H. Kosaka, and Victoria. 1996. Constitutive class I-restricted exogenous presentation of self antigens in vivo. *J. Exp. Med.* 184: 923–930.

221. Latchman, Y. E., S. C. Liang, Y. Wu, T. Chernova, R. A. Sobel, M. Klemm, V. K. Kuchroo, G. J. Freman, and A. H. Sharpe. 2004. PD-L1-deficient mice show that PD-L1 on T cells, antigen-presenting cells, and host tissues negatively regulates T cells. *Proc. Natl. Acad. Sci. U. S. A.* 101: 10691–10696.

222. Maekawa, Y., Y. Minato, C. Ishifune, T. Kurihara, A. Kitamura, H. Kojima, H. Yagita, M. Sakata-Yanagimoto, T. Saito, I. Taniuchi, S. Chiba, S. Sone, and K. Yasutomo. 2008. Notch2 integrates signaling by the transcription factors RBP-J and CREB1 to promote T cell cytotoxicity. *Nat. Immunol.* 9: 1140–1147.

223. Flanagan, S. P. 1966. “Nude”, a new hairless gene with pleiotropic effects in the mouse. *Genet. Res.* 8: 295–309.

224. Nishimura, H., M. Nose, H. Hiai, N. Minato, and T. Honjo. 1999. Development of lupus-like autoimmune diseases by disruption of the PD-1 gene encoding an ITIM motif-carrying immunoreceptor. *Immunity* 11: 141–151.

225. Watanabe, N., M. Gavrieli, J. R. Sedy, J. Yang, F. Fallarino, S. K. Loftin, M. A. Hurchla, N. Zimmerman, J. Sim, X. Zang, T. L. Murphy, J. H. Russell, J. P. Allison, and K. M. Murphy. 2003. BTLA is a lymphocyte inhibitory receptor with similarities to CTLA-4 and PD-1. *Nat. Immunol.* 4: 670–679.

226. Lu, H. C., Q. Tan, M. W. C. Rousseaux, W. Wang, J. Y. Kim, R. Richman, Y. W. Wan, S. Y. Yeh, J. M. Patel, X. Liu, T. Lin, Y. Lee, J. D. Fryer, J. Han, M. Chahrour, R. H. Finnell, Y.

Lei, M. E. Zurita-Jimenez, P. Ahimaz, K. Anyane-Yeboa, L. Van Maldergem, D. Lehalle, N. Jean-Marcais, A. L. Mosca-Boidron, J. Thevenon, M. A. Cousin, D. E. Bro, B. C. Lanpher, E. W. Klee, N. Alexander, M. N. Bainbridge, H. T. Orr, R. V. Sillitoe, M. C. Ljungberg, Z. Liu, C. P. Schaaf, and H. Y. Zoghbi. 2017. Disruption of the ATXN1-CIC complex causes a spectrum of neurobehavioral phenotypes in mice and humans. *Nat. Genet.* 49: 527–536.

227. Baldwin, T. A., M. M. Sandau, S. C. Jameson, and K. A. Hogquist. 2005. The timing of TCRα expression critically influences T cell development and selection. *J. Exp. Med.* 202: 111–121.

228. Barnden, M. J., J. Allison, W. R. Heath, and F. R. Carbone. 1998. Defective TCR expression in transgenic mice constructed using cDNA- based α- and β-chain genes under the control of heterologous regulatory elements. *Immunol. Cell Biol.* 76: 34–40.

229. Lucille Delisle, Maria Doyle, F. H. ATAC-Seq data analysis (Galaxy Training Materials). https://training.galaxyproject.org/training-material/topics/epigenetics/tutorials/atac-seq/tutorial.html Online; accessed Apr 03 2024. .

230. Hiltemann, S., H. Rasche, S. Gladman, H. R. Hotz, D. Larivière, D. Blankenberg, P. D. Jagtap, T. Wollmann, A. Bretaudeau, N. Goué, T. J. Griffin, C. Royaux, Y. Le Bras, S. Mehta, A. Syme, F. Coppens, B. Droesbeke, N. Soranzo, W. Bacon, F. Psomopoulos, C. Gallardo-Alba, J. Davis, M. C. Föll, M. Fahrner, M. A. Doyle, B. Serrano-Solano, A. C. Fouilloux, P. van Heusden, W. Maier, D. Clements, F. Heyl, B. Grüning, and B. Batut. 2023. Galaxy Training: A powerful framework for teaching! *PLOS Comput. Biol.* 19: e1010752.

231. Batut, B., S. Hiltemann, A. Bagnacani, D. Baker, V. Bhardwaj, C. Blank, A. Bretaudeau, L. Brillet-Guéguen, M. Čech, J. Chilton, D. Clements, O. Doppelt-Azeroual, A. Erxleben, M. A.

Freeberg, S. Gladman, Y. Hoogstrate, H. R. Hotz, T. Houwaart, P. Jagtap, D. Larivière, G. Le Corguillé, T. Manke, F. Mareuil, F. Ramírez, D. Ryan, F. C. Sigloch, N. Soranzo, J. Wolff, P. Videm, M. Wolfien, A. Wubuli, D. Yusuf, J. Taylor, R. Backofen, A. Nekrutenko, and B. Grüning. 2018. Community-Driven Data Analysis Training for Biology. *Cell Syst.* 6: 752-758.e1.

232. Langmead, B., and S. L. Salzberg. 2012. Fast gapped-read alignment with Bowtie 2. *Nat. Methods* 9: 357.

233. Zhang, Y., T. Liu, C. A. Meyer, J. Eeckhoute, D. S. Johnson, B. E. Bernstein, C. Nussbaum, R. M. Myers, M. Brown, W. Li, and X. S. Shirley. 2008. Model-based analysis of ChIP-Seq (MACS). *Genome Biol.* 9: R137.

234. Canté-Barrett, K., E. M. Gallo, M. M. Winslow, and G. R. Crabtree. 2006. Thymocyte negative selection is mediated by protein kinase C- and Ca2+-dependent transcriptional induction of bim [corrected]. *J. Immunol.* 176: 2299–2306.

235. Liston, A., S. Lesage, D. H. D. Gray, L. A. O'Reilly, A. Strasser, A. M. Fahrer, R. L. Boyd, J. Wilson, A. G. Baxter, E. M. Gallo, G. R. Crabtree, K. Peng, S. R. Wilson, and C. C. Goodnow. 2004. Generalized resistance to thymic deletion in the NOD mouse; a polygenic trait characterized by defective induction of Bim. *Immunity* 21: 817–830.

236. Kovalovsky, D., M. Pezzano, B. D. Ortiz, and D. B. Sant'Angelo. 2010. A novel TCR transgenic model reveals that negative selection involves an immediate, Bim-dependent pathway and a delayed, Bim-independent pathway. *PLoS One* 5: e8675.

237. Jorgensen, T. N., A. McKee, M. Wang, E. Kushnir, J. White, Y. Refaeli, J. W. Kappler, and P. Marrack. 2007. Bim and Bcl-2 mutually affect the expression of the other in T cells. *J.*

Immunol. 179: 3417–3424.

238. Hu, Q. N., and T. A. Baldwin. 2015. Differential roles for Bim and Nur77 in thymocyte clonal deletion induced by ubiquitous self-antigen. *J. Immunol.* 194: 2643–53.

239. Hogquist, K. A., S. C. Jameson, W. R. Heath, J. L. Howard, M. J. Bevan, and F. R. Carbone. 1994. T cell receptor antagonist peptides induce positive selection. *Cell* 76: 17–27.

240. Tsai, S., A. Shameli, J. Yamanouchi, X. Clemente-Casares, J. Wang, P. Serra, Y. Yang, Z. Medarova, A. Moore, and P. Santamaria. 2010. Reversal of Autoimmunity by Boosting Memory-like Autoregulatory T Cells. *Immunity* 32: 568–580.

241. Vuddamalay, Y., M. Attia, R. Vicente, C. Pomié, G. Enault, B. Leobon, O. Joffre, P. Romagnoli, and J. P. M. van Meerwijk. 2016. Mouse and human CD8(+) CD28(low) regulatory T lymphocytes differentiate in the thymus. *Immunology* 148: 187–96.

242. Schönrich, G., F. Momburg, G. J. Hämmerling, and B. Arnold. 1992. Anergy induced by thymic medullary epithelium. *Eur. J. Immunol.* 22: 1687–1691.

243. Alfei, F., K. Kanev, M. Hofmann, M. Wu, H. E. Ghoneim, P. Roelli, D. T. Utzschneider, M. von Hoesslin, J. G. Cullen, Y. Fan, V. Eisenberg, D. Wohlleber, K. Steiger, D. Merkler, M. Delorenzi, P. A. Knolle, C. J. Cohen, R. Thimme, B. Youngblood, and D. Zehn. 2019. TOX reinforces the phenotype and longevity of exhausted T cells in chronic viral infection. *Nature* 571: 265–269.

244. Gearty, S. V., F. Dündar, P. Zumbo, G. Espinosa-Carrasco, M. Shakiba, F. J. Sanchez-Rivera, N. D. Socci, P. Trivedi, S. W. Lowe, P. Lauer, N. Mohibullah, A. Viale, T. P. DiLorenzo, D. Betel, and A. Schietinger. 2021. An autoimmune stem-like CD8 T cell population

drives type 1 diabetes. *Nature* 602: 156–161.

245. Gebhardt, T., S. L. Park, and I. A. Parish. 2023. Stem-like exhausted and memory CD8+ T cells in cancer. *Nat. Rev. Cancer* 23: 780–798.

246. Love, M. I., W. Huber, and S. Anders. 2014. Moderated estimation of fold change and dispersion for RNA-seq data with DESeq2. *Genome Biol.* 15: 550.

247. Stark, R., and G. Brown. 2011. DiffBind: Differential binding analysis of ChIP-Seq peak data. *https://bioconductor.org/packages/release/bioc/vignettes/DiffBind/inst/doc/DiffBind.pdf* .

248. Ross-Innes, C. S., R. Stark, A. E. Teschendorff, K. A. Holmes, H. R. Ali, M. J. Dunning, G. D. Brown, O. Gojis, I. O. Ellis, A. R. Green, S. Ali, S. F. Chin, C. Palmieri, C. Caldas, and J. S. Carroll. 2012. Differential oestrogen receptor binding is associated with clinical outcome in breast cancer. *Nature* 481: 389–393.

249. Yu, G., L.-G. Wang, Y. Han, and Q.-Y. He. 2012. ClusterProfiler: An R package for comparing biological themes among gene clusters. *Omi. A J. Integr. Biol.* 16: 284–287.

250. Wu, T., E. Hu, S. Xu, M. Chen, P. Guo, Z. Dai, T. Feng, L. Zhou, W. Tang, L. Zhan, X. Fu, S. Liu, X. Bo, and G. Yu. 2021. clusterProfiler 4.0: A universal enrichment tool for interpreting omics data. *Innovation* 2: 100141.

251. Odagiu, L., J. May, S. Boulet, T. A. Baldwin, and N. Labrecque. 2021. Role of the Orphan Nuclear Receptor NR4A Family in T-Cell Biology. *Front. Endocrinol. (Lausanne).* 11: 624122.

252. Liu, X., Y. Wang, H. Lu, J. Li, X. Yan, M. Xiao, J. Hao, A. Alekseev, H. Khong, T. Chen, R. Huang, J. Wu, Q. Zhao, Q. Wu, S. Xu, X. Wang, W. Jin, S. Yu, Y. Wang, L. Wei, A. Wang, B. Zhong, L. Ni, X. Liu, R. Nurieva, L. Ye, Q. Tian, X.-W. Bian, and C. Dong. 2019. Genome-

wide analysis identifies NR4A1 as a key mediator of T cell dysfunction. *Nature* 567: 525–529.

253. Chen, J., I. F. López-Moyado, H. Seo, C.-W. J. Lio, L. J. Hempleman, T. Sekiya, A. Yoshimura, J. P. Scott-Browne, and A. Rao. 2019. NR4A transcription factors limit CAR T cell function in solid tumours. *Nature* 567: 530–534.

254. Tietscher, S., J. Wagner, T. Anzeneder, C. Langwieder, M. Rees, B. Sobottka, N. de Souza, and B. Bodenmiller. 2023. A comprehensive single-cell map of T cell exhaustion-associated immune environments in human breast cancer. *Nat. Commun.* 14: 1–20.

255. Clouthier, D. L., and T. H. Watts. 2014. Cell-specific and context-dependent effects of GITR in cancer, autoimmunity, and infection. *Cytokine Growth Factor Rev.* 25: 91–106.

256. Chan, S., N. Belmar, S. Ho, B. Rogers, M. Stickler, M. Graham, E. Lee, N. Tran, D. Zhang, P. Gupta, M. Sho, T. MacDonough, A. Woolley, H. Kim, H. Zhang, W. Liu, P. Zheng, Z. Dezso, K. Halliwill, M. Ceccarelli, S. Rhodes, A. Thakur, C. M. Forsyth, M. Xiong, S. S. Tan, R. Iyer, M. Lake, E. Digiammarino, L. Zhou, L. Bigelow, K. Longenecker, R. A. Judge, C. Liu, M. Trumble, J. P. Remis, M. Fox, B. Cairns, Y. Akamatsu, D. Hollenbaugh, F. Harding, and H. M. Alvarez. 2022. An anti-PD-1–GITR-L bispecific agonist induces GITR clustering-mediated T cell activation for cancer immunotherapy. *Nat. Cancer* 3: 337–354.

257. Chen, Z., E. Stelekati, M. Kurachi, S. Yu, Z. Cai, S. Manne, O. Khan, X. Yang, and E. J. Wherry. 2017. miR-150 Regulates Memory CD8 T Cell Differentiation via c-Myb. *Cell Rep.* 20: 2584–2597.

258. Gautam, S., J. Fioravanti, W. Zhu, J. B. Le Gall, P. Brohawn, N. E. Lacey, J. Hu, J. D. Hocker, N. V. Hawk, V. Kapoor, W. G. Telford, D. Gurusamy, Z. Yu, A. Bhandoola, H. H. Xue, R. Roychoudhuri, B. W. Higgs, N. P. Restifo, T. P. Bender, Y. Ji, and L. Gattinoni. 2019. The

transcription factor c-Myb regulates CD8+ T cell stemness and antitumor immunity. *Nat. Immunol.* 20: 337–349.

259. Tsui, C., L. Kretschmer, S. Rapelius, S. S. Gabriel, D. Chisanga, K. Knöpper, D. T. Utzschneider, S. Nüssing, Y. Liao, T. Mason, S. V. Torres, S. A. Wilcox, K. Kanev, S. Jarosch, J. Leube, S. L. Nutt, D. Zehn, I. A. Parish, W. Kastenmüller, W. Shi, V. R. Buchholz, and A. Kallies. 2022. MYB orchestrates T cell exhaustion and response to checkpoint inhibition. *Nature* 609: 354–360.

260. Yu, G., L. G. Wang, and Q. Y. He. 2015. ChIPseeker: an R/Bioconductor package for ChIP peak annotation, comparison and visualization. *Bioinformatics* 31: 2382–2383.

261. Wang, Q., M. Li, T. Wu, L. Zhan, L. Li, M. Chen, W. Xie, Z. Xie, E. Hu, S. Xu, and G. Yu. 2022. Exploring Epigenomic Datasets by ChIPseeker. *Curr. Protoc.* 2.

262. Ashburner, M., C. A. Ball, J. A. Blake, D. Botstein, H. Butler, J. M. Cherry, A. P. Davis, K. Dolinski, S. S. Dwight, J. T. Eppig, M. A. Harris, D. P. Hill, L. Issel-Tarver, A. Kasarskis, S. Lewis, J. C. Matese, J. E. Richardson, M. Ringwald, G. M. Rubin, and G. Sherlock. 2000. Gene Ontology: tool for the unification of biology. *Nat. Genet.* 25: 25–29.

263. Carbon, S., E. Douglass, N. Dunn, B. Good, N. L. Harris, S. E. Lewis, C. J. Mungall, S. Basu, R. L. Chisholm, R. J. Dodson, E. Hartline, P. Fey, P. D. Thomas, L. P. Albou, D. Ebert, M. J. Kesling, H. Mi, A. Muruganujan, X. Huang, S. Poudel, T. Mushayahama, J. C. Hu, S. A. LaBonte, D. A. Siegele, G. Antonazzo, H. Attrill, N. H. Brown, S. Fexova, P. Garapati, T. E. M. Jones, S. J. Marygold, G. H. Millburn, A. J. Rey, V. Trovisco, G. Dos Santos, D. B. Emmert, K. Falls, P. Zhou, J. L. Goodman, V. B. Strelets, J. Thurmond, M. Courtot, D. S. Osumi, H. Parkinson, P. Roncaglia, M. L. Acencio, M. Kuiper, A. Lreid, C. Logie, R. C. Lovering, R. P.

Huntley, P. Denny, N. H. Campbell, B. Kramarz, V. Acquaah, S. H. Ahmad, H. Chen, J. H. Rawson, M. C. Chibucos, M. Giglio, S. Nadendla, R. Tauber, M. J. Duesbury, N. T. Del, B. H. M. Meldal, L. Perfetto, P. Porras, S. Orchard, A. Shrivastava, Z. Xie, H. Y. Chang, R. D. Finn, A. L. Mitchell, N. D. Rawlings, L. Richardson, A. Sangrador-Vegas, J. A. Blake, K. R. Christie, M. E. Dolan, H. J. Drabkin, D. P. Hill, L. Ni, D. Sitnikov, M. A. Harris, S. G. Oliver, K. Rutherford, V. Wood, J. Hayles, J. Bahler, A. Lock, E. R. Bolton, J. De Pons, M. Dwinell, G. T. Hayman, S. J. F. Laulederkind, M. Shimoyama, M. Tutaj, S. J. Wang, P. D'Eustachio, L. Matthews, J. P. Balhoff, S. A. Aleksander, G. Binkley, B. L. Dunn, J. M. Cherry, S. R. Engel, F. Gondwe, K. Karra, K. A. MacPherson, S. R. Miyasato, R. S. Nash, P. C. Ng, T. K. Sheppard, A. Shrivatsav Vp, M. Simison, M. S. Skrzypek, S. Weng, E. D. Wong, M. Feuermann, P. Gaudet, E. Bakker, T. Z. Berardini, L. Reiser, S. Subramaniam, E. Huala, C. Arighi, A. Auchincloss, K. Axelsen, G. P. Argoud, A. Bateman, B. Bely, M. C. Blatter, E. Boutet, L. Breuza, A. Bridge, R. Britto, H. Bye-A-Jee, C. Casals-Casas, E. Coudert, A. Estreicher, L. Famiglietti, P. Garmiri, G. Georghiou, A. Gos, N. Gruaz-Gumowski, E. Hatton-Ellis, U. Hinz, C. Hulo, A. Ignatchenko, F. Jungo, G. Keller, K. Laiho, P. Lemercier, D. Lieberherr, Y. Lussi, A. Mac-Dougall, M. Magrane, M. J. Martin, P. Masson, D. A. Natale, N. N. Hyka, I. Pedruzzi, K. Pichler, S. Poux, C. Rivoire, M. Rodriguez-Lopez, T. Sawford, E. Speretta, A. Shypitsyna, A. Stutz, S. Sundaram, M. Tognolli, N. Tyagi, K. Warner, R. Zaru, C. Wu, J. Chan, J. Cho, S. Gao, C. Grove, M. C. Harrison, K. Howe, R. Lee, J. Mendel, H. M. Muller, D. Raciti, K. Van Auken, M. Berriman, L. Stein, P. W. Sternberg, D. Howe, S. Toro, and M. Westerfield. 2019. The Gene Ontology Resource: 20 years and still GOing strong. *Nucleic Acids Res.* 47: D330–D338.

264. Ou, J. 2023. ATACseqTFEA: Transcription Factor Enrichment Analysis for ATAC-seq. *R Packag. version 1.4.0, , https//github.com/jianhong/ATACseqTFEA* .

265. Foletta, V. C., D. H. Segal, and D. R. Cohen. 1998. Transcriptional regulation in the immune system: all roads lead to AP-1. *J. Leukoc. Biol.* 63: 139–152.

266. Wagner, E. F., R. Eferl, D. K. Matsuo, J.-P. David, R. Zenz, L. Bakiri, P. Hasselblatt, A. Bozec, M. Sibilia, G. Karsenty, and J. Smolen. 2005. Fos/AP-1 proteins in bone and the immune system. *Immunol. Rev.* 208: 126–140.

267. Wherry, E. J., S. J. Ha, S. M. Kaech, W. N. Haining, S. Sarkar, V. Kalia, S. Subramaniam, J. N. Blattman, D. L. Barber, and R. Ahmed. 2007. Molecular Signature of CD8+ T Cell Exhaustion during Chronic Viral Infection. *Immunity* 27: 670–684.

268. Zhou, M., L. McPherson, D. Feng, A. Song, C. Dong, S.-C. Lyu, L. Zhou, X. Shi, Y.-T. Ahn, D. Wang, C. Clayberger, and A. M. Krensky. 2007. Krüppel-Like Transcription Factor 13 Regulates T Lymphocyte Survival In Vivo. *J. Immunol.* 178: 5496–5504.

269. Outram, S. V., A. R. Gordon, A. L. Hager-Theodorides, J. Metcalfe, T. Crompton, and P. Kemp. 2008. KLF13 influences multiple stages of both B and T cell development. *Cell Cycle* 7: 2047–2055.

270. Mookerjee-Basu, J., R. Hooper, S. Gross, B. Schultz, C. K. Go, E. Samakai, J. Ladner, E. Nicolas, Y. Tian, B. Zhou, M. R. Zaidi, W. Tourtellotte, S. He, Y. Zhang, D. J. Kappes, and J. Soboloff. 2020. Suppression of Ca2+ signals by EGR4 controls Th1 differentiation and anti-cancer immunity in vivo. *EMBO Rep.* 21: e48904.

271. Feng, X., G. C. Ippolito, L. Tian, K. Wiehagen, S. Oh, A. Sambandam, J. Willen, R. M. Bunte, S. D. Maika, J. V. Harriss, A. J. Caton, A. Bhandoola, P. W. Tucker, and H. Hu. 2010. Foxp1 is an essential transcriptional regulator for the generation of quiescent naive T cells during thymocyte development. *Blood* 115: 510–518.

272. Feng, X., H. Wang, H. Takata, T. J. Day, J. Willen, and H. Hu. 2011. Transcription factor Foxp1 exerts essential cell-intrinsic regulation of the quiescence of naive T cells. *Nat. Immunol.* 12: 544–550.

273. Stephen, T. L., M. R. Rutkowski, M. J. Allegrezza, A. Perales-Puchalt, A. J. Tesone, N. Svoronos, J. M. Nguyen, F. Sarmin, M. E. Borowsky, J. Tchou, and J. R. Conejo-Garcia. 2014. Transforming growth factor β-mediated suppression of antitumor T cells requires Foxp1 transcription factor expression. *Immunity* 41: 427–439.

274. Blighe K, Rana S, L. M. 2023. EnhancedVolcano: Publication-ready volcano plots with enhanced colouring and labeling. *R Packag. version 1.20.0, https//github.com/kevinblighe/EnhancedVolcano* .

275. Richards, D. M., B. Kyewski, and M. Feuerer. 2016. Re-examining the nature and function of self-reactive T cells. *Trends Immunol.* 37: 114–125.

276. Truckenbrod, E. N., K. S. Burrack, T. P. Knutson, H. B. da Silva, K. E. Block, S. D. O'flanagan, K. R. Stagliano, A. A. Hurwitz, R. B. Fulton, K. R. Renkema, and S. C. Jameson. 2021. CD8+ t cell self-tolerance permits responsiveness but limits tissue damage. *Elife* 10: e65615.

277. Ramsdell, F., T. Lantz, and B. J. Fowlkes. 1989. A nondeletional mechanism of thymic self tolerance. *Science* 246: 1038–1041.

278. Mishra, S. 2021. CD8+ Regulatory T Cell – A Mystery to Be Revealed. *Front. Immunol.* 12: 708874.

279. Singer, M., C. Wang, L. Cong, N. D. Marjanovic, M. S. Kowalczyk, H. Zhang, J. Nyman,

K. Sakuishi, S. Kurtulus, D. Gennert, J. Xia, J. Y. H. Kwon, J. Nevin, R. H. Herbst, I. Yanai, O. Rozenblatt-Rosen, V. K. Kuchroo, A. Regev, and A. C. Anderson. 2016. A distinct gene module for dysfunction uncoupled from activation in tumor-infiltrating T cells. *Cell* 166: 1500-1511.e9.

280. Lin, J., A. Harding, E. Giurisato, and A. S. Shaw. 2009. KSR1 Modulates the Sensitivity of Mitogen-Activated Protein Kinase Pathway Activation in T Cells without Altering Fundamental System Outputs. *Mol. Cell. Biol.* 29: 2082–2091.

281. Giurisato, E., J. Lin, A. Harding, E. Cerutti, M. Cella, R. E. Lewis, M. Colonna, and A. S. Shaw. 2009. The Mitogen-Activated Protein Kinase Scaffold KSR1 Is Required for Recruitment of Extracellular Signal-Regulated Kinase to the Immunological Synapse. *Mol. Cell. Biol.* 29: 1554–1564.

282. Wherry, E. J. 2011. T cell exhaustion. *Nat. Immunol.* 12: 492–499.

283. Salerno, F., A. Guislain, J. J. Freen-Van Heeren, B. P. Nicolet, H. A. Young, and M. C. Wolkers. 2019. Critical role of post-transcriptional regulation for IFN-γ in tumor-infiltrating T cells. *Oncoimmunology* 8: e1532762.

284. Villarino, A. V., S. D. Katzman, E. Gallo, O. Miller, S. Jiang, M. T. McManus, and A. K. Abbas. 2011. Posttranscriptional Silencing of Effector Cytokine mRNA Underlies the Anergic Phenotype of Self-Reactive T Cells. *Immunity* 34: 50–60.

285. Yukawa, M., S. Jagannathan, S. Vallabh, A. V. Kartashov, X. Chen, M. T. Weirauch, and A. Barski. 2020. AP-1 activity induced by co-stimulation is required for chromatin opening during T cell activation. *J. Exp. Med.* 217: e20182009.

286. Jain, J., V. E. Valge-Archer, and A. Rao. 1992. Analysis of the AP-1 sites in the IL-2

promoter. *J. Immunol.* 148: 1240–1250.

287. Dolmetsch, R. E., R. S. Lewis, C. C. Goodnow, and J. I. Healy. 1997. Differential activation of transcription factors induced by Ca2+ response amplitude and duration. *Nature* 386: 855–858.

288. Marangoni, F., T. T. Murooka, T. Manzo, E. Y. Kim, E. Carrizosa, N. M. Elpek, and T. R. Mempel. 2013. The transcription factor NFAT exhibits signal memory during serial T cell interactions with antigen-presenting cells. *Immunity* 38: 237–249.

289. Oh-hora, M., M. Yamashita, P. G. Hogan, S. Sharma, E. Lamperti, W. Chung, M. Prakriya, S. Feske, and A. Rao. 2008. Dual functions for the endoplasmic reticulum calcium sensors STIM1 and STIM2 in T cell activation and tolerance. *Nat. Immunol.* 9: 432–443.

290. Blackburn, S. D., H. Shin, W. N. Haining, T. Zou, C. J. Workman, A. Polley, M. R. Betts, G. J. Freeman, D. A. A. Vignali, and E. J. Wherry. 2008. Coregulation of CD8+ T cell exhaustion by multiple inhibitory receptors during chronic viral infection. *Nat. Immunol.* 10: 29–37.

291. Odorizzi, P. M., and E. J. Wherry. 2012. Inhibitory receptors on lymphocytes: insights from infections. *J. Immunol.* 188: 2957–2965.

292. Baitsch, L., S. A. Fuertes-Marraco, A. Legat, C. Meyer, and D. E. Speiser. 2012. The three main stumbling blocks for anticancer T cells. *Trends Immunol.* 33: 364–372.

293. Kim, P. S., and R. Ahmed. 2010. Features of responding T cells in cancer and chronic infection. *Curr. Opin. Immunol.* 22: 223–230.

294. Grosso, J. F., C. C. Kelleher, T. J. Harris, C. H. Maris, E. L. Hipkiss, A. De Marzo, R. Anders, G. Netto, D. Getnet, T. C. Bruno, M. V. Goldberg, D. M. Pardoll, and C. G. Drake.

2007. LAG-3 regulates CD8+ T cell accumulation and effector function in murine self- and tumor-tolerance systems. *J. Clin. Invest.* 117: 3383–3392.

295. Blackburn, S. D., H. Shin, G. J. Freeman, and E. J. Wherry. 2008. Selective expansion of a subset of exhausted CD8 T cells by αPD-L1 blockade. *Proc. Natl. Acad. Sci. U. S. A.* 105: 15016–15021.

296. Pauken, K. E., M. A. Sammons, P. M. Odorizzi, S. Manne, J. Godec, O. Khan, A. M. Drake, Z. Chen, D. R. Sen, M. Kurachi, R. A. Barnitz, C. Bartman, B. Bengsch, A. C. Huang, J. M. Schenkel, G. Vahedi, W. N. Haining, S. L. Berger, and E. J. Wherry. 2016. Epigenetic stability of exhausted T cells limits durability of reinvigoration by PD-1 blockade. *Science* 354: 1160–1165.

297. Francisco, L. M., P. T. Sage, and A. H. Sharpe. 2010. The PD-1 pathway in tolerance and autoimmunity. *Immunol. Rev.* 236: 219–242.

298. Ribas, A., and J. D. Wolchok. 2018. Cancer Immunotherapy Using Checkpoint Blockade. *Science* 359: 1350–1355.

299. Yokosuka, T., M. Takamatsu, W. Kobayashi-Imanishi, A. Hashimoto-Tane, M. Azuma, and T. Saito. 2012. Programmed cell death 1 forms negative costimulatory microclusters that directly inhibit T cell receptor signaling by recruiting phosphatase SHP2. *J. Exp. Med.* 209: 1201–1217.

300. Parry, R. V., J. M. Chemnitz, K. A. Frauwirth, A. R. Lanfranco, I. Braunstein, S. V. Kobayashi, P. S. Linsley, C. B. Thompson, and J. L. Riley. 2005. CTLA-4 and PD-1 Receptors Inhibit T-Cell Activation by Distinct Mechanisms. *Mol. Cell. Biol.* 25: 9543–9553.

301. Nishimura, H., Y. Agata, A. Kawasaki, M. Sato, S. Imamura, N. Minato, H. Yagita, T.

Nakano, and T. Honjo. 1996. Developmentally regulated expression of the PD-1 protein on the surface of double-negative(CD4–CD8–) thymocytes. *Int. Immunol.* 8: 773–780.

302. Brown, J. A., D. M. Dorfman, F.-R. Ma, E. L. Sullivan, O. Munoz, C. R. Wood, E. A. Greenfield, and G. J. Freeman. 2003. Blockade of programmed death-1 ligands on dendritic cells enhances T cell activation and cytokine production. *J. Immunol.* 170: 1257–1266.

303. Liang, S. C., Y. E. Latchman, J. E. Buhlmann, M. F. Tomczak, B. H. Horwitz, G. J. Freeman, and A. H. Sharpe. 2003. Regulation of PD-1, PD-L1, and PD-L2 expression during normal and autoimmune responses. *Eur. J. Immunol.* 33: 2706–2716.

304. Prokunina, L., C. Castillejo-López, F. Öberg, I. Gunnarsson, L. Berg, V. Magnusson, A. J. Brookes, D. Tentler, H. Kristjansdóttir, G. Gróndal, A. Isine Bolstad, E. Svenungsson, I. Lundberg, G. Sturfelt, A. Jönssen, L. Truedsson, G. Lima, J. Alcocer-Varela, R. Jonsson, U. B. Gyllensten, J. B. Harley, D. Alarcón-Segovia, K. Steinsson, and M. E. Alarcón-Riquelme. 2002. A regulatory polymorphism in PDCD1 is associated with susceptibility to systemic lupus erythematosus in humans. *Nat. Genet.* 32: 666–669.

305. Kong, E. K. P., L. Prokunina-Olsson, W. H. S. Wong, C. S. Lau, T. M. Chan, M. Alarcón-Riquelme, and Y. L. Lau. 2005. A new haplotype of PDCD1 is associated with rheumatoid arthritis in Hong Kong Chinese. *Arthritis Rheum.* 52: 1058–1062.

306. Kroner, A., M. Mehling, B. Hemmer, P. Rieckmann, K. V. Toyka, M. Mäurer, and H. Wiendl. 2005. A PD-1 polymorphism is associated with disease progression in multiple sclerosis. *Ann. Neurol.* 58: 50–57.

307. Blank, C., I. Brown, R. Marks, H. Nishimura, T. Honjo, and T. F. Gajewski. 2003. Absence of programmed death receptor 1 alters thymic development and enhances generation of

CD4/CD8 double-negative TCR-transgenic T cells. *J. Immunol.* 171: 4574–4581.

308. Han, P., O. D. Goularte, K. Rufner, B. Wilkinson, and J. Kaye. 2004. An inhibitory Ig superfamily protein expressed by lymphocytes and APCs is also an early marker of thymocyte positive selection. *J. Immunol.* 172: 5931–9.

309. Nüssing, S., I. G. House, C. J. Kearney, A. X. Y. Chen, S. J. Vervoort, P. A. Beavis, J. Oliaro, R. W. Johnstone, J. A. Trapani, and I. A. Parish. 2020. Efficient CRISPR/Cas9 Gene Editing in Uncultured Naive Mouse T Cells for In Vivo Studies. *J. Immunol.* 204: 2308–2315.

310. Jiang, T. T., T. Martinov, L. Xin, J. M. Kinder, J. A. Spanier, B. T. Fife, and S. S. Way. 2016. Programmed Death-1 Culls Peripheral Accumulation of High-Affinity Autoreactive CD4 T Cells to Protect against Autoimmunity. *Cell Rep.* 17: 1783–1794.

311. Fife, B. T., I. Guleria, M. G. Bupp, T. N. Eagar, Q. Tang, H. Bour-Jordan, H. Yagita, M. Azuma, M. H. Sayegh, and J. A. Bluestone. 2006. Insulin-induced remission in new-onset NOD mice is maintained by the PD-1-PD-L1 pathway. *J. Exp. Med.* 203: 2737–2747.

312. Fife, B. T., K. E. Pauken, T. N. Eagar, T. Obu, J. Wu, Q. Tang, M. Azuma, M. F. Krummel, and J. A. Bluestone. 2009. Interactions between programmed death-1 and programmed death ligand-1 promote tolerance by blocking the T cell receptor-induced stop signal. *Nat. Immunol.* 10: 1185–1192.

313. Lühder, F., P. Höglund, J. P. Allison, C. Benoist, and D. Mathis. 1998. Cytotoxic T lymphocyte-associated antigen 4 (CTLA-4) regulates the unfolding of autoimmune diabetes. *J. Exp. Med.* 187: 427–432.

314. Fife, B. T., and K. E. Pauken. 2011. The role of the PD-1 pathway in autoimmunity and

peripheral tolerance. *Ann. N. Y. Acad. Sci.* 1217: 45–59.

315. Policheni, A. N., C. E. Teh, A. Robbins, S. Tuzlak, A. Strasser, and D. H. D. Gray. 2022. PD-1 cooperates with AIRE-mediated tolerance to prevent lethal autoimmune disease. *Proc. Natl. Acad. Sci.* 119: e2120149119.

316. Keir, M. E., S. C. Liang, I. Guleria, Y. E. Latchman, A. Qipo, L. A. Albacker, M. Koulmanda, G. J. Freeman, M. H. Sayegh, and A. H. Sharpe. 2006. Tissue expression of PD-L1 mediates peripheral T cell tolerance. *J. Exp. Med.* 203: 883–895.

317. Ouyang, W., O. Beckett, Q. Ma, and M. O. Li. 2010. Transforming growth factor-beta signaling curbs thymic negative selection promoting regulatory T cell development. *Immunity* 32: 642–653.

318. Kisanuki, Y. Y., R. E. Hammer, J. ichi Miyazaki, S. C. Williams, J. A. Richardson, and M. Yanagisawa. 2001. Tie2-Cre transgenic mice: A new model for endothelial cell-lineage analysis in vivo. *Dev. Biol.* 230: 230–242.

319. Stadtfeld, M., and T. Graf. 2005. Assessing the role of hematopoietic plasticity for endothelial and hepatocyte development by non-invasive lineage tracing. *Development* 132: 203–213.

320. Lee, P. P., D. R. Fitzpatrick, C. Beard, H. K. Jessup, S. Lehar, K. W. Makar, M. Pérez-Melgosa, M. T. Sweetser, M. S. Schlissel, S. Nguyen, S. R. Cherry, J. H. Tsai, S. M. Tucker, W. M. Weaver, A. Kelso, R. Jaenisch, and C. B. Wilson. 2001. A critical role for Dnmt1 and DNA methylation in T cell development, function, and survival. *Immunity* 15: 763–774.

321. Kieper, W. C., J. T. Burghardt, and C. D. Surh. 2004. A Role for TCR Affinity in

Regulating Naive T Cell Homeostasis. *J. Immunol.* 172: 40–44.

322. Leishman, A. J., L. Gapin, M. Capone, E. Palmer, H. R. MacDonald, M. Kronenberg, and H. Cheroutre. 2002. Precursors of functional MHC class I- or class II-restricted CD8alphaalpha(+) T cells are positively selected in the thymus by agonist self-peptides. *Immunity* 16: 355–364.

323. Ebertl, G., and D. R. Litman. 2004. Thymic origin of intestinal alphabeta T cells revealed by fate mapping of RORgammat+ cells. *Science* 305: 248–251.

324. Gangadharan, D., F. Lambolez, A. Attinger, Y. Wang-Zhu, B. A. Sullivan, and H. Cheroutre. 2006. Identification of pre- and postselection TCRalphabeta+ intraepithelial lymphocyte precursors in the thymus. *Immunity* 25: 631–641.

325. Azzam, H. S., A. Grinberg, K. Lui, H. Shen, E. W. Shores, and P. E. Love. 1998. CD5 expression is developmentally regulated by T cell receptor (TCR) signals and TCR avidity. *J. Exp. Med.* 188: 2301–11.

326. Scholzen, T., and J. Gerdes. 2000. The Ki-67 protein: from the known and the unknown. *J. Cell. Physiol.* 182: 311–322.

327. Clarke, S. Rm. K., M. Barnden, C. Kurts, F. R. Carbone, J. F. Miller, and W. R. Heath. 2000. Characterization of the ovalbumin-specific TCR transgenic line OT-I: MHC elements for positive and negative selection. *Immunol. Cell Biol.* 78: 110–117.

328. McConkey, D. J., P. Hartzell, J. F. Amador-Pérez, S. Orrenius, and M. Jondal. 1989. Calcium-dependent killing of immature thymocytes by stimulation via the CD3/T cell receptor complex. *J. Immunol.* 143: 1801–1806.

329. Tadakuma, T., H. Kizaki, C. Odaka, R. Kubota, Y. Ishimura, H. Yagita, and K. Okumura. 1990. CD4+CD8+ thymocytes are susceptible to DNA fragmentation induced by phorbol ester, calcium ionophore and anti-CD3 antibody. *Eur. J. Immunol.* 20: 779–784.

330. Shi, Y. F., R. P. Bissonnette, N. Parfrey, M. Szalay, R. T. Kubo, and D. R. Green. 1991. In vivo administration of monoclonal antibodies to the CD3 T cell receptor complex induces cell death (apoptosis) in immature thymocytes. *J. Immunol.* 146: 3340–3346.

331. Zhan, Y., Y. Zhang, D. Gray, E. M. Carrington, P. Bouillet, H.-J. Ko, L. O'Reilly, I. P. Wicks, A. Strasser, and A. M. Lew. 2011. Defects in the Bcl-2-regulated apoptotic pathway lead to preferential increase of CD25 low Foxp3+ anergic CD4+ T cells. *J. Immunol.* 187: 1566–1577.

332. Perry, J. S. A., and C. S. Hsieh. 2016. Development of T-cell tolerance utilizes both cell-autonomous and cooperative presentation of self-antigen. *Immunol. Rev.* 271: 141–155.

333. Yates, A. J. 2014. Theories and quantification of thymic selection. *Front. Immunol.* 5: 13.

334. Miller, I., M. Min, C. Yang, C. Tian, S. Gookin, D. Carter, and S. L. Spencer. 2018. Ki67 is a Graded Rather than a Binary Marker of Proliferation versus Quiescence. *Cell Rep.* 24: 1105-1112.e5.

335. Tubo, N. J., A. J. Pagán, J. J. Taylor, R. W. Nelson, J. L. Linehan, J. M. Ertelt, E. S. Huseby, S. S. Way, and M. K. Jenkins. 2013. Single naïve CD4+ T cells from a diverse repertoire produce different effector cell types during an infection. *Cell* 153: 785–796.

336. Surh, C. D., and J. Sprent. 2005. Regulation of mature T cell homeostasis. *Semin. Immunol.* 17: 183–191.

337. Takada, K., and S. C. Jameson. 2009. Naive T cell homeostasis: from awareness of space to a sense of place. *Nat. Rev. Immunol.* 9: 823–832.

338. Carrette, F., and C. D. Surh. 2012. IL-7 signaling and CD127 receptor regulation in the control of T cell homeostasis. *Semin. Immunol.* 24: 209–217.

339. Miller, B. C., D. R. Sen, R. Al Abosy, K. Bi, Y. V. Virkud, M. W. LaFleur, K. B. Yates, A. Lako, K. Felt, G. S. Naik, M. Manos, E. Gjini, J. R. Kuchroo, J. J. Ishizuka, J. L. Collier, G. K. Griffin, S. Maleri, D. E. Comstock, S. A. Weiss, F. D. Brown, A. Panda, M. D. Zimmer, R. T. Manguso, F. S. Hodi, S. J. Rodig, A. H. Sharpe, and W. N. Haining. 2019. Subsets of exhausted CD8+ T cells differentially mediate tumor control and respond to checkpoint blockade. *Nat. Immunol.* 20: 326–336.

340. Khan, O., J. R. Giles, S. McDonald, S. Manne, S. F. Ngiow, K. P. Patel, M. T. Werner, A. C. Huang, K. A. Alexander, J. E. Wu, J. Attanasio, P. Yan, S. M. George, B. Bengsch, R. P. Staupe, G. Donahue, W. Xu, R. K. Amaravadi, X. Xu, G. C. Karakousis, T. C. Mitchell, L. M. Schuchter, J. Kaye, S. L. Berger, and E. J. Wherry. 2019. TOX transcriptionally and epigenetically programs CD8+ T cell exhaustion. *Nature* 571: 211–218.

341. Scott, A. C., F. Dündar, P. Zumbo, S. S. Chandran, C. A. Klebanoff, M. Shakiba, P. Trivedi, L. Menocal, H. Appleby, S. Camara, D. Zamarin, T. Walther, A. Snyder, M. R. Femia, E. A. Comen, H. Y. Wen, M. D. Hellmann, N. Anandasabapathy, Y. Liu, N. K. Altorki, P. Lauer, O. Levy, M. S. Glickman, J. Kaye, D. Betel, M. Philip, and A. Schietinger. 2019. TOX is a critical regulator of tumour-specific T cell differentiation. *Nature* 571: 270–274.

342. Seo, H., J. Chen, E. González-Avalos, D. Samaniego-Castruita, A. Das, Y. H. Wang, I. F. López-Moyado, R. O. Georges, W. Zhang, A. Onodera, C. J. Wu, L. F. Lu, P. G. Hogan, A.

Bhandoola, and A. Rao. 2019. TOX and TOX2 transcription factors cooperate with NR4A transcription factors to impose CD8+ T cell exhaustion. *Proc. Natl. Acad. Sci. U. S. A.* 116: 12410–12415.

343. Schietinger, A., M. Philip, V. E. Krisnawan, E. Y. Chiu, J. J. Delrow, R. S. Basom, P. Lauer, D. G. Brockstedt, S. E. Knoblaugh, G. J. Hämmerling, T. D. Schell, N. Garbi, and P. D. Greenberg. 2016. Tumor-Specific T Cell Dysfunction Is a Dynamic Antigen-Driven Differentiation Program Initiated Early during Tumorigenesis. *Immunity* 45: 389–401.

344. Philip, M., L. Fairchild, L. Sun, E. L. Horste, S. Camara, M. Shakiba, A. C. Scott, A. Viale, P. Lauer, T. Merghoub, M. D. Hellmann, J. D. Wolchok, C. S. Leslie, and A. Schietinger. 2017. Chromatin states define tumor-specific T cell dysfunction and reprogramming. *Nature* 545: 452–456.

345. Johnson, D. G., and R. Schneider-Broussard. 1998. Role of E2F in cell cycle control and cancer. *Front. Biosci.* 3: D447-458.

346. Cao, Z., X. Sun, B. Icli, A. K. Wara, and M. W. Feinberg. 2010. Role of Krüppel-like factors in leukocyte development, function, and disease. *Blood* 116: 4404–4414.

347. Chuang, E., M. Augustine, M. Jung, R. H. Schwartz, and N. J. Singh. 2017. Density dependent re-tuning of autoreactive T cells alleviates their pathogenicity in a lymphopenic environment. *Immunol. Lett.* 192: 61–71.

348. Macián, F., S. H. Im, F. J. García-Cózar, and A. Rao. 2004. T-cell anergy. *Curr. Opin. Immunol.* 16: 209–216.

349. Perez, V. L., L. Van Parijs, A. Biuckians, X. X. Zheng, T. B. Strom, and A. K. Abbas. 1997.

Induction of peripheral T cell tolerance in vivo requires CTLA-4 engagement. *Immunity* 6: 411–417.

350. Bhattacharyya, N. D., and C. G. Feng. 2020. Regulation of T Helper Cell Fate by TCR Signal Strength. *Front. Immunol.* 11: 624.

351. Powell, J. D., and G. M. Delgoffe. 2010. The mammalian target of rapamycin: linking T cell differentiation, function, and metabolism. *Immunity* 33: 301–311.

352. Quigley, M., F. Pereyra, B. Nilsson, F. Porichis, C. Fonseca, Q. Eichbaum, B. Julg, J. L. Jesneck, K. Brosnahan, S. Imam, K. Russell, I. Toth, A. Piechocka-Trocha, D. Dolfi, J. Angelosanto, A. Crawford, H. Shin, D. S. Kwon, J. Zupkosky, L. Francisco, G. J. Freeman, E. J. Wherry, D. E. Kaufmann, B. D. Walker, B. Ebert, and W. N. Haining. 2010. Integrative genomic analysis of HIV-specific CD8+ T cells reveals that PD-1 inhibits T cell function by upregulating BATF. *Nat. Med.* 16: 1147–1151.

353. Xing, Y., and K. A. Hogquist. 2014. Isolation, Identification, and Purification of Murine Thymic Epithelial Cells. *J. Vis. Exp.* e51780.

354. Cunningham, C. A., E. Y. Helm, and P. J. Fink. 2018. Reinterpreting recent thymic emigrant function: defective or adaptive? *Curr. Opin. Immunol.* 51: 1–6.

355. Yost, K. E., A. T. Satpathy, D. K. Wells, Y. Qi, C. Wang, R. Kageyama, K. L. McNamara, J. M. Granja, K. Y. Sarin, R. A. Brown, R. K. Gupta, C. Curtis, S. L. Bucktrout, M. M. Davis, A. L. S. Chang, and H. Y. Chang. 2019. Clonal replacement of tumor-specific T cells following PD-1 blockade. *Nat. Med.* 25: 1251–1259.

356. Wei, S. C., C. R. Duffy, and J. P. Allison. 2018. Fundamental mechanisms of immune

checkpoint blockade therapy. *Cancer Discov.* 8: 1069–1086.

357. Yin, Q., L. Wu, L. Han, X. Zheng, R. Tong, L. Li, L. Bai, and Y. Bian. 2023. Immune-related adverse events of immune checkpoint inhibitors: a review. *Front. Immunol.* 14: 1167975.

358. Hwang, J. R., Y. Byeon, D. Kim, and S. G. Park. 2020. Recent insights of T cell receptor-mediated signaling pathways for T cell activation and development. *Exp. Mol. Med.* 52: 750–761.

359. Keenan, S. E., S. A. Blythe, R. A. Marmion, N. J. V. Djabrayan, E. F. Wieschaus, and S. Y. Shvartsman. 2020. Rapid Dynamics of Signal-Dependent Transcriptional Repression by Capicua. *Dev. Cell* 52: 794-801.e4.

360. McCaughtry, T. M., R. Etzensperger, A. Alag, X. Tai, S. Kurtulus, J. H. Park, A. Grinberg, P. Love, L. Feigenbaum, B. Erman, and A. Singer. 2012. Conditional deletion of cytokine receptor chains reveals that IL-7 and IL-15 specify CD8 cytotoxic lineage fate in the thymus. *J. Exp. Med.* 209: 2263–2276.

361. Huesmann, M., B. Scott, P. Kisielow, and H. von Boehmer. 1991. Kinetics and efficacy of positive selection in the thymus of normal and T cell receptor transgenic mice. *Cell* 66: 533–540.

362. Wong, P., A. W. Goldrath, and A. Y. Rudensky. 2000. Competition for Specific Intrathymic Ligands Limits Positive Selection in a TCR Transgenic Model of CD4+ T Cell Development. *J. Immunol.* 164: 6252–6259.

363. Bautista, J. L., C. W. J. Lio, S. K. Lathrop, K. Forbush, Y. Liang, J. Luo, A. Y. Rudensky, and C. S. Hsieh. 2009. Intraclonal competition limits regulatory T cell fate determination in the thymus. *Nat. Immunol.* 10: 610–617.

364. Ernst, B., D. S. Lee, J. M. Chang, J. Sprent, and C. D. Surh. 1999. The peptide ligands mediating positive selection in the thymus control T cell survival and homeostatic proliferation in the periphery. *Immunity* 11: 173–181.

365. Tan, J. T., B. Ernst, W. C. Kieper, E. LeRoy, J. Sprent, and C. D. Surh. 2002. Interleukin (IL)-15 and IL-7 jointly regulate homeostatic proliferation of memory phenotype CD8+ cells but are not required for memory phenotype CD4+ cells. *J. Exp. Med.* 195: 1523–1532.

366. Cho, J.-H., H.-O. Kim, C. D. Surh, and J. Sprent. 2010. T Cell Receptor-Dependent Regulation of Lipid Rafts Controls Naive CD8+ T Cell Homeostasis. *Immunity* 32: 214–226.